



HAL
open science

**Genome editing to understand neural circuits formation :
a novel CRISPR/Cas9-based strategy for conditional
mutagenesis and functional study of the role of the
meteorin gene family in zebrafish neurodevelopment**

Flavia de Santis

► **To cite this version:**

Flavia de Santis. Genome editing to understand neural circuits formation : a novel CRISPR/Cas9-based strategy for conditional mutagenesis and functional study of the role of the meteorin gene family in zebrafish neurodevelopment. *Neurons and Cognition [q-bio.NC]*. Université Pierre et Marie Curie - Paris VI, 2017. English. NNT : 2017PA066269 . tel-02301987

HAL Id: tel-02301987

<https://theses.hal.science/tel-02301987>

Submitted on 1 Oct 2019

HAL is a multi-disciplinary open access archive for the deposit and dissemination of scientific research documents, whether they are published or not. The documents may come from teaching and research institutions in France or abroad, or from public or private research centers.

L'archive ouverte pluridisciplinaire **HAL**, est destinée au dépôt et à la diffusion de documents scientifiques de niveau recherche, publiés ou non, émanant des établissements d'enseignement et de recherche français ou étrangers, des laboratoires publics ou privés.

Université Pierre et Marie Curie

Ecole Doctorale Cerveau Cognition Comportement
Institut Curie, Unité Génétique Biologie du Développement
Equipe Développement des circuits neuronaux

Sujet de la thèse:

**Genome editing to understand neural circuits formation:
*a novel CRISPR/Cas9-based strategy for conditional mutagenesis
and functional study of the role of the meteorin gene family in
zebrafish neurodevelopment***

Présentée par
Flavia DE SANTIS

Thèse de doctorat de Neurosciences

Dirigée par
Filippo DEL BENE

Présentée et soutenue publiquement le
29/09/2017

Devant un jury composé de:

Dr. Filippo Del Bene (Directeur de thèse)
Dr. Patrick Blader (Rapporteur)
Dr. Alessandra Pierani (Rapporteur)
Dr. Sonia Garel (Examineur)
Dr. Xavier Nicol (Examineur)

ACKNOWLEDGEMENTS

First and foremost, I would like to thank my supervisor, Filippo. Thanks for giving me the opportunity to join your lab and be part of such a great team, working with you has never been boring. Thank you for having pushed me to do my best without being on my back all the time, for being an endless source of motivation and for your always positive attitude toward our results. And most importantly thanks for all the gossips, the nice words you spent for me over these years and for the patience you had with my two left hands.

I am extremely thankful to the members of my PhD jury (Patrick Blader, Sonia Garel, Xavier Nicol and Alessandra Pierani) for having accepted to evaluate my work and to the members of my TAC committee, Sonia and Claire, for all the inputs and encouragement you gave me over these years.

I deep thank goes to all the members of my team. During my PhD, I spent most of my days in the lab, and if I make it to the end it was also because each of you gave his special contribution to create a great work environment. Karine, your golden hands saved my experiments so many times that I would need more than 50 chocolate bars to thank you enough! Shahad, thanks to be there to support and sustain me all the time I need you. Chris, thank you for being my best example of scientific integrity and for all the encouraging smiles you gave me during these years. Celine, it was always nice to discuss science or chat with you over a coffee break. Valerie, thanks for the flowers, for feeding me in the moments of need and for sharing the stress of deadlines in these last months. Giulia, thanks for being always a source of positive energy, despite all your “problems”. Juliette, you brought a shot of life in the lab: thanks for being the co-founder of the “chi-chi club”. Gokul and Marion, you are the new generation of PhD students and the future of the “Del Bene lab”, keep great our reputation!

A big thank goes to the former members of the lab: Tom, Federica and Vincenzo. I think that I shared with you the best moments of my PhD. Vin, I don't need many words for you, just thanks for having been my partner in crime for all these years.

I am extremely grateful to Jean-Paul, with whom I moved my first steps in the CRISPRs world. You have been there in the more stressful moment of my PhD, always providing helpful advices during the craziness of the CaCACreZ.

A great thank goes to Irene and Natalia, with whom I had my first experience as a supervisor: it was really fun to work with both of you.

I would also like to thank all the BDD people, especially the 3rd floor, for all the parties and the fruitful discussions we had over these years.

Angelo, we have known each other for more than 10 years and during this long time you became one of my best friends. Thanks for having been an anchor in the moment of sadness, for all the "asocial Fridays" and for the "bulimic weekends" that made this writing less painful.

My biggest gratitude goes to the gym attack (+1) group: Ale, Sara, Robi and Marta. Thanks for all the sweating in the gym, the drinking, the dancing, the singing, the shopping, the eating, the failed starving and all the other moments we shared outside of the lab.

An immense "merci" to all the colocs that have been living in the rooms of rue du temple (Damian, Stefania, Coralie, Mattia, Giulio, Solene, Simon). It was always a pleasure to find you home and share a beer or a dinner after a long day of experiments.

Thanks also to my oldest friends (Mu, Giuseppe, Daniela, Giorgia, Gino), because we all ended up in different places but we still manage to be there for each other.

My strongest thank goes to my family, that always supported me and who kept on feeding me being an endless source of "pacchi da giù".

TABLE OF CONTENTS

List of figures and tables	p.III
Abbreviations	p.IV
Preamble	p.V

CHAPTER I: INTRODUCTION

I.I CRISPR/Cas9-based strategy for conditional mutagenesis in Zebrafish

I.I.I Genome editing in zebrafish.....	p. 1
I.I.II The CRISPR/Cas9 system.....	p.2
I.I.III CRISPR/Cas9 and tissue specific knock-out.....	p.3
I.I.IV CRISPR/Cas9 and clonal analysis.....	p. 7
Aim of the project I	p. 8

I.II Study of the role of the *meteorin* gene family in axon guidance

I.II.I General mechanisms of axonal navigation.....	p.9
I.II.II Axon guidance factors	
Canonical axon guidance factors	
<i>Netrins</i>	p. 11
<i>Slits</i>	p. 12
<i>Semaphorins</i>	p. 14
<i>Ephrins</i>	p. 15
Non-canonical guidance molecules: Morphogens, growth factors and ECM molecules.....	p. 15
I.II.III The role of the midline in axon guidance	p. 17
I.II.IV Opened questions in the field.....	p. 19
I.II.V Meteorin proteins: novel players in axonal guidance?.....	p. 20
I.II.VI Zebrafish and axon guidance research.....	p. 21
I.II.VII Axon guidance mechanisms in zebrafish.....	p. 22

<i>Development of the first commissural tracts: the AC/POC.....</i>	p.22
<i>The retino-tectal system.....</i>	p.24
<i>Commissural and longitudinal tracts in the hindbrain.....</i>	p.27
Aim of the project II.....	p.29

CHAPTER II: RESULTS

Article I summary.....	p.31
2C-Cas9: a versatile tool for clonal analysis of gene function.....	p.33
Article II summary.....	p.51
Meteorins are conserved midline-secreted proteins regulating axonal pathfinding in the Zebrafish nervous system.....	p.53

CHAPTER III: DISCUSSION AND PERSPECTIVES

III.I.I The 2C-Cas9 system allow the induction of conditional mutagenesis and the simultaneous labeling of mutant cells.....	p. 81
III.I.II Advantages and limitation of the 2C-Cas9 system.....	p. 83
III.II.I Metrns are involved in the patterning of the axonal projection in the CNS of zebrafish embryos.....	p. 85
III.II.II Possible models for Metrns induced modulation of axonal pathfinding in Zebrafish.....	p. 87
<i>A. FP induction, Midline differentiation and tissue homeostasis.....</i>	p. 87
<i>B. Direct interaction with pathfinding axons and modulation of axon guidance pathways.....</i>	p. 88

CHAPTER IV: Conclusions

I. Conclusions I	p. 93
II. Conclusions II	p. 94

BIBLIOGRAPHY

ANNEXES.....

LIST OF TABLES AND FIGURES

Figure 1: Schematic of sgRNA mediated recruitment of the Cas9 enzyme to a target site.....	p.3
Figure 2: TALEN- and HR-based generation of floxed alleles in zebrafish.....	p.5
Figure 3 Design of a vector system allowing CRISPR/Cas9-based conditional knock-out.....	p.6
Figure 4 Illustration of the axonal growth cone.....	p.9
Figure 5 Schematic of the different guidance cues acting on growing axons.....	p. 10
Figure 6 Canonical axon guidance ligands and receptors.....	p. 16
Figure 7 Pattern of navigation defects induced by defects in floor plate specification.....	p. 18
Figure 8 Schematic of the axonal scaffold in the rostral forebrain of zebrafish embryos.....	p.23
Figure 9 Illustration of the RGCs projections in the Optic Tectum.....	p.25
Figure 10 Axonal tracts in the hindbrain of 24 hpf zebrafish larvae.....	p.28
Table 1 Genes involved in the patterning of RGC axons.....	p.26

ABBREVIATIONS

AC: anterior commissure
CNS: central nervous system
CRISPR/Cas9: Clustered Regularly Interspaced Palindromic Repeats/
CRISPR associated protein 9
DPF: days post fertilization
DRC: dorsal rostral cluster
DRG: dorsal root ganglion
DSB: double strand break
ECM: extracellular matrix
FP: floor plate
Flp: flippase
FRT: flippase recognition target
HPF: hours post fertilization
HSP: heat shock promoter
KI: knock-in
KO: knock-out
LLF: lateral longitudinal fascicle
LOF: loss of function
MLF: medial longitudinal fascicle
NHEJ: non-homologous end-joining
ORF: open reading frame
PAM: protospacer adjacent motif
POC: post-optic commissure
RGC: retinal ganglion cells
sgRNA: single guide RNA
SOT: Supra optic tract
TALEN: transcription activator-like effector nucleases
TPOC: tract of the post optic commissure
UAS: upstream activating sequence
VRC: ventro rostral cluster

PREAMBLE

The possibility of easily manipulating the zebrafish (*Danio rerio*) genome with a broad spectrum of genome editing approaches, makes this organism a valuable model to study neuronal circuit development and function. In recent years, the CRISPR/Cas9 technology has revolutionized the possibilities of inducing targeted gene modifications, further expanding the advantages of this model.

This thesis provides both a technical description of new CRISPR/Cas9-based tool that we have implemented to induce targeted and tightly controlled gene disruption, and a report of the utility of the CRISPR/Cas9 system for the generation of mutant lines for the study of genes of interest in developmental neurobiology.

In the first part, we will present a novel approach that we have developed to induce conditional gene knock-out in zebrafish. Our strategy is based on the combination of the CRISPR/Cas9 and the Gal4/UAS technologies and allows, at the same time, to induce targeted gene inactivation and labeling of the cells potentially carrying a loss-of-function allele.

In the second part of this thesis, we took advantage of the CRISPR/Cas9 technology to investigate the biological role of the *meteorin* gene family during embryonic neurodevelopment. Meteorins are conserved midline-secreted proteins, potentially involved in the patterning of the embryonic CNS. Here, we explore the possibility that these molecules are implicated in the process of axonal pathfinding in zebrafish and we investigate the effects of *meteorins* gene disruption on the establishment of the axonal navigation path of different neuronal populations.

CHAPTER I: INTRODUCTION

I.I CRISPR/Cas9-based strategy for conditional mutagenesis in zebrafish

I.I.I Genome editing in zebrafish

A number of unique advantages makes the zebrafish (*Danio rerio*) model one of the most attractive for developmental biologists. Being a vertebrate, it shows high genetic homology with most mammalian animals, with the majority of orthologues proteins displaying evolutionary conserved functions. Adult fish are able to generate a very large number of offsprings per lay (about 200-300), providing a high number of embryos undergoing a rapid extra-uterine development. Moreover, zebrafish larvae are optically transparent, making them ideally suited for the live imaging of several developmental processes. Importantly, in recent years, different technologies allowing the manipulation of zebrafish genome have been established, making it possible to generate transgenic and mutant lines for diverse experimental approaches.

The first zebrafish loss-of-function (LOF) alleles were generated by non-targeted strategies during forward genetic screens based on the use of mutagens like N-ethyl N-nitrosourea (Driever, Solnica-Krezel et al. 1996) or retroviral vectors (Gaiano, Amsterdam et al. 1996). The possibility of introducing targeted mutations, thus allowing reverse genetic approaches, was introduced by the development of Zinc Finger Nucleases (McCammon, Doyon et al. 2011) and subsequently boosted by the establishment of the Transcription Activator-Like Effector Nucleases (TALEN) (Huang, Xiao et al. 2011) and the CRISPR/Cas (clustered regularly interspaced palindromic repeats/CRISPR-associated) technologies (Hwang, Fu et al. 2013).

To date, genome editing techniques enable to perform controlled

knock-in (KI) and knock-out (KO) approaches in zebrafish, expanding the advantages of this model in biological research (Li, Zhao et al. 2016, Albadri, Del Bene et al. 2017). The next paragraph will focus on the description of the CRISPR/Cas9 system and will provide a summary of the different strategies that have been developed to apply this and other genome editing techniques to the generation of constitutive and conditional knock-out lines in zebrafish and other organisms.

I.I.II The CRISPR/Cas9 system

In prokaryote organisms, the CRISPR/Cas system is an essential component of the adaptive immunity that allows bacteria and archaea to antagonize the invasion of exogenous genetic material deriving from bacteriophages or plasmids (Barrangou, Fremaux et al. 2007, Marraffini and Sontheimer 2008, Hale, Zhao et al. 2009, Garneau, Dupuis et al. 2010, Bhaya, Davison et al. 2011). The CRISPR/Cas systems have been classified into three major types, each of which relies on the ability of RNA molecules to guide a non-specific nuclease to cut foreign nucleic acids. Among these, the type II has been specifically optimized to serve as a genome editing tool for the precise manipulation of eukaryotic genomes (Jinek, Chylinski et al. 2012, Cong, Ran et al. 2013, Mali, Yang et al. 2013, Malina, Mills et al. 2013). The resulting system is based on the coordinated activity of two components: an engineered single guide RNA (sgRNA) containing a 5' sequence of 20 nucleotides (nt) complementary to the target genomic region and the Cas9 endonuclease catalyzing double-strand breaks (DSBs) at the desired genomic location. Interaction between the two components is guaranteed by the 3' region of the sgRNA, forming a secondary structure recognized and bound by the Cas9 enzyme. To catalyze efficient DNA cleavage, the Cas9 nuclease requires a short motif (named the protospacer adjacent motif, PAM) flanking the 20 nt targeted by the sgRNA on the genomic DNA. The Cas9 protein derived from *Streptococcus pyogenes* is the most widely used for genome editing techniques and requires NGG as PAM sequence (a typical genomic target site consists of a N21-GG consensus) (Figure 1). Following Cas9-induced DNA cleavage, the targeted locus is vulnerable to mutagenesis events induced by the imperfect repair mechanisms mediated by the non-homologous end-joining (NHEJ) pathway. NHEJ is an error-prone process and, while promoting the ligation between the two ends of the damaged DNA, it could lead to the

generation of small insertions and deletions (indel). Therefore, sgRNAs binding within the coding region of a gene cause disruption of its open reading frame (ORF), which, in turn, leads to gene loss-of-function. The possibility of targeting any region of interest by simply customizing a 20 nt long complementary oligo on the 5' of sgRNAs makes the CRISPR/Cas9 system an extremely versatile tool for genome editing approaches. For this reason, in recent years, this technology has imposed itself as the method of choice for the generation of LOF alleles in diverse model organisms, including zebrafish (Friedland, Tzur et al. 2013, Gratz, Cummings et al. 2013, Hwang, Fu et al. 2013, Wang, Yang et al. 2013).

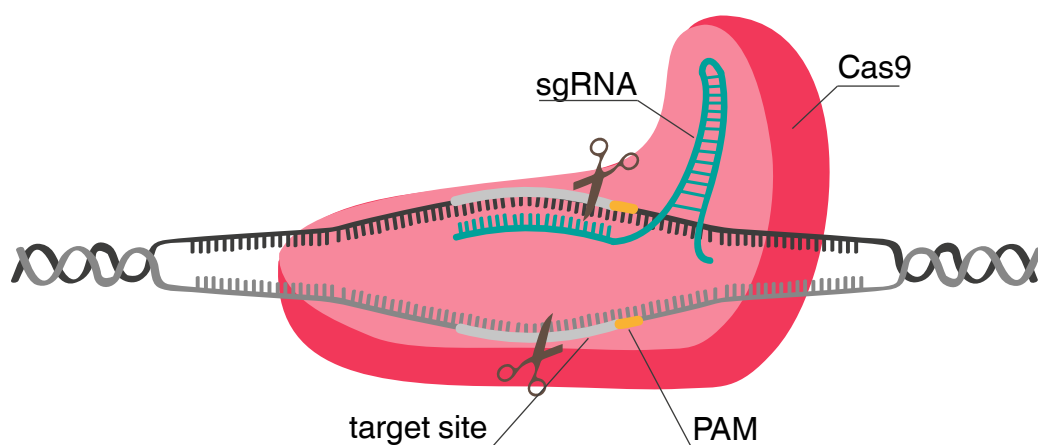


Figure 1

Schematic illustration of the CRISPR/Cas9-induced DNA cleavage. Disruption of the selected locus is achieved by the synergistic activity of two components: a sgRNA (containing a 20 nt sequence complementary to the target sequence on the genomic DNA) and the Cas9 endonuclease that cut the target site after complex formation with the sgRNA.

I.I.III CRISPR/Cas9 and tissue specific knock-out

The possibility of generating animals carrying constitutive KO alleles represents one of the most powerful strategies to explore the function of a gene of interest. Nevertheless, a number of limitations can result from a stable gene disruption. Indeed, the analysis of mutant animals might be strongly impaired by embryonic lethality, compensation mechanisms, and pleiotropic phenotypes that could be induced by constitutive gene mutations. In this context, the ability to control gene LOF in a precisely spatiotemporal-regulated fashion represents a great step forward in reverse genetic studies. Before the establishment of the CRISPR/Cas9

technology, the golden standard techniques for conditional mutagenesis in mouse and *Drosophila melanogaster* were based on the Cre/loxP and Flippase (Flp)/Flippase recognition target (FRT) systems (Theodosiou and Xu 1998, Bouabe and Okkenhaug 2013). The first technique makes use of homologous recombination events to create transgenic animals carrying a floxed target allele having a couple of loxP sites at the 5' and 3' ends of its sequence. These sites are recognized by the Cre enzyme, having the ability of catalyzing site-specific recombination in genomic regions containing loxP sequences. Cre activity promotes the excision of the floxed allele and results in the subsequent induction of gene inactivation. Therefore, the generation of Cre-based conditional gene disruption is possible if animals carrying a floxed target sequence are crossed to a driver line in which cre expression is controlled by a tissue-specific promoter (Kuhn, Schwenk et al. 1995). The use of an engineered version of the Cre recombinase, in which the enzyme is fused to the estrogen receptor (Cre-ER), allows an additional level of control of gene inactivation, permitting tamoxifen-induced temporal regulation of Cre activity (Feil, Brocard et al. 1996). An analogous strategy has been extensively used in *D. melanogaster* and is based on the activity of the Flp enzyme, catalyzing site-directed recombination of DNA sequences flanked by FRT sites (Choi, Vilain et al. 2009). A method for Cre/loxP- and Flp/FRT-induced tissue specific gene inactivation has also been established in zebrafish (Ni, Lu et al. 2012). This approach is based on the intronic integration of a gene-trap cassette that can be inverted by both the Cre or Flp enzymes. The insertion of this transgene in its neutral orientation does not affect the expression of the host gene. On the contrary, its integration in the gene-trap orientation severely disrupt the expression of the targeted locus. Cre or Flp can be used to invert the orientation of this cassette, thus inducing conditional KO, in the first case, or conditional rescue, in the second. Nevertheless, being based on the random integration of the gene-trap cassette, this system does not allow targeted gene disruption.

A possible alternative strategy has been proposed by Bedell et al. (Bedell, Wang et al. 2012), who took advantage of TALEN to insert loxP sites at precise genomic locations. The TALEN approach is suitable for a relatively simple genetic engineering allowing for site-specific DNA targeting. Indeed, TALENs are based on the fusion of a non-specific DNA cutting domain, derived from the FokI nuclease, and a customizable TALE DNA-binding domain. This module consists in series of monomers, each of which specifically binding to one nucleotide, and is responsible for the

precise and specific targeting of selected DNA sequences. The technique proposed by Bedell and colleagues uses single stranded DNA (ssDNA) oligonucleotides as donors for homology directed integration after TALEN-mediated cleavage (Figure 2). A high-efficiency pair of TALEN is injected into one cell-stage embryos together with a ssDNA molecule containing a loxP site. A pair of homology arms, complementary to the genomic regions flanking the TALEN cutting site, are positioned at the 5' and 3' ends of the ssDNA and are responsible for the insertion of the loxP site at the selected locus by homology directed repair. The “knock-in” of these sequences, if targeted to the genomic regions flanking a gene of interest, allows the generation of animals carrying a floxed allele. However, the really low efficiency of homologous recombination during zebrafish embryonic development and the long generation time of transgenic lines carrying floxed alleles represent an important constraint and this approach remain to be implemented *in vivo*.

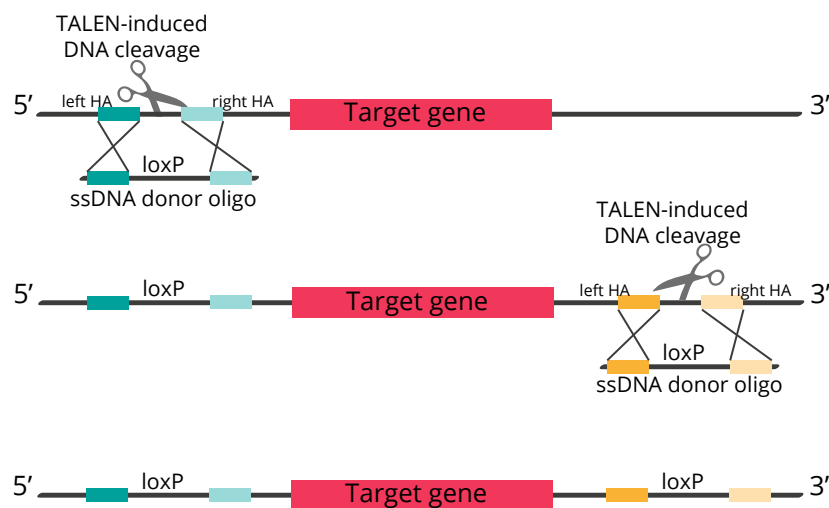


Figure 2

Schematic representation of the TALEN-mediated generation of a floxed allele for Cre-based conditional gene inactivation.

A. A pair of TALENs is used to specifically cut the region at the 5' of the target gene. The simultaneous injection of a ssDNA oligo containing a loxP site flanked by two homology arms (HA) allows the genomic insertion of the loxP sequence by homologous recombination (HR). Injected embryos are raised to adulthood and screened for successful insertions.

B. Fish carrying the loxP site upstream the locus of interest are subsequently injected with a second pair of TALENs directed against the 3' regions of the target gene. HR mediate the insertion of an additional loxP site, allowing the generation of a floxed allele (C) in which the target region is flanked by the two loxP sites. Conditional expression of *cre* would induce targeted gene disruption at the engineered locus.

Similarly, the CRISPR/Cas9 technology has been used for the knock in of loxP sites at desired genomic location in different model organisms (Chang, Sun et al. 2013, Hwang, Fu et al. 2013, Yang, Wang et al. 2013).

Additionally, it is possible to use the CRISPR/Cas9 system to induce tissue-specific knock-out by combining the conditional expression of the Cas9 enzyme with the constitutive expression of sgRNAs (driven by constitutive U6 promoters recognized by type III RNA polymerase). In mouse, conditional expression of the Cas9 enzyme has been possible thanks to the generation of animals carrying a floxed allele in which a *loxP-STOP-loxP* cassette is positioned between a constitutive CAG promoter and the coding sequence of the Cas9. By crossing these animals with tissue specific *cre*-lines, it is possible to achieve Cre-dependent spatiotemporal regulation of Cas9 expression (Platt, Chen et al. 2014). A similar control of Cas9 activity was described in *Drosophila* by Port et al. (Port, Chen et al. 2014). The authors reported the use of the Gal4/upstream activating sequence (UAS) binary system to obtain tissue-specific expression of the Cas9 enzyme. In this strategy, the Cas9 CDS is placed behind a UAS sequence and its transcription depends on the activity of the Gal4 transactivator. If a tissue-specific promoter is used to drive the Gal4 expression it is possible to drive conditional activation of the Cas9 enzyme.

Similar strategies have also been developed in zebrafish. A first report (Ablain, Durand et al. 2015) described a modular vector in which a cell-type specific promoter is used to drive *cas9* expression and a U6 promoter regulates the ubiquitous transcription of a sgRNA targeting a gene of choice. The flexibility of the system relies on the possibility of readily changing both the promoter driving Cas9 expression and the sgRNA sequence targeting a specific ORF (Figure 3).

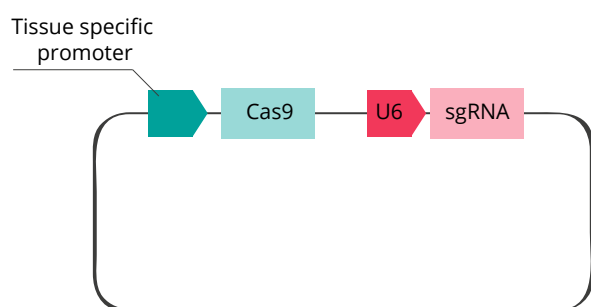


Figure 3

Schematic illustration of the vector system allowing Cas9-based conditional gene inactivation by tissue-specific expression of the *cas9* enzyme and simultaneous ubiquitous expression of the sgRNA.

Yin and colleagues recently developed a method allowing the tight temporal regulation of Cas9 expression (Yin, Jao et al. 2015).

This methodology is based on the generation of two transgenic lines: one carrying a floxed allele (*hsp70:loxP-mCherry-STOP-loxP-cas9*) allowing heat-shock induction of *cas9* expression upon Cre dependent recombination; the other harboring a U6 cassette for the transcription of a sgRNA targeting the gene of interest (*U6:sgRNA*). Therefore, injection of *cre* mRNA into one-cell stage double transgenic embryos and subsequent heat-shock induction would result in a timely controlled *cas9* expression.

Importantly, these last strategies do allow the generation of conditional gene disruption but are not suitable for the direct visualization of the cells carrying KO alleles, an important feature for the direct correlation between genotype and phenotype in LOF studies.

I.I.IV CRISPR/Cas9 and clonal analysis

In the past years, the generation of chimeric animals, in which the fate of clones derived from a mutant progenitor could be followed in a wild type environment, has been obtained by different approaches. To this end, an efficient repertoire of transplantation techniques has been implemented in several model organisms. Indeed, mouse embryonic stem cells, carrying the selected mutation together with an independent genetic marker, can be transplanted into wild type blastocyst, thus generating genetic chimeras (Rossant and Spence 1998). Similarly, transplantation strategies can be performed in *Drosophila* (Technau 1986, Kemp, Carmany-Rampey et al. 2009) or zebrafish (Kemp, Carmany-Rampey et al. 2009) by transferring cells derived from a mutant donor embryo into wild type hosts. Nevertheless, transplantation-based strategies are often technically complicated and can only be used to assess the role of genes active during the earliest phases of embryonic development. The Cre/loxP system has been employed in mouse and *Drosophila* (Zong, Espinosa et al. 2005, Nakazawa, Taniguchi et al. 2012) to develop alternative approaches combining the generation of targeted gene disruption and the activation of a reporter for lineage tracing, but an analogue technique is still challenging in Zebrafish. Most recently, a novel CRISPR-based strategy has been described in mouse. The technique (Chen, Rosiene et al. 2015) is based on the simultaneous in utero electroporation of a CRISPR-based plasmid (inducing gene LOF) together with a Piggybac transposase vector (necessary for the expression of fluorescent reporters for the lineage tracing of the cells carrying loss-of-function mutations) (Chen, Rosiene,

Che, Becker, & LoTurco, 2015).

Aim of the project I

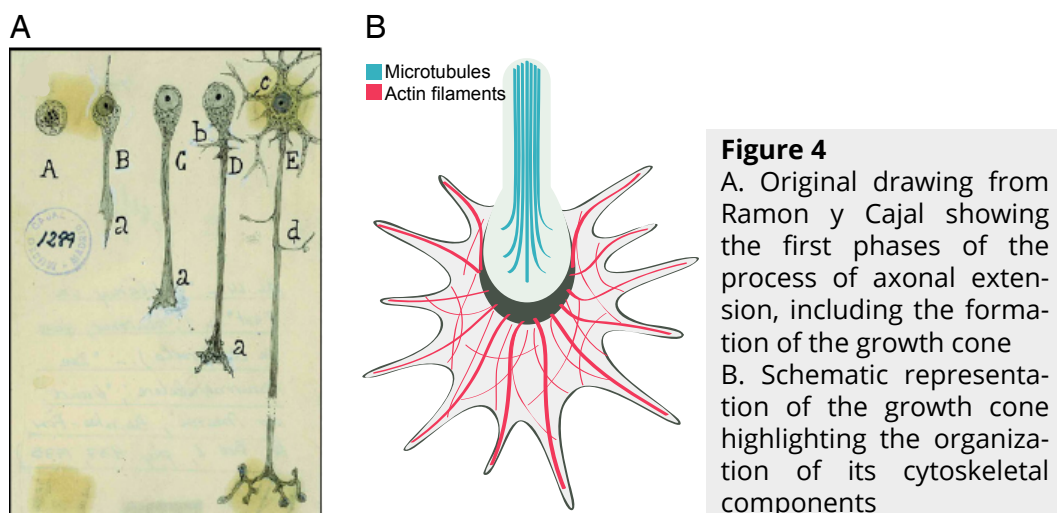
In the past five years, the CRISPR/Cas9 technology has revolutionized reverse genetic approaches in a variety of model organisms including zebrafish. So far genetic manipulation in this model has been limited to the generation of constitutive loss-of-function alleles and the spatiotemporal control of gene inactivation remains challenging. In this study, we explore the possibility to develop a CRISPR/Cas9 and Gal4/UAS-based strategy enabling the analysis of gene inactivation in a cell-type- specific manner. Furthermore, we aim at providing a genetic tool allowing, at the same time, the generation of tissue-specific somatic mutations and the labeling of mutant cell clones or single cells.

I.II Study of the role of the *meteorin* gene family in axon guidance

I.II.I General mechanisms of axon navigation

In the embryonic nervous system, the building of complex neural wiring patterns relies on the ability of newly generated axons to follow precise and well-defined paths towards their correct synaptic partners. Over the past decades, one of the major goals of developmental neurobiology has been the understanding of the molecular mechanisms that guide developing axons along these stereotyped tracks, paving the way for the formation of specific synaptic contacts.

The first neuronal connections are established through a series of guidance events that are directed by a complex network of receptor/ligand interactions occurring between the axons and the surrounding environment. Axonal response to environmental guidance signals is mostly controlled by a highly motile structure located at the distal tips of growing axons: the growth cone, described for the first time a century ago by Ramon y Cajal (Cajal 1890). Axonal growth cones are characterized by an extremely dynamic cytoskeleton and can be divided into a microtubules-enriched central domain and a peripheral domain of Actin-rich filopodia and lamellipodia (Figure 4).



Growth cones express a specific set of guidance receptors that enable developing neurites to sense the extracellular environment and decipher the directions for their correct navigation (Tamariz and Varela-Echavarria

2015). Changes in the environmental signals induce the alternation of the assembling and disassembling of growth cones' cytoskeletal components, thus promoting morphological changes responsible for axonal elongation and navigation. The formation of an axon tract is normally initiated by a single axon, named pioneer axon, whose function is the establishment of the appropriate trajectory that will be subsequently followed by all axons belonging to the same neuronal population (Raper and Mason 2010). The guidelines allowing growth cones to follow the proper neuronal paths are provided by a precisely regulated combination of molecules, forming instructive guidance cues along the axonal navigation tracks. These guidance signals can be both mediated by diffusible factors or regulated by non-diffusible molecules bound to cell membranes or extracellular matrix (ECM). In organisms with bilateral symmetry, a population of specialized glia cells, located at the ventral midline (or floor plate, FP), play an essential role in this process, being the main source of secreted guidance molecules (Kaprielian, Runko et al. 2001). The coordinate action of guidance factors generates four types of guidance cues: short-range or long-range cues, each of which can act as an attractant or a repellent. These cues are not mutually exclusive but act in concert to ensure accurate and reproducible axons elongation along the right track: single neurites might be “pushed” from behind by a long-range repellent, “pulled” from in front by a long-range attractant, and kept in a tight bundle by attractive and repulsive local cues (Figure 5) (Dickson 2002, Kolodkin and Tessier-Lavigne 2011).

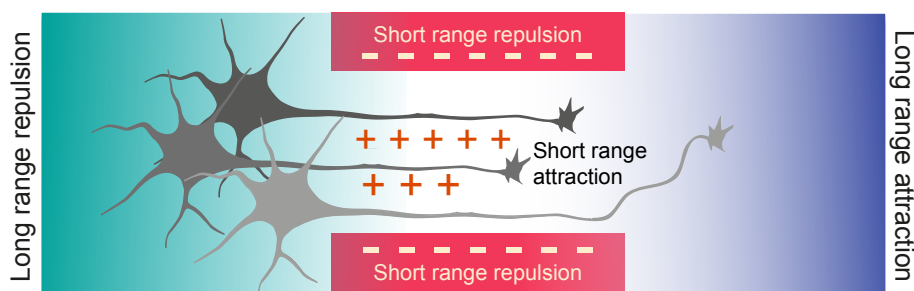


Figure 5

Schematic of the different guidance forces acting on the growth cones of developing axonal projections. Axons move away from a long-range repellent while growing toward a long-range attractant. Short range attractive and repulsive cues maintain the axons in tight bundles.

Axonal navigation is a highly dynamic process: the same molecule might have a bifunctional role (attractive or repulsive), allowing different axons to display different response to the same cue. Additionally, having to navigate over long distances, the same axon might need to change its response to a specific guidance factor along its journey. As a result of this complex but finely regulated process, an intricate pattern of commissural connections (crossing the midline and linking the left and right side of the brain) and longitudinal projections (running parallel to the midline and forming ipsilateral circuits) is established in the mature CNS.

I.II.II Axon guidance factors

Over the past decades, the biological mechanisms regulating axonal pathfinding have been object of intense studies that led to the identification of several conserved families of axon guidance molecules. The role of four major protein families (Netrins, Slits, Semaphorins and Ephrins), often referred to as “canonical axon guidance molecules”, has been extensively dissected and the effect of these proteins on axonal behavior has been broadly characterized (Kolodkin and Tessier-Lavigne 2011). In recent years, morphogens, growth factors and ECM components have also been shown to play a pivotal role in the process, defining an intricate puzzle in which single growth cones will have to integrate multiple and diverse signals in order to make the correct navigation choice. Complex regulatory mechanisms modulate the balance of different guidance cues in the extracellular environment and specific genetic programs allow developing axons to initiate the appropriate response to the combination of guidance signals they are exposed to. The next paragraphs will focus on the description of the best-characterized guidance molecules and on the analysis of their specific contribution to the process of axonal navigation.

Canonical axon guidance factors

Netrins

Over 25 years ago, pioneer studies in *C.elegans* identified UNC-6 (the orthologue of the vertebrate Netrin-1) as the first molecule able to influence axonal navigation (Ishii, Wadsworth et al. 1992). Since its discovery, proteins belonging to the Netrin family have been object of intense studies that unraveled their critical function in several biological

processes including neuronal migration and axon guidance. Netrin-1 is the best characterized member of the family and shows a conserved expression pattern along the midline and in the FP in the vertebrate hindbrain and spinal cord (Kennedy, Serafini et al. 1994, Livesey and Hunt 1997, Hamasaki, Goto et al. 2001). It has been shown that this protein can act both as a chemo-attractant or chemo-repellent, depending on the set of receptors expressed by the targeted neuronal populations. All Netrin receptors belong to the immunoglobulin (Ig) gene superfamily and include deleted in colorectal cancer (DCC), Neogenin (a DCC paralogue), UNC-5(A-D) and Down syndrome cell adhesion molecule (DSCAM). DCC family receptors and DSCAM are the main responsible for Netrin-mediated attraction while UNC-5 receptors are mostly involved in Netrin induced repulsion. In addition, Netrin function can be modulated by Heparan sulphate proteoglycans (HSPGs) and Integrins (Lai Wing Sun, Correia et al. 2011).

The function of Netrins has been extensively analyzed *in vivo*, showing a conserved role in the process of axonal navigation across different species. It has been demonstrated that, in *D. melanogaster*, Netrin is expressed at the midline of the developing CNS and is involved in the guidance of commissural and peripheral motor axons (Mitchell, Doyle et al. 1996). Homozygous mice carrying a *netrin 1* LOF allele die few hours after birth and display a number of neurodevelopmental defects including misrouted axons in the ventral spinal commissure, the corpus callosum and the anterior and hippocampal commissures (Serafini, Colamarino et al. 1996). Closely related phenotypes are observed in *dcc* mutant mice, confirming the role of DCC as main transducer of Netrin-mediated attraction (Fazeli, Dickinson et al. 1997). Based on *in vivo* and *in vitro* evidences, it was proposed that, in the hindbrain and spinal cord, FP-secreted Netrin-1 forms a gradient exerting a long-range attractive force on elongating commissural axons (Kennedy, Serafini et al. 1994, Serafini, Colamarino et al. 1996, Kennedy, Wang et al. 2006). Nevertheless, more recent observations from Varadarajan et al. and Dominici et al. (Dominici, Moreno-Bravo et al. 2017, Varadarajan, Kong et al. 2017) pointed out that the protein produced by the neuronal progenitors located at the midline (and not the one expressed by FP cells) is responsible of the correct navigation of commissural neurons.

Slits

Slit ligands and their main receptors (Robos) have been first discovered

in a genetic screen for genes affecting axonal navigation in *D. melanogaster* (Seeger, Tear et al. 1993, Kidd, Bland et al. 1999) and their role in axonal pathfinding have been confirmed afterward in other species.

In most vertebrates, the *slit* gene family includes three members, *slit1-3*, each of which encodes for a 200 kDa protein (Blockus and Chedotal 2016). Slits are secreted by midline cells and act as long-range repellent on Slit-sensitive growth cones that express the Roundabout (Robo) receptors. The Robo protein family is highly conserved across different species: one Robo orthologue (SAX-3) has been described in *C. elegans*, while the family comprises three members in chick and *Xenopus leavis*, and four in mammals and zebrafish (Kidd, Brose et al. 1998). All Robo receptors have a single transmembrane domain and lack any autocatalytic or enzymatic activity, indicating that their function depends on downstream signaling and scaffolding molecules. Furthermore, Slit/Robo interaction can be stabilized by HSPGs by the establishment of a ternary complex (Hohenester 2008).

In addition to the well documented involvement of Robos, additional receptors might be implicated in the transduction of Slit signaling. Indeed, a putative Slit receptor, *Eva1C*, has been discovered in *C. elegans* (Fujisawa, Wrana et al. 2007) and its expression can be detected in a population of mouse axons responding to Slit (James, Foster et al. 2013). Moreover, a C-terminal Slit fragment displayed the ability to exert a repellent force on pathfinding axons by interacting with the Semaphorin receptor Plexin A1, suggesting a cross-talk between the two pathways (Delloye-Bourgeois, Jacquier et al. 2015). Slit activity can be additionally influenced by homophilic interactions or heterophilic binding with other molecules, including Neurexins, Type IV Collagens (Xiao, Staub et al. 2011), Netrin 1 (Brose, Bland et al. 1999), dystroglycan (Wright, Lyon et al. 2012), Glypican (Liang, Annan et al. 1999) and Syndecan (Johnson, Ghose et al. 2004). Moreover, Robo receptors have the ability to mediate axonal elongation by binding to Slit-unrelated ligands. Indeed, it has been recently demonstrated that Robo3 can be activated by the binding of the Neuronal growth factor-like 2 (Nell2) protein (Jaworski, Tom et al. 2015).

After its first discovery in fly, Slit/Robo capacity of regulating axonal elongation in vivo has been confirmed in mammals. In particular, the role of the pathway in the organization of commissural axons in the hindbrain and spinal cord has been object of intense studies. The spinal cord of triple *slit1/2/3* knockout mice show several misrouted axons stalling at the midline or navigating across the FP multiple times (Long, Sabatier

et al. 2004). Analysis of *robo* mutant mice revealed that Slit function is only partially mediated by Robo proteins, since *robo1* mutants and *robo1/2* double knockout only partially phenocopy the *slit1/2/3* triple mutant mice (Jaworski, Long et al. 2010). It has been observed that all commissural neurons fail to cross the midline in *robo3*^{-/-} mice, suggesting that Robo3 might differ from its two paralogues in the way it regulates axonal navigation (Marillat, Sabatier et al. 2004, Sabatier, Plump et al. 2004). Based on this and other evidences, a first model proposes that, by binding the Robo1 and Robo2 receptors, Slit proteins exert a repulsive force keeping pre-crossing commissures away from the midline. In contrast, their binding to Robo3, whose expression on commissural axons is increased during midline crossing, would counteract this repulsion, thus allowing axonal navigation across the FP (Sabatier, Plump et al. 2004). Interestingly, Zelina et al. recently proposed that the mammalian Robo3 underwent a process of divergent evolution causing the loss of the Slit-binding ability in favor of a novel and direct interaction with the Netrin/DCC signaling pathway (Zelina, Blockus et al. 2014). Thus, the mammalian Robo3 would support Netrin-mediated attraction instead of counterbalance Slit-induced repulsion. How the protein works in other vertebrates is still poorly understood.

Finally, Slit/Robo signaling is additionally involved in the navigation of longitudinal tracts as aberrant trajectories and severe defasciculation are observed if this pathway is disrupted (Farmer, Altick et al. 2008).

Semaphorins

The Semaphorin family is composed by approximately 20 proteins and includes both secreted and membrane-bound molecules. A distinctive semaphorin (sema) domain (of about 500 amino acids) is detectable in each member of the family and is responsible for the protein homo-dimerization and for the interaction with Semaphorin receptors (Yazdani and Terman 2006). The best characterized class of Semaphorin receptors is a family of single-pass transmembrane proteins named Plexins. Nine Plexins exist in vertebrates (Plexins A1-A4, B1-B3, C1, D1) while two orthologues have been identified in invertebrates (PlexA and PlexB) (Tamagnone and Comoglio 2000). Even if most Semaphorins can bind Plexins directly, other molecules, including the transmembrane proteins Neuropilins (Nrp), can modulate their ligand/receptor binding (Tran, Kolodkin et al. 2007). *In vivo* studies have shown that Semaphorins exert a strong repellent action on axonal projections, providing a local repulsion responsible for the proper

fasciculation of many peripheral nerves. Indeed, in mouse, the secretion of Semaphorin3A in the environment surrounding motor and sensory axons defines a permissive corridor in which the developing projections can grow as a compact bundle and the disruption of the *sema3A* gene results in a severe defasciculation of several peripheral tracts (Kitsukawa, Shimizu et al. 1997).

Ephrins

Ephrin proteins are expressed on the surface of neuronal projections and can be divided into two subfamilies (class A and B) depending on the way they are attached to the cell membrane. The first group of ephrins includes Glycosylphosphatidylinositol (GPI)-anchored proteins while the second is composed by transmembrane molecules (Klein 2004). Ephrin signals are transduced by Eph receptors, a class of tyrosine kinases distinguishable in two groups (A or B) depending on the type of Ephrins they preferentially interact with. It has been demonstrated that Ephrin can only act as short-range cues, as they are not functional if released from the cell membrane (Kullander and Klein 2002). Visual system development is, perhaps, the process where the function of Ephrins has been studied most intensively. Several reports have shown that this class of guidance molecules is essential for the correct pattern of connectivity between the axons of retinal ganglion cells (RGCs), the sole output neurons of the retina, and their target cells in the appropriate portion of brain retinorecipient nuclei, namely the optic tectum in lower vertebrates and the lateral geniculate nucleus of the thalamus in higher vertebrates (Feldheim and O'Leary 2010). Overall, Ephrins role in the establishment of the so-called retinotopic maps display a high degree of flexibility, as the same molecules can attract a specific set of axons while repelling some others (McLaughlin and O'Leary 2005).

Non-canonical guidance molecules: Morphogens, growth factors and ECM molecules

During early embryogenesis, secreted morphogenic factors coordinate cell proliferation and fate-specification. Moreover, growing evidences suggest that, at later stages, members of the Sonic hedgehog (Shh), Wnt and Transforming growth factorB/Bones morphogenetic protein (TGFB/Bmp) family are involved in the process of axon guidance, behaving as attractive or repulsive cues for different classes of neurons. In the spinal cord, Shh is secreted by FP cells and is able to attract commissural axons

(Charron, Stein et al. 2003) while it acts as a repellent on RGCs (Trousse, Marti et al. 2001). Wnt proteins have been shown to push axons away from the posterior commissure in *D. melanogaster* (Yoshikawa, McKinnon et al. 2003) and to form an attractive cue guiding post-crossing motor axons in the anterior direction in mammals (Lyuksyutova, Lu et al. 2003, Yoshikawa, McKinnon et al. 2003). BMPs form a repellent cue pushing spinal cord axons along the dorso-ventral axis (Yamauchi, Phan et al. 2008).

Growth factors represent another class of molecules involved in axonal pathfinding. It seems that these factors have really specialized functions, acting only on a subset of responsive neurons, mostly as attractive cues. It has been shown that Hepatocyte growth factor (HGF) (Ebens, Brose et al. 1996), Fibroblast growth factors (FGFs) (Shirasaki, Lewcock et al. 2006) and Glial cell-derived neurotrophic factor (GDNF) (Kramer, Knott et al. 2006) are able to instruct a subsets of motor axons, while sensory axons are sensitive to Neurotrophins (Rochlin, O'Connor et al. 2000) and thalamocortical axons respond to Neuregulins (Lopez-Bendito, Cautinat et al. 2006).

ECM components (including Laminin, Fibronectin, Collagen, Tenascin and HSPGs) can also influence axonal navigation by regulating cell motility and axon elongation through the interaction with neuronal Integrins. Additionally, forming stable complexes with many secreted axon guidance factors, ECM molecules can directly modulate their signaling thus influencing axonal outgrowth (Holt and Dickson 2005, Myers, Santiago-Medina et al. 2011).

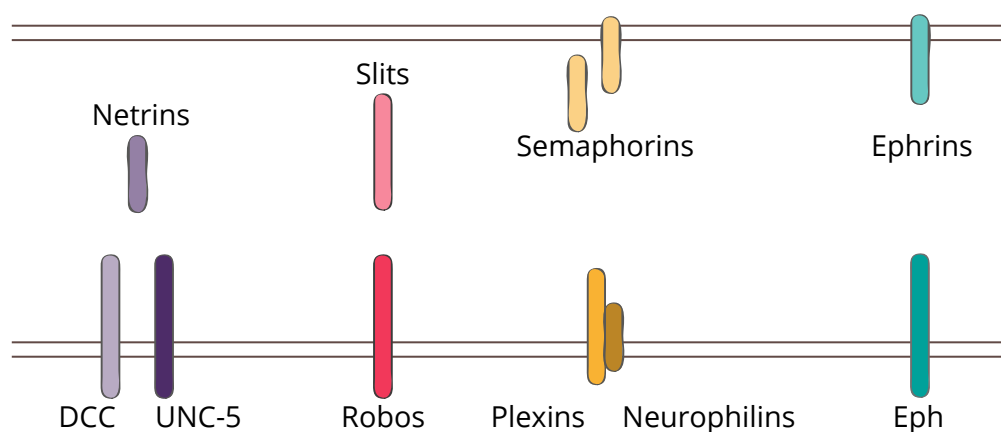


Figure 6 Families of canonical axon guidance molecules and their ligand/receptor interactions (Netrin/DCC and Netrin/UNC-5; Slits/Robos; Semaphorins/Plexins-Neurophilins; Ephrins/Eph receptors).

I.II.III The role of the midline in axon guidance

According to the most accepted current model, growing axons rarely respond to a single guidance molecule but need to integrate multiple and simultaneous directional information while moving along their path. Before reaching their synaptic partners, axons often require to cover long distances and have to frequently modify their response to a multitude of environmental cues to be able to switch direction and keep a correct trajectory. To simplify this complicated task, in most cases axonal navigation routes are subdivided into shorter segments, each of which ends with an "intermediate target" or "choice point" directing axonal behavior *in vivo*. In the CNS of bilaterally symmetrical organisms, the midline represents perhaps the most important one, and surely the best-characterized, of these choice points for pathfinding axons. Cells that lie at the midline provide both long and short-range cues directing the navigation choices of both longitudinal and commissural axons (Tear 1999, Kaprielian, Runko et al. 2001, Mastick, Farmer et al. 2010).

The importance of the midline and, more specifically, its most ventral region (the FP), has been revealed thanks to the study of model organisms in which this structure was depleted or failed to correctly differentiate (Thomas, Crews et al. 1988, Yamada, Placzek et al. 1991, Klambt, Jacobs et al. 1991, Bovolenta and Dodd 199, Matise, Lustig et al. 1999). In *D. melanogaster*, mutations in the *single-minded (sim)* gene abrogates the specification of midline cells and, as a consequence, induces several guidance defects including the failure of the formation of commissural tracts and the collapse of longitudinal bundles (Thomas, Crews et al. 1988). Differently, in *slit* mutants, midline cells differentiate correctly but appear displaced ventrally. As a result, commissural tracts initially form but, due to the mis-positioning of midline cells, longitudinal tracts fuse and collapse onto the midline (Klambt, Jacobs et al. 1991). Related phenotypes can be also observed in vertebrate models. In chick embryos, the ablation of the notochord prevents the formation of the FP, thus inducing turning mistakes in commissural axons (Yamada, Placzek et al. 1991). Similarly, in the *Danforth's short-tail (sd)* mouse mutant, missing both the FP and the underlying notochord, commissural axons in the spinal cord undertake aberrant trajectories. Guided by a number of midline-secreted factors, in wild type animals, commissural axons in the spinal cord first elongate toward the FP in the dorso-ventral direction, subsequently navigate across the ventral midline and finally turn in the

rostral directions (Figure 7A). In contrast, in *sd* mouse mutants, axons are able to reach the FP but display crossing defects or make mistakes in the following turning in the anterior direction (Bovolenta and Dodd 1991) (Figure 7B). Commissural axons behave in a similar fashion in *Gli Family Zinc Finger 2* (*gli2*) mutants, missing the FP due to the disruption of the CDS of the *gli2* transcription factor involved in the regulation of Shh signaling (Matise, Lustig et al. 1999). In the same mutants, longitudinal axonal trajectories are also affected, with the presence of multiple axons crossing the midline, turning on the wrong anterior/posterior direction and being severely defasciculated (Farmer, Altick et al. 2008) (Figure 7C,D).

Interestingly, recent reports suggest that the FP is not the only regulator of midline axon guidance but other cells lying at the midline (such as neuronal progenitor cells) might contribute to the process by secreting instructive guidance molecules (Dominici, Moreno-Bravo et al. 2017, Varadarajan, Kong et al. 2017).

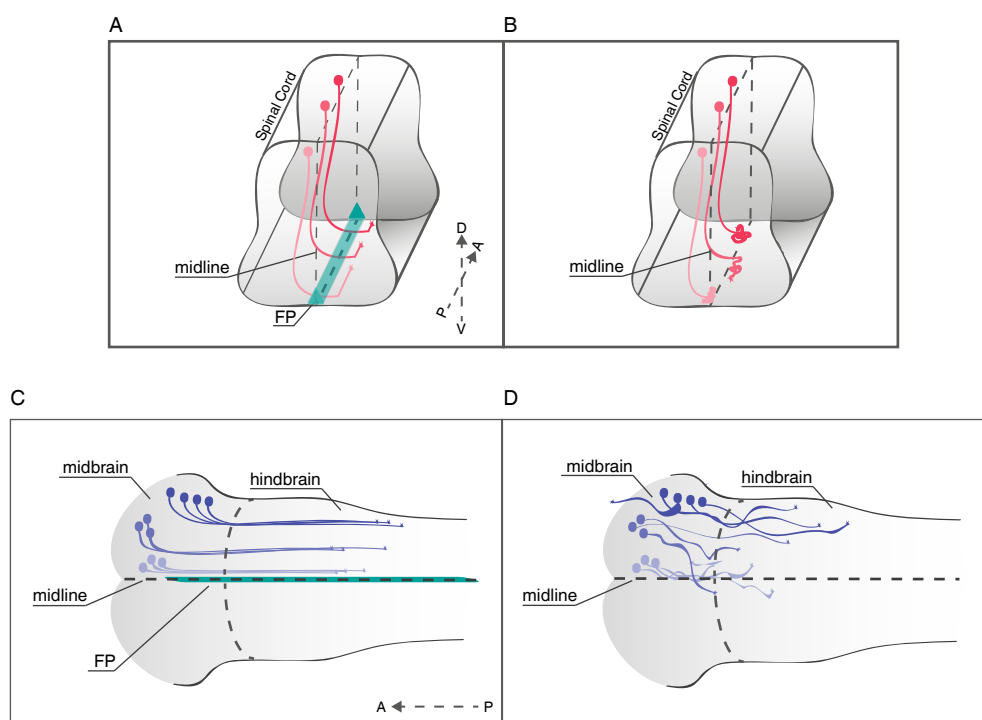


Figure 7

A. Schematic illustration of pathfinding axons in the mouse spinal cord. Neurons begin to extend their axons ventrally to reach the FP. Commissural axons navigate across the midline and turn in the anterior direction once they are in the contralateral side.

B. In the *Danforth's short-tail* (*sd*) and *gli2* mouse mutants the FP fail to correctly differentiate. As a result, commissural axons in the spinal cord are able to reach the ventral midline but fail to reach the contralateral side

C. Representation of longitudinal tracts in the hindbrain of mouse embryos. Axons form tight bundles and grow parallel to the midline

D. Misrouted and defasciculated axons in the hindbrain of *gli2* mutants

I.II.IV Open questions in the field

Although many guidance molecules have been discovered and their instructive role on axonal navigation has been broadly analyzed in the past years, an exhaustive understanding of how the exceptionally diverse repertoire of guidance factors influences axonal behavior is still missing.

It is still unclear whether other major families of guidance cues need to be identified and if additional factors might have more specialized functions in directing the navigation of specific set of responsive axons. Indeed, to explain how the exceptionally complex network of neuronal connections is established during embryogenesis, we would need to unravel the signaling pathways allowing any subpopulation of axons to react to a constantly changing extracellular environment and navigate towards their proper synaptic partners. Due to the high redundancy of biological systems, it is possible that guidance molecules with highly specific functions still need to be added to the collection of axon guidance factors.

Additionally, we still lack the complete mechanistic insight of the regulatory processes by which axonal growth cones are able to modulate their response to a particular cue, switching from an attractive to a repulsive behavior at precise positions of their navigation paths. This response might be regulated at different levels by transcriptional, translational, and post-translational mechanisms, ensuring a finely controlled expression and function of the correct combination of guidance receptors and co-receptors on each growth cone. At every choice point, a change in the transcriptional program active in the neuron might be responsible for the re-shuffling of the pattern of receptors expressed at the surface of each growing axon. To date, little is known about the transcription factors regulating the expression of guidance receptors and how signaling from environmental guidance cues might change neuronal gene expression profiles. The control of axonal response to guidance signals also involves the alternative splicing of mRNA encoding for guidance receptors (ensuring the possibility for the same locus to control different axonal behaviors) and the regulation of mRNA stability. Additionally, protein synthesis, maturation, proteolytic modification, trafficking and turn-over might strongly influence guidance decisions, thus adding a further level of complexity to the process of axonal navigation. In recent years, some of the above-mentioned mechanisms regulating the expression and function of guidance molecules have been unraveled and reviewed (Bashaw and

Klein 2010, Nawabi and Castellani 2011, Stoeckli 2017).

Importantly, the mechanisms ensuring the proper integration of the multitude of signals present in the extracellular environment are still poorly characterized and it is still unclear how different pathways interact with each other to ensure proper axonal navigation (Dudanova and Klein 2013). Taken together, these observations suggest that a deeper understanding of the mechanisms underlying axonal pathfinding and, more in general, neural circuit formation, would require the identification of additional factors acting as guidance molecules, involved in the regulation of known guidance signals or responsible for the cross-talk between different cues.

I.II.V Meteorin proteins: novel players in axonal guidance?

Meteorin proteins belong to a family of midline-secreted proteins that is conserved among vertebrates, whose biological function during neuronal development is still poorly described. This family includes two members in mammals (Meteorin, *Metrn* and Meteorin-like, *Metrn1*), while it counts three proteins in Zebrafish (*Metrn*, *Metrn11* and *Metrn12*).

Metrn was first discovered as a secreted neurotrophic factor having the ability to promote axonal extension in dorsal root ganglion (DRG) explants and to induce glial cells differentiation *in vitro* (Nishino, Yamashita et al. 2004). In mouse embryos, *metrn* is highly expressed in the central and peripheral nervous system, mostly by neural and glial progenitors and in cells belonging to the astrocyte lineage. Immunohistochemistry experiments on adult mouse brain detected high Meteorin expression in Bergmann glia and in distinct neuronal populations in the *superior colliculus*, the ocular motor nucleus, the raphe and pontine nuclei, and in various thalamic nuclei. Low level of protein could also be found in ubiquitously distributed astrocytes (Jorgensen, Thompson et al. 2009). It has been shown that embryonic *metrn* is expressed by perivascular astrocytes and regulates angiogenesis at the gliovascular interface (Park, Lee et al. 2008). Importantly, a more recent study, demonstrated that *metrn* LOF is lethal due to defects in mesoderm development (Kim, Moon et al. 2014). In adult mice, it has been shown that *Metrn* exert a neuroprotective function (Jorgensen, Emerich et al. 2011, Tornøe, Torp et al. 2012) and has the capability of driving gliogenesis as well as inducing neural progenitor proliferation after CNS injury (Wang, Andrade et al. 2012, Wright, Ermine

et al. 2016). *Metrn* is an orphan ligand, nevertheless it seems that the JAK/STAT and MEK/ERK pathways are key mediators of its biological activity (Nishino, Yamashita et al. 2004, Lee, Han et al. 2010).

Metrn1 (also known as Cometin or Subfatin) was identified shortly after *Metrn* as a downstream target of Pax2/5/8 signaling during otic vesicle development (Ramialison, Bajoghli et al. 2008). During mouse embryogenesis, *metrn1* expression can be detected in FP cells starting from embryonic day E9.5. Later, beginning from E13.5, the transcript is also present in DRGs and in the inner ear (Zheng, Li et al. 2016). Similar to *Metrn*, *Metrn1* displays an axogenic activity, being able to induce outgrowth of DRG neurites via a Jak/STAT3 and MEK/ERK-dependent mechanism (Jorgensen, Fransson et al. 2012). Additionally, *metrn1* knockdown in PC12 cells also affects axonal elongation by inhibiting NGF-induced neurite extension (Watanabe, Akimoto et al. 2012).

In adult animals *metrn1* strongest expression is located in subcutaneous white adipose tissue and, a recent study, demonstrated that *Metrn1* mediates muscle-fat crosstalk promoting the browning of the white adipose tissue (Rao, Long et al. 2014). The same function has been also described for a C-terminal proteolytic fragment of Slit2 (Slit2-C) (Svensson, Long et al. 2016), suggesting that the two proteins might be involved in related pathways.

Due to their interesting expression patterns in the developing CNS, their capacity of promoting axon elongation, *in vitro*, and considering the similar role of *Metrn1* and Slit2-C in the adipose tissue, we reasoned that *Metrn* family members could represent novel potential players in the process of axonal pathfinding.

I.II.VI Zebrafish and axon guidance research

Due to the relatively simple and highly stereotyped organization of their nervous system, the zebrafish has been extensively studied to assess the mechanisms regulating the establishment and function of neural circuits. In this context, the process of axonal pathfinding has been intensely investigated and it has been demonstrated that it is coordinated by the same set of molecules driving axonal elongation in mammals. The next paragraphs will describe how diverse guidance factors direct the formation of different embryonic axonal tracts, pointing out the

importance for a developing axon to integrate multiple and simultaneous cues for making the correct choice. The attention will be focused on the navigation paths that have served more often as a model to understand the conserved mechanisms driving axonal elongation. Nevertheless, the molecules listed are obviously able to influence the growth of other axons that will not be mentioned here.

I.II.VII Axon guidance mechanisms in zebrafish

Development of the first commissural tracts: the AC/POC

By one day post fertilization (dpf), a bilaterally symmetrical axonal scaffold is established in the embryonic zebrafish. This stereotyped structure is composed by both commissural and longitudinal tracts and will serve as a template for the subsequent development and refinement of the embryonic nervous system. In the most rostral region of the developing forebrain, two big commissures originate from two neuronal nuclei: the dorsal rostral cluster (DRC) and the ventro rostral cluster (VRC). At 24 hours post fertilization (hpf) a bundle of axons connects the left and right VRCs, forming the post-optic commissure (POC). In addition to commissural axons, the VRC projects a longitudinal tract that grows caudally (the tract of the post optic commissure, TPOC). Shortly after the POC is established, a second commissure (the anterior commissure, AC) is formed between the two DRCs. A distinct group of axons originates from the DRC and navigates in the dorso-ventral direction toward the VRC, thus forming the supra-optic tract (SOT). Once they reach the VRC, neurites from the SOT can turn caudally and be included in the TPOC, or can grow rostral, joining the VRC axons in the POC (Hjorth and Key 2002) (Figure 8).

It has been demonstrated that axonal navigation along the AC and POC is directed by a complex set of guidance factors. Indeed, if the expression of single or multiple guidance molecules is lost or altered, the formation of the two commissures results severely affected (Macdonald, Scholes et al. 1997, Shanmugalingam, Houart et al. 2000, Wolman, Liu et al. 2004, Barresi, Hutson et al. 2005, Gaudin, Hofmeister et al. 2012, Zhang, Gao et al. 2012).

In the *noi* mutant (lacking the Pax2 transcription factor), axons of the POC display several pathfinding defects: although their ability of crossing

the midline is not fully abolished, they look less fasciculated than in wild type animals and, in some cases, they undertake aberrant and ectopic trajectories. Interestingly, in *noi* mutant fish, the guidance molecules *netrin-1* and *shh* are mis-expressed, suggesting that neurons elongating along the POC are sensitive to the guidance cues provided by these factors (Macdonald, Scholes et al. 1997). Similarly, disrupted AC and POC can be observed in the *ace* mutant, in which LOF of *fgf8* causes severe defects in midline cells differentiation. In *ace* mutant embryos, axons from the two commissures appear strongly defasciculated and often extend misrouted projections on the lateral side of the midline. The analysis of the gene expression profiles of different guidance factors reveals that, like in the *noi* mutant, the expression of a number of instructive molecules including *netrin 1* and *2* and *semaphorin 3D* is downregulated in *ace* mutant larvae, supporting the hypothesis that commissural axons of the AC and POC respond to canonical guidance signals (Shanmugalingam, Houart et al. 2000). Interestingly, in both *noi* and *ace* mutants, the two main commissures fail to correctly elongate their axons because of the inappropriate differentiation of the midline glial cells regulating the balance between different guidance factors.

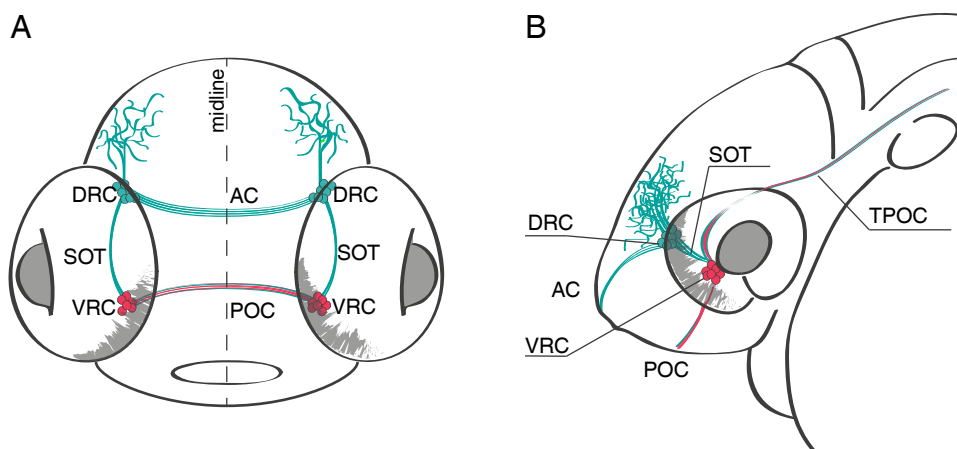


Figure 8

Frontal (A) and lateral (B) representations of the more rostral portion of the scaffold of axon tracts established in the embryonic zebrafish brain at 24 hpf. Neurons of the dorso-rostral cluster (DRC, green) extend axons to form the supra-optic tract (SOT) and the anterior commissure (AC). Axons from neurons of the ventro-rostral cluster (VRC, pink) form the tract of the post-optic commissure (TPOC) and the post-optic commissure (POC).

Barresi et al. (Barresi, Hutson et al. 2005) suggested that the AC and POC require the Slit signaling for the establishment of their right

projection pattern. They proposed a model in which the navigation path of the two commissures is built on a glial bridge, composed by *GFAP* and *slit1a* expressing cells, forming a permissive corridor that allows axons to elongate along the right route. Differently from their third paralog, *silt2* and *slit3* are highly expressed in the region spanning the two commissures, suggesting that they exert a repulsive force keeping the axonal bundles highly fasciculated, thus avoiding abnormal branching in the dorso-ventral direction.

Additional evidences supporting the role of the Slit/Robo and Netrin/DCC pathways in establishing the early axonal scaffold of the embryonic brain came from the analysis of knockdown animals (Gaudin, Hofmeister et al. 2012, Zhang, Gao et al. 2012). In particular, Gaudin et al. demonstrated that the injection of morpholino antisense oligonucleotides targeting *netrin 1a*, *netrin 1b*, *slit 1a* or *dcc* results in defects in the formation of the AC and they surprisingly observed that the targeted disruption of *netrins* and *dcc* expression induces the growth of an aberrant axon tract in the dorsal telencephalon (Gaudin, Hofmeister et al. 2012). Differently, *slit2/3* or *robo* down-regulation did not affect the formation of the AC but, had an impact of the establishment of the SOT. In morpholino-injected embryos, this axonal tract resulted strongly impaired, being severely reduced or absent in most injected fish. Increased *slit2* expression has been observed in the forebrain region of embryos in which the expression of the Wnt receptor *frizzled-3a* was reduced (Hofmeister, Devine et al. 2012). In these fish, defects in the Wnt signaling pathway cause the expansion of the *slit2* repellent domain, thus impeding DRC neurons to elongate their axons across the midline. Furthermore, additional families of guidance factors seem to be involved in the process. In particular, Semaphorins demonstrated to play a pivotal role, as the knockdown of *semaphorin 3D*, *neuropilin 1A* or *neuropilin 2B* also results in defects in AC formation (Wolman, Liu et al. 2004).

Overall, these observations suggest that, during early embryogenesis, a complex pattern of guidance factors is needed for the axons to make their appropriate navigation choices and that midline glial cells play a pivotal role in maintaining and regulating such a balanced combination of molecules.

The retino-tectal system

In a large number of studies, the zebrafish visual system has been used as a valuable model for the investigation of the mechanisms regulating

axonal pathfinding. This structure is composed by two main areas: the retina, sensitive to light stimuli and responsible for the transmission of the visual information through the RGCs, and the optic tectum, the main midbrain target region, homologous to the mammalian *superior colliculus*, responsible for the integration of the visual inputs. After exiting each eye, RGC axons form a dense axonal bundle, the optic nerve, which navigates in the ventral diencephalon toward the midline, where axons from the two sides meet and form the optic chiasm. Importantly, differently from mammalian vertebrates, the zebrafish have entirely crossed retino-tectal projections. Once they leave the midline, retinal axons form the optic tract and grow in the dorso-caudal direction, thus reaching the contralateral lobe of the optic tectum. Here, single neurites terminate their journey in an extremely organized manner, establishing stereotyped retinotopic maps that reflect the position of their cell bodies in the retina (Stuermer 1988, Burrill and Easter 1994, Baier, Klostermann et al. 1996). Additionally, RGC projections are organized in a finely regulated laminar structure, with single axons innervating single synaptic laminae in the tectal neuropil (Robles, Filosa et al. 2013) (Figure 9).

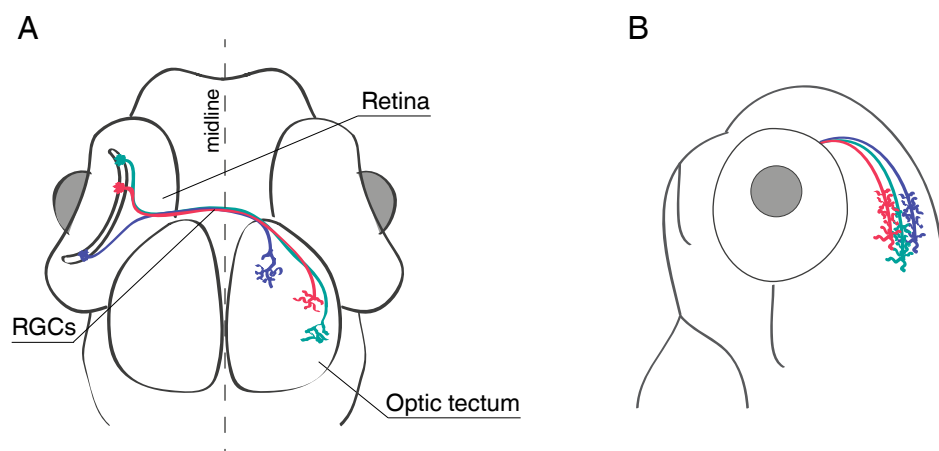


Figure 9

Schematic of the zebrafish retinotectal system. (A) Frontal view showing RGCs axons connecting the retina to the contralateral lobe of the optic tectum. (B) Lateral view showing the laminar organization of RGCs axons in the tectal neuropile.

Thanks to a forward genetic approach it has been possible to perform large-scale screens of mutations affecting the patterning of the retino-tectal projections, uncovering many factors responsible for the correct navigation of RGCs (Karlstrom, Trowe et al. 1997, Hutson and Chien 2002). Defects in axonal elongation could be detected at different point

of the axonal path. Indeed, it has been reported that RGC axons can take aberrant paths while exiting the eye, during the navigation from the eye to the midline, in the process of midline crossing, in the route between the midline and the contralateral tectum, in the establishment of the retinotopic maps or in the organization of their synaptic lamination (Baier, Klostermann et al. 1996, Karlstrom, Trowe et al. 1996, Trowe, Klostermann et al. 1996). Importantly, genes affecting midline differentiation as well as canonical guidance molecules and ECM components have been shown to affect retinal axons navigation, suggesting that the integration of multiple and diverse signals is required for building appropriate retino-tectal trajectories (representative mutants showing RGCs guidance mistakes are listed in Table 1).

Table 1.

Mutant	Gene	RGC pathfinding defects	Reference
<i>Acerebellar (ace)</i>	<i>fgf8</i>	Midline crossing/ Pathfinding to the tectum/ Topography	(Shanmugalingam, Houart et al. 2000)
<i>Astray (ast)</i>	<i>robo2</i>	Midline crossing/ Pathfinding to the tectum	(Hutson and Chien 2002)
<i>Bashful (bal)</i>	<i>lamininα4</i>	Retinal exit/ Midline crossing/ Pathfinding to the tectum	(Paulus and Halloran 2006)
<i>Belladonna (bel)</i>	<i>Lim homeobox gene lhx2</i>	Midline crossing	(Seth, Culverwell et al. 2006)
<i>Boxer (box)</i>	<i>Exostosin extl3</i>	Tract sorting	(Lee, von der Hardt et al. 2004)
<i>Chameleon (con)</i>	<i>dispatched 1 (disp1)</i>	Retinal exit/ Midline crossing	(Karlstrom, Trowe et al. 1996, Nakano, Kim et al. 2004)
<i>Dackerl (Dak)</i>	<i>ext2</i>	Tract sorting	(Lee, von der Hardt et al. 2004)
<i>No isthmus (noi)</i>	<i>pax2.1</i>	Midline crossing/ Pathfinding to the tectum	(Macdonald, Scholes et al. 1997)
<i>Sonic you (syu)</i>	<i>shh</i>	Retinal exit/ Midline crossing	(Schauerte, van Eeden et al. 1998)
<i>You-too (yot)</i>	<i>gli2</i>	Retinal exit/ Midline crossing/ Pathfinding to the tectum	(Karlstrom, Talbot et al. 1999)

Among the canonical guidance molecules, the role of the Slit/Robo in the regulation of RGCs axonal pathfinding is perhaps the best characterized.

In *astray/robo2* mutant zebrafish larvae, RGCs display a high number of misrouted axons projecting to the ipsilateral tectum or to several

ectopic extra-tectal targets (Fricke, Lee et al. 2001, Hutson and Chien 2002). According to the current model, Robo2-expressing RGCs are sensitive to the repellent action of the guidance molecules Slit2 and Slit3, expressed along their axonal navigation path. If the expression of the receptor is abolished, RGC axons lose the ability to respond to Slit signaling, thus taking aberrant trajectories instead of navigating toward the contra-lateral tectum. Importantly, if Robo2 function is missing, the laminar segregation of RGC neurites in the tectal neuropil is also impaired, suggesting that Slit/Robo are involved in multiple aspects of RGCs elongation (Xiao, Staub et al. 2011). Similar defects could be detected in *dragnet* mutant embryos, missing the ECM component Collagen 4 α 5 (Col4 α 5), or in case of knockdown of the secreted guidance factor Slit1. Xiao et al. demonstrated a direct interaction between Slit1 and Col4 α 5 proposing a model in which a superficial-to-deep gradient of Slit1 is maintained in the tectal neuropil by the interaction between Slit1 and Col4 α 5 at the basement membrane and is responsible for the correct lamination of RGCs axons.

Commissural and longitudinal tracts in the hindbrain

The vertebrate hindbrain is composed by an arrangement of sensory-motor networks responsible for controlling essential functions like vision, respiration, mastication, and locomotion (Garcia-Campmany, Stam et al. 2010). The embryonic zebrafish hindbrain is characterized by a distinctive morphological organization consisting in a series of eight segments named rhombomeres (Moens and Prince 2002). The first neurons emerging in this brain region are two large reticulospinal neurons: the Mauthner cells. The cell bodies of these neurons are symmetrically located in the center of the 4th rhombomere and, starting from 21-23 hpf, they begin to extend an axon that, after crossing the midline, turns in the caudal direction pioneering the hindbrain medial longitudinal fascicle (MLF). Later on, axons from other reticulo-spinal neurons, whose soma are stereotypically placed in the hindbrain rhombomeres, will join the ipsilateral or contralateral MLF, thus forming a pair of thick axonal bundles positioned parallel to the FP. A second pair of tracts, the lateral longitudinal fascicles (LLFs), originates from the trigeminal sensory neurons and grows caudally (Hjorth and Key 2002) (Figure 10).

In the past decades, several experimental evidences demonstrated that the FP has an essential function in patterning the axonal projections of zebrafish hindbrain neurons, confirming that defects in FP specification and maturation result in several guidance mistakes. In the *cyclops* (*cyc*)

fish, carrying a LOF allele for a *nodal related protein (ndr2)* (Sampath, Rubinstein et al. 1998), the population of glial cells composing the FP fails to differentiate and mutant embryos display a number of misrouted axons in different brain regions, including the hindbrain (Hatta 1992). Instead of forming a bilateral set of axonal tracts, in most *cyc* embryos the two MLFs fuse in a single bundle at the ventral midline. Importantly, in the same mutant fish line, the LLFs elongate along the correct paths, suggesting that these neurons are not sensitive to FP secreted guidance molecules but might respond to environmental cues generated by other sources. Selective labeling of the Mauthner neurons in *cyc* embryos revealed that, in most cases, after correctly joining the contralateral MLF, their axons do not maintain a parallel course but re-cross the midline multiple times, supporting the idea that the FP represents a repellent barrier for post-crossing Mauthner axons.

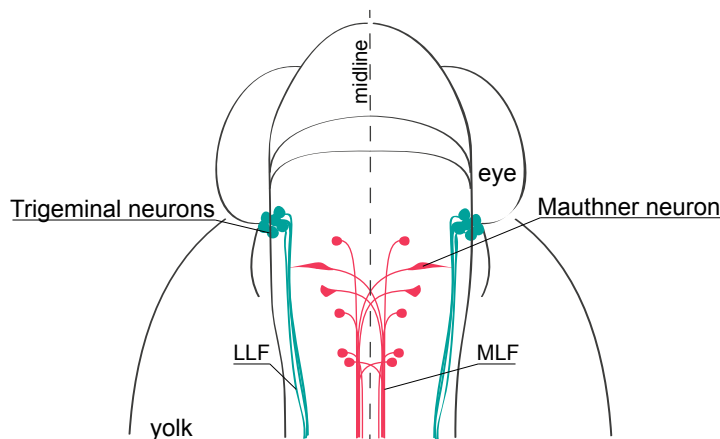


Figure 10

Dorsal view of the zebrafish hindbrain at 24 hpf. Mauthner neurons axons navigate across the midline and grow caudally pioneering the medial longitudinal fasciculus (MLF). Axons from other reticulospinal neurons (pink) join the ipsilateral or contralateral MLF shortly after. A second axonal tract, the lateral longitudinal fasciculus (LLF), originate from the trigeminal sensory neurons (green).

Several experimental observations revealed that canonical guidance molecules are involved in the regulation of axonal behavior in the embryonic hindbrain. Among these, the Slit/Robo pathway is essential for the navigation of several commissural hindbrain neurons, including the Mauthner cells. Indeed, in *twitch twice (robo3)* mutants, hindbrain commissures are highly disorganized and defasciculated (Burgess, Johnson et al. 2009). In these mutant fish, Mauthner axons frequently fail to cross the midline, projecting to the ipsilateral spinal cord instead of

navigating across the FP before turning caudally.

Similarly, if the Robo ligand *slit2* is overexpressed, comparable defects in hindbrain axons fasciculation and Mauthner cells navigation can be observed (Yeo, Miyashita et al. 2004).

Semaphorins are also part of the guidance cues defining the trajectories of hindbrain projections, as *sema3D* or *nrp-1A* knockdown results in the formation of a highly disorganized MLF. Axons from this tract appears severely defasciculated or misrouted, extending in the rostral direction instead of moving on a descending path (Wolman, Liu et al. 2004).

Additionally, it has been demonstrated that activation of the Netrin pathway is required to modulate axonal pathfinding of several commissural hindbrain neurons (Jain, Bell et al. 2014). In zebrafish *spaced out (spo)* fish, a mutation in the *dcc* gene leads to a single amino acid substitution that disrupts the Netrin binding site, making the axons insensitive to Netrin signaling. As a result, a number of commissural hindbrain neurons misproject their axons, often developing ectopic ipsilateral neurites.

Aim of the project II

In the past years, intense studies in the field of axon guidance contributed to the identification of the main molecular players orchestrating axonal navigation choices. Nevertheless, a growing number of observations suggest that the plethora of factors controlling axonal pathfinding is more diverse than initially envisaged and propose that growth cones might be sensitive to additional midline-secreted proteins that are still uncharacterized.

With the objective of uncovering novel molecules able to influence axonal behavior, we explored the possibility that the Meteorin protein family plays a role during embryonic brain development. In particular, we focused our attention on the analysis of the putative function of these proteins in the fine organization of axonal projections, taking advantage of the zebrafish embryonic CNS to investigate how Meteorin proteins influence axonal navigation in different brain regions.

By doing so, we meant to contribute to the understanding of the biological mechanisms driving and maintaining developing axons on their correct trajectory and, more generally, to the investigation of the biological processes regulating neural circuits formation.

CHAPTER II: RESULTS

Summary

In recent years the CRISPR/Cas9 technology has dramatically improved the efficiency and specificity of targeted gene inactivation. To date, in zebrafish, this method allows for the generation of constitutive LOF alleles but has not been optimized to induce tissue-specific gene disruption. In this report, we take advantage of different genetic tools to provide a novel strategy enabling simultaneous conditional gene KO and labeling of the potentially mutant *cas9*-expressing cells.

Results:

We generated a plasmid to drive the transcription of the *cas9* endonuclease and a fluorescent reporter via Gal4/UAS while constitutively expressing two sgRNA targeting a gene of interest

We demonstrated that this construct successfully promotes the generation of LOF alleles in a tissue-specific manner, as shown by the selective loss of eye pigmentation observed when targeting the *tyrosinase* gene in retinal progenitor cells (RPCs).

We combined our Cas9-mediated KO strategy with the activity of the Cre recombinase (2C-Cas9 system) to allow long-term tracking of *cas9*-expressing cells.

We showed that the 2C-Cas9 system permits the labeling of cell clones arising from a *cas9*-expressing mutant progenitor cells: by targeting the *atho7* gene (encoding for a transcription factor controlling the specification of RGCs) in RPCs, we could analyze clones of *ath7*-depleted retinal neurons lacking the population of RGCs.

We implemented a system allowing the direct comparison of mutant and wild type cells based on the combination of the 2C-Cas9 vector with the Brainbow technology. This approach allowed us to compare, in the same animal, the axonal branching of a *kif5aa*^{-/-} RGC (displaying a reduced arbor complexity) with the wild type counterpart.

In conclusion, we present a tool enabling CRISPR/Cas9 and Gal4/UAS mediated tissue-specific KO, providing, at the same time, a strategy to mark *cas9*-expressing cells to facilitate their phenotypic analysis. This approach is suitable for the analysis of gene LOF in specific tissues or single cells or for tracing the fate of *cas9*-expressing progenitors.

Method

2C-Cas9: a versatile tool for clonal analysis of gene function

Vincenzo Di Donato,^{1,4} Flavia De Santis,^{1,4} Thomas O. Auer,^{1,5} Noé Testa,¹ Héctor Sánchez-Iranzo,² Nadia Mercader,² Jean-Paul Concordet,³ and Filippo Del Bene¹

¹Institut Curie, PSL Research University, INSERM U 934, CNRS UMR3215, F-75005, Paris, France; ²Department of Cardiovascular Development and Repair, Atherothrombosis and Imaging, Centro Nacional de Investigaciones Cardiovasculares (CNIC), 28028 Madrid, Spain; ³Muséum National d'Histoire Naturelle, INSERM U1154, CNRS UMR 7196, Paris F-75231, France

CRISPR/Cas9-mediated targeted mutagenesis allows efficient generation of loss-of-function alleles in zebrafish. To date, this technology has been primarily used to generate genetic knockout animals. Nevertheless, the study of the function of certain loci might require tight spatiotemporal control of gene inactivation. Here, we show that tissue-specific gene disruption can be achieved by driving *Cas9* expression with the Gal4/UAS system. Furthermore, by combining the Gal4/UAS and Cre/loxP systems, we establish a versatile tool to genetically label mutant cell clones, enabling their phenotypic analysis. Our technique has the potential to be applied to diverse model organisms, enabling tissue-specific loss-of-function and phenotypic characterization of live and fixed tissues.

[Supplemental material is available for this article.]

The CRISPR (Clustered Regularly Interspaced Short Palindromic Repeats)/CRISPR-associated (Cas) system has recently emerged as a powerful tool to generate constitutive loss-of-function alleles, enabling detailed analyses of gene function (Cho et al. 2013; Cong et al. 2013; Hwang et al. 2013b; Mali et al. 2013). Gene disruption is achieved by the activity of two components: a single guide RNA (sgRNA) that contains 20 nt complementary to a DNA target, and a Cas9 endonuclease that catalyzes DNA cleavage at the target site after complex formation with the sgRNA. Following DNA cleavage, mutations are efficiently induced upon imperfect repair by the nonhomologous end-joining (NHEJ) pathway at the targeted sequence. sgRNAs that bind within the coding region of a gene thereby allow disruption of the open reading frame (ORF), leading to loss of gene activity. Pioneer studies in worms (Shen et al. 2014), fruit fly (Port et al. 2014), mouse (Platt et al. 2014), and, more recently, zebrafish (Ablain et al. 2015) have taken advantage of this methodology to induce conditional gene knockouts by driving tissue-specific expression of *Cas9*. However, in zebrafish, this approach relies on cell-type-specific promoter sequences to control *Cas9* expression, usually requiring the screening of several lines to achieve sufficient and nonectopic transgene expression. One alternative and powerful method for cell-specific expression of transgenes in model organisms is the Gal4/UAS binary system (Asakawa and Kawakami 2008), in which transcription is driven by the binding of the Gal4 transcription factor to tandem upstream activation sequences (UAS) placed at the 5' end of a gene of interest. An important resource of Gal4 transgenic lines has been established by gene- and enhancer-trap screens (Davison et al. 2007; Asakawa et al. 2008; Scott and

Baier 2009; Kawakami et al. 2010; Balciuniene et al. 2013) based on random integration of the Gal4 ORF via Tol2 transposition (Kawakami 2004) into the fish genome. In particular, Gal4 driver lines have been identified for many tissues as well as for novel and previously uncharacterized cell types, especially in the nervous system (Scott et al. 2007; Asakawa et al. 2008). More recently, we have developed a simple and efficient method for converting GFP- into Gal4-transgenic lines, significantly expanding the potential resource of Gal4 driver lines (Auer et al. 2014a,b). Finally, Gal4-driven expression of transgenes from UAS promoters is robust and can often be revealed in cells where *Gal4* expression itself is difficult to detect. In this report, we show that flexible and efficient gene disruption is achieved as a result of tissue-specific expression of *Cas9* via the Gal4/UAS system. In addition, we overcome the challenge of visualizing loss-of-function mutations in specific cells by coexpressing the Cas9 endonuclease with GFP or Cre recombinase, allowing the labeling of potentially mutant cells and thereby facilitating their phenotypic analysis. This step is essential to correlate phenotype with genotype for analysis of gene function, a task that was not addressed with previously published methods.

Results

Design of a vector system for spatiotemporal control of Cas9 activity via Gal/UAS

The generation of conditional knockout models requires the specific targeting of a gene of interest in a given tissue and, ideally, the labeling of targeted cells. In order to develop a flexible tool

⁴These authors contributed equally to this work.

⁵Present address: Center for Integrative Genomics, Faculty of Biology and Medicine, University of Lausanne, 1015 Lausanne, Switzerland
Corresponding authors: filippo.del-bene@curie.fr, jean-paul.concordet@mnhn.fr

Article published online before print. Article, supplemental material, and publication date are at <http://www.genome.org/cgi/doi/10.1101/gr.196170.115>.

© 2016 Di Donato et al. This article is distributed exclusively by Cold Spring Harbor Laboratory Press for the first six months after the full-issue publication date (see <http://genome.cshlp.org/site/misc/terms.xhtml>). After six months, it is available under a Creative Commons License (Attribution-NonCommercial 4.0 International), as described at <http://creativecommons.org/licenses/by-nc/4.0/>.

for efficient spatiotemporal control of gene disruption, we generated a Tol2-based vector ensuring Gal4/UAS-mediated cell-type-specific expression of the Cas9 enzyme and ubiquitous expression of sgRNAs. Due to its strong transactivating properties, the Gal4/UAS system directs effective expression of the Cas9 endonuclease, even in the case of weak tissue-specific *Gal4* transcription by an endogenous promoter. Furthermore, this system renders our vector design compatible with many readily available Gal4 transgenic lines generated in previous Gal4 gene- and enhancer-trap screens (including those where the regulatory elements driving *Gal4* expression are not known) (Davison et al. 2007; Asakawa et al. 2008; Scott and Baier 2009; Kawakami et al. 2010; Balciuniene et al. 2013). In our vector design, the use of a viral T2A self-cleaving peptide (Probst et al. 2007) to synthesize a GFP reporter from the same transgene (*UAS:Cas9T2AGFP*) allows Cas9-positive cells to be unambiguously marked by GFP fluorescence. This feature is critical for the analysis of cellular phenotypes resulting from Cas9-induced gene inactivation. Our vector also contains two sgRNA expression cassettes, each driven by the ubiquitous *U6-1* promoter (Halbig et al. 2008; Yin et al. 2015) (*UAS:Cas9T2AGFP*; *U6:sgRNA1*; *U6:sgRNA2*) (Fig. 1A). By using two sgRNAs, we sought to increase the probability of generating loss-of-function alleles, since genomic deletions might be induced, in addition to frame-shifts caused by insertions and deletions (indels). To verify that cell-type-specific expression of *Cas9* can be driven by Gal4 transcriptional activation, we generated a stable transgenic line with this vector, *Tg(UAS:Cas9T2AGFP*; *U6:sgRNA1*; *U6:sgRNA2*), and crossed it to different Gal4 driver lines (Fig. 1B). The motor neuron-specific *Tg(mnx1:Gal4)* transgenic line, the enhancer-trap line *Tg(s1020t)* expressed in the thalamus and spinal cord, and the optic tectum-specific gene-trap line *Tg(SA2AzGFF49A)* were used as drivers. We compared the expression of the *UAS:Cas9T2AGFP* with an independent reporter of the Gal4 activity by crossing the same driver lines with a *Tg(UAS:RFP*; *cry:GFP*). In the embryos analyzed, GFP was specifically detected in the expected Gal4 transactivation domain, indicating nonectopic *Cas9* expression. Modest differences in GFP and RFP expression were observed, the RFP-positive cells being on average more numerous than the GFP-positive ones. This might be due to transgene specific differences likely linked to positional effect of the integration as commonly seen for other zebrafish transgenic lines. Overall, these expression patterns demonstrate that our approach can be used to both express Cas9 nuclease in a tissue-specific manner and to simultaneously label Cas9-expressing cells with GFP.

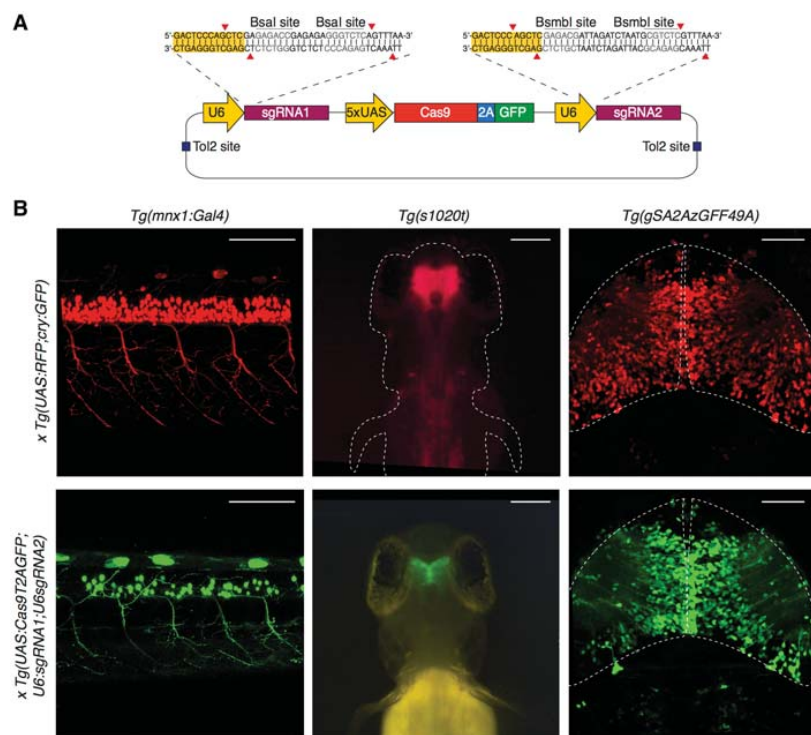


Figure 1. Spatiotemporal control of Cas9 activity via the Gal4/UAS expression system. (A) Schematic illustration of the expression vector design. Spatial and temporal control of Cas9 synthesis is achieved by the Gal4/UAS system and monitored by GFP expression. Two constitutively active *U6* promoters drive the transcription of single guide RNAs (*sgRNAs*) specifically targeting a gene of interest. To facilitate cloning of *sgRNA* target sequences, Bsmbl and Bsal restriction sites (red arrows) were introduced. Tol2 allows efficient transgenesis after injection into one-cell stage zebrafish embryos. (B) (Left panel) Confocal imaging of the spinal cord of 2 dpf *Tg(mnx1:Gal4)* embryos. The upper image shows the Gal4-induced RFP expression of a double transgenic embryo deriving from a cross between *Tg(mnx1:Gal4)* and *Tg(UAS:RFP*; *cry:GFP)* fish. The same pattern is observed in the GFP channel in a double transgenic *Tg(mnx1:Gal4)* × *Tg(UAS:Cas9T2AGFP*; *U6:sgRNA1*; *U6:sgRNA2)* embryo (lower image). Scale bar = 100 μ m. (Middle panel) Imaging of whole-mount 3 dpf *Tg(s1020t)* enhancer-trap line. The GFP expression pattern (lower panel) recapitulates RFP (upper panel). Scale bar = 100 μ m. (Right panel) Confocal imaging of 5 dpf optic tectum in the double transgenic embryos deriving from a cross of *Tg(SA2AzGFF49A)* gene-trap line and *Tg(UAS:RFP*; *cry:GFP)* (upper image) and *Tg(UAS:Cas9T2AGFP*; *U6:sgRNA1*; *U6:sgRNA2)* (lower image). Scale bar = 50 μ m. No target sequence was inserted in the vector for the generation of the *Tg(UAS:Cas9T2AGFP*; *U6:sgRNA1*; *U6:sgRNA2)* line.

Targeting the *tyrosinase* gene in the optic primordium leads to loss of pigmentation in the retinal pigmented epithelium (RPE)

To test the efficiency of our approach for tissue-specific gene disruption, we targeted the *tyrosinase* (*tyr*) gene, which codes for a key enzyme in melanin production (Camp and Lardelli 2001), by including two sgRNAs targeting the *tyr* in our vector locus (*pUAS:Cas9T2AGFP*; *U6:tyrsgRNA1*; *U6:tyrsgRNA2*). We previously assessed the mutagenesis rate of each sgRNA by injection of in vitro-transcribed sgRNA with synthetic *Cas9* mRNA into one-cell stage wild-type embryos (Supplemental Table S1). Loss-of-function of the *tyr* locus results in pigmentation defects, offering a clear visual read-out of biallelic gene inactivation (Jao et al. 2013). We used fluorescence-activated cell sorting (FACS) to verify that site-specific cleavage only occurs in GFP-expressing cells and to quantify the mutation rate induced by our vector. The quasi-ubiquitous *Tg(rpl5b:Gal4)* line (Amsterdam et al. 2004) was chosen to enlarge

the number of GFP-positive cells in the assay (Supplemental Fig. S1A). We thereby transiently expressed the pUAS: *Cas9T2AGFP*; *U6:tyrsgRNA1*; *U6:tyrsgRNA2* by injection into one-cell stage *Tg(trpl5b:Gal4)* embryos. After separating the pool of GFP-positive cells from the GFP-negative control cells derived from 200 injected embryos, total DNA was extracted from the two cell populations. Upon PCR amplification and sequencing of single amplicons from the DNA of GFP-positive cells, we detected indel out-of-frame mutations at the *tyr* target region in 30% (4/12) of the analyzed sequences (Supplemental Fig. S1B). In this cell population, we also observed a 488-bp deletion at the *tyr* gene resulting from simultaneous targeting of the locus by both sgRNAs. In contrast, no *tyr* mutations were found in the GFP-negative cells (0/15). These data confirm that locus-specific knockout events are restricted to the cells expressing the fluorescent reporter. Subsequently, we tested whether spatiotemporally regulated *tyr* loss-of-function can be induced by our vector system. For this purpose, we used a transgenic line expressing *Gal4* under the promoter of the zebrafish *retinal homeobox gene 2 (rx2)* (Heermann et al. 2015), *Tg(rx2:Gal4;myl7:GFP)*. We identified transgenic embryos using the *myl7* (*myosin, light chain 7, regulatory*) promoter, driving heart-specific GFP expression, which was incorporated in the same transgene. *Rx2* is active in the optic primordium in the progenitors of the neural retina and the retinal-pigmented epithelium (RPE) (Chuang and Raymond 2001). Thus, transient, cell-specific expression of Cas9 from the pUAS: *Cas9T2AGFP*; *U6:tyrsgRNA1*; *U6:tyrsgRNA2* in *Tg(rx2:Gal4;myl7:GFP)* embryos should promote targeted disruption of the *tyr* locus uniquely in Gal4-positive cells, leading to pigmentation defects exclusively in the RPE after biallelic gene inactivation. In agreement with the known expression pattern of the *rx2* promoter (Supplemental Fig. S2A), we detected sparse green fluorescent cells in the embryonic retina of Gal4-positive larvae, at 24 hours post-fertilization (hpf) (Fig. 2A). Of the embryos analyzed at 5 days post-fertilization (dpf), 15% displayed loss of pigmentation specifically in the RPE (16/107 embryos in three independent experiments) compared to 0% (0/116 in three independent experiments) in embryos injected with a plasmid containing control sgRNA sequences (Fig. 2B,C). We observed a variable degree of pigmentation loss, and all the embryos displaying the phenotype were scored as positives. Importantly, no pigmentation defects were detected outside of the eye-specific Gal4 expression domain. Together, these results indicate that knockout of the *tyr* gene driven by the *rx2* promoter leads to tissue-specific pigmentation defects. Having this proof of principle for our approach, we decided to create a stable integration of the UAS-based transgene to achieve a more robust and more reliable expression and to evaluate the penetrance of the pigmentation phenotype. We generated a *Tg(UAS:Cas9T2AGFP;U6:tyrsgRNA1;U6:tyrsgRNA2)* transgenic line

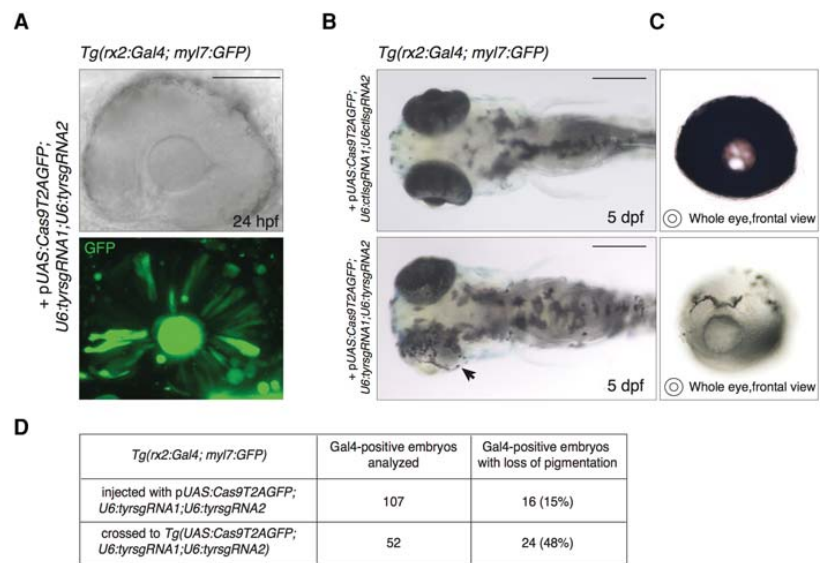


Figure 2. Tissue-specific disruption of the *tyrosinase* locus induced by the expression of the UAS-based vector in the retinal progenitor cells. (A) Transmitted light and confocal imaging of eye of a 24 hpf *Tg(rx2:Gal4;myl7:GFP)* embryo injected with pUAS: *Cas9T2AGFP*; *U6:tyrsgRNA1*; *U6:tyrsgRNA2* together with *Tol2* mRNA. GFP fluorescence indicates Gal4-driven expression of the Cas9 enzyme in the retinal progenitor cells (RPCs) giving rise to the retinal pigmented epithelium (RPE) and to the neural retina. Scale bar = 100 μ m. (B) (Lower panel) Specific loss of pigmentation in the RPE of a 5 dpf zebrafish embryo induced by injection of pUAS: *Cas9T2AGFP*; *U6:tyrsgRNA1*; *U6:tyrsgRNA2* in *Tg(rx2:Gal4; myl7:GFP)* at one-cell stage. Arrowhead indicates the eye with lost pigmentation. (Upper panel) Control embryo injected with the same vector containing a control sgRNA sequence (*ctfsgRNA*). Scale bar = 300 μ m. (C) Frontal view of eyes with absent pigmentation (lower panel) and wild-type (upper panel) explanted from the larvae shown in B. (D) Table showing the percentage of Gal4-positive larvae displaying loss of pigmentation in the RPE. (First row) Injection of the pUAS: *Cas9T2AGFP*; *U6:tyrsgRNA1*; *U6:tyrsgRNA2* into one-cell-stage *Tg(rx2:Gal4; myl7:GFP)* embryos. (Second row) Cross of *Tg(rx2:Gal4; myl7:GFP)* fish with *Tg(UAS:Cas9T2AGFP;U6:tyrsgRNA1;U6:tyrsgRNA2)*.

and crossed it with *Tg(rx2:Gal4;myl7:GFP)* fish. Gal4-positive embryos were prescreened by *myl7:GFP* expression and subsequently analyzed to assess *tyr* inactivation. The rate of larvae displaying RPE pigmentation defects increased to 48% (24/52) (Fig. 2D); therefore, *tyr* loss-of-function most likely occurred in all double transgenic progeny of the cross, as only half of the Gal4-positive larvae were expected to carry the UAS transgene. This observation shows that stable expression of the Cas9/sgRNA complex dramatically improves the efficiency of gene inactivation, most likely due to higher levels and more widespread expression in retinal progenitor cells (RPCs). Based on these data, we conclude that our vector system is capable of inducing loss-of-function alleles at given genomic loci in a defined spatiotemporal manner. However, at the developmental stage of the phenotypic analysis (5 dpf), GFP fluorescence could no longer be detected since the *rx2* promoter is not active in the differentiated RPE. This result reflects the fact that GFP expression is strictly dependent on the temporal activity of the promoter driving *Gal4* expression, thus restricting direct detection of potential mutant cells to a limited time window.

Cre-mediated recombination allows permanent labeling of Cas9-expressing cells

By using the pUAS: *Cas9T2AGFP*; *U6:sgRNA1*; *U6:sgRNA2* vector, potentially mutated cells are labeled by simultaneous expression

of the Cas9 endonuclease and a GFP reporter. Nevertheless, the possibility of phenotypic analysis of the cells expressing the transgene strongly depends on the activity window of the chosen promoter, as it determines when the GFP reporter can be detected. Therefore, the long-term visualization of cells displaying loss-of-function phenotypes that are not self-revealing (unlike the loss of pigmentation induced by mutations on the *tyr* locus) requires permanent labeling of Cas9-expressing cells and their progeny. To obtain such a labeling, we replaced the GFP ORF with the one of Cre recombinase (Fig. 3A), an enzyme catalyzing site-specific recombination events (Branda and Dymecki 2004; Pan et al. 2005). In order to detect Cre-mediated labeling of Cas9-expressing cells, we used transgenic lines carrying a cassette where a ubiquitous promoter drives constitutive expression of a fluorescent reporter only upon excision of a floxed STOP sequence by Cre recombinase. The tissue-specific Gal4-driven transcription of a *UAS:Cas9T2ACre* transgene ensures concomitant expression of the Cas9 and Cre enzymes inducing, respectively, double-strand breaks (DSBs) at the target locus and activation of the floxed reporter transgene within the same cell (Fig. 3B). Most importantly, Cre-dependent expression of the fluorescent reporter will persist in all cells derived from a specific Cas9-expressing precursor. This approach, that

we name 2C-Cas9 (Cre-mediated recombination for Clonal analysis of Cas9 mutant cells) allows targeted mutagenesis of a cell population and the genetic labeling of the derived mutant cell clones.

Visualizing 2C-Cas9-mediated gene inactivation

In order to explore the possibility of directly visualizing protein loss, we sought to induce eye-specific loss-of-function at the *parvalbumin 6* (*pvalb6*) locus, coding for a calcium-binding protein expressed in a subpopulation of amacrine cells (ACs) in the inner nuclear layer (INL) and retinal ganglion cell layer (GCL) of the differentiated retina (Fig. 4A). The *pvalb6* gene is the only paralog expressed in mature retinal neurons as reported by the ZFIN in situ database (Sprague et al. 2008). This gene represents an ideal target for unbiased detection of locus disruption, since its expression can be easily revealed by immunohistochemistry with a commercially available antibody (Nevin et al. 2008). To achieve *pvalb6* inactivation, we first generated a *pUAS:Cas9T2ACre;U6:pvalb6sgRNA1;U6:pvalb6sgRNA2* vector. The mutagenesis rate of the sgRNA used was tested in transient injection in wild-type embryos prior to cloning in the 2C-Cas9 vector (Supplemental Table S1). As a single efficient sgRNA could be identified for this gene, the same target sequence was inserted downstream from each of the two U6 promoters. We chose the *rx2:Gal4* driver to express this UAS construct targeting *pvalb6* in multipotent retinal progenitor cells as the *rx2* promoter is active during early eye field development (Chuang and Raymond 2001; Heermann et al. 2015). It has been previously reported that one single RPC can give rise to clones including all of the different retinal cell types spanning all retinal layers (Livesey and Cepko 2001). Thus, a loss-of-function mutation, when induced at the level of a RPC, is expected to propagate to a clone of cells derived from the progenitor. To obtain clonal labeling of mutant retinal cells, we injected the *pUAS:Cas9T2ACre;U6:pvalb6sgRNA1;U6:pvalb6sgRNA2* into one-cell stage embryos of a cross of *Tg(rx2:Gal4;myl7:GFP)* and *Tg(-3.5ubb:loxP-lacZ-loxP-eGFP)cn2* fish. The latter reporter line allows visualization of Cre-mediated recombination by switching from *lacZ* to *GFP* expression. This cross enables the detection in the retina of radial columns of GFP-positive cells arising from RPCs having expressed the *Cas9* during the activation time of the *rx2* promoter. Discrete clones of GFP-positive Cas9-expressing cells were analyzed in retinas of 5 dpf larvae after double immunohistochemistry for GFP and Pvalb. For each clone, we counted the total number of cells labeled by the GFP reporter, excluding photoreceptors, and the number of cells simultaneously stained for GFP and Pvalb. This second

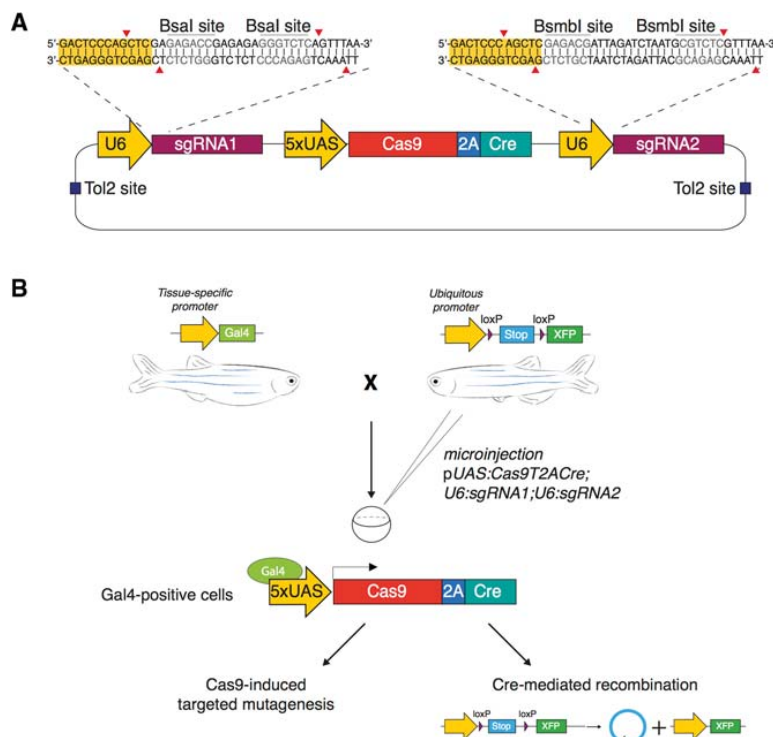


Figure 3. Permanent labeling of Cas9-expressing cells by Cre-mediated recombination. (A) Schematic illustration of the *pUAS:Cas9T2ACre;U6sgRNA1;U6sgRNA2* expression vector design. The vector contains two U6-sgRNA expression cassettes targeting the same gene. Bsal and BsmBI restriction sites are used for the sgRNA target sequence cloning. UAS elements drive the expression of Cas9 and Cre recombinase linked via the T2A peptide. (B) Microinjection of the *pUAS:Cas9T2ACre;U6sgRNA1;U6sgRNA2* construct in the double transgenic embryos *Tg(Tissue specific promoter:Gal4) × Tg(Ubiquitous promoter:loxP-STOP-loxP-XFP)* triggers simultaneous synthesis of Cas9 and Cre in a chosen spatiotemporal pattern, defined by the promoter driving Gal4 expression. Cell-specific Cas9 endonuclease activity induces targeted disruption of the gene of interest and Cre-mediated recombination induces permanent expression of a fluorescent reporter gene (XFP) by deletion of the floxed stop sequence.

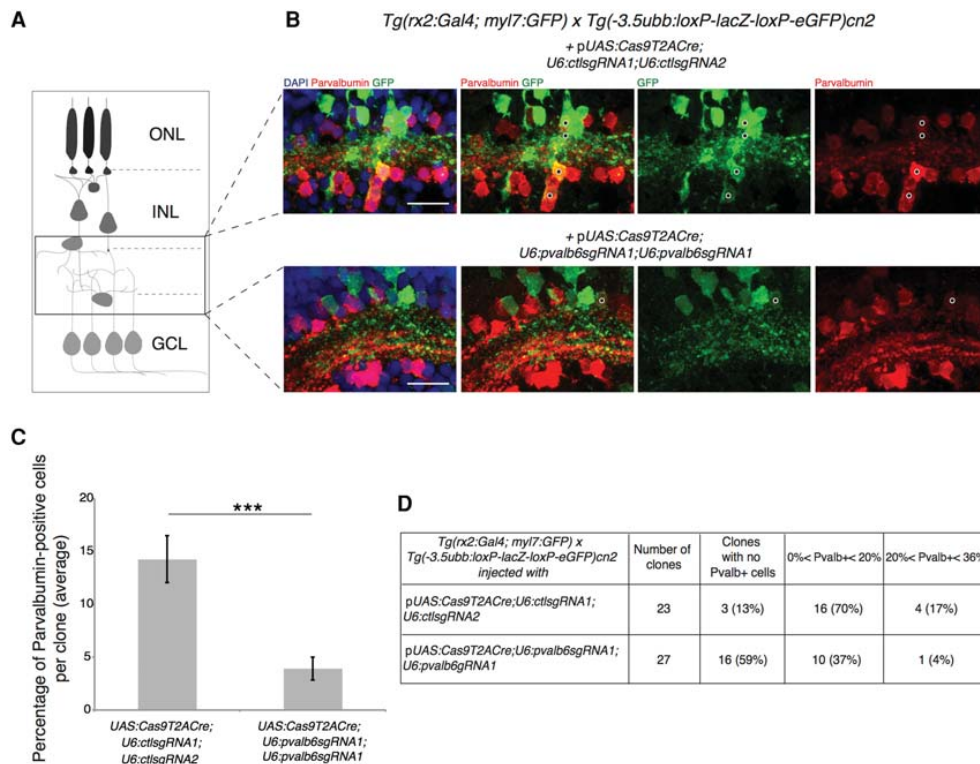


Figure 4. Targeting of the *pvalb6* locus leads to loss of Pvalb expression in ACs. (A) Schematic of a clone of cells deriving from a single RPC. The black frame defines the position of the amacrine cell population. (ONL) Outer nuclear layer, (INL) inner nuclear layer, (GCL) ganglion cell layer. (B) GFP-positive Cas9-expressing cells in the retinal section of a 5 dpf double transgenic *Tg(rx2:Gal4; myl7:GFP) × Tg(-3.5ubb:loxP-lacZ-loxP-eGFP)cn2* embryos transiently expressing the 2C-Cas9 vector containing control sgRNAs (upper panel) or *pvalb6*-specific sgRNAs (lower panel). The same sgRNA target sequence was inserted downstream from each U6 promoter (*U6:pvalb6sgRNA1*). The number of Pvalb- and GFP-double-positive cells (black dots) is reduced if *pvalb6* is targeted compared to control. Scale bar = 50 μ m. (C) Quantification of the percentage of Pvalb-positive cells per GFP-positive clone in the retinal sections of double transgenic *Tg(rx2:Gal4; myl7:GFP) × Tg(-3.5ubb:loxP-lacZ-loxP-eGFP)cn2* larvae microinjected with the 2C-Cas9 plasmid containing control sgRNAs (first row) or *pvalb6*-targeting sgRNAs (second row). (D) Table showing the percentage of Pvalb-positive cells per GFP-positive clone in the retinal sections of double transgenic *Tg(rx2:Gal4; myl7:GFP) × Tg(-3.5ubb:loxP-lacZ-loxP-eGFP)cn2* larvae microinjected with the 2C-Cas9 plasmid containing control sgRNAs (first row) or *pvalb6*-targeting sgRNAs (second row).

population represents the subset of amacrine cells deriving from Cas9-expressing RPCs that escaped *pvalb6* biallelic inactivation. We observed that the total number of cells was not affected in the examined clones (15 ± 1 in controls vs. 16 ± 1 in *pvalb6* sgRNA clones; $P = 0.9$, Wilcoxon Mann-Whitney test), while the number of cells showing colocalization of Pvalb and GFP signals was considerably reduced by the targeting of *pvalb6* (1.9 ± 0.3 in controls vs. 0.8 ± 0.2 in *pvalb6* sgRNA clones; $P < 0.005$, Wilcoxon Mann-Whitney test) (Fig. 4B). Overall, in control retinas the number of GFP-positive cells expressing Pvalb represented 12% of each clone on average ($n = 23$ clones; 345 cells analyzed). On the contrary, in clones where the *pvalb6* gene was targeted, only 4% of GFP-positive cells were also positive for Pvalb ($n = 27$ clones; 435 cells analyzed), representing cells that escaped biallelic *pvalb6* inactivation (Fig. 4C,D). Altogether, *pvalb6* targeting led to a reduction of two thirds of the *pvalb6*-expressing ACs. These results confirm that 2C-Cas9 can mediate gene loss-of-function and that antibody staining can efficiently reveal protein loss at a cellular resolution, offering a clear read-out of the proportion of cells carrying biallelic mutations within the analyzed population.

atoh7 gene inactivation in retinal progenitors inhibits determination of retinal ganglion cells (RGCs) in clonally derived cell populations

We next wanted to test the utility of the 2C-Cas9 system in the analysis of a loss-of-function phenotype in cell clones. We chose to target the *atoh7* gene because a characterized loss-of-function allele (*lakritz*) shows a clearly identifiable retinal phenotype (Kay et al. 2001). The *lak* mutation results in the loss of retinal ganglion cell (RGC) specification during eye development. Because *rx2* expression precedes *atoh7* activation, mutations induced by *rx2*-driven Cas9 may give rise to *atoh7* mutant cells in RPCs before endogenous *atoh7* is expressed. We therefore transiently expressed a pUAS:Cas9T2ACre;U6:*atoh7*sgRNA1;U6:*atoh7*sgRNA2 vector in double transgenic embryos deriving from a cross of *Tg(rx2:Gal4;myl7:GFP)* and *Tg(-3.5ubb:loxP-lacZ-loxP-eGFP)cn2* fish to induce targeted mutations at the *atoh7* locus in RPCs. The mutagenesis efficiency of the sgRNAs used was assessed prior to insertion in the transgenesis vector (Supplemental Table S1) in transient injection experiments. Clones of GFP-positive cells were analyzed in sections of

Di Donato et al.

differentiated retinas of 5 dpf larvae (Fig. 5A–C). For this analysis, we chose to quantify only spatially well-separated clones that could be unambiguously identified, ranging from 10 to 55 cells per clone. We observed that the total number of cells per clone was not affected (25 ± 3 in controls vs. 24 ± 2 in *atoh7* sgRNA clones; $P=0.91$, Wilcoxon Mann–Whitney test), while the number of RGCs was significantly reduced in *atoh7* targeted clones (6.1 ± 1.2 in controls vs. 2.4 ± 0.5 in *atoh7* sgRNA clones; $P<0.01$, Wilcoxon Mann–Whitney test). On average, in control retinas the RGC population represented 23% of the cells in each clone (57/247 cells analyzed). In contrast, in potentially *atoh7*-depleted clones only 9% of GFP-positive cells corresponded to differentiated RGCs (48/532 cells analyzed) (Fig. 5D). In the retinas of embryos injected with the control plasmid, all clones of cells (10/10) contained RGCs, representing, in the majority of clones (7/10), >20% of the GFP-positive cell population (Fig. 5E). In the

retinal sections of embryos where the *atoh7* locus was targeted, one third of the examined clones (7/22) displayed complete absence of RGCs, while only in a few cases (2/22 clones) the percentage of specified RGCs per clone was higher than 20% (Fig. 5E). These observations indicate that *atoh7* loss-of-function is effectively induced by our vector system in *rx2*-expressing retinal progenitors.

Analysis of genetic chimeras by combining tissue-specific loss-of-function with Brainbow single-cell labeling

To gain insights into complex loss-of-function phenotypes, it is necessary to understand if the biological effect of gene inactivation is cell-autonomous or non-cell-autonomous. Our method can be applied to generate genetic mosaics in which the phenotype of single mutant cells can be analyzed in a wild-type

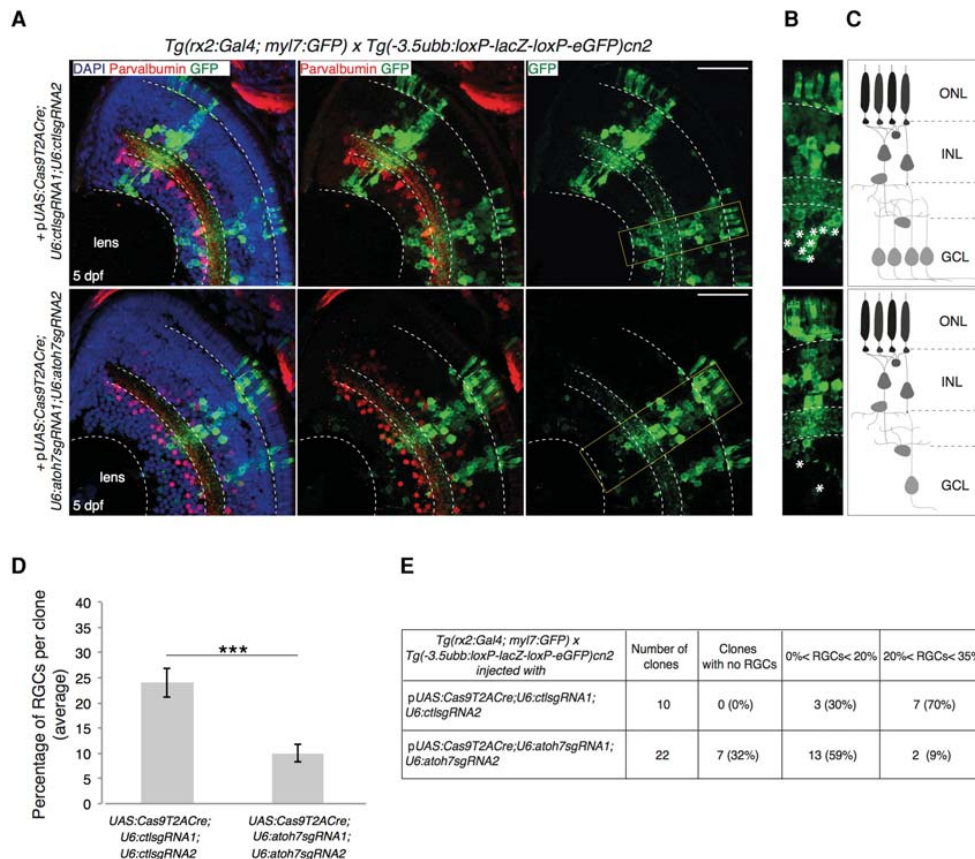


Figure 5. Clonal deletion of *atoh7* leads to reduction in RGCs differentiation. Targeting of the *atoh7* gene. *Atoh7* is a transcription factor essential for the differentiation of retinal ganglion cells (RGCs). The pUAS-Cas9T2ACre;U6sgRNA1;U6sgRNA2 construct, with control or *atoh7*-specific sgRNAs, was injected in double transgenic embryos *Tg(rx2:Gal4; myl7:GFP) x Tg(-3.5Subb:loxP-lacZ-loxP-eGFP)cn2*. The latter transgene drives *Gal4* expression in retinal progenitor cells. (A) (Upper panel) Differentiated RGCs are detected in wild-type clones injected with the DNA construct containing control sgRNAs. (Lower panel) GFP-labeled mutant clones show reduction of RGCs in the retinal type of a 5 dpf larva, as expected from *atoh7* loss-of-function. Quantification of RGCs was done according to soma location in the ganglion cell layer (GCL), and displaced amacrine cells were distinguished by Parvalbumin counterstaining. Scale bar = 100 μ m. (B) Higher magnification of the wild-type (upper panel) and *atoh7* (lower panel) mutant retinal cell layers. RGCs are indicated by asterisks. (C) A schematic of labeled clones in the zebrafish retinal layers. (ONL) Outer nuclear layer, (INL) inner nuclear layer, (GCL) ganglion cell layer. (D) Quantification of the percentage of RGCs per clone derived from *Cas9*-expressing cells. Data are represented as mean \pm SEM. (***) P -value < 0.001 following Wilcoxon Mann–Whitney test. (E) Table showing the percentage of RGCs per GFP-positive clone in the retinal sections of double transgenic *Tg(rx2:Gal4; myl7:GFP) x Tg(-3.5Subb:loxP-lacZ-loxP-eGFP)cn2* embryos microinjected with the 2C-Cas9 vector containing control sgRNAs (first row) or *atoh7*-specific sgRNAs (second row).

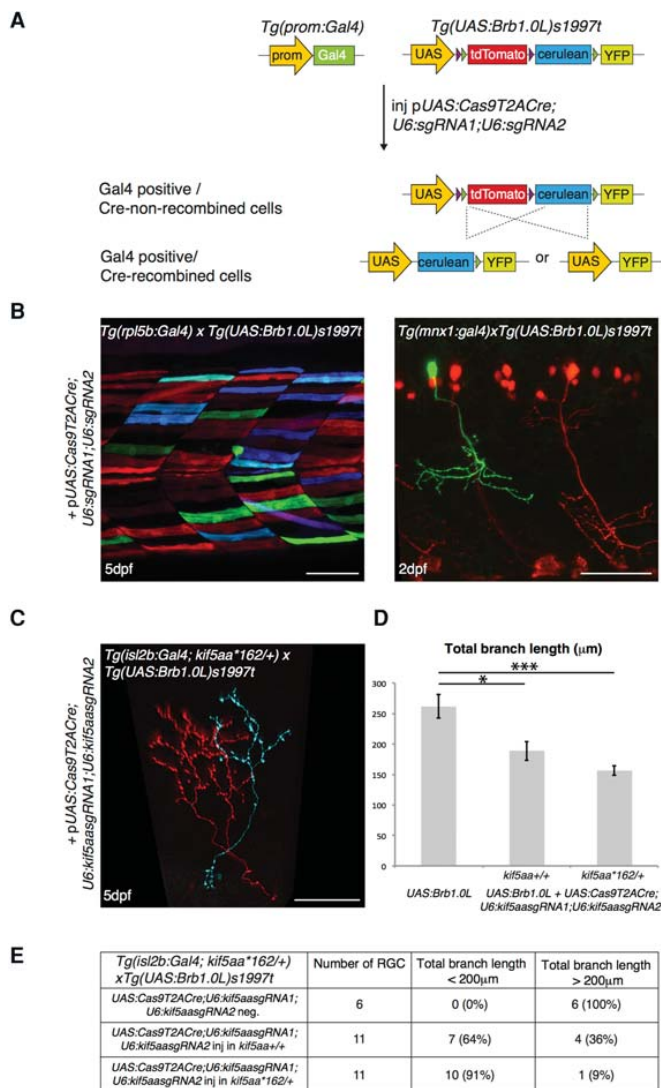


Figure 6. Labeling of mutant single cells by combining the 2C-Cas9 and the Brainbow methodologies. (A) Microinjection of the pUAS:Cas9T2ACre;U6sgRNA1;U6sgRNA2 construct in the double transgenic embryos *Tg(promoter:Gal4) × Tg(UAS:Brb1.0L)s1997t* leads to synthesis of both Cas9 and Cre. In *Gal4*-expressing cells, Cas9 promotes targeted cleavage of the chosen genomic locus. At the same time, Cre activity induces stochastic recombination of the *UAS:Brb1.0L* cassette, thus promoting a switch from the default tdTomato to YFP or Cerulean fluorescence in the same cells. (B) Recombination of the *UAS:Brb1.0L* cassette in a tissue-specific pattern induced by injection of the pUAS:Cas9T2ACre;U6sgRNA1;U6sgRNA2 plasmid. No target sequence was inserted in the vector prior to injection. (Left panel) Multicolor labeling of muscle cells in the *Tg(rpl5b:Gal4)* transgenic line. (Right panel) Single YFP motor neuron labeled by expression of *UAS:Cas9T2ACre;U6sgRNA1;U6sgRNA2* transgene in the double transgenic embryos *Tg(mnx1:Gal4) × Tg(UAS:Brb1.0L)s1997t*. tdTomato marks motor neurons that do not express the *UAS* transgenic cassette. Scale bar = 50 μm. (C) Double transgenic *Tg(isl2b:Gal4; kif5aa*162/+)* × *Tg(UAS:Brb1.0L)s1997t* larva, injected with pUAS:Cas9T2ACre;U6:Kif5aasgRNA1;U6:Kif5aasgRNA2. *isl2b:Gal4* drives the expression of *UAS:Brb1.0L* transgene in RGC axons in the optic tectum. Note that the axon marked by *cerulean* expression, and therefore by Cre recombinase activity, shows reduced arbor size as expected from the phenotype of *kif5aa*^{-/-} RGCs transplanted in wild-type host (Auer et al. 2015). Scale bar = 30 μm. (D) Quantification of total branch length in tdTomato-positive wild-type and potentially mutant Cerulean- or YFP-positive RGC axons (analyzed in *kif5aa*^{+/+}: [*] *P*-value < 0.05 following Wilcoxon Mann–Whitney test, and *kif5aa*^{*162/+}: [***] *P*-value < 0.001 following Wilcoxon Mann–Whitney test). Data are represented as mean ± SEM. (E) Table describing the percentage of RGCs displaying a wild-type-like (axonal length > 200 μm) and a mutant-like (axonal length < 200 μm) phenotype in the tectum of double transgenic *Tg(isl2b:Gal4; kif5aa*162/+)* × *Tg(UAS:Brb1.0L)s1997t* larva, injected with pUAS:Cas9T2ACre;U6:Kif5aasgRNA1;U6:Kif5aasgRNA2. (First row) tdTomato-positive cells (*UAS:Cas9T2ACre;U6:Kif5aasgRNA1;U6:Kif5aasgRNA2*-negative). (Second row) Cerulean- or YFP-positive neurons (*UAS:Cas9T2ACre;U6:Kif5aasgRNA1;U6:Kif5aasgRNA2*-positive) in *kif5aa*^{+/+} fish. (Third row) Cerulean- or YFP-positive neurons (*UAS:Cas9T2ACre;U6:Kif5aasgRNA1;U6:Kif5aasgRNA2*-positive) in *kif5aa*^{*162/+} fish.

background, thus allowing the evaluation of cell-autonomous gene function. To this end, we combined our conditional knock-out strategy with the Brainbow technology (Livet 2007; Pan et al. 2013), in which Cre recombinase stochastically activates the expression of different fluorescent proteins, allowing the differential labeling of single mutant cells in a wild-type tissue. In the *UAS:Brainbow* transgene (*Tg[UAS:Br1.0L]^{s1997t}*) (Robles et al. 2013), Cre recombinase sites separate the cDNAs of the fluorescent proteins tdTomato, Cerulean, and YFP. When crossing a transgenic line carrying this cassette to cell-type-specific *Gal4* lines, the *Gal4* transactivator leads to the expression of *tdTomato*, in the absence of Cre-mediated recombination. In contrast, if Cre recombinase expression is induced, transcription of either *cerulean* or *YFP* is triggered (Fig. 6A). We first verified that transient expression of the pUAS:Cas9T2ACre;U6:sgRNA1;U6:sgRNA2 construct induces stochastic recombination of the *UAS:Brainbow* allele by injecting the plasmid into one-cell stage

Tg(rpl5b:Gal4) or *Tg(mnx1:Gal4) × Tg(UAS:Br1.0L)^{s1997t}* double transgenic embryos. Mosaic expression of fluorescent proteins was detected, as expected, in *Gal4*-positive cells (Fig. 6B) in agreement with the known *Gal4* expression patterns of the two promoters (Fig. 1B; Supplemental Fig. S2B). We next used the 2C-Cas9 vector system to generate genetic chimeras where tdTomato- fluorescent cells are wild-type, while Cerulean- or YFP-labeled cells represent potentially mutant cells. In order to achieve this differential labeling, we injected the 2C-Cas9 vector in double transgenic embryos (carrying tissue-specific *Gal4* driver and *UAS:Brainbow*). In our construct, *Cas9* and *Cre* expression occur from the same transcript; therefore, *Gal4*-expressing cells that received the *Cas9T2ACre* plasmid will recombine the *UAS:Br1.0L* allele, inducing expression of *cerulean* or *YFP* and will potentially be knockout for the target gene. On the contrary, *Gal4*-expressing cells that did not receive the *Cas9T2ACre* plasmid will be marked by tdTomato fluorescence and wild-type (Fig. 6A).

To confirm that cell-autonomous gene function can be examined by this method, we targeted the *kif5aa* gene, coding for the motor protein Kinesin family member 5A, a (Campbell and Marlow 2013; Auer et al. 2015). We selected this gene because we have recently shown that *kif5aa* inactivation results in the reduction of axon arbor complexity via a cell-autonomous mechanism: *kif5aa*^{-/-} cells transplanted into wild-type host, after differentiation into RGCs, showed a severe reduction in axon arbor total length (Auer et al. 2015). We decided to apply the 2C-Cas9 system to inactivate the *kif5aa* gene in single RGCs while differentially labeling wild-type and potentially mutant cells in the same embryos. We used *Tg(isl2b:Gal4)* larvae to express the *Gal4* transactivator in RGCs and drive 2C-Cas9-mediated gene disruption in this neuronal population. To further increase the efficiency of the knockout strategy, we used *Tg(isl2b:Gal4)* embryos heterozygous for an existing loss-of-function mutation in the *kif5aa* locus (*kif5aa*^{162/+}). We hypothesized that, if only one wild-type allele needs to be targeted by the Cas9/sgRNA complex, a loss-of-function phenotype would be generated with a higher probability. We therefore cloned two sgRNAs targeting the *kif5aa* locus (Auer et al. 2014b) (Supplemental Table S1) in the 2C-Cas9 vector and injected the resulting pUAS:Cas9T2ACre;U6:kif5aasgRNA1;U6:kif5aasgRNA2 in double transgenic embryos *Tg(isl2b:Gal4;kif5aa*^{162/+}) × *Tg(UAS:Br1.0L)s1997t*. In the injected embryos, YFP- or Cerulean-fluorescent RGCs (potentially *kif5aa* mutant) showed a decrease of total branch length compared to *tdTomato*-expressing RGCs (wild-type). As expected, an overall reduction of axonal length was detected in YFP or Cerulean RGCs compared to *tdTomato* RGCs, and it was more severe in *kif5aa*^{162/+} than in *kif5aa*^{+/+} embryos (*tdTomato*-expressing RGCs = 261.8 ± 19.3 μm, *n* = 6; *cerulean*- or *YFP*-expressing RGCs in *kif5aa*^{+/+} = 188.8 ± 15.7 μm, *n* = 11, *P* < 0.05, Wilcoxon Mann–Whitney test; *cerulean*- or *YFP*-expressing RGCs in *kif5aa*^{162/+} = 156.6 ± 7.7 μm, *n* = 11, *P* < 0.001, Wilcoxon Mann–Whitney test) (Fig. 6D). In addition, we noted the presence of two distinct RGC phenotypes in the Cre-labeled neurons: a wild-type-like (axonal length >200 μm) and a mutant-like (axonal length <200 μm). Remarkably, the number of cells showing a mutant-like phenotype was more abundant in the *kif5aa*^{162/+} fish (91% of analyzed axons, *n* = 11) than in the *kif5aa*^{+/+} embryos (64% of analyzed axons, *n* = 11) (Fig. 6E). This observation confirms that the activation of the 2C-Cas9 system in a heterozygous genetic background leads to an increase of the proportion of mutant cells.

Our results demonstrate the utility of this method to generate genetic mosaic embryos and allow the labeling of multiple axons with different genotypes in distinct color combinations.

Discussion

The constant improvement of CRISPR/Cas9-mediated technologies over the past years is revolutionizing reverse genetic approaches in model organisms. Using the Gal4/UAS system for the first time in a vertebrate model to drive *Cas9* expression, our method expands the possibility of spatiotemporally regulated gene knockout, allowing researchers to tap into the resource of existing Gal4 driver lines. The generation of a stable *Tg(UAS:Cas9T2AGFP;U6:sgRNA1;U6:sgRNA2)* transgenic line, represents an advantage in the study of *in vivo* gene function in diverse cell types and tissues, as tissue-specific gene inactivation can be obtained simply by crossing to already established Gal4 driver lines. Although this transgenic expression system has been shown to experience somatic mosaicism from epigenetic silencing (Akitake et al.

2011), this has not diminished its great popularity and use in zebrafish and other organisms. Indeed, in some applications mosaic gene expression can even be a positive feature, allowing the analysis of the effect of gene inactivation in a sparse manner in single cells or cell clones. However, even when tissue-specific gene inactivation is achieved, the visualization of mutant cells is essential to the phenotypic analysis, an integral element that was not possible with previously published approaches.

In our work, we tested two methods to identify cells carrying loss-of-function alleles. In both cases, the use of a T2A self-cleaving peptide allows for the stoichiometric expression of the *Cas9* and a reporter gene that are translated as a single polypeptide from the same mRNA (Provost et al. 2007; Kim et al. 2011). First, we used a GFP reporter whose expression is linked to that of the *Cas9* to allow for efficient visualization of *Cas9*-expressing cells. *Cas9T2AGFP* transcription being dependent on transactivation by Gal4, the analysis of gene loss-of-function can be performed during the time frame of *Gal4* expression, which is detected by GFP fluorescence. In some cases, the phenotypic evaluation of mutant cells may be required after *Gal4* expression has terminated. For instance, when targeting the *tyr* gene with a Gal4 driver active in retinal progenitors, we could observe cells lacking pigmentation in larvae, but they did not express *GFP*, and therefore, absence of pigmentation could not be strictly correlated to inactivation of the *tyrosinase* gene in the unpigmented cells. The second method that we tested, 2C-Cas9, addresses the time frame issue by enabling both conditional generation of mutant cells and their permanent lineage tracing. In this assay, we used Cre activity to permanently label the population of *Cas9*-expressing cells, making it possible to analyze the phenotype resulting from targeted gene disruption after *Cas9* expression has ceased. Importantly, if Cre-mediated recombination of a floxed allele results in the expression of a fluorescent protein driven by a constitutive promoter, the label would be transmitted from the *Cas9*-expressing founder cell to its progeny and remain detectable, thus generating a clone of labeled mutant cells. By using this method in retinal progenitor cells, we successfully disrupted the *pvalb6* and *atoh7* genomic loci, thus modifying molecular identity and cell-fate determination of their progeny, respectively.

To expand further the possibility to analyze tissue-specific gene inactivation, we took advantage of the flexibility of the pUAS:Cas9T2ACre;U6:sgRNA1;U6:sgRNA2 construct to achieve labeling of single mutant cells in an otherwise wild-type animal. So far, generation of genetic chimeras in biological systems has mainly been possible in the mouse and the fruit fly, greatly contributing to the preeminence of these animal models in genetic studies (Perrimon 1998; Wijgerde et al. 2002). In these models, the use of recombination-based approaches such as Cre/LoxP has been accepted as a gold standard technique for conditional mutagenesis. Until now, a similar approach has not been available in zebrafish. The phenotypic analysis of single mutant cells in a wild-type genetic background has relied on technically challenging transplantation experiments limited to embryonic development, which could not be temporally controlled. For this reason, genetic chimera experiments allow the investigation of only early phenotypes and cannot be used to examine the role of genes and pathways that are used repeatedly during development. Our multicolor labeling approach, that we achieved by combining the 2C-Cas9 system with the Brainbow technology (Livet 2007; Pan et al. 2013), permits the analysis of tissue-specific phenotypes of gene inactivation at a single cell resolution and enables the direct comparison of potentially mutant cells with their wild-type

counterpart in the same animal. Cre/LoxP-based approaches in zebrafish, if properly developed, could also circumvent these limitations but would require much longer generation time and challenging homologous recombination-based genomic manipulations. Furthermore the efficiency of Cre-mediated recombination is well known to depend strongly on the Cre driver line used and the target locus, and potential mosaic inactivation needs to be taken into account also in this case (Branda and Dymecki 2004).

Although the 2C-Cas9 system is meant to allow the phenotypic evaluation of mutant cells, different parameters may influence the interpretation of phenotypes arising from the targeting of a specific locus with this method. To unambiguously follow the fate of mutant cells (or clones of cells), it would be necessary to activate a reporter gene exclusively in these populations. However, in the zebrafish model system, the tools to obtain this kind of tracking are still missing. As an alternative, we propose to mark potentially mutant cells by coexpressing the Cas9 enzyme together with GFP or Cre reporters. By using this approach, not all the analyzed cells will be mutant and each mutant cell will have independently induced mutations (a percentage of these might be silent in-frame mutations). If an antibody recognizing the protein encoded by the targeted gene is available, a single staining could identify all the cells carrying protein null-mutations. Indeed, we could reveal *pvalb6* loss-of-function in the zebrafish neural retina by staining the population of Cas9-expressing cells with an antibody directed against this protein. In other cases, a molecular evaluation of the proportion of truly mutant cells within the analyzed population would be ideally needed to facilitate the statistical analysis of the behavior of the Cas9-expressing cells. A possibility to estimate the rate of mutation in the targeted tissue would be the separation of the marked Cas9-expressing cells by fluorescence-activated cell sorting (FACS). To be efficient, this procedure requires a highly pure and concentrated single-cell suspension, and it might be prone to contamination with debris or nonfluorescent cells. In addition, many transgenic lines contain fluorescent transgenesis markers (such as *myl7:GFP* or *cry:GFP*), which are wild-type fluorescent cells limiting the accuracy of the FACS for the evaluation of the mutagenesis efficiency.

In addition, the strength of the Gal4 driver used is essential in determining the efficiency of the 2C-Cas9 system, and its variability may result in differences in gene disruption. For instance, when using the *Tg(tpl5:Gal4)* line to target the *tyr* locus, we detected a mutagenesis rate that appeared lower than when using the *rx2:Gal4* driver, where we observed phenotypes suggesting a highly efficient gene disruption. This result suggests that, in driver lines displaying low expression of the Gal4 transactivator, gene inactivation may be insufficient to observe phenotypic effects of loss-of-function. Therefore strong Gal4 carrier lines need to be used in order to achieve high mutagenesis rates. The intra-cellular levels of Cas9 expression provided by the 5×UAS of our vector system were sufficient to induce gene inactivation in cell clones or single cells in our experiments. Nevertheless, further improvements in the Cas9 expression cassette could increase Cas9 protein levels. Recently, noncoding elements of the zebrafish genome have been used to increase expression of transgenes and have been incorporated in UAS vectors (Horstick et al. 2015). The addition of such features to our vector design may have a strong impact on the expression of the Cas9, thus leading to a more penetrant tissue-specific loss-of-function. In addition to strong and stable Cas9 expression, the generation of a high rate of biallelic mutations re-

quires highly active sgRNAs that will be facilitated by recently reported efficiency predictions (Moreno-Mateos et al. 2015). Furthermore, the design of sgRNAs recognizing genomic loci coding for essential domains of a protein would increase the possibility of inducing a null phenotype, even in the case of in-frame mutations (Shi et al. 2015). Importantly, we also show that one simple and powerful way to increase the efficiency of gene disruption is to inject the *pUAS:Cas9T2ACre;U6:sgRNA1;U6:sgRNA2* in a heterozygous mutant background, where one allele is already constitutively mutated.

In this report, we present for the first time in zebrafish a strategy to track the fate of individual genetically modified cells within a wild-type whole animal environment, thus allowing detection of cell-autonomous defects resulting from mutations. The genetic lineage tracing of potentially mutant cells allows the phenotypic analysis of cell populations of interest until adulthood, broadening the use of the 2C-Cas9 in fields ranging from stem cells and regeneration to cancer biology and aging. Finally, because none of the tools that we generated are restricted to zebrafish, similar experiments are readily possible in virtually any organism where transgenesis and DNA injection are feasible.

Methods

Fish lines and husbandry

For this study, the transgenic and mutant lines used are listed in Supplemental Table S2. Zebrafish strains were maintained according to standard protocols (Westerfield 2000).

Molecular cloning

The *Cas9T2AGFP* fragment was generated by inserting a PCR-amplified fragment containing the *T2AGFP* sequence from the *pCas9_GFP* plasmid (Addgene, #44719) into the *pCS2-nCas9n* plasmid (Addgene, #47929). Primers used (5' to 3') were *bgIII-Cas9-T2A* fwd: GGTGAGATCTCCTAAGAAGAGAAAGGTTGAGGTCCGGCGCGGAG, and *GFP XbaI* rev: AGCTTCTAGATTA CTTGTACAGCTC. *Bgl*II and *Xba*I enzymes were used to digest both plasmid and PCR product prior to ligation.

The *U6:sgRNA1* sequence was synthesized as G-block from IDT. *Bsm*BI restriction sites were introduced to clone the 20-bp target sequence at the predicted transcription start site (+1). The Gibson assembly kit (NEB) was used to clone the *U6:sgRNA1* and the *Cas9T2AGFP* fragments into a *pminiToI2* vector (Balciunas et al. 2006) containing a 5×UAS cassette and digested with *Eco*RI and *Cl*aI. Primers used were (5' to 3'): *U6* fwd: GCAATAAACCTTGTACAAAGTGGGGGATC, and *U6* rev: GAGC TCGAATTAATTCATAATTGAAAAAAGCACCCGAC to amplify the *U6:sgRNA* fragment, and *Cas9-T2A-GFP* fwd: CTGAATAGGGAA TTGGGGCCACCATGGCTTCTCCA, and *Cas9-T2A-GFP* rev: TTG TACAAGGTTTATTGCAGCTTATAATGGTTACAAATAAAG to amplify the *Cas9T2AGFP* fragment.

The second *U6:sgRNA2* cassette was designed with *S*all overhangs for insertion into the *p(UAS:Cas9T2AGFP;U6:sgRNA1)* plasmid linearized with the same enzyme. *B*saI sites were used to clone the 20-nt sgRNA target sequence at the +1 position.

The *Cas9T2ACre* fragment was synthesized by fusion of individual PCR products using Phusion High-Fidelity DNA Polymerase (Thermo Scientific). The Cre sequence was amplified from the *pCR8GW-Cre-FRT-kan-FRT 2* plasmid (Suster et al. 2011). Primers used (5' to 3') were *T2A-Cre* fwd: GAGGAAGTCTTCTAACAT GCGGTGACGTGGAGGAGAATCCCGGCCCAATGGCCAATTTAC TGACCGTACAC, and *Cre-XbaI* rev: CGATTCTAGACTAATCGCC

ATCTTCCAGC. The *Cas9T2A* fragment was amplified from the pUAS:*Cas9T2AGFP;U6:sgRNA1;U6:sgRNA2*. Primers used (5' to 3') were Cas9 KpnI fwd: GGTCGGTACCGCACTGATCAAGAAATAC, and T2A rev: GTCACCGCATGTTAGAAGACTTCC. Both fragments were fused, amplified, and inserted into the pUAS:*Cas9T2AGFP;U6:sgRNA1;U6:sgRNA2* digested with KpnI and XbaI. The sequence of all constructs was verified by sequencing.

Generation of stable transgenic lines

The *Tg(UAS:Cas9T2AGFP;U6:sgRNA1;U6:sgRNA2)* and *Tg(UAS:Cas9T2AGFP;U6:tyrsgRNA1;U6:tyrsgRNA2)* were generated by injecting the previously described plasmids into one-cell stage wild-type embryos. The *rx2:Gal4* vector was generated by three-way-Gateway cloning recombining a 5' entry vector carrying the *rx2* promoter fragment (Heermann et al. 2015) with a Gal4 middle entry, a polyA 3' entry vector, and a *myl7:eGFP-Tol2* destination vector (Kwan et al. 2007). To generate the *rpl5b:Gal4* vector, we cloned a 5700-bp promoter fragment of the ribosomal gene *rpl5b* in a 5' entry vector and recombined it with a Gal4 middle entry, a polyA 3' entry vector, and a Tol2 destination vector (Kwan et al. 2007). To generate the *Tg(-3.5Subb:loxP-lacZ-loxP-eGFP)cn2* transgenic line (also known as cn2Tg or Hulk), we used a three-way-Gateway cloning system. p5E -3.5Subb:loxP-lacZ-loxP was generated by inserting the result of digesting the iZEG plasmid (Novak et al. 2000) with XbaI and XhoI and making blunt ends into the p5E *ubi* (Mosimann et al. 2011) after being linearized with BamHI and blunting the ends. pDest *cry:GFP* was generated by inserting the result of digesting the p1 *cry:GFP* (Love et al. 2011) with SacII and making blunt ends into the pDestTol2pA2 (Kwan et al. 2007) that was linearized with BglII. The -3.5Subb:loxP-lacZ-loxP-eGFP; *cry:GFP* construct was generated combining these four plasmids into a single one using Gateway LR Clonase II, Life Technologies: p5E -3.5Subb:loxP-lacZ-loxP, pME GFP (Kwan et al. 2007), p3E pA (Kwan et al. 2007), and pDest *cry:GFP*. Stable transgenic lines were generated injecting plasmid DNA with *Tol2* mRNA transposase and founders identified by genetic crossing and transgene transmission. The *cry:GFP* cassette contained in this transgene allows the selection of transgenic embryos due to the *GFP* expression in the developing lens under the control of the *gamma-crystallin* promoter.

Injections

To test the mutagenesis efficiency of *sgRNAs*, a mixture of *sgRNA* and *Cas9* mRNA was injected into one-cell stage zebrafish embryos. The final concentration was 75 ng/μL for *sgRNA* and 150 ng/μL for *Cas9* mRNA. For Tol2-mediated transgenesis, p(UAS:*Cas9T2AGFP;U6:sgRNA1;U6:sgRNA2*) or p(UAS:*Cas9T2ACre;U6:sgRNA1;U6:sgRNA2*) were co-injected at a concentration of 30 ng/μL with the *Tol2* transposase mRNA (50 ng/μL) into the selected *Tg(Promoter:Gal4)* lines. Genomic DNA was extracted from either single embryos or pools of embryos and then used for PCR and DNA sequencing experiments.

Whole-embryos DNA extraction

For genomic DNA extraction, pools of 25 embryos at 5 dpf were digested for 1 h at 55°C in 0.5 mL lysis buffer (10 mM Tris, pH 8.0, 10 mM NaCl, 10 mM EDTA, and 2% SDS) with proteinase K (0.17 mg/mL, Roche Diagnostics). To check for frequency of indel mutations, target genomic loci were PCR-amplified using Phusion High-Fidelity DNA polymerase (Thermo Scientific). PCR amplicons were subsequently cloned into the pCR-bluntII-TOPO vector (Invitrogen). Plasmid DNA was isolated from single colonies and

sent for sequencing. Mutant alleles were identified by comparison with the wild-type sequence.

Cryosections

Embryos at the stage of 5 dpf were fixed in 4% paraformaldehyde in PBS (pH 7.4) for 2 h at room temperature and subsequently cryoprotected overnight in a 30% sucrose/0.02% sodium azide/PBS solution. Embryos were transferred to plastic molds and embedded in OCT after removal of the sucrose. The blocks were placed on dry ice before sectioning. The sections were cut with a thickness of 14 μm and mounted on Fisherbrand Superfrost plus slides (No. 12-550-15).

Immunohistochemistry

Cryosections of 5 dpf retinas were washed twice in 1× PBS/0.1% Tween-20 (PBS-T) solution. Subsequently, they were incubated 1 h at room temperature in 10% normal goat serum (Invitrogen) in PBS-T blocking solution followed by overnight incubation with 1/500 dilution of chicken primary anti-GFP (Genetex) or mouse anti-Parvalbumin antibody (Millipore). The Alexa Fluor 488 secondary antibody goat anti-chicken IgG or the Alexa Fluor 568 secondary antibody goat anti-mouse IgG (1/500, Molecular Probes) and a 1/500 dilution of DAPI (50 μg/μL) in blocking solution were added for 2 h at room temperature. After five washings in wash buffer (1× PBS/0.1% Tween-20) coverslips were placed on the slides after addition of Vectashield drops. Slides were left at room temperature for 1 h before microscopy analysis.

sgRNAs and Cas9 mRNA generation

sgRNA sequences (listed in Supplemental Table S1) were cloned into the BsaI-digested pDR274 (Addgene, #42250) vector. The *sgRNAs* were synthesized by in vitro transcription (using the Megascript T7 transcription kit #AM1334, Ambion). After transcription, *sgRNAs* were purified using an RNAeasy Mini Kit (Qiagen). The quality of purified *sgRNAs* was checked by electrophoresis on a 2% agarose gel. As a control, we used RFP-specific *sgRNAs*, whose sequence is not present in the fish genome (Supplemental Table S1). *Cas9* mRNA was generated as described previously (Hwang et al. 2013a).

FACS

Fluorescent *Cas9*-expressing cells were isolated from wild-type cells by fluorescence-activated cell sorting. 3 dpf embryos were dissociated as previously described by Manoli and Driever (2012). Cell sorting was performed on FACS Aria (BD Biosciences), and data were analyzed using FACSDiva version 6.1.2 (BD Biosciences). The GFP fluorescence was detected in the gfpBlue-B-530/30-A channel. GFP-positive and -negative cells were sorted in lysis buffer provided in the NucleoSpin Tissue Kit (Macherey-Nagel), and genomic DNA was extracted with the same kit. PCR on target genomic loci and DNA sequencing were performed as described above.

Microscopy

Low magnification images were acquired with a Leica MZ FLIII stereomicroscope (Leica) equipped with a Leica DFC310FX digital camera (Leica). Whole-eye pictures were taken with a Leica upright wide-field epifluorescence microscope using a 20× oil immersion objective. A Zeiss LSM 780 confocal microscope (Zeiss) was used for confocal microscopy, employing a 40× water immersion or 10× objective. Z-volumes were acquired with a 1- to 2-μm

resolution, and images were processed using ImageJ, Adobe Photoshop, and Adobe Illustrator software.

Data access

The sequences of mutant *tyr* clones from this study have been submitted to the NCBI GenBank (<http://www.ncbi.nlm.nih.gov/genbank/>) under accession numbers KU751772–KU751776. The sequences and the maps relative to the plasmids pUAS: *Cas9T2AGFP;U6:sgRNA1;U6:sgRNA2* and pUAS: *Cas9T2ACre;U6:sgRNA1;U6:sgRNA2* are available in Addgene (<https://www.addgene.org>). Plasmid numbers are #74009 and #74010.

Acknowledgments

We thank Allison Bardin, Allison Mallory, Yohanns Bellaiche, Christoph Gebhardt, Shahad Albadri, Celine Revenu, and Valerie Bercier for critical reading of the manuscript. We also thank Herwig Baier, Estuardo Robles, Joachim Wittbrodt, Koichi Kawakami, Claire Wyatt, Nadine Peyri ras, and Georges Lutfalla for sharing reagents and transgenic lines. We thank all members of the Del Bene lab for fruitful discussions. We thank the Developmental Biology Curie imaging facility (PICT-IBISA@BDD, Paris, France, UMR3215/U934) member of the France-BioImaging national research infrastructure for their help and advice with confocal microscopy and the Flow Cytometry and Cell Sorting Platform at Institute Curie for their expertise. The Del Bene laboratory “Neural Circuits Development” is part of the Laboratoire d’Excellence (LABEX) entitled DEEP (ANR -11-LABX-0044), and of the  cole des Neurosciences de Paris Ile-de-France network. V.D.D. was supported by a doctoral fellowship of the Fondation Pierre-Gilles de Gennes pour la recherche and Fondation Recherche Medicale (FRM) 4th year doctoral fellowship. F.D.S. was supported by a doctoral fellowship of the Curie International PhD program. T.O.A. was supported by a Boehringer Ingelheim Fonds PhD fellowship. H.S. was funded through FPU12/03007. This work has been supported by an ATIP/AVENIR program starting grant (F.D.B.), ERC-StG #311159-Zebrarectum (F.D.B.), ANR-II-INBS-0014 (J.P.C.), CNRS, INSERM, Institut Curie (F.D.B.), and Mus um National d’Histoire Naturelle (J.P.C.) core funding, the Fundaci n CNIC Carlos III (N.M.), the Fundaci n ProCNIC (N.M.), the Spanish Ministry of Economy and Competitiveness (Tercel and BFU2011-25297) (N.M.), and ERC Starting grant 337703 – zebraHeart (N.M.).

Author contributions: V.D.D., F.D.S., T.O.A., J.P.C., and F.D.B. conceived and designed experiments. V.D.D., F.D.S., and N.T. performed molecular cloning experiments. V.D.D. and F.D.S. performed microinjections, immunohistochemistry, and imaging experiments. T.O.A. generated essential transgenic lines. V.D.D. and F.D.S. analyzed the data. V.D.D., F.D.S., J.P.C., and F.D.B. wrote the manuscript with inputs from all the coauthors. H.S. and N.M. provided essential unpublished reagents (*Tgf-3.Subb:loxP-lacZ-loxP-eGFP* *cn2* transgenic line).

References

Ablain J, Durand EM, Yang S, Zhou Y, Zon LI. 2015. A CRISPR/Cas9 vector system for tissue-specific gene disruption in zebrafish. *Dev Cell* **32**: 756–764.
 Akitake CM, Macurak M, Halpern ME, Goll MG. 2011. Transgenerational analysis of transcriptional silencing in zebrafish. *Dev Biol* **352**: 191–201.
 Amsterdam A, Nissen RM, Sun Z, Swindell EC, Farrington S, Hopkins N. 2004. Identification of 315 genes essential for early zebrafish development. *Proc Natl Acad Sci* **101**: 12792–12797.
 Asakawa K, Kawakami K. 2008. Targeted gene expression by the Gal4-UAS system in zebrafish. *Dev Growth Differ* **50**: 391–399.

Asakawa K, Suster ML, Mizusawa K, Nagayoshi S, Kotani T, Urasaki A, Kishimoto Y, Hibi M, Kawakami K. 2008. Genetic dissection of neural circuits by *Tol2* transposon-mediated Gal4 gene and enhancer trapping in zebrafish. *Proc Natl Acad Sci* **105**: 1255–1260.
 Auer TO, Duroure K, Concordet JP, Del Bene F. 2014a. CRISPR/Cas9-mediated conversion of *eGFP* into *Gal4*-transgenic lines in zebrafish. *Nat Protoc* **9**: 2823–2840.
 Auer TO, Duroure K, De Cian A, Concordet JP, Del Bene F. 2014b. Highly efficient CRISPR/Cas9-mediated knock-in in zebrafish by homology-independent DNA repair. *Genome Res* **24**: 142–153.
 Auer TO, Xiao T, Bercier V, Gebhardt C, Duroure K, Concordet JP, Wyatt C, Suster M, Kawakami K, Wittbrodt J, et al. 2015. Deletion of a kinesin I motor unmasks a mechanism of homeostatic branching control by neurotrophin-3. *eLife* **4**. doi: 10.7554/eLife.05061.
 Balciunas D, Wangenstein KJ, Wilber A, Bell J, Geurts A, Sivasubbu S, Wang X, Hackett PB, Largaespada DA, McIvor RS, et al. 2006. Harnessing a high cargo-capacity transposon for genetic applications in vertebrates. *PLoS Genet* **2**: e169.
 Balciunienė J, Nagelberg D, Walsh KT, Camerota D, Georgette D, Biemar F, Bellipanni G, Balciunas D. 2013. Efficient disruption of Zebrafish genes using a Gal4-containing gene trap. *BMC Genomics* **14**: 619.
 Branda CS, Dymecki SM. 2004. Talking about a revolution: the impact of site-specific recombinases on genetic analyses in mice. *Dev Cell* **6**: 7–28.
 Camp E, Lardelli M. 2001. Tyrosinase gene expression in zebrafish embryos. *Dev Genes Evol* **211**: 150–153.
 Campbell PD, Marlow FL. 2013. Temporal and tissue specific gene expression patterns of the zebrafish *kinesin-1* heavy chain family, *kif5s*, during development. *Gene Expr Patterns* **13**: 271–279.
 Cho SW, Kim S, Kim JM, Kim JS. 2013. Targeted genome engineering in human cells with the Cas9 RNA-guided endonuclease. *Nat Biotechnol* **31**: 230–232.
 Chuang JC, Raymond PA. 2001. Zebrafish genes *rx1* and *rx2* help define the region of forebrain that gives rise to retina. *Dev Biol* **231**: 13–30.
 Cong L, Ran FA, Cox D, Lin S, Barretto R, Habib N, Hsu PD, Wu X, Jiang W, Marraffini LA, et al. 2013. Multiplex genome engineering using CRISPR/Cas systems. *Science* **339**: 819–823.
 Davison JM, Akitake CM, Goll MG, Rhee JM, Gosse N, Baier H, Halpern ME, Leach SD, Parsons MJ. 2007. Transactivation from Gal4-VP16 transgenic insertions for tissue-specific cell labeling and ablation in zebrafish. *Dev Biol* **304**: 811–824.
 Halbig KM, Lekven AC, Kunkel GR. 2008. Zebrafish *U6* small nuclear RNA gene promoters contain a SPH element in an unusual location. *Gene* **421**: 89–94.
 Heermann S, Schutz L, Lemke S, Kriegstein K, Wittbrodt J. 2015. Eye morphogenesis driven by epithelial flow into the optic cup facilitated by modulation of bone morphogenetic protein. *eLife* **4**. doi: 10.7554/eLife.05216.
 Horstick EJ, Jordan DC, Bergeron SA, Tabor KM, Serpe M, Feldman B, Burgess HA. 2015. Increased functional protein expression using nucleotide sequence features enriched in highly expressed genes in zebrafish. *Nucleic Acids Res* **43**: e48.
 Hwang WY, Fu Y, Reyon D, Maeder ML, Kaini P, Sander JD, Joung JK, Peterson RT, Yeh JR. 2013a. Heritable and precise zebrafish genome editing using a CRISPR-Cas system. *PLoS One* **8**: e68708.
 Hwang WY, Fu Y, Reyon D, Maeder ML, Tsai SQ, Sander JD, Peterson RT, Yeh JR, Joung JK. 2013b. Efficient genome editing in zebrafish using a CRISPR-Cas system. *Nat Biotechnol* **31**: 227–229.
 Jao LE, Wente SR, Chen W. 2013. Efficient multiplex biallelic zebrafish genome editing using a CRISPR nuclease system. *Proc Natl Acad Sci* **110**: 13904–13909.
 Kawakami K. 2004. Transgenesis and gene trap methods in zebrafish by using the *Tol2* transposable element. *Methods Cell Biol* **77**: 201–222.
 Kawakami K, Abe G, Asada T, Asakawa K, Fukuda R, Ito A, Lal P, Mouri N, Muto A, Suster ML, et al. 2010. zTrap: zebrafish gene trap and enhancer trap database. *BMC Dev Biol* **10**: 105.
 Kay JN, Finger-Baier KC, Roeser T, Staub W, Baier H. 2001. Retinal ganglion cell genesis requires *lakritz*, a zebrafish *atonal* homolog. *Neuron* **30**: 725–736.
 Kim JH, Lee SR, Li LH, Park HJ, Park JH, Lee KY, Kim MK, Shin BA, Choi SY. 2011. High cleavage efficiency of a 2A peptide derived from porcine teschovirus-1 in human cell lines, zebrafish and mice. *PLoS One* **6**: e18556.
 Kwan KM, Fujimoto E, Grabher C, Mangum BD, Hardy ME, Campbell DS, Parant JM, Yost HJ, Kanki JP, Chien CB. 2007. The Tol2kit: a multisite gateway-based construction kit for *Tol2* transposon transgenesis constructs. *Dev Dyn* **236**: 3088–3099.
 Livesey FJ, Cepko CL. 2001. Vertebrate neural cell-fate determination: lessons from the retina. *Nat Rev Neurosci* **2**: 109–118.
 Livet J. 2007. [The brain in color: transgenic “Brainbow” mice for visualizing neuronal circuits]. *Med Sci (Paris)* **23**: 1173–1176.

- Love NR, Thuret R, Chen Y, Ishibashi S, Sabherwal N, Paredes R, Alves-Silva J, Dorey K, Noble AM, Guille MJ, et al. 2011. pTtransgenesis: a cross-species, modular transgenesis resource. *Development* **138**: 5451–5458.
- Mali P, Yang L, Esvelt KM, Aach J, Guell M, DiCarlo JE, Norville JE, Church GM. 2013. RNA-guided human genome engineering via Cas9. *Science* **339**: 823–826.
- Manoli M, Driever W. 2012. Fluorescence-activated cell sorting (FACS) of fluorescently tagged cells from zebrafish larvae for RNA isolation. *Cold Spring Harb Protoc* **2012**. doi: 10.1101/pdb.prot069633.
- Moreno-Mateos MA, Vejnar CE, Beaudoin JD, Fernandez JP, Mis EK, Khokha MK, Giraldez AJ. 2015. CRISPRscan: designing highly efficient sgRNAs for CRISPR-Cas9 targeting *in vivo*. *Nat Methods* **12**: 982–988.
- Mosimann C, Kaufman CK, Li P, Pugach EK, Tamplin OJ, Zon LI. 2011. Ubiquitous transgene expression and Cre-based recombination driven by the *ubiquitin* promoter in zebrafish. *Development* **138**: 169–177.
- Nevin LM, Taylor MR, Baier H. 2008. Hardwiring of fine synaptic layers in the zebrafish visual pathway. *Neural Dev* **3**: 36.
- Novak A, Guo C, Yang W, Nagy A, Lobe CG. 2000. Z/EG, a double reporter mouse line that expresses enhanced green fluorescent protein upon Cre-mediated excision. *Genesis* **28**: 147–155.
- Pan X, Wan H, Chia W, Tong Y, Gong Z. 2005. Demonstration of site-directed recombination in transgenic zebrafish using the Cre/loxP system. *Transgenic Res* **14**: 217–223.
- Pan YA, Freundlich T, Weissman TA, Schoppik D, Wang XC, Zimmerman S, Ciruna B, Sanes JR, Lichtman JW, Schier AF. 2013. Zebrafish: multispectral cell labeling for cell tracing and lineage analysis in zebrafish. *Development* **140**: 2835–2846.
- Perrimon N. 1998. Creating mosaics in *Drosophila*. *Int J Dev Biol* **42**: 243–247.
- Platt RJ, Chen S, Zhou Y, Yim MJ, Swiech L, Kempton HR, Dahlman JE, Parnas O, Eisenhaure TM, Jovanovic M, et al. 2014. CRISPR-Cas9 knockin mice for genome editing and cancer modeling. *Cell* **159**: 440–455.
- Port F, Chen HM, Lee T, Bullock SL. 2014. Optimized CRISPR/Cas tools for efficient germline and somatic genome engineering in *Drosophila*. *Proc Natl Acad Sci* **111**: E2967–E2976.
- Provost E, Rhee J, Leach SD. 2007. Viral 2A peptides allow expression of multiple proteins from a single ORF in transgenic zebrafish embryos. *Genesis* **45**: 625–629.
- Robles E, Filosa A, Baier H. 2013. Precise lamination of retinal axons generates multiple parallel input pathways in the tectum. *J Neurosci* **33**: 5027–5039.
- Scott EK, Baier H. 2009. The cellular architecture of the larval zebrafish tectum, as revealed by Gal4 enhancer trap lines. *Front Neural Circuits* **3**: 13. doi: 10.3389/neuro.04.013.2009.
- Scott EK, Mason L, Arrenberg AB, Ziv L, Gosse NJ, Xiao T, Chi NC, Asakawa K, Kawakami K, Baier H. 2007. Targeting neural circuitry in zebrafish using GAL4 enhancer trapping. *Nat Methods* **4**: 323–326.
- Shen Z, Zhang X, Chai Y, Zhu Z, Yi P, Feng G, Li W, Ou G. 2014. Conditional knockouts generated by engineered CRISPR-Cas9 endonuclease reveal the roles of Coronin in *C. elegans* neural development. *Dev Cell* **30**: 625–636.
- Shi J, Wang E, Milazzo JP, Wang Z, Kinney JB, Vakoc CR. 2015. Discovery of cancer drug targets by CRISPR-Cas9 screening of protein domains. *Nat Biotechnol* **33**: 661–667.
- Sprague J, Bayraktaroglu L, Bradford Y, Conlin T, Dunn N, Fashena D, Frazer K, Haendel M, Howe DG, Knight J, et al. 2008. The Zebrafish Information Network: The zebrafish model organism database provides expanded support for genotypes and phenotypes. *Nucleic Acids Res* **36**: D768–D772.
- Suster ML, Abe G, Schouw A, Kawakami K. 2011. Transposon-mediated BAC transgenesis in zebrafish. *Nat Protoc* **6**: 1998–2021.
- Westerfield M. 2000. *The zebrafish book. A guide for the laboratory use of zebrafish (Danio rerio)*, 4th ed. University of Oregon Press, Eugene, OR.
- Wijgerde M, McMahon JA, Rule M, McMahon AP. 2002. A direct requirement for Hedgehog signaling for normal specification of all ventral progenitor domains in the presumptive mammalian spinal cord. *Genes Dev* **16**: 2849–2864.
- Yin L, Maddison LA, Li M, Kara N, LaFave MC, Varshney GK, Burgess SM, Patton JG, Chen W. 2015. Multiplex conditional mutagenesis using transgenic expression of Cas9 and sgRNAs. *Genetics* **200**: 431–441.

Received June 22, 2015; accepted in revised form February 24, 2016.



2C-Cas9: a versatile tool for clonal analysis of gene function

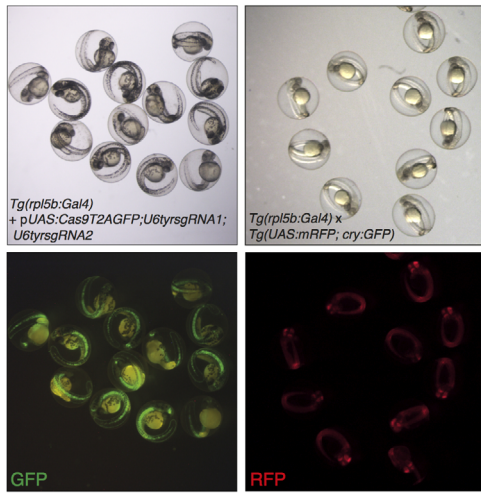
Vincenzo Di Donato, Flavia De Santis, Thomas O. Auer, et al.

Genome Res. 2016 26: 681-692 originally published online March 8, 2016
Access the most recent version at doi:[10.1101/gr.196170.115](https://doi.org/10.1101/gr.196170.115)

Supplemental Material	http://genome.cshlp.org/content/suppl/2016/04/08/gr.196170.115.DC1
References	This article cites 52 articles, 18 of which can be accessed free at: http://genome.cshlp.org/content/26/5/681.full.html#ref-list-1
Creative Commons License	This article is distributed exclusively by Cold Spring Harbor Laboratory Press for the first six months after the full-issue publication date (see http://genome.cshlp.org/site/misc/terms.xhtml). After six months, it is available under a Creative Commons License (Attribution-NonCommercial 4.0 International), as described at http://creativecommons.org/licenses/by-nc/4.0/ .
Email Alerting Service	Receive free email alerts when new articles cite this article - sign up in the box at the top right corner of the article or click here .

To subscribe to *Genome Research* go to:
<http://genome.cshlp.org/subscriptions>

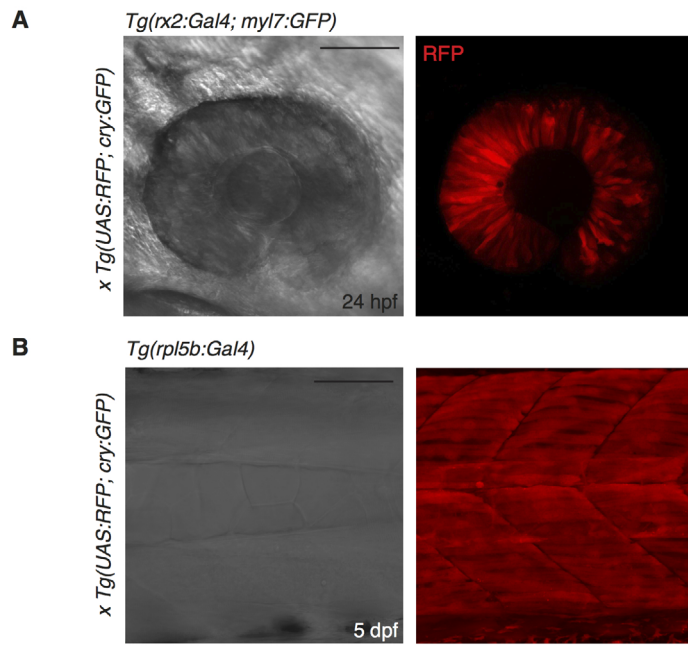
A



B

Target 1 mutations

5'-AGCGTTTGGACTGGAGGACTTCTGGGGAGGTGCAGACT-3'
5'-AGCGTTTGGACTGGAGGACTTCTG ----- ACT-3' Δ11 (x3)
5'-AGCGTTTGGACTGGAGGACTTCTGGGG - TGTGCAGACT-3' Δ2; +1



Supplementary Figure 2

sgRNA name	Target gene	Target sequence	Mutagenesis efficiency
TyrsgRNA1	Tyrosinase	GGACTGGAGGACTTCTGGGG	90% (18/20)
TyrsgRNA2	Tyrosinase	GGCGTTTCTGCCTTGGCATC	10% (2/20)
Ath5sgRNA1	Ath5	GGCATATAAACCCAATCCAC	20% (4/20)
Ath5sgRNA2	Ath5	GGCCGAGCTGTGCAGACTCC	13% (4/32)
Kif5aasgRNA1	Kif5aa	GGAATGATGCCCATCTGCTG	22% (4/18)
Kif5aasgRNA2	Kif5aa	GGGACGACACGGTCATCATC	38% (6/16)
Pvalb6sgRNA	Pvalb6	CGCTATTGTCGGCATCCAGG	47% (9/19)
ctlsgRNA1	RFP	GGCCACGAGTTCGAGATCGA	-
ctlsgRNA2	RFP	GGACATCACCTCCCACAACG	-

Transgenic or mutant zebrafish line used in this study	Gene	Description	Original Reference
<i>kif5aa</i> ^{*162 +/-}	<i>kif5aa</i>	TALEN mediated loss-of-function allele of <i>kif5aa</i> .	(Auer et al., 2015)
<i>Tg(isl2b:Gal4)</i>		A promoter fragment of the <i>isl2b</i> gene drives expression of the Gal4 transactivator in the entire RGC population of the retina.	(Ben Fredj et al., 2010)
<i>Tg(gSA2AzGFF49A)</i>		Transgenic line generated by gene-trap approach. An optimized version of the Gal4 (GFF) is expressed in periventricular neurons (PVNs) at the level of the optic tectum (OT).	(Muto et al., 2013)
<i>Tg(rpl5b:Gal4)</i>		A promoter fragment of the <i>rpl5b</i> ribosomal gene drives quasi-ubiquitous expression of the <i>Gal4</i> transactivator.	generated in this report
<i>Tg(s1020t)</i>		Transgenic line generated by an enhancer-trap screen. <i>Gal4</i> is expressed in the thalamus, spinal cord and bipolar cells of the retina.	(Scott and Baier, 2009)
<i>Tg(mnx1:Gal4)</i>		A promoter containing three copies of the <i>mnx1</i> enhancer drives the expression of <i>Gal4</i> in spinal cord primary motor neurons.	(Zelenchuch and Brusés, 2011)
<i>Tg(rx2:Gal4; myl7:GFP)</i>		A promoter fragment of the <i>rx2</i> gene drives expression of <i>Gal4</i> in retinal progenitors. The heart-specific promoter <i>myl7</i> drives <i>GFP</i> (<i>myl7:GFP</i>) as transgenesis marker.	generated in this report
<i>Tg(UAS:Cas9T2AGF-P;U6sgRNA1;U6sgRNA2)</i>		The simultaneous expression of the <i>Cas9</i> endonuclease and the <i>GFP</i> reporter depends on the activation of an UAS. Two sgRNAs empty expression cassettes are present.	generated in this report
<i>Tg(UAS:Cas9T2AGF-P;U6tyrsgRNA1;U6tyrsgRNA2)</i>	<i>tyr</i>	The simultaneous expression of the <i>Cas9</i> endonuclease and the <i>GFP</i> reporter depends on the activation of an UAS. Two <i>U6</i> promoter sequences drive the transcription of sgRNAs targeting the <i>tyrosinase</i> gene.	generated in this report
<i>Tg(-3.5ubb:loxP-lacZ-loxP-eGFP)cn2</i>		The ubiquitin promoter (Mosimann et al, 2011) is placed 5' of a floxed lacZ sequence followed by GFP cDNA. Expression of <i>GFP</i> in the lens driven by a crystalline promoter fragment (<i>cry</i>) is used as transgenesis reporter.	generated in this report
<i>Tg(UAS:Brb1.0L)^{s1997t}</i>		The expression of a Brainbow cassette (Pan et al., 2013) is dependent of the activation of an upstream activator sequence (UAS).	(Robles et al., 2013)
<i>Tg(UAS:RFP; cry:GFP)</i>		A UAS drives the Gal4-mediated transcription of the cDNA sequence of the red fluorescent protein (RFP). Expression of <i>GFP</i> in the lens driven by a crystalline promoter fragment (<i>cry</i>) is used as transgenesis reporter.	(Auer et al., 2014)

Supplementary Legends

Figure S1 Mutagenesis efficiency at the *tyr* locus in the *Tg(rpl5b:Gal4)* line

(A) Left panel: whole mount image of *Tg(rpl5b:Gal4)* embryos transiently expressing the *pUAS:Cas9T2AGFP;U6:tyrsgRNA1;U6:tyrsgRNA2* used for FACS analysis. Right panel: double transgenic *Tg(rpl5b:Gal4) x Tg(UAS:RFP; cry:GFP)* larvae. RFP is used as an independent reporter of Gal4 transactivation and confirms non-ectopic expression of the *pUAS:Cas9T2AGFP;U6:tyrsgRNA1;U6:tyrsgRNA2*.

(B) Representative mutations at the *tyr* locus.

Figure S2 *Gal4* expression domains in the *Tg(rx2:Gal4; myl7:GFP)* and *Tg(rpl5b:Gal4)* lines

(A) Confocal image of Gal4-induced eye-specific expression of *UAS:RFP* in a 24 hpf double transgenic *Tg(rx2:Gal4; myl7:GFP) x Tg(UAS:RFP; cry:GFP)* embryo. Scale bar: 100 μ m.

(B) Confocal image of muscle cells expressing *UAS:RFP* in a 5 dpf double transgenic *Tg(rpl5b:Gal4) x Tg(UAS:RFP; cry:GFP)* embryo. Scale bar: 50 μ m.

Table S1 Sequence and efficiency of the sgRNAs used in this study.

The mutagenesis rate was assessed by injection of in vitro transcribed sgRNA with synthetic Cas9 mRNA into one-cell stage wild-type embryos. To estimate the number of mutations induced we extracted DNA from a pool of 25 injected embryos and subsequently PCR amplified the targeted locus. Single PCR amplicons were sequenced and mutant alleles were identified after alignment with the wild-type sequence.

Table S2 Transgenic lines used in the report

Summary

The establishment of proper neuronal connections in the embryonic brain relies on the ability of differentiated neurons to extend their axons in the direction of their correct synaptic partners. This task is controlled by midline-produced molecular cues in the extracellular environment providing directional information to navigating axons.

In this study, we explore the possibility that the proteins belonging to the *Metrn* family play a role in the regulation of axonal pathfinding.

Results:

We show that the *metrn* gene family is conserved across vertebrates and represent a family of secreted factors with a still unknown function.

We demonstrated that zebrafish *metrn* genes are expressed in the embryonic CNS along the midline and at the floor plate, an expression pattern coherent with a possible role in axon guidance.

We generated and analysed LOF alleles for the three zebrafish paralogues, proving that *metrns* inactivation affects the navigation path of different neuronal populations. In particular, our results suggest that these proteins are implicated in the patterning of the AC, in the laminar organization of RGC axonal projections and in the fasciculation of trigeminal axons.

In conclusion, we described a functional role for a new class of proteins providing data supporting their implication in the modulation of axonal pathfinding.

Meteorins are conserved midline-secreted proteins regulating axonal pathfinding in the Zebrafish nervous system

Flavia De Santis¹, Natalia Belen Beiza-Canelo¹, Vincenzo Di Donato¹, Karine Duroure¹, Thomas Auer², Filippo Del Bene¹

1. Institut Curie, PSL Research University, INSERM, U 934, CNRS UMR3215, F-75005, Paris, France.5. Muséum National d'Histoire naturelle, Paris F-75231, France

2. Center for Integrative Genomics, Faculty of Biology and Medicine, University of Lausanne, Lausanne, Switzerland

Abstract

In the embryonic nervous system axons are guided toward their specific targets by attractive and repulsive cues in the extracellular environment. Here, we present a family of secreted proteins (the Meteorin family) whose members represents novel uncharacterized molecules involved in the process of axon guidance. We investigated the role of Meteorin proteins in directing the navigation of axonal projections in the developing nervous system of zebrafish embryos, identifying a number of axonal tracts responsive to the Meteorin signal. We demonstrated that, if Meteorin function is disrupted, axons from the anterior commissure, the retinal ganglion cells and the trigeminal neurons display several navigation errors, supporting a model where Meteorin proteins are new players involved in the process of axonal pathfinding.

Introduction

A functional nervous system is composed by a stereotyped pattern of neuronal circuits in which different populations of neurons are linked to each other by specific synaptic contacts. The central nervous system (CNS) of bilateral organisms is composed by a combination of commissural circuits, connecting the left and right side of the brain, and ipsilateral connections, established by neurons located on the same side of the longitudinal body axis. Importantly, a precise balance of commissural and non-commissural connections is essential to the CNS physiology and is needed for the proper integration of sensory stimuli/inputs (Nugent, Kolpak et al. 2012, Van Battum, Brignani et al. 2015). The assembly of the brain wiring pattern starts during the early stages of embryonic

development, when differentiated neurons begin to extend their axons and to elongate them toward their correct synaptic partner. While navigating along their path, axons are exposed to environmental attractive and repulsive guidance cues, most of which are produced by specialized cells located at the midline. In the past three decades, our understanding of the process of axon guidance at the CNS midline has progressed rapidly from the identification of specific molecules modulating axon navigation choices (e.g. Netrins, Slits, Ephrins, Semaphorins) to the description of guidance mechanisms that seem highly conserved across evolution (Dickson 2002, Nawabi and Castellani 2011). Despite the great advance in the axon guidance field, a comprehensive picture of this process is far to be completed and additional molecular players still need to be identified to reach a deeper understanding of this extremely complex and finely regulated biological phenomenon.

We have recently identified a new family of midline-secreted factors (the *meteorin* family) whose members represent promising candidates to be part of the complex repertoire of molecules regulating axonal navigation. Meteorin (Metrn) was first discovered as a secreted neurotrophic factor expressed by radial glia and neuronal progenitors in mouse embryos (Nishino, Yamashita et al. 2004, Jorgensen, Thompson et al. 2009). It has been reported that, *in vitro*, Metrn is able to modulate the processes of neurons/glia differentiation and neurite outgrowth (Lee, Han et al. 2010). A close homolog of Metrn, named Meteorin-like 1 (Metrn1, also known as Cometin or Subfatin), has been identified as a downstream target of Pax2/5/8 signaling during otic vesicle development (Ramialison, Bajoghli et al. 2008) and later found to have neurotrophic properties comparable to the ones of Metrn (Jorgensen, Fransson et al. 2012). Both Metrn and Metrn1 promote axonal extension, and appear associated with the JAK/STAT and MEK/ERK pathways *via* the activation of a still unknown receptor. Importantly, *metrn1* knockdown has been shown to influence axonal development by inhibiting NGF-induced neurite elongation, *in vitro* (Watanabe, Akimoto et al. 2012). Both proteins are also expressed in other organs and, recently, Metrn1 has been recognized as a cytokine-like protein regulating thermogenesis and anti-inflammatory processes in the adipose tissue (Rao, Long et al. 2014). Interestingly, a cleaved fragment of the guidance molecule Slit2 (Slit2-C) have been recently shown to exert the same function in this tissue (Svensson, Long et al. 2016).

By using the zebrafish as a model, we investigated the possibility that Meteorin proteins have a role in the embryonic development of the

CNS, focusing our attention on their potential function in the process of axon guidance. Taken together our results suggest that Meteorins activity is involved, *in vivo*, in the regulation of axonal navigation and in the definition of the proper organization of different axon tracts in the embryonic zebrafish brain.

Results

Meteorin gene family is conserved among vertebrates

With the objective of identifying novel midline-secreted molecules regulating the process of axonal development and pathfinding, we performed a candidate gene approach that raised our attention on the *meteorin* gene family. Due to their strong expression in the mouse embryonic CNS and their positive impact on axonal elongation *in vitro* (Nishino, Yamashita et al. 2004), we speculated that Meteorin proteins might have a conserved role during embryonic brain development and we reasoned that their activity might influence axonal elongation, *in vivo*. To verify the conservation of the *meteorin* gene family across different organisms, we took advantage of the *Ensembl* and NCBI databases in order to find genes annotated as *meteorin* or *meteorin-like* in different species. Interestingly, we found *meteorin* genes exclusively in organisms belonging to different classes of vertebrates (including mammals, bony fishes, birds, reptiles and amphibians), indicating that *metrns* are vertebrate-specific genes. This finding would be in sharp contrast with many other well-characterized players on axon guidance (e.g. Netrins, Slits, Ephrins, Semaphorins, among others), which are conserved in function and biochemical pathway among metazoans. In mammals, the *metrn* gene family includes two annotated members (*meteorin*, *metrn* and *meteorin-like metrn1*) while it only counts one gene in *Xenopus leavis* (*metrn1*) and three in zebrafish (*metrn*, *metrn11* and *metrn12*) (Figure 1A).

A comparative analysis between the sequences of the human, mouse and zebrafish *Metrns* revealed that homologues and paralogues proteins display overall about the 50% of identity and a higher level of similarity (Figure 1B). This high degree of sequence conservation suggests a likely common biological function for *Metrn* proteins. All *Metrns* are small proteins (of about 300 amino acids) and contain a short N-terminal signal

peptide responsible for the secretion in the extracellular environment. In order to understand if *Metrn* aminoacidic sequences encode for conserved protein domains, we analyzed the human, mouse and zebrafish *Metrn* and *Metrn1* sequences on the online NCBI conserved domain database (<https://www.ncbi.nlm.nih.gov/Structure/bwrpsb/bwrpsb.cgi>). Interestingly, we could detect a Netrin-like domain (NTR-like) in the C-terminal half of the zebrafish *Metrn1*. This domain, present in Netrins and other proteins including complement proteins, tissue inhibitors of metalloproteases (TIMP), and procollagen C-proteinase enhancers (PCOLCE), has been shown to mediate the binding to extracellular matrix components like Heparan sulfate proteoglycans (HSPG) (Banyai and Patthy 1999, Kappler, Franken et al. 2000). Given the high conservation of this region among paralogues and orthologues Meteorins (Figure 1B) it is likely that this domain is present and conserved in other family members but not detected by our preliminary bioinformatic approach.

Overall, our analysis confirmed that the *metrn* gene family is conserved among vertebrates and suggests that these proteins might share the same role in different species.

***meteorin* genes are expressed in the CNS and at the midline in zebrafish embryos**

After having confirmed that the *metrn* family is conserved across vertebrates, we wondered whether the expression pattern of its genes is also preserved in different species. Specifically, we focused our attention on the zebrafish *metrns*, as this model system is particularly suited for the study of the mechanisms regulating embryonic brain development in vertebrates. It has been reported that *metrns* are highly expressed by neural and glial progenitors in the central and peripheral nervous system of mouse embryos. To verify that a comparable expression exists in zebrafish, we performed *in situ* hybridization experiments at different stages of embryonic development. High level of all *metrns* could be detected in the CNS of 24 hpf larvae (Figure 2A,B,C upper panels). At this stage *metrn* and *metrn2* mRNA displayed a broad expression in the embryonic brain while a stronger *metrn1* signal could be detected at the midbrain/hindbrain boundary, in the presumptive otic vesicles and at boundary regions between hindbrain rhombomeres. The expression pattern became more restricted for all the genes starting from 48 hpf,

when *metrn* and *metrn11* mRNAs were distinguishable along the midline and in periventricular regions of the CNS while *metrn12* transcripts mostly localized at the somite boundaries and in the otic vesicles (Figure 2A,B,C lower panels and Figure D,E). At later stages the expression pattern of *metrns* in the CNS strongly decreased (data not shown), suggesting that the function of these proteins in the CNS is accomplished in the earliest phases of brain development, when the basic layout of the main axonal connections is established. Interestingly, as in mouse, *metrn* and *metrn11* expression is abundant in regions enriched of neural and glial progenitors and, most importantly, the expression along the midline and at the floor plate is consistent with a role of Metrns proteins in the modulation of axonal elongation. Indeed, the expression of *metrn11* at the floorplate is highly reminiscent of the one of other guidance factors, including *slits*. To confirm that *metrn11* and *slits* are, at least partially, expressed by the same cell populations, we performed a double fluorescent *in situ* hybridization demonstrating that *metrn11* nicely co-localizes with tree out of the four zebrafish *slit* paralogues at the hindbrain floorplate (Figure 2F,G,H). This suggests that *metrns* and *slits* might have a similar role in the patterning of the embryonic nervous system, supporting our idea of Metrns being involved in axonal pathfinding.

***metrn* mutants are adult viable**

We speculated that, if Metrns are involved in axon elongation, axon tracts extending in the close proximity of *metrn*-expressing domains should be sensitive to their signaling and would display navigation errors in case of gene inactivation. To explore this possibility, we took advantage of the CRISPR/Cas9 technology to generate LOF alleles for all the three *metrn* paralogues existing in the zebrafish genome. We targeted the second exon of each gene, thus inducing out-of-frame deletions leading to the formation of a premature STOP codon (figure 3 A,B,C,D,E,F). Furthermore, by performing qPCR experiments, we verified that this mutagenic approach resulted in the generation of null alleles, as, at 24 hpf, *metrns* gene expression is strongly reduced in triple mutant embryos compared to wild type, thus suggesting that that the mRNA produced by the targeted locus is degraded by non-sense-mediated decay (relative gene expression in *metrn* triple mutants compared to wild type: *metrn*=19,85+/-4,95%; *metrn11*=22,11+/-3,89%; *metrn12*=12,42+/-2,57%) (figure 3G).

In contrast to what previously reported for mouse, where *metrn* gene disruption results in an early embryonic lethality due to gastrulation defects (Kim, Moon et al. 2014), all single (*metrn*^{-/-}; *metrn11*^{-/-}; *metrn12*^{-/-}), double (*metrn*^{-/-}, *metrn11*^{-/-}; *metrn*^{-/-}, *metrn12*^{-/-}; *metrn11*^{-/-}, *metrn12*^{-/-}) and triple (*metrn*^{-/-}, *metrn11*^{-/-}, *metrn12*^{-/-}) mutant zebrafish lines are adult viable, allowing for the assessment of later phenotypes in the developing and mature CNS.

We therefore decided to analyze the effect of *metrn* LOF in different neuronal population, focusing on the formation of their axonal projections. In order to avoid compensation effects, we decided to perform the phenotypic analysis of *metrns* LOF starting from the triple mutants, subsequently assessing the specific contribution of each *metrn* gene.

Meteorins are required for the establishment of the AC

During the earliest stages of brain development, *metrn* genes are broadly transcribed in the embryonic CNS. Considering the early onset of their expression, we thought that Meteorins activity might influence the elongation of the very first axonal tracts extending in the embryonic zebrafish brain. To test this hypothesis, we stained the axonal projections of 28 hpf wild type and mutant embryos by acetylated tubulin staining. At the chosen developmental stage, a stereotyped axonal scaffold, including both commissural and longitudinal tracts, is fully developed in wild type animals. In the more rostral region of the embryonic forebrain, this structure includes two big commissures (the dorsal anterior commissure, AC and the ventral post-optic commissure, POC) connecting the left and right side of the brain (Hjorth and Key 2002).

Confocal imaging of the stained embryos revealed that, as expected, wild type fish display a complete and fully organized AC and POC (Figure 4A,C,E). Differently, triple mutant embryos show a delayed and reduced formation of the commissural axons of the AC, while the POC does not seem to be affected by *metrns* LOF (Figure 4B,D,F). The mutant AC appears always thinner than the wild type counterpart, being often defasciculated or even absent. We subsequently wondered if the phenotype observed in the triple mutants was due to the synergistic activity of the three proteins or was caused by the inactivation of a single *metrn* gene. To answer this question, we measured the thickness of the axonal bundles in wild type, triple and single mutant embryos. Interestingly, we could detect a

significantly reduced AC in triple and single *metrn*^{-/-} mutants while the LOF of *metrn11* and *metrn12* did not seem to affect the formation of this commissural tract (wt= 5,7+/-0,44µm, n=15; triple mutants=3,6+/-0,31µm, n=17; *metrn*^{-/-}= 3,16+/-0,48µm, n=7; *metrn11*^{-/-}= 5,82+/-0,60 µm, n=9; *metrn12*^{-/-}= 6,70+/-0,55µm, n=13. Wild type vs triple mutants: p=0,0004; wild type vs *metrn*^{-/-}: p=0,0023; wild type vs *metrn11*^{-/-}: p=0,872; wild type vs *metrn12*^{-/-}: p=0,165; unpaired t-test) (Figure 3G). Interestingly, we did not observe a significant difference between *metrn*^{-/-} and triple mutant embryos (p=0,456; unpaired t-test), suggesting that the loss of other paralogues does not enhance the deleterious effect of *metrn* inactivation. This observation led us to the conclusion that, among the three family members, only Meteorin is involved in the proper establishment of the AC during the zebrafish nervous system development.

Meteorins support RGC axonal lamination

Previous reports have shown that, at later stages, the knock out or knock down of genes involved in the patterning of the AC or POC are often associated to pathfinding errors in retinal ganglion cells (RGCs) projections (Macdonald, Scholes et al. 1997; Shanmugalingam, Houart et al. 2000). Interestingly, *metrn* and *metrn11* are expressed at the midline, in the region where RGC axons coming from the two eyes form the optic chiasm, and in the marginal zone of the optic tectum, exhibiting an expression profile coherent with an instructive role of Meteorins on RGC axons. Therefore, we decided to investigate the possibility that *metrns* inactivation affects the formation of the optic chiasm or influence the elongation of RGC axons toward the contralateral tectum. In order to achieve this objective, we labeled the RGC projections of wild type and mutant embryos by using the lipophilic carbocyanine dyes DiI and DiO. After injection into the eyes of fixed larvae, these dyes allow the anterograde tracing of RGC projections, thus staining the overall population of RGC axons. By filling the two eyes of 48 hpf embryos with different dyes, we were able to stain the optic chiasm, in order to evaluate the contribution of each eye to the formation of this commissural structure. Interestingly, in both wild type and triple mutant embryos, RGC axons originating from one eye were able to navigate across the midline and no misprojection to the ipsilateral side of the optic tectum could be observed (Figure 4A,B). Similarly, by injecting the two dyes into different positions of the

same eye, we demonstrated that the formation of retinotopic maps is not affected in *metrns* mutants (Figure 4 C,D,E,F). We subsequently wondered if *Metrns* were able to influence the laminar organization of RGC axons. To answer this question, we genetically labeled single RGCs by the transient mosaic expression of a membrane targeted GFP under the control of the *isl2b* promoter (active in RGC from 48 hpf). To this end, we injected a *isl2b:GFPcaax* plasmid into one cell stage wild type and triple mutant embryos and we imaged the RGC terminals in the tectal neuropil after 5 days. Misrouted axons meandering between multiple tectal laminae were observed in about half of the mutant fish (n=4/9) (Figure 4G,H) but never detected in wild type larvae (n=0/9) (Figure 4E-F). To verify how single *Metrns* influence RGC lamination, we performed the same experiment in single mutants. Importantly, we could not see any lamination defects in the three single mutants, suggesting that *Metorins* could act redundantly on RGC axons in this biological context.

Overall, the analysis of RGC projections in *metrns* mutants suggests that the activity of this protein family is not required for the formation of the optic chiasm or for the organization of the retinotopic maps, but might influence the laminar organization of RGC axons.

Meteorins are involved in the fasciculation of trigeminal neurons

Longitudinal axons are capable of growing over long distances maintaining an ipsilateral trajectory. It has been proposed that their guidance choices are influenced by midline-secreted factors exerting a repulsive force that prevents aberrant midline crossing and maintains the axons at a fixed distance from the midline (Farmer, Altick et al. 2008). Due to their strong expression at the hindbrain midline, we reasoned that Meteorin proteins may affect the elongation profile of longitudinal tracts growing in this brain region. In wild type embryos, the axons of the trigeminal sensory neurons form a tight axonal bundle running laterally to the midline in the hindbrain and spinal cord. This projection profile makes the trigeminal nerve a perfect candidate to be sensitive to *Metrn* biological activity. To verify if *metrns* LOF affects the elongation of the trigeminal axons, we selectively labeled this neuronal population by transiently expressing the *isl2b:GFPcaax* plasmid (*isl2b* is expressed in trigeminal cells). Injected fish were analyzed by confocal microscopy at 3 dpf. All the wild type embryos displayed a well-organized trigeminal tract,

whose axons correctly elongated along a perfectly defined trajectory in the rostro-caudal direction (Figure 6A,B). In contrast, the trigeminal nerve appeared strongly defasciculated in triple mutant embryos, with axons often approaching the midline while navigating towards the posterior direction (Figure 6C,D). To quantify the effect of *metrns* LOF on the fasciculation of trigeminal axons and to verify the contribution of single Meteorin, we measured the thickness of the axonal bundle in the different genetic backgrounds. Interestingly, we found a significantly increased defasciculation in the triple and single *metrn* and *metrn11* mutants while *metrn12* didn't seem to be involved in instructing trigeminal projections (wt=27,29 μ m +/- 1,99, n=14; triple mutants=46,22 μ m +/- 3,48, n=14; *metrn*^{-/-}=41,66 μ m +/- 2,33, n=14; *metrn11*^{-/-}=40,53 μ m +/- 1,65 n=6; *metrn12*^{-/-}= 24,43 μ m +/-1,85, n=13. Wild type vs triple mutants: p<0,0001; wild type vs *metrn*^{-/-}: p<0,0001; wild type vs *metrn11*^{-/-}: p=0,0004; wild type vs *metrn12*^{-/-}: p=0,303; unpaired t-test).

This result suggests that trigeminal axons are sensitive to *Metrns* signaling, whose activity is likely required to maintain the axonal navigation path parallel to the midline.

Interestingly, other neurons elongating their axons in the same region does not seem to be affected by *metrn* inactivation. As revealed by neurofilament staining, the navigation path of Mauthner cell axons is not impaired if all *metrn* genes are disrupted. These neurons correctly project their axons across the midline, subsequently taking a longitudinal rostro-caudal trajectory (Figure S1A, B). We additionally observed that the distance between these axons and the midline is not impaired (Figure S1C), thus suggesting that *metrns* selectively acts on a specific subset of responsive neurons.

Discussion

In this report, we explored the contribution of the *metrn* gene family to the process of axon guidance. Meteorin proteins have been shown to mediate neuronal progenitor differentiation and axonal elongation, *in vitro*, but, to date, a description of their role during neuronal development, *in vivo*, is still missing.

First, we verified that *Metrns* are conserved across different classes of vertebrates, suggesting that their function might have been preserved during vertebrate evolution. The presence of a signal peptide in the

N-terminal region of all the *Metrns* confirms that they are secreted factors, a feature suitable for the cooperation with different pathways regulating axonal elongation during embryonic development. A further support to this hypothesis is given by the presence of a putative NTR-like domain in the C-terminal region of the zebrafish *Metrn1*. In our preliminary bioinformatics analysis, we were not able to detect this domain in other paralogues, nevertheless, given the observed sequence conservation, it is likely that this module is present in other proteins but not detected by our approach. It has been previously shown that this domain is responsible for the binding of Netrins to ECM components like HSPGs and might contribute to their accumulation and multimerisation in the extracellular environment (Kappler, Franken et al. 2000). It is possible that this module plays a similar function in *Metrns*, regulating their activity by modulating their spatial distribution.

Importantly, the spatiotemporal expression patterns of *metrn* genes is coherent with a role of these proteins in the modulation of axonal navigation. Indeed, in both mouse and zebrafish, *metrns* are expressed by glia and neuronal progenitor cells at the midline and the floor plate, both being a platform for the secretion of guidance factors controlling the behavior of elongating axons. In particular, we could find a population of hindbrain floor plate cells co-expressing *metrn11* and three *slit* paralogues (*slit1a*, *slit1b* and *slit2*), pointing out that *Metrn* proteins are at least partially expressed by the same cell population responsible for the formation of one of the major guidance cues in the embryonic brain. Whether the co-localization of *metrn11* and *slits* transcripts reflects a functional cooperation between the two classes of molecules is still unclear. Nevertheless, our results pave the ground for the investigation of a possible interaction between the two pathways in establishing the embryonic neural circuits.

By using a LOF approach, we demonstrated that, in zebrafish embryos, at least three neuronal populations are sensitive to *Metrns* signaling, as their axons display navigation defects in case of *metrns* gene inactivation. Our observations suggest that different axons might respond to different combinations of *Metrns*: axons forming the AC seem to be exclusively influenced by *Metrn* while *Metrn* and *Metrn11* appear to have a synergistic activity on trigeminal neurons. As RGC axons did not display any aberrant projection in case of single *metrns* disruption, we speculated that *Metrns* might act redundantly on the coordination of their laminar organization.

Whether the effect of *Metrns* is directly linked to the binding of

these factors to their receptor on the targeted axons or is caused by the modulation of other pathways involved in axonal navigation is still ambiguous.

Taken together, our experiments revealed the role of a novel family of secreted proteins in the patterning of the embryonic CNS, suggesting that Metrns are a new class of molecules cooperating to the formation of the complex pattern of axonal projections in the vertebrate developing brain.

Figure Legends

Figure 1. Metrns are secreted proteins conserved across vertebrates

A. Phylogenetic tree of Metrns proteins. The scale bar indicates the number of amino acid substitution per site.

B. Alignment of the amino acid sequences of the human, mouse and zebrafish Metrns and Metrnl. Regions with different similarity scores are highlighted in orange.

C. Schematic representation of the structure of the three zebrafish Metrns. A signal peptide is present at the N-terminal region of all the proteins while a NTR-like domain is detectable in the C-term region of Metrnl1

Figure 2. Zebrafish *metrn* genes are expressed in the embryonic CNS

A,B,C. Whole mount *in situ* hybridization showing the expression pattern of the zebrafish *metrn* (A), *metrnl1* (B) and *metrnl2* (C). Dorsal views are shown on the left side of each panel, lateral views are of the right side. At 1 dpf (upper panels) the three mRNAs are detectable in the CNS, where *metrn* and *metrnl2* have a broader expression while *metrnl1* is highly transcribed in the presumptive otic vesicles and in the hindbrain rhombomeres boundary regions. At 2 dpf (lower panels) *metrn* and *metrnl1* are expressed at the midline and in periventricular regions of the CNS, *metrnl2* is expressed at the otic vesicle and at the somite boundary.

D,E. Vibratome sections of 2dpf embryos showing the expression pattern of *metrn* (D) and *metrnl1* (E). Longitudinal sections are on the upper panels,

transversal sections on the lower panels. The two mRNAs are detectable at the midline in the antero-posterior and dorso-ventral axis. *metrn11* is also expressed at the floor plate in the spinal cord.

F,G,H. Double fluorescent *in situ* hybridization showing the colocalization of *metrn11* with *slit1a*, *slit1b* and *slit2* at the hindbrain floor plate.

Figure 3. CRISPR/Cas9 based generation of LOF alleles

A,C,E. schematic representation of the three *metrn* loci in the zebrafish genome. The targeted 20 nt in the exon 2 of each gene are highlighted in red; the PAM sequence is indicated in green.

B,D,F. wild type and putative truncated Metrn proteins

G. Quantification of the reduction of the amount of *metrn* transcripts in triple mutants compared to wild type fish. Error bars = SEM

Figure 4. *meteorins* loss-of-functions affects the formation of the anterior commissure

A,B. Schematic representation of the wild type (A) and mutant (B) anterior and post-optic commissures (AC and POC) in the rostral forebrain of a 28 hpf embryo.

C,D. Frontal view of the AC and POC in a wild type (C) and triple mutant (D) embryo. A fully developed commissural bundles can be observed in both the AC and POC of wild type fish while the triple mutant shows an incomplete development of the AC (Scale bar: 30µm).

E,F. dorsal view of the AC highlighting the developmental defects of the commissure in triple mutants (F) compared to wild type (E) (Scale bar: 30µm).

G. Measure of the width of the AC in wild type, triple and single mutants showing a significant impairment of the AC in triple and single *metrn* and *metrn11* mutants. AC establishment is not affected in *metrn12* mutants. Error bars = SEM

Figure 5. Meteorins are involved in the patterning of RGCs axons

A,B. Optic chiasm of 48 hpf wild type and triple mutant embryos labeled

with DiI and DiO and showing no misrouted axons (Scale bar: 30µm)
C,D,E,F. Schematic representation of the retinotopic targeting of RGC axons coming from different retina locations. Injections of the lipophilic dyes DiI and DiO in different quadrants of the contralateral retina (left panels) show that retinotopic mapping to the optic tectum (right panels) is not altered in *metrn* triple mutants (C) compared to wild type embryos (D).

Figure 6. Meteorins regulate the fasciculation of the trigeminal nerve

A,C. Schematic representation of the wild type (A) and mutant (B) trigeminal nerve fasciculation.

B,D. Dorsal view of 3 dpf wild type (B) and mutant (D) trigeminal neurons transiently expressing the *islt2b:GFPcaax* plasmid. Mutant axons appear extremely disorganized and defasciculated if compared to wild type (Scale bar: 30µm).

E,F Measure of the width of the trigeminal tract in wild type, single and triple mutants showing a significant increase in the bundle thickness in triple and single *metrn* and *metrn11* mutants compared to wild type fish. Error bars = SEM

Figure S1. Meteorin are not implied in the navigation of Mauthner neurons

A,B. Dorsal view of 48 hpf wild type (A) and triple mutant (B) embryos in which the Mauthner cells are labeled by 3A10 staining. No difference between wild type and mutants can be detected

C. Quantification of the distance between Mauthner axons and the midline in wild type and mutant larvae. No differences exist between the two genetic backgrounds

Materials and methods

Phylogenetic analysis and identification of conserved domains

Molecular cloning

Protein sequences were obtained from the Ensembl Genome Browser after searching for annotated *metrn* and *metrnl* genes in all organisms. The following sequences were used: D. Rerio *metrn* (ENSDARP00000041804), D. Rerio *metrnl1* (ENSDARP00000131064), D. Rerio *metrnl2* (ENSDARP00000021463), G. Gallus *metrn* (ENSGALP00000054530), G. Gallus *metrnl* (ENSGALP00000041582), H. Sapiens *metrn* (ENSP00000455068), H. Sapiens *metrnl* (ENSP00000315731), L. Oculatus *metrn* (ENSLOCP00000003703), M. Musculus *metrn* (ENSMUSP00000127275), M. Musculus *metrnl* (ENSMUSP00000038126), X. Leavis *metrnl* (ENSXETP00000020278). Phylogenetic tree was reconstructed with the geneious © software using the neighbor joining method and choosing the L. oculatus *metrn* as outgroup. The search of conserved domains was performed on the online NCBI Conserved Domain database (<https://www.ncbi.nlm.nih.gov/Structure/cdd/wrpsb.cgi>).

Single and double fluorescent situ hybridization

The cDNA fragments of *metrn*, *metrnl*, *metrnl2*, *slit1a*, *slit1b*, *slit2* and were amplified by PCR from the cDNA of 2 dpf zebrafish embryos using the following primers (5'-3'):

metrn: for: GGGGATTTAGGAGTGTTGCG; rev: AGTCTTTATATCTTGGAGCG

metrnl1: for: GTGATCAGTGCAGCTGGAGG; rev: TGTAGCGTGGAGCGCAGCTG

metrnl2: for: CTGAAGGCTCTCTGCAGTGG; rev: ATCACAGCGCTGCAGAATCT

slit1a: for: TGAGCAGCTGGTTGAGGAAC; rev: GTAGCCGTCTGTCTGATCCG

slit1b: for: CACGGACTTAACCTGGCAGA; rev: TTGGGTGGACAAACAGGCTT

slit2: for: TTGCTGATTTGGCCTGTCCA; rev: TGTGAACTCGTTGCCATCGA

In vitro transcription of Digoxigenin-labeled probes was performed using the RNA Labeling Kit (Roche Diagnostics Corporation) according to manufacturer's instructions. Decorionated embryos at the appropriate developmental stage(s) were fixed in 4% paraformaldehyde in PBS (pH 7.4) for 2 hours at room temperature and whole-mount in situ hybridisation was performed as previously described (Thisse and Thisse 2008).

Vibratome sections

Whole-mount embryos were washed twice in 1X PBS/0.1% Tween-20 (PBS-Tw) solution. The samples were embedded in gelatin/albumin with 4% of Glutaraldehyde

and sectioned (20 μ m) on a VT1000 S vibrating blade microtome (Leica). Sections were mounted in Fluoromount Aqueous Mounting Medium (Sigma).

sgRNAs and Cas9 mRNA generation

sgRNA guide sequences were cloned into the BsaI digested DR274 (Addgene ref 42250) plasmid vector. The sgRNAs were synthesized by *in vitro* transcription (using the Megascript T7 transcription kit, Ambion ref AM1334). After transcription, sgRNAs were purified using RNAeasy Mini Kit (Qiagen). The target sequences are the following (5'-3'): *metrn*: CCACCACACCCGGCCAGCC, *metrn1*: GGTGTATCTCCGCTGCGCCC; *metrn2*: CCAGAAACAGCGCCCCCTCCTGC. The quality of purified sgRNAs was checked by electrophoresis on a 2 % agarose gel. Cas9 mRNA was generated as previously described (Hwang, Fu et al. 2013)

Injections of sgRNA and Cas9 mRNA

To induce targeted mutagenesis at the *metrn*, *metrn1* and *metrn2* loci, 200 ng/ μ l of sgRNA were injected into one-cell stage zebrafish embryos together with 150 ng/ μ l of Cas9 mRNA. Injected embryos were grown to adulthood and screened for mutation in their offspring.

Whole embryo DNA extraction and analysis of CRISPR/Cas9-mediated mutagenesis

For genomic DNA extraction, pools of 25 5-dpf embryos were digested for 1 h at 55°C in 0.5mL lysis buffer (10 mM Tris, pH 8.0, 10 mM NaCl, 10 mM EDTA, and 2% SDS) with proteinase K (0.17 mg/mL, Roche Diagnostics). To check for frequency of indel mutations, target genomic loci were PCR amplified using Phusion High-Fidelity DNA polymerase (Thermo Scientific). PCR amplicons were subsequently cloned into the pCR-bluntII-TOPO vector (Invitrogen). Plasmid DNA was isolated from single colonies and sent for sequencing. Mutant alleles were identified by comparison with the wild-type sequence.

Genotyping of mutant lines

Genotyping of *metrn*s mutants was performed as follows : after genomic DNA extraction PCR amplification reactions were conducted in final volumes of 20 μ l containing 1x PCR reaction buffer, 1,5mM MgCl₂, 70 ng of gDNA, Taq DNA Polymerase (5U/ μ l) (LifeTechnologies) and 0.5 μ M of each primer.

Gene-specific primers are the following (5'-3'):

metrn: for: TCTGTGTTGACTGCTGGCTG; rev:
GTGTTTTAGTGGTGTTCCTTACAATGA
metrn1: for: TCCCATGCCTGGACCTCATA; rev:
AGACGGAGAGAAGAGACGCT
metrn2: for: TGTTGATCAGCAGTGTGTGCGTAGC; rev:
GTCCTCCGCTGATCTACGTG

The DNA amplification was performed with 30 cycles at the annealing temperature of 60°C. Metrn and metrn2 amplicons were loaded on 2 % agarose gel to discriminate between wild type and mutant alleles (for metrn, the size of wild type allele is 598bp while the mutant is 482bp long; for metrn2, the size of wild type allele is 242bp while the mutant is 156bp long). Metrn1 PCR product was digested at 55°C ON with the *PasI* enzyme (Thermo Fisher scientific) and the resulting digestion was subsequently analysed on a 2% agarose gel. The wildtype allele results in two fragments of 107bp and 94bp length, respectively. The mutant alleles are not digested and show a band at 201bp.

Quantitative RT-PCR

Total RNA was prepared from 1 dpf embryos with TRIzol reagent (ThermoFisher Scientific) and TURBO DNA-free reagents (ThermoFisher Scientific). RNA (1 µg) was retrotranscribed using random primers and the SuperScript III First-Strand Synthesis system (ThermoFisher Scientific). For q-RT-PCR, the SYBR Green PCR Master Mix (ThermoFisher Scientific) was used according to the manufacturers protocol and the PCR reaction was performed on an ABI PRISM 7900HT instrument. *Ef1a* and *RPL13a* were used as reference genes as reported previously (Tang, Dodd et al. 2007). All assays were performed in triplicate using 11.25 ng of cDNA per reaction. The mean values of triplicate experiments were calculated according to the delta CT quantification method. Primer used are the following (5'-3'):

metrn: for: TCCGCTACGAGCTGAGAGGG; rev:
GTGCAGACGGCCATCAGGATC
metrn1:for:ATTGCGCGCTCCAGTACTC;rev:CGCAGCGGAGATACACCTGC
metrn2:for:CTGAAGGCTCTCTGCAGTGG;rev:GGCTTCACACACACGCTAG

Immunohistochemistry (IHC)

Embryos were fixed at the chosen developmental stage in 4% paraformaldehyde in PBS-Tw for 2 h at RT and subsequently washed three times in PBS-1% Triton X 100 to promote their permeabilization.

Consequently, they were incubated for 1 hour at room temperature

in blocking solution (10% Normal Goat Serum, Invitrogen, in PBS-Tw) followed by overnight (ON) incubation, at 4 °C, with a 1/200 dilution of the mouse anti acetylated tubulin monoclonal antibody (Sigma # T7451) or 3A10 (DSHB, AB_531874)

in blocking solution. After five washes in PBS-Tw, the embryos were incubated ON with the Alexa Fluor 488 anti- mouse IgG secondary antibody (Life Technologies) and DAPI (Sigma) diluted at a final concentration of 1/200 and 1/500 respectively in blocking solution. The following day embryos were washed five times in PBS-Tw and mounted in 1% low melting point agarose in glass-bottom cell tissue culture dish (Fluorodish, World Precision Instruments, USA) for imaging.

DiDo injections

For the tracing of RGC axonal projections, 2 and 5 dpf embryos were fixed in 4% paraformaldehyde in PBS for 2 hours. DiO and DiI injection were performed as previously described (Baier, Klostermann et al. 1996).

Molecular cloning

The pIsl2b:Gal4:GFP-Caax construct was generated by a Gateway reaction (MultiSite Gateway Three-Fragment Vector Construction Kit, ThermoFisher Scientific, Waltham, MA) using the p5E-Isl2b39, pME-GFP-caax, p3E-pA and the pDest-Tol2;cmlc2:eGFP40 vectors.

Microscopy and image analysis

In situ hybridization sections were imaged on a Leica MZ FLIII stereomicroscope (Leica) equipped with a Leica DFC310FX digital camera. A Zeiss LSM 780 confocal microscope (Zeiss) was used for confocal microscopy, employing a 40x water immersion objective. Z-volumes were acquired with a

0,5- to 2- μ m resolution and images processed using ImageJ or Adobe Photoshop softwares. 3D reconstructions of Z- volumes of single RGC axons were done using Imaris.

For in vivo imaging embryos were anesthetized using 0.02% tricaine (MS-222, Sigma) diluted in egg water and embedded in 1% low melting-point agarose in glass-bottom cell tissue culture dish (Fluorodish, World Precision Instruments, USA).

Bibliography

Baier, H., S. Klostermann, T. Trowe, R. O. Karlstrom, C. Nusslein-Volhard and F. Bonhoeffer (1996). "Genetic dissection of the retinotectal projection." *Development* 123: 415-425.

Banyai, L. and L. Patthy (1999). "The NTR module: domains of netrins, secreted frizzled related proteins, and type I procollagen C-proteinase enhancer protein are homologous with tissue inhibitors of metalloproteases." *Protein Sci* 8(8): 1636-1642.

Dickson, B. J. (2002). "Molecular mechanisms of axon guidance." *Science* 298(5600): 1959-1964.

Farmer, W. T., A. L. Altick, H. F. Nural, J. P. Dugan, T. Kidd, F. Charron and G. S. Mastick (2008). "Pioneer longitudinal axons navigate using floor plate and Slit/Robo signals." *Development* 135(22): 3643-3653.

Hjorth, J. and B. Key (2002). "Development of axon pathways in the zebrafish central nervous system." *Int J Dev Biol* 46(4): 609-619.

Hwang, W. Y., Y. Fu, D. Reyon, M. L. Maeder, P. Kaini, J. D. Sander, J. K. Joung, R. T. Peterson and J. R. Yeh (2013). "Heritable and precise zebrafish genome editing using a CRISPR-Cas system." *PLoS One* 8(7): e68708.

Jorgensen, J. R., A. Fransson, L. Fjord-Larsen, L. H. Thompson, J. P. Houchins, N. Andrade, M. Torp, N. Kalkkinen, E. Andersson, O. Lindvall, M. Ulfendahl, S. Brunak, T. E. Johansen and L. U. Wahlberg (2012). "Cometin is a novel neurotrophic factor that promotes neurite outgrowth and neuroblast migration in vitro and supports survival of spiral ganglion neurons in vivo." *Exp Neurol* 233(1): 172-181.

Jorgensen, J. R., L. Thompson, L. Fjord-Larsen, C. Krabbe, M. Torp, N. Kalkkinen, C. Hansen and L. Wahlberg (2009). "Characterization of Meteorin--an evolutionary conserved neurotrophic factor." *J Mol Neurosci* 39(1-2): 104-116.

Kappler, J., S. Franken, U. Junghans, R. Hoffmann, T. Linke, H. W. Muller and K. W. Koch (2000). "Glycosaminoglycan-binding properties and secondary structure of the C-terminus of netrin-1." *Biochem Biophys Res Commun* 271(2): 287-291.

Kim, Y. Y., J. S. Moon, M. C. Kwon, J. Shin, S. K. Im, H. A. Kim, J. K. Han and Y. Y. Kong (2014). "Meteorin regulates mesendoderm development by enhancing nodal expression." *PLoS One* 9(2): e88811.

Lee, H. S., J. Han, S. H. Lee, J. A. Park and K. W. Kim (2010). "Meteorin promotes the formation of GFAP-positive glia via activation of the Jak-STAT3 pathway." *J Cell Sci* 123(Pt 11): 1959-1968.

Nawabi, H. and V. Castellani (2011). "Axonal commissures in the central nervous system: how to cross the midline?" *Cell Mol Life Sci* 68(15): 2539-2553.

Nishino, J., K. Yamashita, H. Hashiguchi, H. Fujii, T. Shimazaki and H. Hamada (2004).

"Meteorin: a secreted protein that regulates glial cell differentiation and promotes axonal extension." *EMBO J* 23(9): 1998-2008.

Nugent, A. A., A. L. Kolpak and E. C. Engle (2012). "Human disorders of axon guidance." *Curr Opin Neurobiol* 22(5): 837-843.

Ramialison, M., B. Bajoghli, N. Aghaallaei, L. Ettwiller, S. Gaudan, B. Wittbrodt, T. Czerny and J. Wittbrodt (2008). "Rapid identification of PAX2/5/8 direct downstream targets in the otic vesicle by combinatorial use of bioinformatics tools." *Genome Biol* 9(10): R145.

Rao, R. R., J. Z. Long, J. P. White, K. J. Svensson, J. Lou, I. Lokurkar, M. P. Jedrychowski, J. L. Ruas, C. D. Wrann, J. C. Lo, D. M. Camera, J. Lachey, S. Gygi, J. Seehra, J. A. Hawley and B. M. Spiegelman (2014). "Meteorin-like is a hormone that regulates immune-adipose interactions to increase beige fat thermogenesis." *Cell* 157(6): 1279-1291.

Svensson, K. J., J. Z. Long, M. P. Jedrychowski, P. Cohen, J. C. Lo, S. Serag, S. Kir, K. Shinoda, J. A. Tartaglia, R. R. Rao, A. Chedotal, S. Kajimura, S. P. Gygi and B. M. Spiegelman (2016). "A Secreted Slit2 Fragment Regulates Adipose Tissue Thermogenesis and Metabolic Function." *Cell Metab* 23(3): 454-466.

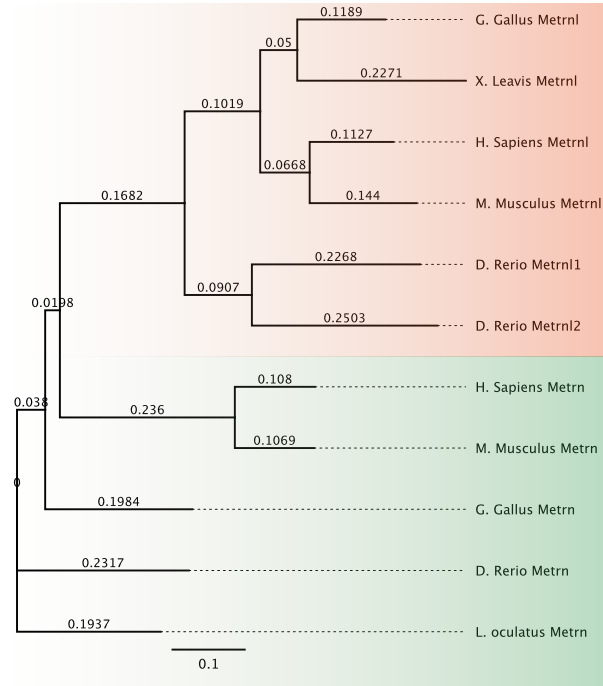
Tang, R., A. Dodd, D. Lai, W. C. McNabb and D. R. Love (2007). "Validation of zebrafish (*Danio rerio*) reference genes for quantitative real-time RT-PCR normalization." *Acta Biochim Biophys Sin (Shanghai)* 39(5): 384-390.

Thisse, C. and B. Thisse (2008). "High-resolution in situ hybridization to whole-mount zebrafish embryos." *Nat Protoc* 3(1): 59-69.

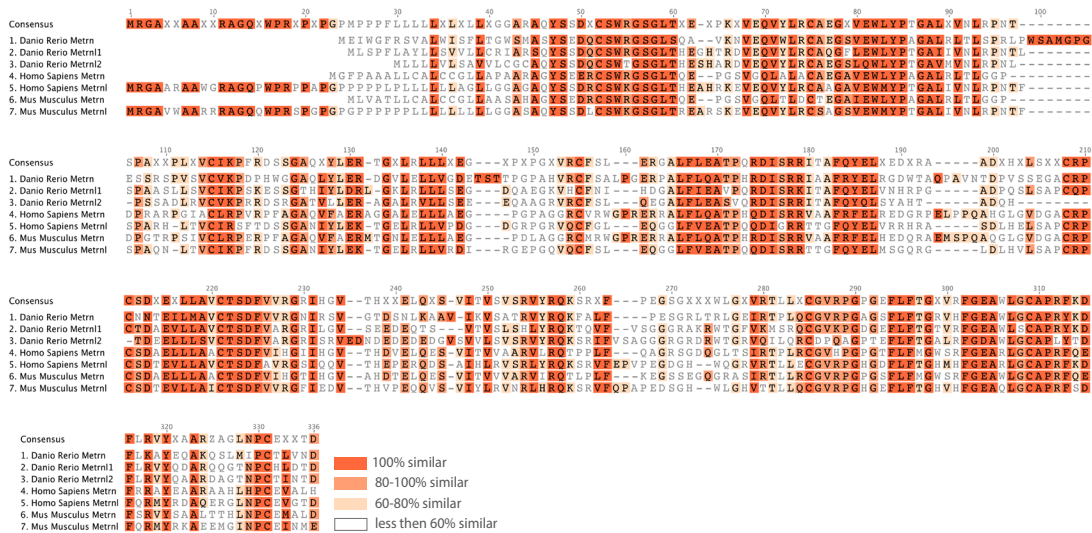
Van Battum, E. Y., S. Brignani and R. J. Pasterkamp (2015). "Axon guidance proteins in neurological disorders." *Lancet Neurol* 14(5): 532-546.

Watanabe, K., Y. Akimoto, K. Yugi, S. Uda, J. Chung, S. Nakamuta, K. Kaibuchi and S. Kuroda (2012). "Latent process genes for cell differentiation are common decoders of neurite extension length." *J Cell Sci* 125(Pt 9): 2198-2211.

A



B



C

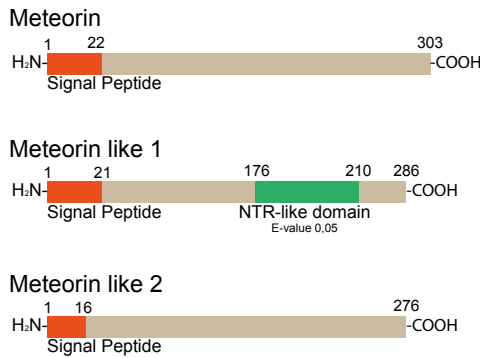


Figure 1

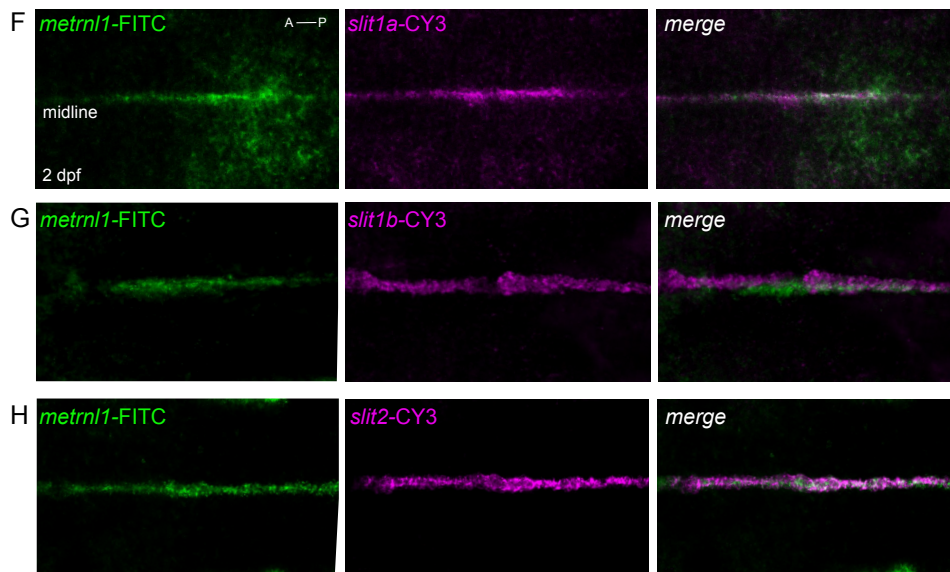
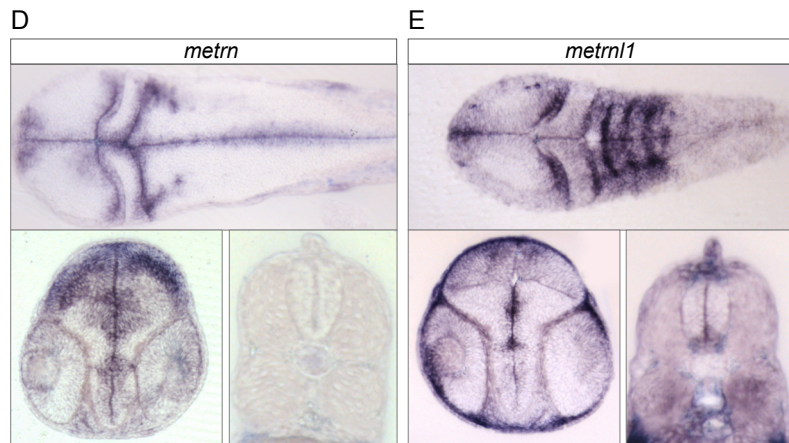
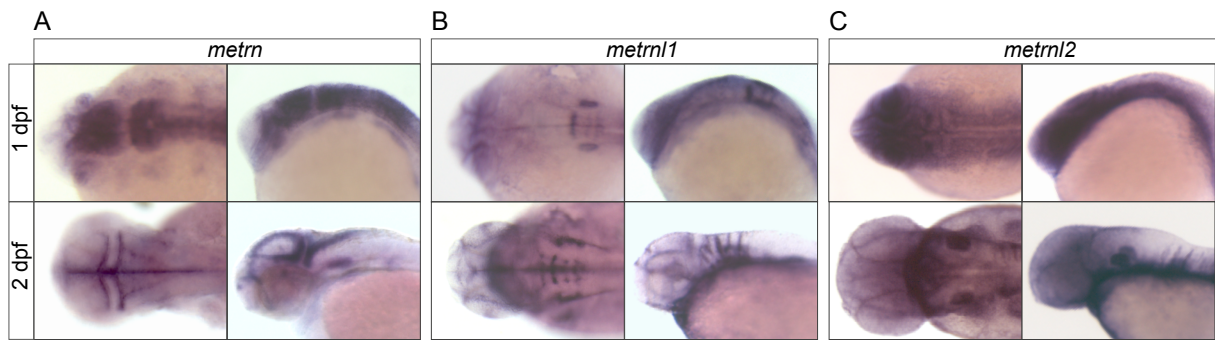


Figure2

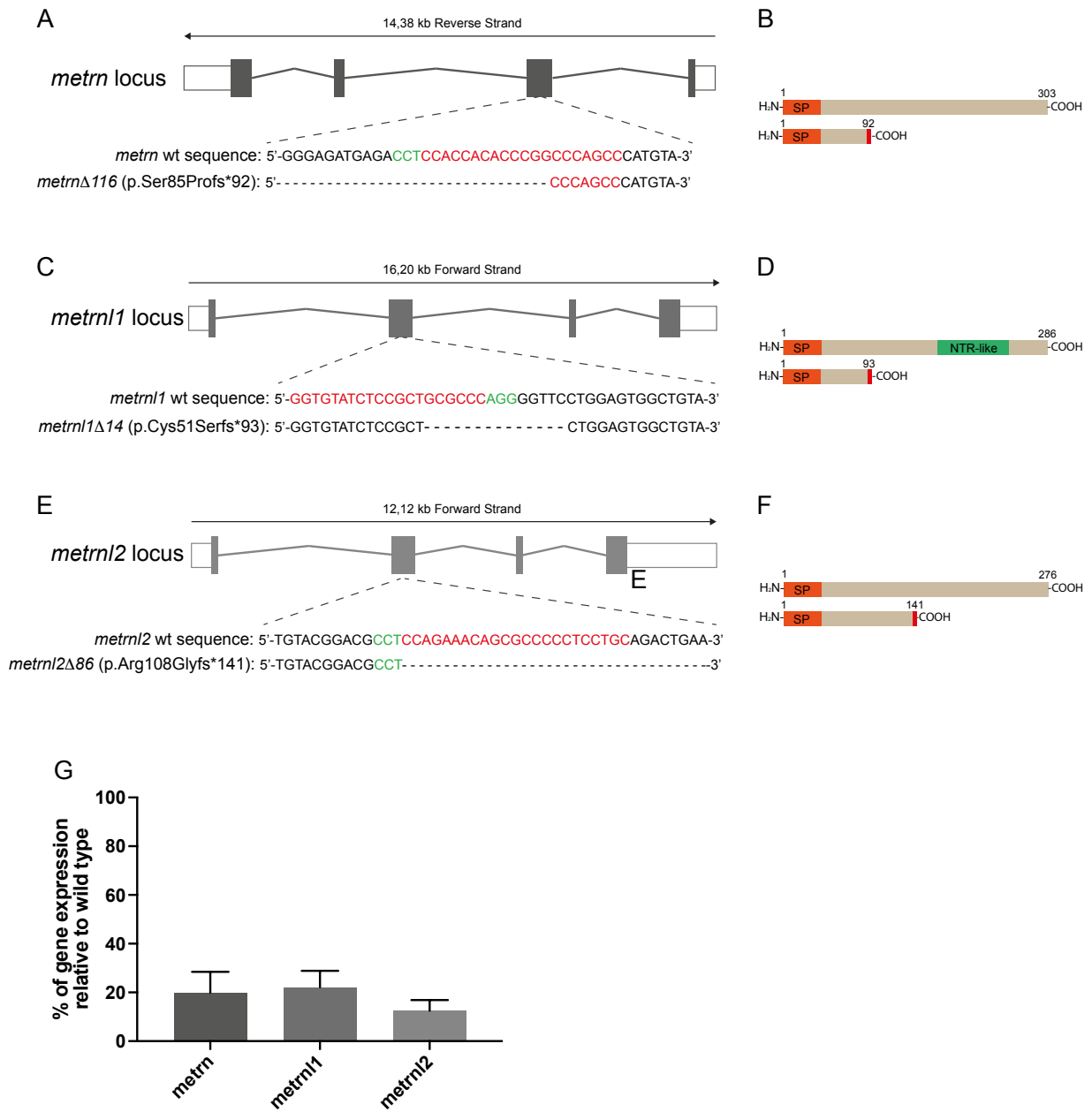


Figure 3

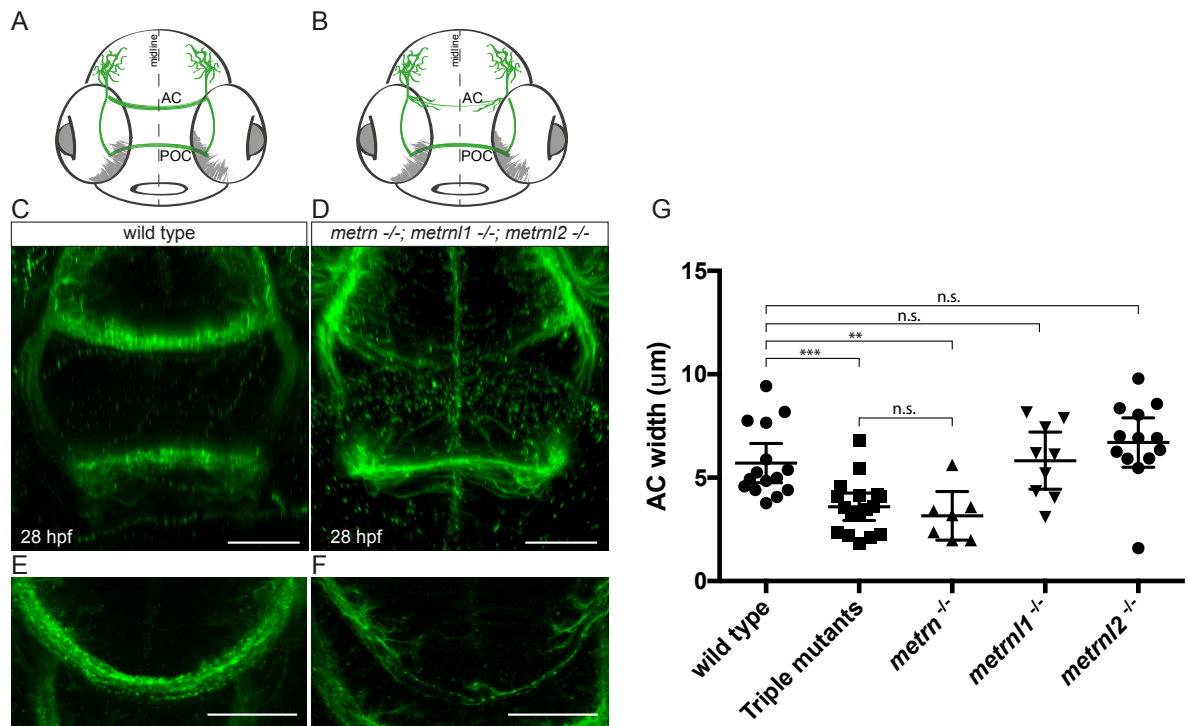


Figure 4

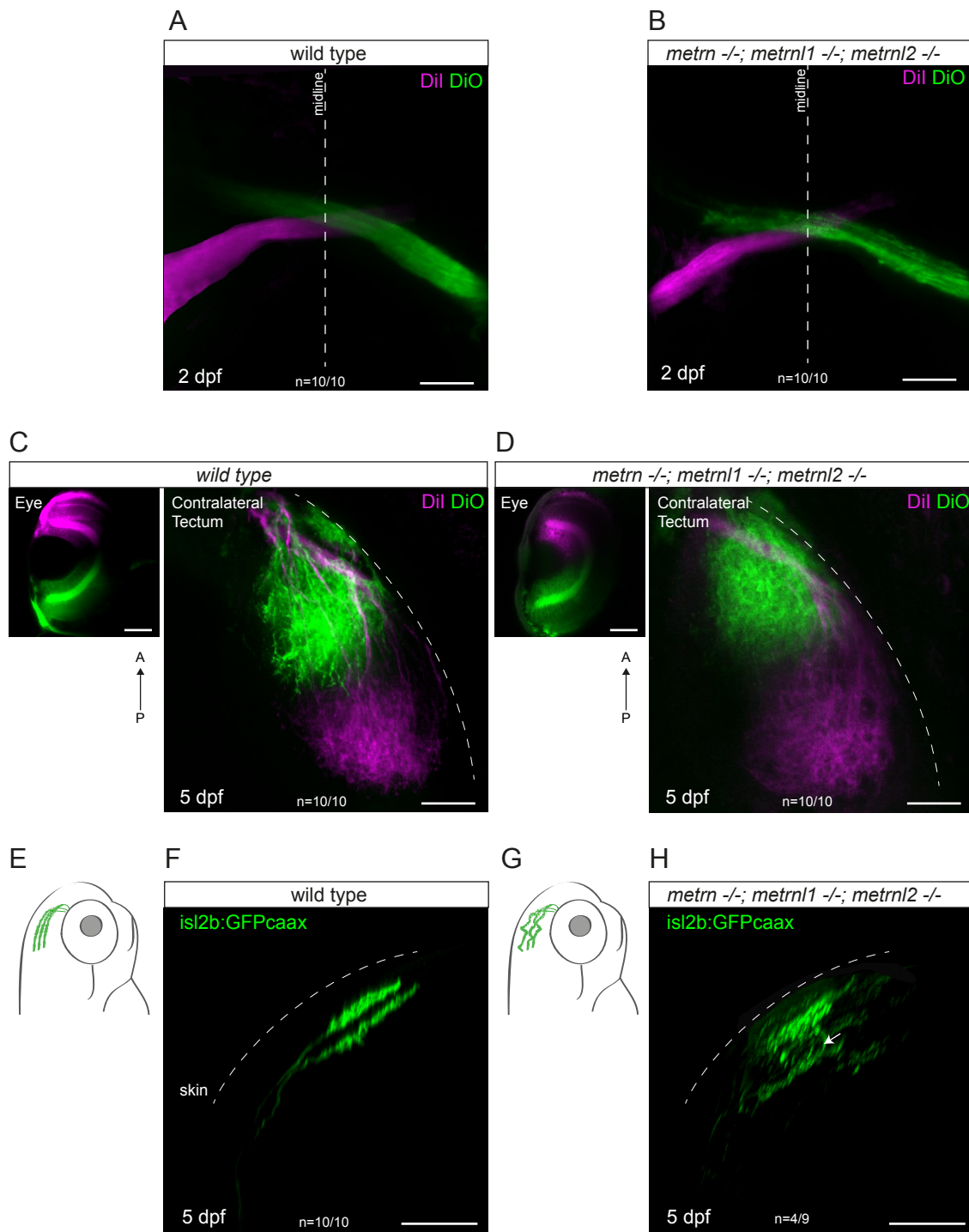


Figure 5

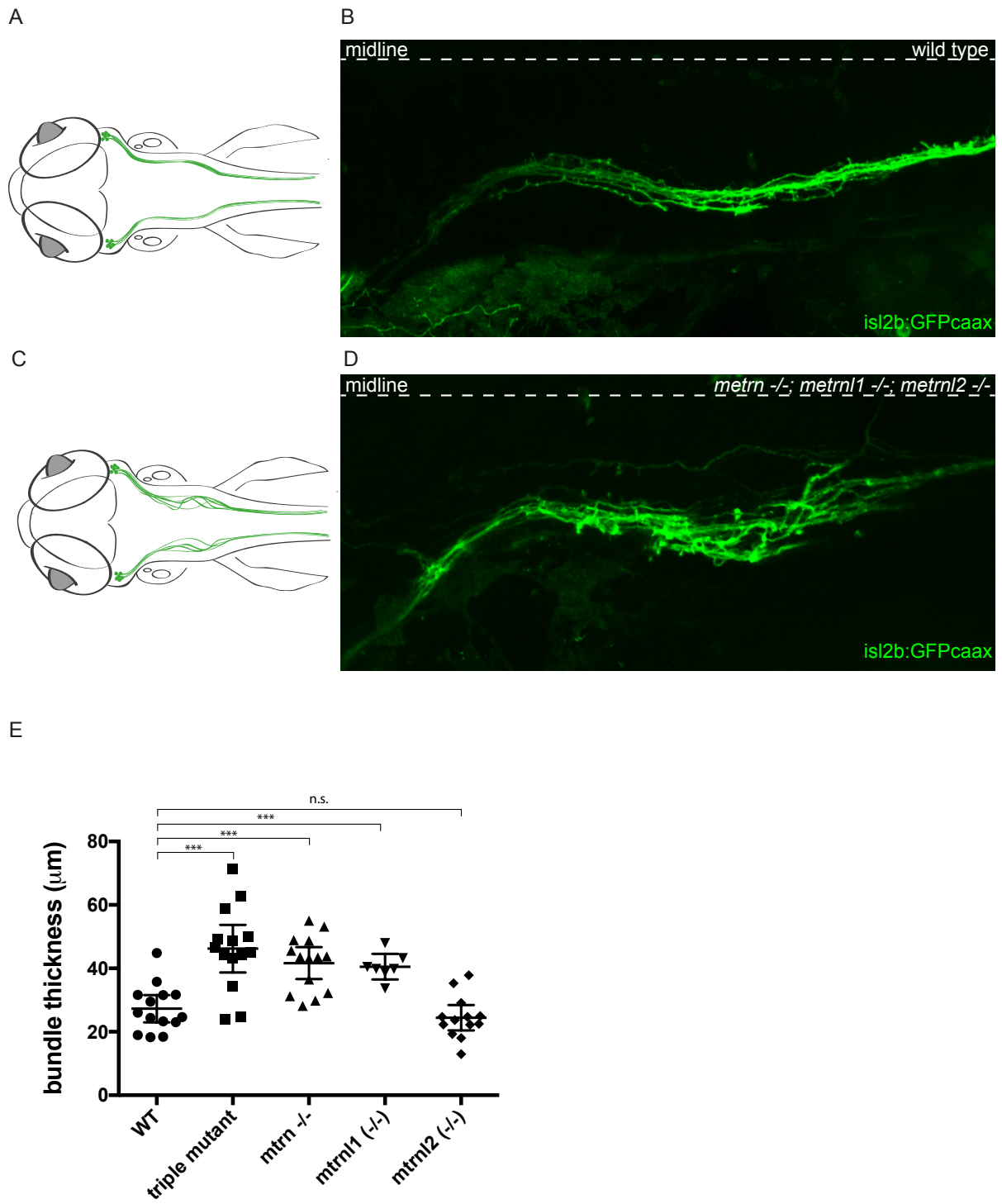


Figure 6

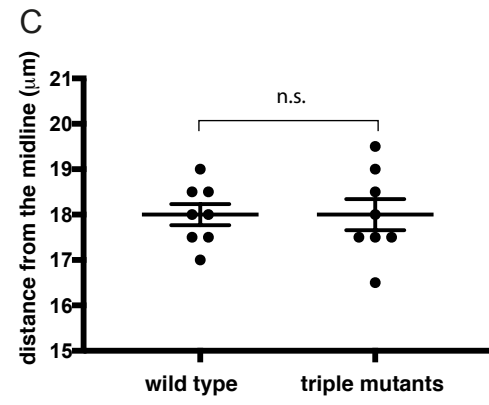
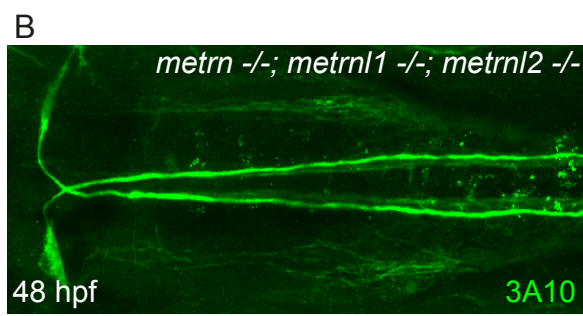
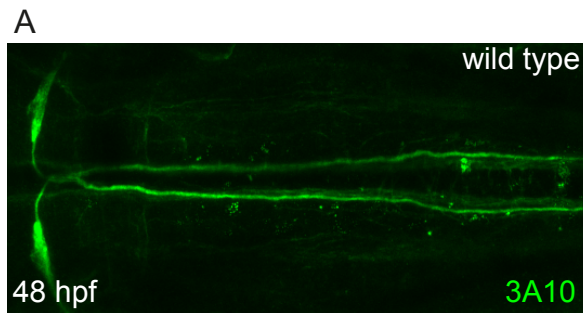


Figure S1

CHAPTER III: DISCUSSION AND PERSPECTIVES

DISCUSSION AND PERSPECTIVES

III.1.1 The 2C-Cas9 system allows the induction of conditional mutagenesis and the simultaneous labeling of mutant cells

TALENs and the CRISPRs/Cas9 technologies have recently revolutionized the field of genome editing, making readily accessible the possibility of inducing precise and targeted disruption at any locus of choice. These methodologies allow the generation of constitutive LOF alleles, representing a great advantage for the study of the biological function of a given gene. Nevertheless, the KO of genes involved in the earliest processes of embryonic development might be lethal, thus impeding the analysis of gene functions arising at later developmental stages. To overcome this limitation, a study from Ablain et al. (Ablain, Durand et al. 2015) proposed the use of the CRISPR/Cas9 system to induce tissue-specific gene inactivation. The proposed strategy is based on the use of a modular plasmid permitting the simultaneous expression of the *cas9* enzyme (driven by a tissue-specific promoter) and a sgRNAs (transcribed by a ubiquitous U6 promoter). Few cloning steps are needed to insert in the system a promoter of interest driving *cas9* expression, making the technique relatively flexible. However, to efficiently generate tissue-specific gene inactivation, the sequence of the cell-type specific promoter needs to be precisely annotated. Unfortunately, the genomic sequence of a big number of zebrafish promoters is not fully characterized, thus limiting the applicability of this system. The Gal4/UAS binary system offers a valuable alternative to the use of specific promoters, thanks to the availability of many tissue-specific Gal4 lines generated by enhancer- and gene-trap screenings. In these lines, the Gal4 expression pattern results from the random insertion of its CDS in the zebrafish genome and, in most cases, the promoter sequence controlling its transcription is not mapped. Taking advantage of this system, we developed a strategy for a CRISPR/Cas9-mediated conditional KO based on the Gal4-induced tissue-specific

expression of the Cas9 enzyme. Thanks to the concomitant UAS-dependent expression of the Cas9 enzyme and U6-driven production of gene-specific sgRNAs, our method allows the inactivation of any gene of interest in any Gal4 driver line.

Importantly, we co-expressed the *GFP* or *cre* reporters in combination with the Cas9 endonuclease, thus enabling the visualization of the potentially mutant *cas9*-expressing cells. The possibility to unambiguously mark the population of cells in which the Cas9 is active represents a great advantage in the analysis of the phenotypes arising from the induced targeted mutagenesis. At first, we labeled the population of *cas9*-expressing cells with the fluorescent reporter GFP, ensuring the stoichiometric translation of the two proteins thanks to the use of the viral T2A self-cleaving peptide. By using this strategy against the *tyrosinase* locus, we were able to induce eye-specific loss of pigmentation when expressing our transgene in the progenitors of the neural retina and the retinal-pigmented epithelium.

Crucially, in this case, the GFP expression is strictly dependent on the temporal activity of the promoter driving Gal4 expression, preventing the possibility of detecting the cells potentially carrying a LOF allele after Gal4 transactivation has terminated.

To circumvent this limitation and to permanently label the cells in which the Cas9 enzyme was expressed, we developed a strategy where the *GFP* CDS was substituted by the cDNA of the *cre* enzyme (Branda & Dymecki 2004, Pan et al 2005), a topoisomerase that catalyzes the site-specific recombination of DNA between loxP sites. The visualization of *cre*-expressing cells can be achieved by using zebrafish lines carrying a transgene where a constitutive promoter drives the expression of a fluorescent reporter upon the Cre-mediated excision of a floxed stop codon. Therefore, in cells carrying a floxed allele, the simultaneous expression of Cas9 and Cre enzymes would induce, at the same time, double-strand breaks at the selected genomic location and recombination of the floxed locus. Importantly, if the expression of the reporter on the floxed allele is driven by a constitutive promoter after Cre-mediated recombination all the cells deriving from a single Cas9-expressing cell will be labeled by the reporter, allowing long-term visualization of potentially mutated clones of cells after Gal4 expression has ended.

Our work demonstrated that this approach (2C-Cas9, Cre-mediated recombination for Clonal analysis of **Cas9** mutant cells) is suitable for the phenotypic analysis of LOF phenotypes arising in both progenitor and

differentiated cells. Indeed, by employing the 2C-Cas9 vector to target the *atoh7* transcription factor, we were able to modify the fate specification of retinal progenitor cells, generating and permanently labeling cell clones missing the population of RGCs.

With a similar efficiency, we applied the 2C-Cas9 system to target gene LOF in differentiated cells, generating genetic chimera allowing for the assessment of cell-autonomous phenotypes. To obtain this result, we combined the 2C-Cas9 system with the Brainbow technology, allowing the differential labeling of wild type and mutant cells and permitting their direct comparison in the same animal. We tested this system by targeting the motor protein Kinesin family member 5A (*kif5aa*) in differentiated RGCs. As expected, inactivation of the *kif5aa* gene resulted in a reduction of axonal branch complexity in a cell autonomous manner. In addition, thanks to the 2C-Cas9 approach, the expression of different fluorescent reporters allowed us to mark and compare, in the same tectum, wild type and potentially mutant *cas9*-expressing cells.

Taken together, our experiments are the proof-of-principle for the efficiency of a novel technique permitting, at the same time, conditional mutagenesis and labeling of the cells potentially carrying a LOF allele.

III.1.II Advantages and limitations of the 2C-Cas9 system

Based on use of the Gal4/UAS system to selectively express the Cas9 enzyme, the 2C-Cas9 system represents a flexible tool to induce conditional biallelic gene disruption. A broad range of studies could potentially benefit from this innovative strategy, allowing, at the same time, targeted gene inactivation and the labeling of the *cas9*-expressing cells. The fields of stem cell and cancer cell biology could take great advantage from the possibility of performing genetic lineage tracing of potentially mutant *cas9*-expressing clones by using the 2C-Cas9 system in progenitor cells. At the same time, the expression of the 2C-Cas9 vector in differentiated cells could be advantageous in the field of neurobiology, where neurodevelopment processes and mechanisms involved in the maintenance and function of neural networks are often assessed in post-mitotic neurons.

Furthermore, this method imposes itself as a powerful alternative to the technically challenging transplantation experiments, representing, to date, the only approach allowing the generation of genetic mosaics in zebrafish.

One of the main advantages of our strategy is the genetic fluorescent labeling of *cas9*-expressing cells. Nevertheless Cas9-activity is not unequivocally associated with the induction of biallelic LOF, and, in some cases, the labeled cells or clones will carry in frame mutations or efficiently repaired alleles. This observation points out the need of a method to distinguish mutant and wild-type cells in the mixed population of Cas9-expressing cells. As proposed in our report, a clear readout of the protein loss induced by targeted gene disruption can be obtained by performing immunofluorescence experiments.

In parallel, to maximize the proportion of cells harboring out of frame mutations, it would be required to optimize the efficiency of the 2C-Cas9 technology. In order to increase the mutagenesis rate, we could improve different parts of our vector system. First, it is of crucial importance the selection of a highly efficient sgRNA to successfully induce DSBs at the target genomic locus. Additionally, the design of sgRNAs targeting essential functional domains could reduce the deleterious effects of in-frame mutations, as the a simple aminoacidic substitution could cause the loss of their biological acidity. As shown by our results, the efficiency of gene disruption can be enhanced by the expression of the 2C-Cas9 plasmid in a heterozygous background, where one allele already carries a null mutation. Furthermore, it is possible to act on the expression level of the Cas9 enzyme, maximizing the amount of protein targeting the gene of interest. This result could be obtained by the use of a strong Gal4 driver line, leading to a high intracellular expression of Cas9 endonuclease. As a complementary approach, additional improvements in the Cas9 expression cassette may be performed. One possibility could be the incorporation of noncoding elements of the zebrafish genome that have been shown to strongly increase the expression of transgenes in UAS-based plasmids (Horstick et al 2015).

Finally, despite the above-listed drawbacks, the genetic labeling of potentially mutant cells generated by the 2C-Cas9 system represents a valuable approach to correlate phenotype and genotype in a tissue specific manner, a challenge that cannot be addressed with other genetic tools currently available in zebrafish.

III.II.I Metrns are involved in the patterning of the axonal projection in the CNS of zebrafish embryos

In the past three decades, the identification of proteins modulating axonal elongation during embryonic development has driven a significant progress towards our understanding of the molecular mechanisms leading to the assembly of functional neural circuits. A number of instructive molecular guidance cues has been identified and the study of their mechanisms of action has allowed scientists to sketch out the main aspects of the biological processes directing axonal pathfinding. Nevertheless, a comprehensive picture of how axonal navigation choices direct the formation of the proper synaptic connections between different neurons is still missing, and, most importantly, it is still unsure whether additional molecules are involved in this process.

Our lab became recently interested in the *metrn* gene family, encoding for a group of secreted proteins regulating neuronal progenitor differentiation and axonal extension, *in vitro*. By using the zebrafish CNS as a model, we tried to understand if Metrns have a function in the development of the embryonic brain and, more precisely, if they are involved in the regulation of axonal pathfinding.

First, we raised questions about the conservation of the Metrn family across different species and we verified that *metrn*- and *metrn1*-coding genes exist in several classes of vertebrates. As no gene belonging to the family could be found in invertebrate genomes, we concluded that Metrn proteins arose after the evolution of vertebrates, thus implying that their putative role in the patterning of the CNS would be vertebrate-specific. The presence of modules of highly conserved amino acids in the sequence of Metrns belonging to different species provided an indication that Metrns' biological activity has been maintained across evolution. One common feature of Metrn sequences is the presence of a signal peptide in their N-terminal region, indicating that all proteins belonging to this family are secreted in the extracellular environment and, most likely, mediate their biological function by binding to a specific receptor on the surface of their target cells. The hypothesis of Metrn being involved in axonal pathfinding was strengthened by the presence of a supposed NTR-like domain in the C-terminal region of the zebrafish Metrn1. This domain was not detected in other proteins, nevertheless, considering the high degree of sequence conservation existing among Metrns, it is likely that it is also present in other orthologues or paralogues. It still unknown whether this

domain has a functional meaning, nevertheless it is interesting to note that, being present in Netrins and other proteins, this module did not show any chemoattractant or chemorepellent property, but seems to be involved in the interaction with ECM components like HSPGs (Bekhouche, Kronenberg et al. 2010). Therefore, it seems reasonable that this putative domain contributes to the regulation of Metrns activity by modulating their spatial distribution in the extracellular compartment.

To support the hypothesis of Metrns playing a role in defining axonal trajectories during embryonic development, we proved that *metrn* genes are expressed in the embryonic CNS. As already demonstrated for their mouse orthologues (Nishino, Yamashita et al. 2004, Jorgensen, Thompson et al. 2009), in the developing CNS of zebrafish larvae, *metrn* genes are transcribed by glia and neuronal progenitors, and, importantly, a high number of *metrn*- and *metrn1*-expressing cells are located along the midline and at the floor plate. These regions represent well-characterized guideposts for elongating axons and are responsible for the generation of the majority of the environmental cues directing axonal navigation (Tear 1999, Kaprielian, Runko et al. 2001). Interestingly, we found that the mRNA encoding for *metrn1* and for three out of the four zebrafish *slit* paralogues (*slit1a*, *slit1b* and *slit2*) co-localize at the floor plate region in the hindbrain. This observation indicates that the two molecules are, at least in part, produced by the same cell populations, raising the attractive hypothesis of a functional interaction between the Metrn and the Slit signaling.

To investigate the biological role of Metrn proteins, we generated LOF alleles for all the three zebrafish paralogues, demonstrating that the establishment of the axonal paths of several neuronal populations is impaired if *metrn* genes are disrupted. In particular, we noticed that the commissural axons of the AC, the RGC projections and the trigeminal neurons seem to be sensitive to Metrn signaling. More precisely, our results suggest that Metrn is the only zebrafish paralogue to have an impact on the development of the AC, as defects in its elongation and fasciculation can be detected in triple and single *metrn*^{-/-} mutants but not in case of single *metrn1* or *metrn2* gene disruption. Differently, our data indicate that the three paralogues might act redundantly in regulating the laminar patterning of RGC axons in the tectal neuropil while Metrn and Metrn1 (but not Metrn2) showed a possible instructive role on the trigeminal nerve.

Overall, our phenotypic analysis demonstrated a role of Metrn proteins

in defining the axonal projection pattern of several neuronal types, pointing out that distinct axonal populations might be responsive to different combination of Metrnl proteins. Nevertheless, despite they highlight the importance of this new class of proteins in regulating axonal elongation, our experiments do not provide a functional explanation on how Metrnl activity is able to influence axonal behavior. In the next paragraphs, we speculate about possible mechanisms that could explain Metrnl-induced modulation of axonal pathfinding, providing a brief description of the experiments needed to clarify this aspect.

III.II.II Possible models for Metrnl induced modulation of axonal pathfinding in Zebrafish

A. FP induction, Midline differentiation and tissue homeostasis

Based on published *in vitro* and *in vivo* data, a first hypothesis suggests that Metrnl proteins are involved in the patterning and differentiation of the midline glia cells responsible for the generation of instructive guidance cues.

Studies in mouse have shown that Metrnl is a positive regulator of Nodal signaling, demonstrating that its gene inactivation induces lethal defects in mesoderm specification (Kim, Moon et al. 2014). Importantly, it has been proven that, in zebrafish, Nodal activity is required for the FP induction, as the ventral midline fails to properly differentiate in *cyc (ndr2)* mutants (Sampath, Rubinstein et al. 1998). In these embryos, the absence of the FP is associated with remarkable guidance defects, confirming the role of the FP as a key organizer of axonal projections (Hatta 1992). If Metrnl proteins act as enhancers of Nodal signaling, it seems reasonable to hypothesize that, in case of *metrnl* gene disruption, the mutant FP would not be fully developed. This would result in a defective production of guidance molecules which, in turn, would led to the pathfinding defects observed in *metrnl* mutant fish. To test this first model it would be interesting to analyze *nodal* expression in the context of *metrnl* LOF and to verify if morphological defects in the FP organization can be detected in mutant embryos, although, at a first anatomical observation, this does not seem to be the case in the triple mutants.

As an alternative possibility, several groups proposed the involvement

of *Metrn* proteins in the modulation of glia specification. In support to this idea, cultured neurospheres or P19 embryonic cell line were shown to differentiate into GFAP-positive glia cells if exposed to exogenous *Metrn* (Nishino, Yamashita et al. 2004, Lee, Han et al. 2010). The neuron/glia balance is important for the homeostasis of the developing brain, being responsible for the maintenance of the proper amount of trophic and guidance factors (Chotard and Salecker 2004). If *metrns* inactivation leads to defects in glia differentiation, the presence of an unbalanced production of guidance factors could explain the navigation mistakes observed in the mutants. To explore this possibility, it would be needed to assess how neuronal progenitors differentiate in *metrns* mutants, evaluating how the neuron/glia ratio change if *metrns* CDSs are disrupted. To this end it might be useful to differently label post-mitotic neurons and glia cells, staining the two cell types in fixed (e.g. by Huc/GFAP antibody staining) or in live animals (e.g. by generating transgenic lines in which the two cell populations express fluorescent reporters). Preliminary experiments have shown that the number of *GFAP* expressing cells (revealed by immunohistochemistry) or the *GFAP* mRNA levels (detected by qPCR) are not affected in triple mutant embryos, arguing against this hypothesis (data not shown).

Both these hypotheses rely on an indirect action of *Metrns* on the behavior of pathfinding axons. According to these models, *Metrns* biological activity would modulate the extracellular environment which serve as a substrate for axonal elongation rather than directly influence axonal navigation.

B. Direct interaction with pathfinding axons and modulation of axon guidance pathways

A second theory proposes that *Metrns* themselves are capable of controlling axonal navigation choices, either being novel and uncharacterized guidance molecules or *via* the interaction or the regulation of known pathways directing axonal navigation. Despite the intensive investigation of molecular cues in the field of axon guidance research, in the last years, the identification of novel instructive factors has remarkably slowed down. Nevertheless, while the main family of guidance factors have been already uncovered, it is not excluded that the refinement of axonal trajectories might need additional molecules with more specialized functions. As already mentioned, Meteorin

proteins are secreted in the “right place” and at the “right time” in the embryonic CNS, thus representing good candidates to be added to the repertoire of molecules orchestrating the process of axonal elongation. In order to accomplish this task, Metrns would be required to interact with a specific receptor, expressed at the surface of elongating axons and activating a precise signaling pathway leading to a change in axonal behavior. To test the putative binding of Metrns on growing axons I generated expression constructs in which the CDSs of *metrns* is fused to the cDNA of the *alkaline-phosphatase* (AP). AP-fusion proteins have been previously shown to be an extremely efficient tool to investigate the cellular distribution of a putative receptor and could be used to localize the cell populations expressing Metrns receptor(s) (Flanagan, Cheng et al. 2000). Encouraging preliminary results from our collaborators show that, if applied to spinal cord sections, mouse Metrns-AP fusion proteins are able to bind to commissural axons, in particular to their post-crossing segment (A. Chedotal, personal communication, data not shown). This observation supports the hypothesis of a function of Metrns in axon guidance, pointing out the need to identify the receptor(s) responsible for their signal transduction in order to move forward in understanding their biological activity. To strengthen this idea, *in vitro* tests will be needed to investigate the potential chemoattractant or chemorepellent action of Metrns proteins. To this end, we plan to use *in vitro* explant cultures to evaluate the amount of Metrns-induced axonal outgrowth, to test the directionality of the resulting neurite extension and to assess a potential synergistic interaction with known guidance factors such as Netrins or Slits.

An interesting possibility is that Metrns cooperate with canonical guidance pathways, regulating their activity and influencing their impact on axonal elongation. Some indications suggest the tempting idea that Metrns proteins might act in a signaling pathway related to the one of Slits. It has been shown that both proteins have an impact on cultured DRG explants, promoting neurite extension and axonal branching (Zinn and Sun 1999, Nishino, Yamashita et al. 2004, Jorgensen, Thompson et al. 2009). In addition, Metrnl and a cleaved fragment of Slit (Slit2-C) have been proved to have a similar role in the adipose tissue (Rao, Long et al. 2014, Svensson, Long et al. 2016) and we showed that the expression pattern of the two gene families display a partial overlap. The idea of a functional interaction between Metrns and Slit pathways is further reinforced by the observation that the pathfinding choices of all axons affected by *metrns*

LOF are influenced by Slit activity (Xiao, Staub et al. 2011, Pan, Choy et al. 2012) (Zhang, Gao et al. 2012). Therefore, it would be interesting to test if there is a direct interaction between Metrns and proteins belonging to the Slit/Robo pathway (indicating a direct link between the biological activity of the two proteins) or if Metrns have a role in the regulation of *slit/robo* expression levels (suggesting that Metrns function upstream Slit/Robo). Both possibilities seem reasonable if we assume that the putative binding to pathfinding axons, that we have visualized for the mouse orthologues, is conserved in zebrafish Metrns. On one hand, Metrns could influence axonal response to the Slit/Robo pathway by interacting (directly or by forming a complex with Slit proteins) with Robo receptors expressed at the membrane of navigating axon. To test this hypothesis, *in vitro* binding assays will be needed to validate a possible biochemical interaction between Metrns, Slit and Robo proteins. On the other hand, Metrns binding to an unknown receptor on the membrane of growing axons might activate a signaling pathway leading to a change in the expression level of the Robo receptors, thus causing a Metrns-induced modulation of the axonal sensitivity to the Slit-mediated repulsion. A quantitative and qualitative analysis of the expression of *robo* genes in the context of *metrn* LOF would be helpful to evaluate if Metrns are able to enhance or repress *robo* transcription.

Overall, the models proposed in this paragraph assume a more direct activity of Metrns on growing axons, and imply that the biological role of these proteins is mediated by their binding to the membrane of elongating axons.

Importantly, the models proposed above are not mutually exclusive. As shown for many morphogens, it is possible that Metrns proteins have multiple functions during embryonic development, being involved in neuron/glia differentiation at early stages and directly regulating axonal navigation pathways later in development. To distinguish between early and late function of Metrns it would be useful to apply the 2C-Cas9 system to inactivate *metrns* genes after neuronal differentiation is completed, thus assessing the function of Metrns on axon elongation independently from the process of FP and glia differentiation.

CHAPTER IV: CONCLUSIONS

Conclusions I

In the past few years, the CRISPR/Cas9 technology has imposed itself as one of the most efficient and reliable method to induce precise and targeted genetic modifications.

In zebrafish, this technique has been successfully employed to perform constitutive mutagenesis or to generate transgenic reporter lines via knock-in approaches. Nevertheless, in this model organism, the use of CRISPR/Cas9 methodology to induce conditional gene inactivation remains challenging.

Thanks to the combination of the Gal4/UAS and the CRISPR/Cas9 technologies, the 2C-Cas9 method presented in this thesis allows the spatiotemporal control of Cas9 activity, thus enabling the generation of targeted mutagenesis in a chosen tissue or in single cells. Importantly, the use of genetically encoded reporters to identify the population of Cas9-expressing cells represents an important advantage for the analysis of the phenotypes arising from the targeted gene inactivation, allowing the assessment of cell-autonomous defects arising from gene LOF. In addition, the use of the Cre enzyme to permanently label the population of Cas9-expressing cells offers the possibility to perform genetic lineage tracing of potentially mutant progenitors and gives the opportunity to follow their fate until adulthood. Overall, the above listed features make the 2C-Cas9 an extremely versatile tool, potentially useful for a broad range of research fields including cancer biology, neuroscience, stem cell, regeneration and aging.

Conclusion II

During embryogenesis, newborn neurons need to extend their axons in an extremely precise and stereotyped fashion in order to build functional neuronal networks. A complex set of receptor/ligand interactions occurs between the developing axonal projections and the extracellular environment, ensuring the proper establishment of neuronal connections in the developing brain. The second part of this thesis focused on the analysis of the putative conserved function of the Meteorin protein family in the patterning of the embryonic brain during development. We showed that Meteorin proteins are conserved across vertebrates and we confirmed that *metrn* genes are expressed along the midline and at the FP in the developing CNS of zebrafish larvae. Furthermore, we demonstrated that targeted gene disruption of the three zebrafish *metrn* loci induces pathfinding defects in distinct population of axons, suggesting that different neuronal types are responsive to Metrnl signaling. Taken together, these data propose the involvement of Meteorins in the process of axonal elongation and pathfinding and represent an important advance toward a deeper understanding of the mechanisms controlling axonal navigation. This study lays the first stone toward the understanding of the biological role of a novel family of midline secreted proteins, whose activity can, directly or indirectly, impact on the formation of the neural wiring patterns in the embryonic CNS.

BIBLIOGRAPHY

BIBLIOGRAPHY

Ablain, J., E. M. Durand, S. Yang, Y. Zhou and L. I. Zon (2015). "A CRISPR/Cas9 vector system for tissue-specific gene disruption in zebrafish." *Dev Cell* 32(6): 756-764.

Albadri, S., F. Del Bene and C. Revenu (2017). "Genome editing using CRISPR/Cas9-based knock-in approaches in zebrafish." *Methods* 121-122: 77-85.

Baier, H., S. Klostermann, T. Trowe, R. O. Karlstrom, C. Nusslein-Volhard and F. Bonhoeffer (1996). "Genetic dissection of the retinotectal projection." *Development* 123: 415-425.

Banyai, L. and L. Patthy (1999). "The NTR module: domains of netrins, secreted frizzled related proteins, and type I procollagen C-proteinase enhancer protein are homologous with tissue inhibitors of metalloproteases." *Protein Sci* 8(8): 1636-1642.

Barrangou, R., C. Fremaux, H. Deveau, M. Richards, P. Boyaval, S. Moineau, D. A. Romero and P. Horvath (2007). "CRISPR provides acquired resistance against viruses in prokaryotes." *Science* 315(5819): 1709-1712.

Barresi, M. J., L. D. Hutson, C. B. Chien and R. O. Karlstrom (2005). "Hedgehog regulated Slit expression determines commissure and glial cell position in the zebrafish forebrain." *Development* 132(16): 3643-3656.

Bashaw, G. J. and R. Klein (2010). "Signaling from axon guidance receptors." *Cold Spring Harb Perspect Biol* 2(5): a001941.

Bedell, V. M., Y. Wang, J. M. Campbell, T. L. Poshusta, C. G. Starker, R. G. Krug, 2nd, W. Tan, S. G. Penheiter, A. C. Ma, A. Y. Leung, S. C. Fahrenkrug, D. F. Carlson, D. F. Voytas, K. J. Clark, J. J. Essner and S. C. Ekker (2012). "In vivo genome editing using a high-efficiency TALEN system." *Nature* 491(7422): 114-118.

Bekhouche, M., D. Kronenberg, S. Vadon-Le Goff, C. Bijakowski, N. H. Lim, B. Font, E. Kessler, A. Colige, H. Nagase, G. Murphy, D. J. Hulmes and C. Moali (2010). "Role of the netrin-like domain of procollagen C-proteinase

enhancer-1 in the control of metalloproteinase activity." *J Biol Chem* 285(21): 15950-15959.

Bhaya, D., M. Davison and R. Barrangou (2011). "CRISPR-Cas systems in bacteria and archaea: versatile small RNAs for adaptive defense and regulation." *Annu Rev Genet* 45: 273-297.

Blockus, H. and A. Chedotal (2016). "Slit-Robo signaling." *Development* 143(17): 3037-3044.

Bouabe, H. and K. Okkenhaug (2013). "Gene targeting in mice: a review." *Methods Mol Biol* 1064: 315-336.

Bovolenta, P. and J. Dodd (1991). "Perturbation of neuronal differentiation and axon guidance in the spinal cord of mouse embryos lacking a floor plate: analysis of Danforth's short-tail mutation." *Development* 113(2): 625-639.

Brose, K., K. S. Bland, K. H. Wang, D. Arnott, W. Henzel, C. S. Goodman, M. Tessier-Lavigne and T. Kidd (1999). "Slit proteins bind Robo receptors and have an evolutionarily conserved role in repulsive axon guidance." *Cell* 96(6): 795-806.

Burgess, H. A., S. L. Johnson and M. Granato (2009). "Unidirectional startle responses and disrupted left-right co-ordination of motor behaviors in robo3 mutant zebrafish." *Genes Brain Behav* 8(5): 500-511.

Burrill, J. D. and S. S. Easter, Jr. (1994). "Development of the retinofugal projections in the embryonic and larval zebrafish (*Brachydanio rerio*)." *J Comp Neurol* 346(4): 583-600.

Chang, N., C. Sun, L. Gao, D. Zhu, X. Xu, X. Zhu, J. W. Xiong and J. J. Xi (2013). "Genome editing with RNA-guided Cas9 nuclease in zebrafish embryos." *Cell Res* 23(4): 465-472.

Charron, F., E. Stein, J. Jeong, A. P. McMahon and M. Tessier-Lavigne (2003). "The morphogen sonic hedgehog is an axonal chemoattractant that collaborates with netrin-1 in midline axon guidance." *Cell* 113(1): 11-23.

Chen, F., J. Rosiene, A. Che, A. Becker and J. LoTurco (2015). "Tracking and transforming neocortical progenitors by CRISPR/Cas9 gene targeting and piggyBac transposase lineage labeling." *Development* 142(20): 3601-3611.

Choi, C. M., S. Vilain, M. Langen, S. Van Kelst, N. De Geest, J. Yan, P. Verstreken and B. A. Hassan (2009). "Conditional mutagenesis in *Drosophila*." *Science* 324(5923): 54.

Chotard, C. and I. Salecker (2004). "Neurons and glia: team players in axon guidance." *Trends Neurosci* 27(11): 655-661.

Cong, L., F. A. Ran, D. Cox, S. Lin, R. Barretto, N. Habib, P. D. Hsu, X. Wu, W. Jiang, L. A. Marraffini and F. Zhang (2013). "Multiplex genome engineering using CRISPR/Cas systems." *Science* 339(6121): 819-823.

Delloye-Bourgeois, C., A. Jacquier, C. Charoy, F. Reynaud, H. Nawabi, K. Thoinet, K. Kindbeiter, Y. Yoshida, Y. Zagar, Y. Kong, Y. E. Jones, J. Falk, A. Chedotal and V. Castellani (2015). "PlexinA1 is a new Slit receptor and mediates axon guidance function of Slit C-terminal fragments." *Nat Neurosci* 18(1): 36-45.

Dickson, B. J. (2002). "Molecular mechanisms of axon guidance." *Science* 298(5600): 1959-1964.

Dominici, C., J. A. Moreno-Bravo, S. R. Puiggros, O. Rappeneau, N. Rama, P. Vieugue, A. Bernet, P. Mehlen and A. Chedotal (2017). "Floor-plate-derived netrin-1 is dispensable for commissural axon guidance." *Nature* 545(7654): 350-354.

Driever, W., L. Solnica-Krezel, A. F. Schier, S. C. Neuhauss, J. Malicki, D. L. Stemple, D. Y. Stainier, F. Zwartkruis, S. Abdelilah, Z. Rangini, J. Belak and C. Boggs (1996). "A genetic screen for mutations affecting embryogenesis in zebrafish." *Development* 123: 37-46.

Dudanova, I. and R. Klein (2013). "Integration of guidance cues: parallel signaling and crosstalk." *Trends Neurosci* 36(5): 295-304.

Ebens, A., K. Brose, E. D. Leonardo, M. G. Hanson, Jr., F. Bladt, C. Birchmeier, B. A. Barres and M. Tessier-Lavigne (1996). "Hepatocyte growth factor/scatter factor is an axonal chemoattractant and a neurotrophic factor for spinal motor neurons." *Neuron* 17(6): 1157-1172.

Farmer, W. T., A. L. Altick, H. F. Nural, J. P. Dugan, T. Kidd, F. Charron and G. S. Mastick (2008). "Pioneer longitudinal axons navigate using floor plate and Slit/Robo signals." *Development* 135(22): 3643-3653.

Fazeli, A., S. L. Dickinson, M. L. Hermiston, R. V. Tighe, R. G. Steen, C. G. Small, E. T. Stoeckli, K. Keino-Masu, M. Masu, H. Rayburn, J. Simons, R. T. Bronson, J. I. Gordon, M. Tessier-Lavigne and R. A. Weinberg (1997). "Phenotype of mice lacking functional Deleted in colorectal cancer (Dcc) gene." *Nature* 386(6627): 796-804.

Feil, R., J. Brocard, B. Mascrez, M. LeMeur, D. Metzger and P. Chambon (1996). "Ligand-activated site-specific recombination in mice." *Proc Natl Acad Sci U S A* 93(20): 10887-10890.

Feldheim, D. A. and D. D. O'Leary (2010). "Visual map development: bidirectional signaling, bifunctional guidance molecules, and competition." *Cold Spring Harb Perspect Biol* 2(11): a001768.

Flanagan, J. G., H. J. Cheng, D. A. Feldheim, M. Hattori, Q. Lu and P. Vanderhaeghen (2000). "Alkaline phosphatase fusions of ligands or receptors as in situ probes for staining of cells, tissues, and embryos." *Methods Enzymol* 327: 19-35.

Fricke, C., J. S. Lee, S. Geiger-Rudolph, F. Bonhoeffer and C. B. Chien (2001). "astray, a zebrafish roundabout homolog required for retinal axon guidance." *Science* 292(5516): 507-510.

Friedland, A. E., Y. B. Tzur, K. M. Esvelt, M. P. Colaiacovo, G. M. Church and J. A. Calarco (2013). "Heritable genome editing in *C. elegans* via a CRISPR-Cas9 system." *Nat Methods* 10(8): 741-743.

Fujisawa, K., J. L. Wrana and J. G. Culotti (2007). "The slit receptor EVA-1 coactivates a SAX-3/Robo mediated guidance signal in *C. elegans*." *Science* 317(5846): 1934-1938.

Gaiano, N., A. Amsterdam, K. Kawakami, M. Allende, T. Becker and N. Hopkins (1996). "Insertional mutagenesis and rapid cloning of essential genes in zebrafish." *Nature* 383(6603): 829-832.

Garcia-Campmany, L., F. J. Stam and M. Goulding (2010). "From circuits to behaviour: motor networks in vertebrates." *Curr Opin Neurobiol* 20(1): 116-125.

Garneau, J. E., M. E. Dupuis, M. Villion, D. A. Romero, R. Barrangou, P. Boyaval, C. Fremaux, P. Horvath, A. H. Magadan and S. Moineau (2010). "The CRISPR/Cas bacterial immune system cleaves bacteriophage and plasmid DNA." *Nature* 468(7320): 67-71.

Gaudin, A., W. Hofmeister and B. Key (2012). "Chemoattractant axon guidance cues regulate de novo axon trajectories in the embryonic forebrain of zebrafish." *Dev Biol* 367(2): 126-139.

Gratz, S. J., A. M. Cummings, J. N. Nguyen, D. C. Hamm, L. K. Donohue, M. M. Harrison, J. Wildonger and K. M. O'Connor-Giles (2013). "Genome engineering of *Drosophila* with the CRISPR RNA-guided Cas9 nuclease." *Genetics* 194(4): 1029-1035.

Hale, C. R., P. Zhao, S. Olson, M. O. Duff, B. R. Graveley, L. Wells, R. M. Terns and M. P. Terns (2009). "RNA-guided RNA cleavage by a CRISPR RNA-Cas protein complex." *Cell* 139(5): 945-956.

Hamasaki, T., S. Goto, S. Nishikawa and Y. Ushio (2001). "A role of netrin-1 in the formation of the subcortical structure striatum: repulsive action on the migration of late-born striatal neurons." *J Neurosci* 21(12): 4272-4280.

Hatta, K. (1992). "Role of the floor plate in axonal patterning in the zebrafish CNS." *Neuron* 9(4): 629-642.

Hjorth, J. and B. Key (2002). "Development of axon pathways in the zebrafish central nervous system." *Int J Dev Biol* 46(4): 609-619.

Hofmeister, W., C. A. Devine, J. A. Rothnagel and B. Key (2012). "Frizzled-3a and slit2 genetically interact to modulate midline axon crossing in the telencephalon." *Mech Dev* 129(5-8): 109-124.

Hohenester, E. (2008). "Structural insight into Slit-Robo signalling." *Biochem Soc Trans* 36(Pt 2): 251-256.

Holt, C. E. and B. J. Dickson (2005). "Sugar codes for axons?" *Neuron* 46(2): 169-172.

Huang, P., A. Xiao, M. Zhou, Z. Zhu, S. Lin and B. Zhang (2011). "Heritable gene targeting in zebrafish using customized TALENs." *Nat Biotechnol* 29(8): 699-700.

Hutson, L. D. and C. B. Chien (2002). "Pathfinding and error correction by retinal axons: the role of astray/robo2." *Neuron* 33(2): 205-217.

Hutson, L. D. and C. B. Chien (2002). "Wiring the zebrafish: axon guidance and synaptogenesis." *Curr Opin Neurobiol* 12(1): 87-92.

Hwang, W. Y., Y. Fu, D. Reyon, M. L. Maeder, P. Kaini, J. D. Sander, J. K. Joung, R. T. Peterson and J. R. Yeh (2013). "Heritable and precise zebrafish genome editing using a CRISPR-Cas system." *PLoS One* 8(7): e68708.

Hwang, W. Y., Y. Fu, D. Reyon, M. L. Maeder, S. O. Tsai, J. D. Sander, R. T. Peterson, J. R. Yeh and J. K. Joung (2013). "Efficient genome editing in zebrafish using a CRISPR-Cas system." *Nat Biotechnol* 31(3): 227-229.

Ishii, N., W. G. Wadsworth, B. D. Stern, J. G. Culotti and E. M. Hedgecock (1992). "UNC-6, a laminin-related protein, guides cell and pioneer axon migrations in *C. elegans*." *Neuron* 9(5): 873-881.

Jain, R. A., H. Bell, A. Lim, C. B. Chien and M. Granato (2014). "Mirror movement-like defects in startle behavior of zebrafish dcc mutants are caused by aberrant midline guidance of identified descending hindbrain neurons." *J Neurosci* 34(8): 2898-2909.

James, G., S. R. Foster, B. Key and A. Beverdam (2013). "The expression pattern of EVA1C, a novel Slit receptor, is consistent with an axon guidance role in the mouse nervous system." *PLoS One* 8(9): e74115.

Jaworski, A., H. Long and M. Tessier-Lavigne (2010). "Collaborative and specialized functions of Robo1 and Robo2 in spinal commissural axon guidance." *J Neurosci* 30(28): 9445-9453.

Jaworski, A., I. Tom, R. K. Tong, H. K. Gildea, A. W. Koch, L. C. Gonzalez and M. Tessier-Lavigne (2015). "Operational redundancy in axon guidance through the multifunctional receptor Robo3 and its ligand NELL2." *Science* 350(6263): 961-965.

Jinek, M., K. Chylinski, I. Fonfara, M. Hauer, J. A. Doudna and E. Charpentier (2012). "A programmable dual-RNA-guided DNA endonuclease in adaptive bacterial immunity." *Science* 337(6096): 816-821.

Johnson, K. G., A. Ghose, E. Epstein, J. Lincecum, M. B. O'Connor and D. Van Vactor (2004). "Axonal heparan sulfate proteoglycans regulate the distribution and efficiency of the repellent slit during midline axon guidance." *Curr Biol* 14(6): 499-504.

Jorgensen, J. R., D. F. Emerich, C. Thanos, L. H. Thompson, M. Torp, B. Bintz, L. Fjord-Larsen, T. E. Johansen and L. U. Wahlberg (2011). "Lentiviral delivery of meteorin protects striatal neurons against excitotoxicity and reverses motor deficits in the quinolinic acid rat model." *Neurobiol Dis* 41(1): 160-168.

Jorgensen, J. R., A. Fransson, L. Fjord-Larsen, L. H. Thompson, J. P. Houchins, N. Andrade, M. Torp, N. Kalkkinen, E. Andersson, O. Lindvall, M. Ulfendahl, S. Brunak, T. E. Johansen and L. U. Wahlberg (2012). "Cometin is a novel neurotrophic factor that promotes neurite outgrowth and neuroblast migration in vitro and supports survival of spiral ganglion neurons in vivo." *Exp Neurol* 233(1): 172-181.

Jorgensen, J. R., L. Thompson, L. Fjord-Larsen, C. Krabbe, M. Torp, N. Kalkkinen, C. Hansen and L. Wahlberg (2009). "Characterization of Meteorin--an evolutionary conserved neurotrophic factor." *J Mol Neurosci* 39(1-2): 104-116.

Kappler, J., S. Franken, U. Junghans, R. Hoffmann, T. Linke, H. W. Muller and K. W. Koch (2000). "Glycosaminoglycan-binding properties and secondary structure of the C-terminus of netrin-1." *Biochem Biophys Res Commun* 271(2): 287-291.

Kaprielian, Z., E. Runko and R. Imondi (2001). "Axon guidance at the midline choice point." *Dev Dyn* 221(2): 154-181.

Karlstrom, R. O., W. S. Talbot and A. F. Schier (1999). "Comparative synteny cloning of zebrafish you-too: mutations in the Hedgehog target gli2 affect ventral forebrain patterning." *Genes Dev* 13(4): 388-393.

Karlstrom, R. O., T. Trowe and F. Bonhoeffer (1997). "Genetic analysis of axon guidance and mapping in the zebrafish." *Trends Neurosci* 20(1): 3-8.

Karlstrom, R. O., T. Trowe, S. Klostermann, H. Baier, M. Brand, A. D. Crawford, B. Grunewald, P. Haffter, H. Hoffmann, S. U. Meyer, B. K. Muller, S. Richter, F. J. van Eeden, C. Nusslein-Volhard and F. Bonhoeffer (1996). "Zebrafish mutations affecting retinotectal axon pathfinding." *Development* 123: 427-438.

Kemp, H. A., A. Carmany-Rampey and C. Moens (2009). "Generating chimeric zebrafish embryos by transplantation." *J Vis Exp*(29).

Kennedy, T. E., T. Serafini, J. R. de la Torre and M. Tessier-Lavigne (1994). "Netrins are diffusible chemotropic factors for commissural axons in the embryonic spinal cord." *Cell* 78(3): 425-435.

Kennedy, T. E., H. Wang, W. Marshall and M. Tessier-Lavigne (2006). "Axon guidance by diffusible chemoattractants: a gradient of netrin protein in the developing spinal cord." *J Neurosci* 26(34): 8866-8874.

Kidd, T., K. S. Bland and C. S. Goodman (1999). "Slit is the midline repellent for the robo receptor in *Drosophila*." *Cell* 96(6): 785-794.

Kidd, T., K. Brose, K. J. Mitchell, R. D. Fetter, M. Tessier-Lavigne, C. S. Goodman and G. Tear (1998). "Roundabout controls axon crossing of the CNS midline and defines a novel subfamily of evolutionarily conserved guidance receptors." *Cell* 92(2): 205-215.

Kim, Y. Y., J. S. Moon, M. C. Kwon, J. Shin, S. K. Im, H. A. Kim, J. K. Han and Y. Y. Kong (2014). "Meteorin regulates mesendoderm development by enhancing nodal expression." *PLoS One* 9(2): e88811.

Kitsukawa, T., M. Shimizu, M. Sanbo, T. Hirata, M. Taniguchi, Y. Bekku, T. Yagi and H. Fujisawa (1997). "Neuropilin-semaphorin III/D-mediated chemorepulsive signals play a crucial role in peripheral nerve projection in mice." *Neuron* 19(5): 995-1005.

Klambt, C., J. R. Jacobs and C. S. Goodman (1991). "The midline of the *Drosophila* central nervous system: a model for the genetic analysis of cell fate, cell migration, and growth cone guidance." *Cell* 64(4): 801-815.

Klein, R. (2004). "Eph/ephrin signaling in morphogenesis, neural development and plasticity." *Curr Opin Cell Biol* 16(5): 580-589.

Kolodkin, A. L. and M. Tessier-Lavigne (2011). "Mechanisms and molecules of neuronal wiring: a primer." *Cold Spring Harb Perspect Biol* 3(6).

Kramer, E. R., L. Knott, F. Su, E. Dessaud, C. E. Krull, F. Helmbacher and R. Klein (2006). "Cooperation between GDNF/Ret and ephrinA/EphA4 signals for motor-axon pathway selection in the limb." *Neuron* 50(1): 35-47.

Kuhn, R., F. Schwenk, M. Aguet and K. Rajewsky (1995). "Inducible gene targeting in mice." *Science* 269(5229): 1427-1429.

Kullander, K. and R. Klein (2002). "Mechanisms and functions of Eph and ephrin signalling." *Nat Rev Mol Cell Biol* 3(7): 475-486.

Lai Wing Sun, K., J. P. Correia and T. E. Kennedy (2011). "Netrins: versatile extracellular cues with diverse functions." *Development* 138(11): 2153-2169.

Lee, H. S., J. Han, S. H. Lee, J. A. Park and K. W. Kim (2010). "Meteorin promotes the formation of GFAP-positive glia via activation of the Jak-STAT3 pathway." *J Cell Sci* 123(Pt 11): 1959-1968.

Lee, J. S., S. von der Hardt, M. A. Rusch, S. E. Stringer, H. L. Stickney, W. S. Talbot, R. Geisler, C. Nusslein-Volhard, S. B. Selleck, C. B. Chien and H. Roehl (2004). "Axon sorting in the optic tract requires HSPG synthesis by ext2 (dackel) and extl3 (boxer)." *Neuron* 44(6): 947-960.

Li, M., L. Zhao, P. S. Page-McCaw and W. Chen (2016). "Zebrafish Genome Engineering Using the CRISPR-Cas9 System." *Trends Genet* 32(12): 815-827.

Liang, Y., R. S. Annan, S. A. Carr, S. Popp, M. Mevissen, R. K. Margolis and R. U. Margolis (1999). "Mammalian homologues of the *Drosophila* slit protein are ligands of the heparan sulfate proteoglycan glypican-1 in brain." *J Biol Chem* 274(25): 17885-17892.

Livesey, F. J. and S. P. Hunt (1997). "Netrin and netrin receptor expression in the embryonic mammalian nervous system suggests roles in retinal, striatal, nigral, and cerebellar development." *Mol Cell Neurosci* 8(6): 417-429.

Long, H., C. Sabatier, L. Ma, A. Plump, W. Yuan, D. M. Ornitz, A. Tamada, F. Murakami, C. S. Goodman and M. Tessier-Lavigne (2004). "Conserved roles for Slit and Robo proteins in midline commissural axon guidance." *Neuron* 42(2): 213-223.

Lopez-Bendito, G., A. Cautinat, J. A. Sanchez, F. Bielle, N. Flames, A. N. Garratt, D. A. Talmage, L. W. Role, P. Charnay, O. Marin and S. Garel

(2006). "Tangential neuronal migration controls axon guidance: a role for neuregulin-1 in thalamocortical axon navigation." *Cell* 125(1): 127-142.

Lyuksyutova, A. I., C. C. Lu, N. Milanesio, L. A. King, N. Guo, Y. Wang, J. Nathans, M. Tessier-Lavigne and Y. Zou (2003). "Anterior-posterior guidance of commissural axons by Wnt-frizzled signaling." *Science* 302(5652): 1984-1988.

Macdonald, R., J. Scholes, U. Strahle, C. Brennan, N. Holder, M. Brand and S. W. Wilson (1997). "The Pax protein Noi is required for commissural axon pathway formation in the rostral forebrain." *Development* 124(12): 2397-2408.

Mali, P., L. Yang, K. M. Esvelt, J. Aach, M. Guell, J. E. DiCarlo, J. E. Norville and G. M. Church (2013). "RNA-guided human genome engineering via Cas9." *Science* 339(6121): 823-826.

Malina, A., J. R. Mills, R. Cencic, Y. Yan, J. Fraser, L. M. Schippers, M. Paquet, J. Dostie and J. Pelletier (2013). "Repurposing CRISPR/Cas9 for in situ functional assays." *Genes Dev* 27(23): 2602-2614.

Marillat, V., C. Sabatier, V. Failli, E. Matsunaga, C. Sotelo, M. Tessier-Lavigne and A. Chedotal (2004). "The slit receptor Rig-1/Robo3 controls midline crossing by hindbrain precerebellar neurons and axons." *Neuron* 43(1): 69-79.

Marraffini, L. A. and E. J. Sontheimer (2008). "CRISPR interference limits horizontal gene transfer in staphylococci by targeting DNA." *Science* 322(5909): 1843-1845.

Mastick, G. S., W. T. Farmer, A. L. Altick, H. F. Nural, J. P. Dugan, T. Kidd and F. Charron (2010). "Longitudinal axons are guided by Slit/Robo signals from the floor plate." *Cell Adh Migr* 4(3): 337-341.

Matise, M. P., M. Lustig, T. Sakurai, M. Grumet and A. L. Joyner (1999). "Ventral midline cells are required for the local control of commissural axon guidance in the mouse spinal cord." *Development* 126(16): 3649-3659.

McCammon, J. M., Y. Doyon and S. L. Amacher (2011). "Inducing high rates of targeted mutagenesis in zebrafish using zinc finger nucleases (ZFNs)." *Methods Mol Biol* 770: 505-527.

McLaughlin, T. and D. D. O'Leary (2005). "Molecular gradients and development of retinotopic maps." *Annu Rev Neurosci* 28: 327-355.

Mitchell, K. J., J. L. Doyle, T. Serafini, T. E. Kennedy, M. Tessier-Lavigne, C. S. Goodman and B. J. Dickson (1996). "Genetic analysis of Netrin genes in

Drosophila: Netrins guide CNS commissural axons and peripheral motor axons." *Neuron* 17(2): 203-215.

Moens, C. B. and V. E. Prince (2002). "Constructing the hindbrain: insights from the zebrafish." *Dev Dyn* 224(1): 1-17.

Myers, J. P., M. Santiago-Medina and T. M. Gomez (2011). "Regulation of axonal outgrowth and pathfinding by integrin-ECM interactions." *Dev Neurobiol* 71(11): 901-923.

Nakano, Y., H. R. Kim, A. Kawakami, S. Roy, A. F. Schier and P. W. Ingham (2004). "Inactivation of dispatched 1 by the chameleon mutation disrupts Hedgehog signalling in the zebrafish embryo." *Dev Biol* 269(2): 381-392.

Nakazawa, N., K. Taniguchi, T. Okumura, R. Maeda and K. Matsuno (2012). "A novel Cre/loxP system for mosaic gene expression in the Drosophila embryo." *Dev Dyn* 241(5): 965-974.

Nawabi, H. and V. Castellani (2011). "Axonal commissures in the central nervous system: how to cross the midline?" *Cell Mol Life Sci* 68(15): 2539-2553.

Ni, T. T., J. Lu, M. Zhu, L. A. Maddison, K. L. Boyd, L. Huskey, B. Ju, D. Hesselton, T. P. Zhong, P. S. Page-McCaw, D. Y. Stainier and W. Chen (2012). "Conditional control of gene function by an invertible gene trap in zebrafish." *Proc Natl Acad Sci U S A* 109(38): 15389-15394.

Nishino, J., K. Yamashita, H. Hashiguchi, H. Fujii, T. Shimazaki and H. Hamada (2004). "Meteorin: a secreted protein that regulates glial cell differentiation and promotes axonal extension." *EMBO J* 23(9): 1998-2008.

Nugent, A. A., A. L. Kolpak and E. C. Engle (2012). "Human disorders of axon guidance." *Curr Opin Neurobiol* 22(5): 837-843.

Pan, Y. A., M. Choy, D. A. Prober and A. F. Schier (2012). "Robo2 determines subtype-specific axonal projections of trigeminal sensory neurons." *Development* 139(3): 591-600.

Park, J. A., H. S. Lee, K. J. Ko, S. Y. Park, J. H. Kim, G. Choe, H. S. Kweon, H. S. Song, J. C. Ahn, Y. S. Yu and K. W. Kim (2008). "Meteorin regulates angiogenesis at the gliovascular interface." *Glia* 56(3): 247-258.

Paulus, J. D. and M. C. Halloran (2006). "Zebrafish bashful/laminin-alpha 1 mutants exhibit multiple axon guidance defects." *Dev Dyn* 235(1): 213-224.

Platt, R. J., S. Chen, Y. Zhou, M. J. Yim, L. Swiech, H. R. Kempton, J. E. Dahlman, O. Parnas, T. M. Eisenhaure, M. Jovanovic, D. B. Graham, S.

Jhunjhunwala, M. Heidenreich, R. J. Xavier, R. Langer, D. G. Anderson, N. Hacohen, A. Regev, G. Feng, P. A. Sharp and F. Zhang (2014). "CRISPR-Cas9 knockin mice for genome editing and cancer modeling." *Cell* 159(2): 440-455.

Port, F., H. M. Chen, T. Lee and S. L. Bullock (2014). "Optimized CRISPR/Cas tools for efficient germline and somatic genome engineering in *Drosophila*." *Proc Natl Acad Sci U S A* 111(29): E2967-2976.

Ramialison, M., B. Bajoghli, N. Aghaallaei, L. Ettwiller, S. Gaudan, B. Wittbrodt, T. Czerny and J. Wittbrodt (2008). "Rapid identification of PAX2/5/8 direct downstream targets in the otic vesicle by combinatorial use of bioinformatics tools." *Genome Biol* 9(10): R145.

Rao, R. R., J. Z. Long, J. P. White, K. J. Svensson, J. Lou, I. Lokurkar, M. P. Jedrychowski, J. L. Ruas, C. D. Wrann, J. C. Lo, D. M. Camera, J. Lachey, S. Gygi, J. Seehra, J. A. Hawley and B. M. Spiegelman (2014). "Meteorin-like is a hormone that regulates immune-adipose interactions to increase beige fat thermogenesis." *Cell* 157(6): 1279-1291.

Raper, J. and C. Mason (2010). "Cellular strategies of axonal pathfinding." *Cold Spring Harb Perspect Biol* 2(9): a001933.

Robles, E., A. Filosa and H. Baier (2013). "Precise lamination of retinal axons generates multiple parallel input pathways in the tectum." *J Neurosci* 33(11): 5027-5039.

Rochlin, M. W., R. O'Connor, R. J. Giger, J. Verhaagen and A. I. Farbman (2000). "Comparison of neurotrophin and repellent sensitivities of early embryonic geniculate and trigeminal axons." *J Comp Neurol* 422(4): 579-593.

Rossant, J. and A. Spence (1998). "Chimeras and mosaics in mouse mutant analysis." *Trends Genet* 14(9): 358-363.

Sabatier, C., A. S. Plump, M. Le, K. Brose, A. Tamada, F. Murakami, E. Y. Lee and M. Tessier-Lavigne (2004). "The divergent Robo family protein rig-1/Robo3 is a negative regulator of slit responsiveness required for midline crossing by commissural axons." *Cell* 117(2): 157-169.

Sampath, K., A. L. Rubinstein, A. M. Cheng, J. O. Liang, K. Fekany, L. Solnica-Krezel, V. Korzh, M. E. Halpern and C. V. Wright (1998). "Induction of the zebrafish ventral brain and floorplate requires cyclops/nodal signalling." *Nature* 395(6698): 185-189.

Schauerte, H. E., F. J. van Eeden, C. Fricke, J. Odenthal, U. Strahle and P. Hafter (1998). "Sonic hedgehog is not required for the induction of medial

floor plate cells in the zebrafish." *Development* 125(15): 2983-2993.

Seeger, M., G. Tear, D. Ferres-Marco and C. S. Goodman (1993). "Mutations affecting growth cone guidance in *Drosophila*: genes necessary for guidance toward or away from the midline." *Neuron* 10(3): 409-426.

Serafini, T., S. A. Colamarino, E. D. Leonardo, H. Wang, R. Beddington, W. C. Skarnes and M. Tessier-Lavigne (1996). "Netrin-1 is required for commissural axon guidance in the developing vertebrate nervous system." *Cell* 87(6): 1001-1014.

Seth, A., J. Culverwell, M. Walkowicz, S. Toro, J. M. Rick, S. C. Neuhaus, Z. M. Varga and R. O. Karlstrom (2006). "belladonna/*Ihx2* is required for neural patterning and midline axon guidance in the zebrafish forebrain." *Development* 133(4): 725-735.

Shanmugalingam, S., C. Houart, A. Picker, F. Reifers, R. Macdonald, A. Barth, K. Griffin, M. Brand and S. W. Wilson (2000). "Ace/*Fgf8* is required for forebrain commissure formation and patterning of the telencephalon." *Development* 127(12): 2549-2561.

Shirasaki, R., J. W. Lewcock, K. Lettieri and S. L. Pfaff (2006). "FGF as a target-derived chemoattractant for developing motor axons genetically programmed by the LIM code." *Neuron* 50(6): 841-853.

Stoeckli, E. (2017). "Where does axon guidance lead us?" *F1000Res* 6: 78.

Stuermer, C. A. (1988). "Retinotopic organization of the developing retinotectal projection in the zebrafish embryo." *J Neurosci* 8(12): 4513-4530.

Svensson, K. J., J. Z. Long, M. P. Jedrychowski, P. Cohen, J. C. Lo, S. Serag, S. Kir, K. Shinoda, J. A. Tartaglia, R. R. Rao, A. Chedotal, S. Kajimura, S. P. Gygi and B. M. Spiegelman (2016). "A Secreted *Slit2* Fragment Regulates Adipose Tissue Thermogenesis and Metabolic Function." *Cell Metab* 23(3): 454-466.

Tamagnone, L. and P. M. Comoglio (2000). "Signalling by semaphorin receptors: cell guidance and beyond." *Trends Cell Biol* 10(9): 377-383.

Tamariz, E. and A. Varela-Echavarria (2015). "The discovery of the growth cone and its influence on the study of axon guidance." *Front Neuroanat* 9: 51.

Tang, R., A. Dodd, D. Lai, W. C. McNabb and D. R. Love (2007). "Validation of zebrafish (*Danio rerio*) reference genes for quantitative real-time RT-PCR normalization." *Acta Biochim Biophys Sin (Shanghai)* 39(5): 384-390.

Tear, G. (1999). "Axon guidance at the central nervous system midline." *Cell Mol Life Sci* 55(11): 1365-1376.

Technau, G. M. (1986). "Lineage analysis of transplanted individual cells in embryos of *Drosophila melanogaster* : I. The method." *Roux Arch Dev Biol* 195(6): 389-398.

Theodosiou, N. A. and T. Xu (1998). "Use of FLP/FRT system to study *Drosophila* development." *Methods* 14(4): 355-365.

Thisse, C. and B. Thisse (2008). "High-resolution in situ hybridization to whole-mount zebrafish embryos." *Nat Protoc* 3(1): 59-69.

Thomas, J. B., S. T. Crews and C. S. Goodman (1988). "Molecular genetics of the single-minded locus: a gene involved in the development of the *Drosophila* nervous system." *Cell* 52(1): 133-141.

Tornoe, J., M. Torp, J. R. Jorgensen, D. F. Emerich, C. Thanos, B. Bintz, L. Fjord-Larsen and L. U. Wahlberg (2012). "Encapsulated cell-based biodelivery of meteorin is neuroprotective in the quinolinic acid rat model of neurodegenerative disease." *Restor Neurol Neurosci* 30(3): 225-236.

Tran, T. S., A. L. Kolodkin and R. Bharadwaj (2007). "Semaphorin regulation of cellular morphology." *Annu Rev Cell Dev Biol* 23: 263-292.

Trousse, F., E. Marti, P. Gruss, M. Torres and P. Bovolenta (2001). "Control of retinal ganglion cell axon growth: a new role for Sonic hedgehog." *Development* 128(20): 3927-3936.

Trowe, T., S. Klostermann, H. Baier, M. Granato, A. D. Crawford, B. Grunewald, H. Hoffmann, R. O. Karlstrom, S. U. Meyer, B. Muller, S. Richter, C. Nusslein-Volhard and F. Bonhoeffer (1996). "Mutations disrupting the ordering and topographic mapping of axons in the retinotectal projection of the zebrafish, *Danio rerio*." *Development* 123: 439-450.

Van Battum, E. Y., S. Brignani and R. J. Pasterkamp (2015). "Axon guidance proteins in neurological disorders." *Lancet Neurol* 14(5): 532-546.

Varadarajan, S. G., J. H. Kong, K. D. Phan, T. J. Kao, S. C. Panaitof, J. Cardin, H. Eltzschig, A. Kania, B. G. Novitsch and S. J. Butler (2017). "Netrin1 Produced by Neural Progenitors, Not Floor Plate Cells, Is Required for Axon Guidance in the Spinal Cord." *Neuron* 94(4): 790-799 e793.

Wang, H., H. Yang, C. S. Shivalila, M. M. Dawlaty, A. W. Cheng, F. Zhang and R. Jaenisch (2013). "One-step generation of mice carrying mutations in multiple genes by CRISPR/Cas-mediated genome engineering." *Cell* 153(4): 910-918.

Wang, Z., N. Andrade, M. Torp, S. Wattananit, A. Arvidsson, Z. Kokaia, J. R. Jorgensen and O. Lindvall (2012). "Meteorin is a chemokinetic factor in neuroblast migration and promotes stroke-induced striatal neurogenesis." *J Cereb Blood Flow Metab* 32(2): 387-398.

Watanabe, K., Y. Akimoto, K. Yugi, S. Uda, J. Chung, S. Nakamuta, K. Kaibuchi and S. Kuroda (2012). "Latent process genes for cell differentiation are common decoders of neurite extension length." *J Cell Sci* 125(Pt 9): 2198-2211.

Wolman, M. A., Y. Liu, H. Tawarayama, W. Shoji and M. C. Halloran (2004). "Repulsion and attraction of axons by semaphorin3D are mediated by different neuropilins in vivo." *J Neurosci* 24(39): 8428-8435.

Wright, J. L., C. M. Ermine, J. R. Jorgensen, C. L. Parish and L. H. Thompson (2016). "Over-Expression of Meteorin Drives Gliogenesis Following Striatal Injury." *Front Cell Neurosci* 10: 177.

Wright, K. M., K. A. Lyon, H. Leung, D. J. Leahy, L. Ma and D. D. Ginty (2012). "Dystroglycan organizes axon guidance cue localization and axonal pathfinding." *Neuron* 76(5): 931-944.

Xiao, T., W. Staub, E. Robles, N. J. Gosse, G. J. Cole and H. Baier (2011). "Assembly of lamina-specific neuronal connections by slit bound to type IV collagen." *Cell* 146(1): 164-176.

Yamada, T., M. Placzek, H. Tanaka, J. Dodd and T. M. Jessell (1991). "Control of cell pattern in the developing nervous system: polarizing activity of the floor plate and notochord." *Cell* 64(3): 635-647.

Yamauchi, K., K. D. Phan and S. J. Butler (2008). "BMP type I receptor complexes have distinct activities mediating cell fate and axon guidance decisions." *Development* 135(6): 1119-1128.

Yang, H., H. Wang, C. S. Shivalila, A. W. Cheng, L. Shi and R. Jaenisch (2013). "One-step generation of mice carrying reporter and conditional alleles by CRISPR/Cas-mediated genome engineering." *Cell* 154(6): 1370-1379.

Yazdani, U. and J. R. Terman (2006). "The semaphorins." *Genome Biol* 7(3): 211.

Yeo, S. Y., T. Miyashita, C. Fricke, M. H. Little, T. Yamada, J. Y. Kuwada, T. L. Huh, C. B. Chien and H. Okamoto (2004). "Involvement of Islet-2 in the Slit signaling for axonal branching and defasciculation of the sensory neurons in embryonic zebrafish." *Mech Dev* 121(4): 315-324.

Yin, L., L. E. Jao and W. Chen (2015). "Generation of Targeted Mutations in Zebrafish Using the CRISPR/Cas System." *Methods Mol Biol* 1332: 205-217.

ANNEXES

Albadri S*, **De Santis F***, Di Donato V*, Del Bene F.

CRISPR/Cas9 mediated knock-in and knock-out in Zebrafish

Genome Editing in Neurosciences, Springer editions 2017 (in press)

Fontenas L, **De Santis F**, Di Donato V, Degerny C, Chambraud B, Del Bene F, Tawk M.

Neuronal Ndr4 is required for nodes of Ranvier organization in Zebrafish

PLoS Genet. 2016 Nov 30;12(11)

De Santis F*, Di Donato V*, Del Bene F.

Clonal analysis of gene loss of function and tissue-specific gene deletion in zebrafish via CRISPR/Cas9 technology

Methods Cell Biol. 2016;135:171-88.

CRISPR/Cas9-Mediated Knockin and Knockout in Zebrafish

Shahad Albadri, Flavia De Santis, Vincenzo Di Donato,
and Filippo Del Bene

Abstract The zebrafish (*Danio rerio*) has emerged in recent years as a powerful vertebrate model to study neuronal circuit development and function, thanks to its relatively small size, rapid external development and translucency. These features allow the easy application of in vivo microscopy analysis and optical perturbation of neuronal function. So far, genetic manipulation in zebrafish has been limited to the generation of constitutive loss-of-function alleles and transgenic models. CRISPR/Cas9 offers unprecedented possibilities for genomic manipulation that can be exploited to study neuronal function. In the past few years, we have successfully used CRISPR/Cas9-based technology in zebrafish to achieve two goals crucial for neuronal circuit analysis by developing two CRISPR/Cas9-based approaches that overcome previous major limitations to the study of gene and neuron functions in zebrafish. The study of gene function via tissue- or cell-specific mutagenesis remains challenging in zebrafish when the study of the function of certain loci might require tight spatiotemporal control of gene inactivation, which is particularly true in studying the function of a particular gene in post mitotic neurons, when the same gene may have had an earlier developmental function. To circumvent this limitation, we developed a simple and versatile protocol to achieve tissue-specific and temporally controlled gene disruption based on Cas9 expression under the control of the Gal4/UAS binary system (Di Donato et al. 2016). This strategy allows us to induce somatic mutations in genetically labeled cell clones or single cells and to follow them in vivo via reporter gene expression. We have also been able to target endogenous genomic loci to specifically label the great variety of neuronal cell types with reporter genes such as the transcriptional activator Gal4 (Auer et al. 2014). As a result, we can specifically target the expression of fluorescent proteins, a genetically encoded calcium indicator or optogenetic actuators in defined neuronal subpopulations.

We will present ways that these two methods can be applied to the study of the development of the nervous system in larval zebrafish.

Shahad Albadri, Flavia De Santis and Vincenzo Di Donato made equal contribution.

S. Albadri • F. De Santis • V. Di Donato • F. Del Bene (✉)
Institut Curie, PSL Research University, INSERM, U 934, CNRS UMR3215, 75005 Paris,
France
e-mail: Filippo.Del-Bene@curie.fr

[AUI](#)

© The Author(s) 2017
R. Jaenisch et al. (eds.), *Genome Editing in Neurosciences*, Research and
Perspectives in Neurosciences, DOI 10.1007/978-3-319-60192-2_4

41

33

34 CRISPR/Cas9 and Gal4/UAS Combination for Cell-Specific Gene Inactivation

35 Over the last decades, the analysis of gene function has relied on mutagenesis
36 approaches leading to the generation of loss-of-function alleles. The CRISPR/Cas9
37 system represents a major step forward towards achieving precise and targeted gene
38 disruption. Being readily applicable for the creation of knockout loci in a great
39 variety of animal models used in neuroscience studies, this technology has led to
40 significant advances in the fields of developmental and functional neurobiology
41 (Heidenreich and Zhang 2016). Nonetheless, constitutive gene disruption is often
42 associated with side effects, such as compensation mechanisms and embryonic
43 lethality, representing an important limitation on the analysis of phenotypes specific
44 to the nervous system, since neural circuits are fully established at late stages of
45 development. Recently, studies in worms (Shen et al. 2014), fruit flies (Port et al.
46 2014), mice (Platt et al. 2014) and zebrafish (Ablain et al. 2015) have pioneered the
47 use of the CRISPR/Cas9 methodology to generate conditional gene knockouts via
48 tissue-specific expression of *cas9*. This strategy takes advantage of cell type-
49 specific promoters to control the spatiotemporal expression of the Cas9 enzyme.
50 Importantly, one of the most common methodologies ensuring cell-specific expres-
51 sion of transgenes in zebrafish is the Gal4-UAS binary system (derived from yeast),
52 in which the transcription of genes placed 3' of an upstream activating sequence
53 (UAS) relies on the DNA binding of the Gal4 transcriptional activator (Asakawa
54 and Kawakami 2008). Gene- and enhancer-trap methods have been applied to
55 establish a significant number of Gal4 transgenic lines (Davison et al. 2007;
56 Asakawa et al. 2008; Scott and Baier 2009; Kawakami et al. 2010; Balciuniene
57 et al. 2013), several of which are neural-specific (Scott et al. 2007; Asakawa et al.
58 2008). Notably, in these lines the Gal4 open reading frame (ORF) is randomly
59 integrated in the fish genome through Tol2-based transposition, and the insertion
60 site is not mapped; therefore, the sequence of the promoter elements driving Gal4
61 expression is unknown. In our work, we have developed a flexible conditional
62 knockout strategy based on the CRISPR/Cas9 technology that combines Gal4/
63 UAS-mediated expression of the Cas9 enzyme with a constitutive expression of
64 sgRNAs driven by PolIII U6 promoter sequences. Our strategy does not require
65 previous knowledge of promoter sequences to induce *cas9* expression since this is
66 provided by cell type-specific Gal4 transcription. Additionally, to enable the anal-
67 ysis of the phenotypes arising from Cas9-induced gene disruption, we marked the
68 population of the *cas9*-expressing cells by using the viral T2A self-cleaving peptide
69 (Provost et al. 2007), ensuring the stoichiometric synthesis of the Cas9 enzyme and
70 the fluorescent reporter GFP from the same mRNA. To test our conditional knock-
71 out strategy, we used our vector system to target the *tyrosinase* (*tyr*) locus, coding
72 for a key enzyme involved in melanin production (Camp and Lardelli 2001). We
73 were able to induce eye-specific loss of pigmentation by expressing our transgene
74 exclusively in the progenitors of the neural retina and the retinal-pigmented

epithelium (RPE). For this purpose we used a transgenic line, $Tg(rx2:gal4)$, in which the Gal4 trans-activator is specifically driven in the optic primordium by the promoter of the zebrafish *retinal homeobox gene 2* (*rx2*; Heermann et al. 2015). This result confirmed the ability of our strategy to induce Gal4- and Cas9-mediated tissue-specific gene inactivation. Remarkably, in this first approach, GFP expression was strictly dependent on the temporal activity of the promoter driving Gal4 expression, thus restricting direct detection of potential mutant cells to a limited time window. This caveat reduces the possibility of analyzing loss-of-function phenotypes after Gal4 transactivation activity has terminated. To circumvent this issue, we proposed to use the activity of the Cre enzyme, a topoisomerase that catalyzes the site-specific recombination of DNA between *loxP* sites (Branda and Dymecki 2004; Pan et al. 2005), to constitutively label the population of *Cas9*-expressing cells. We therefore developed a construct where we substituted the GFP with a Cre reporter, enabling the analysis of gene disruption after Cas9 activity has terminated. The visualization of *cre*-expressing cells is commonly achieved with the use of transgenic lines carrying a cassette where a constitutive promoter drives the expression of a fluorescent reporter upon the Cre-mediated excision of a floxed stop codon. Thus, in cells carrying floxed alleles, the concomitant expression of Cas9 and Cre enzymes by a tissue-specific Gal4 promoter would ensure, respectively, double-strand breaks (DSBs) at the targeted locus as well as the recombination of the floxed locus. Notably, if the Cre-dependent expression of a reporter is constitutive after recombination, all the cells deriving from a *cas9*-expressing progenitor will be fluorescent, allowing long-term visualization of potentially mutated clones of cells. By using our system in retinal stem cells, we successfully disrupted the *atoh7* gene, which is involved in the specification of retinal ganglion cells (RGC) in the developing retina. In this case, we could modify cell fate determination of retinal progenitor cells and generate labeled loss-of-function clones lacking the population of RGC.

Additionally, we employed our method to create genetic chimeras in which single mutant cells could be differentially tagged in a wild-type tissue. To obtain this labeling, we combined the 2C-Cas9 system with the Brainbow technology. The $Tg(UAS:brainbow)$ line (Robles et al. 2013) carries a transgene in which the CDSs of the fluorescent proteins tdTomato, Cerulean and YFP are separated by Cre recombinase sites. In double transgenic embryos $Tg(UAS:brainbow) \times Tg(Tissue-specific promoter:gal4)$, tdTomato will be expressed in the Gal4 transactivation domain in the absence of Cre-mediated recombination. In contrast, *cerulean* or *YFP* will be transcribed if Cre recombinase is active. The expression of our transgenesis vector in these embryos provides simultaneous activity of the Cas9 and Cre enzymes. As a result, all the Gal4-positive cells that received the plasmid are potentially mutant and marked by cerulean or YFP fluorescence, whereas the population of Gal4-positive cells that do not express the construct is wild-type and labeled with the reporter tdTomato. This multicolor labeling strategy can be easily applied to neurobiology studies to induce targeted mutations in single neurons and directly compare loss-of-function and wild-type phenotypes in the same animal. To test this potential application, we targeted the genomic locus coding for the motor

120 protein Kinesin family member 5A, a (*kif5aa*) (Campbell and Marlow 2013; Auer
121 et al. 2015), whose inactivation triggers the reduction of RGC axon arbor complexity
122 via a cell-autonomous mechanism (Auer et al. 2015). To target the *kif5aa* gene with
123 the 2C-Cas9 system in single RGC, we used the Tg(*isl2b:gal4*) line. As expected,
124 after injection of our construct into one-cell stage embryos derived from a cross of
125 Tg(*isl2b:gal4*) and Tg(*UAS:brainbow*) fish, we could observe a strong decrease in
126 total branch length in YFP- or Cerulean-expressing RGC (potentially *kif5aa* mutant)
127 compared to tdTomato-fluorescent RGC (wild-type).

128 In conclusion, the 2C-Cas9 system represents a versatile tool to induce biallelic
129 conditional gene inactivation. The use of the Gal4/UAS system allows the targeting
130 of a gene of choice in any cell population. The combination of this bipartite system
131 with simultaneous activation of Cas9 And Cre enzymes in progenitor or differen-
132 tiated cells enables first, the genetic lineage tracing of mutant cells and second, the
133 detection of cell-autonomous gene inactivation at single cell resolution. Addition-
134 ally, permanent labeling of knockout cells offers the possibility of investigating
135 gene function in adult animals, expanding the applicability of the 2C-Cas9 from
136 neurodevelopment to maintenance and function of neural networks. Finally,
137 because the 2C-Cas9 system is based on genetic tools available in several model
138 organisms, this approach allows the same level of investigation in a broad range of
139 animal models.

140 In addition to the use of the Crispr/Cas9 application for the generation of loss-of-
141 function alleles, RNA guide nucleases can be used for more sophisticated genome
142 modifications such as homologous recombination (HR) or non-homologous end
143 joining (NHEJ)-mediated knockin. We herein provide a conceptual outline of the
144 steps involved in the generation of knockin lines based on the Crispr/Cas9 strategy
145 and the latest advances made in the zebrafish genome-editing field.

146 **Crispr/Cas9-Mediated Knockin Approaches in Zebrafish**

147 With its advantage of transparency, the zebrafish model organism rapidly emerged
148 as a powerful experimental system for studies in genetics, developmental biology
149 and neurobiology. The possible integration of exogenous genes into any given loci
150 and the analysis of their function in the living animal have dramatically improved
151 over the past few years with the development of genome editing technologies. Prior
152 to this recent explosion in the field of knockin generation, conventional transgenic
153 zebrafish lines were generated by Tol2-mediated transgenesis, which has success-
154 fully allowed the making of hundreds of new reporter lines essential to the study of
155 particular gene functions in vivo (Davison et al. 2007; Asakawa et al. 2008; Scott
156 and Baier 2009; Kawakami et al. 2010; Balciuniene et al. 2013). Bacterial artificial
157 chromosome-based transgenesis has been and still is one of the go-to methods for
158 making reporter lines. However, this technique comes with one major limitation:
159 the integration of extra coding copies of hundreds of kbs. In addition, it is not
160 known how the integration of such a large construct affects the neighboring site of

insertion. More recently, the transcription activator-like effectors (TALEs) technology, a milestone in the development of zebrafish mutant and transgenic lines, has lifted the limit of loci-specific targeting. With very low off-targeting effects, TALEs were therefore the first successful genome editing method that permitted homologous-directed recombination (HDR) and NHEJ-mediated knockin in zebrafish (Bedell et al. 2012; Zu et al. 2013). Two reports (Chang et al. 2013; Hwang et al. 2013b) showed that double stranded breaks (DSB), which are simpler in design and have higher mutagenesis efficiency, could also be generated using the Crispr/Cas9 technology based on the same approach used by Bedell et al. (2012). Following these studies, Hruscha et al. (2013) achieved the integration of HA-tags into the sequence of single strand oligonucleotides flanked by two short homology arms of the targeted gene. Similarly to previously observed integration events, insertion of the sequences of interest was detected in most targeted alleles with, however, a majority of imprecise and error-prone repair mechanisms. In 2013, Zu et al. reported the first HR gene-targeting event using TALENs and a double stranded vector containing an eGFP cassette flanked by long homology arms and a germ line transmission rate of 1.5%. More recently many other laboratories have developed various methods to generate knockin alleles by HR followed by CRISPR/Cas9-induced DSB, using as donor single stranded DNA, circular or linear plasmids with short (~40 bp) or long (800–1000 bp) homology arms (Hruscha et al. 2013; Hwang et al. 2013a; Irion et al. 2014; Shin et al. 2014; He et al. 2015; Hisano et al. 2015). Although these methods were proven possible, their efficiency remains variable. To circumvent these problems, in 2014 our laboratory employed a strategy taking advantage of homologous independent repair events shown to be tenfold more active than HR events in the one-cell stage embryo (Auer et al. 2014). The plasmid donor vector was engineered with an eGFP bait cassette and a Gal4 transcriptional transactivator cassette. Co-injected with a locus-specific sgRNA, an eGFP targeting sgRNA and *cas9* nuclease mRNA, cleavage of the donor vector was generated along with the endogenous chromosomal integration site. For better readout, the injection was performed into an outcross of two transgenic lines, the first being an eGFP reporter line and the second a Tg(*UAS:RFP*) line. Injected embryos with a successful in-frame integration event (most probably through homologous independent repair mechanisms) therefore displayed RFP signal in cells where GFP signal was normally detected. In this system, the offspring transmission was evaluated at about 30% and increased to 40% when a selection for the RFP signal was performed after injection. The generation of such a donor vector allowed the direct assessment of the efficiency of the strategy by targeting an endogenous locus of the zebrafish genome. Targeting the transcriptional starting site of the *kif5aa* gene, integration of the donor vector was successfully induced and shown to be independent from the orientation of the sgRNA targeting *kif5aa*. In addition, no homologous sequences between the vector and the endogenous targeted site were required for the integration, allowing the re-use of the vector in combination with any given site-specific sgRNA. Using the same approach, Kimura et al. (2014) improved the strategy by adding a heat shock cassette (Hsp70) upstream of the transcription trans-activator Gal4 cassette into the donor vector,

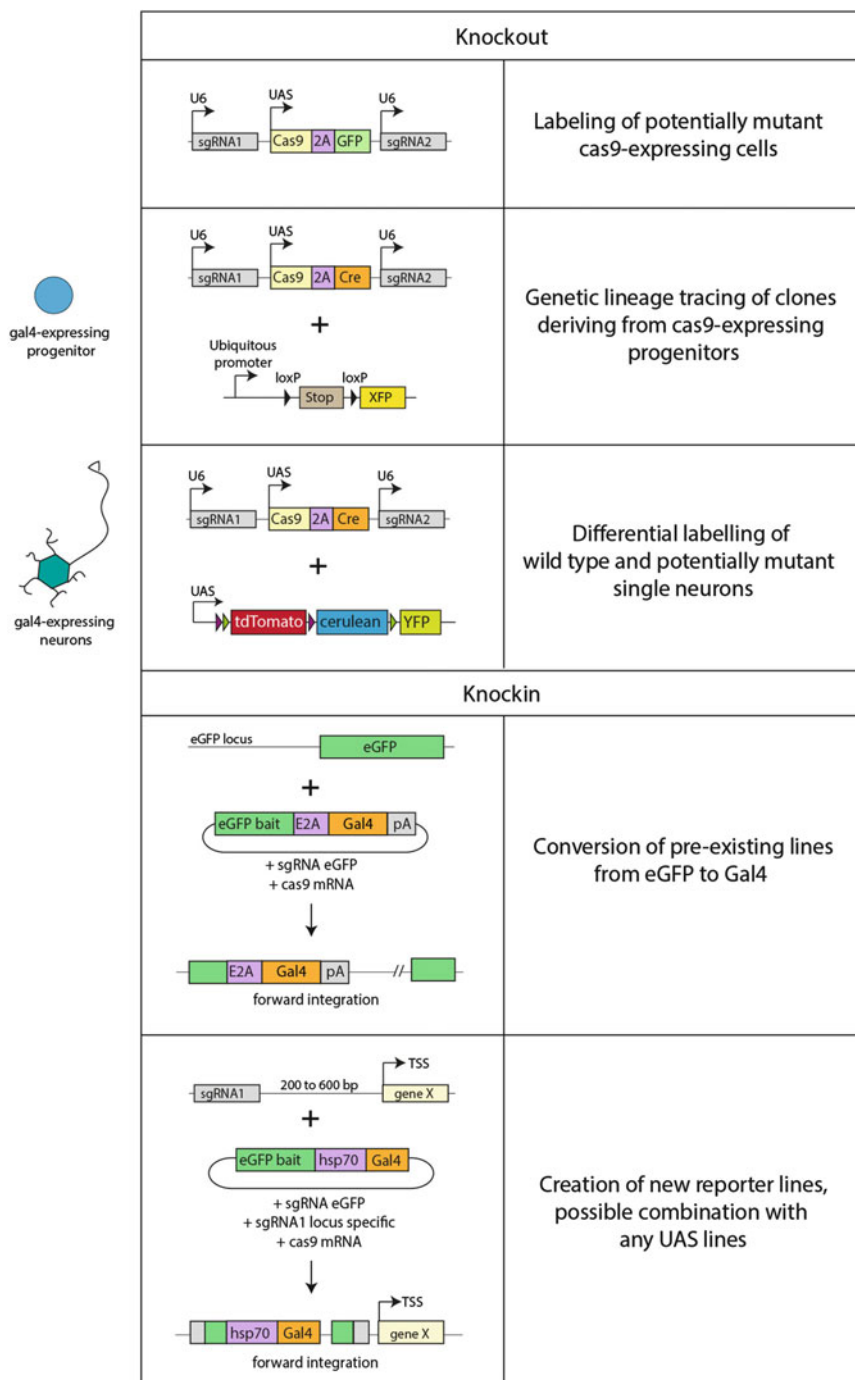


Fig. 1 Knockout and knockin strategies based on the Crispr/Cas9 technology in zebrafish. Schematic representation of the different methods and applications of Crispr/Cas9-mediated genome modifications. From top to bottom: (1) labeling with GFP of *cas9*-expressing cells

[AU2](#)

allowing its expression independently from in-frame insertion events within the 206
transcriptional starting site of the gene of interest. To date, several new reporter 207
lines have been generated using this strategy, providing a powerful alternative for 208
homology-independent repair over HR-mediated integration. Key points for its 209
success are (1) the identification of efficient sgRNAs targeting the chromosomal 210
site of choice, for which new prescreening methods have been developed 211
(Carrington et al. 2015; Prykhozhij et al. 2016); (2) the injection of the sgRNA 212
mix with Cas9 nuclease mRNA over purified Cas9 protein that seems to prevent the 213
donor plasmid insertion; and (3) further screening for the identification of founders 214
due to the error-prone nature of junction sites between the endogenous locus and the 215
donor vector. Hisano et al. (2015) addressed this last point by introducing 10–40 bp 216
homology arms into the donor vector to trigger integration events mediated by HR 217
repair mechanisms. In parallel, Li et al. (2015) developed another approach by 218
targeting intronic regions of the gene of interest, therefore non-HR dependent. 219
While this strategy allows keeping the integrity of the targeted coding sequence, 220
the enriched presence of repeat sequences within the introns makes it difficult to 221
achieve a specific targeting. Finally, the latest advance in knockin approaches is the 222
development of traceable genome editing events that allow the easy recovery of 223
edited alleles (Hoshijima et al. 2016) (Fig. 1). 224

←
Fig. 1 (continued) potentially mutated in locus targeted by the sgRNA1 and sgRNA2 expressed with the PolIII U6 promoters. (2) Genetic labeling with Cre recombinase of *cas9*-expressing cells. Cre activity was revealed by the conditional expression of a fluorescent reporter protein (XFP) after removal of a stop cassette. (3) A similar strategy combined with a brainbow reporter cassette allows the visualization of *cas9*-expressing cells in multiple colors. (4) Genetic knockin of a Gal4 reporter transcription factor into GFP locus of preexisting transgenic lines or (5) into an endogenous genomic location (geneX). *UAS* upstream activating sequence

225 **References**[AU3](#)

- 226 Ablain J, Durand EM, Yang S, Zhou Y, Zon LI (2015) A CRISPR/Cas9 vector system for tissue-
227 specific gene disruption in zebrafish. *Dev Cell* 32:756–764
- 228 Asakawa K, Kawakami K (2008) Targeted gene expression by the Gal4-UAS system in zebrafish.
229 *Dev Growth Differ* 50:391–399
- 230 Asakawa K, Suster ML, Mizusawa K, Nagayoshi S, Kotani T, Urasaki A, Kishimoto Y, Hibi M,
231 Kawakami K (2008) Genetic dissection of neural circuits by Tol2 transposon-mediated Gal4
232 gene and enhancer trapping in zebrafish. *Proc Natl Acad Sci USA* 105:1255–1260
- 233 Auer TO, Del Bene F (2014) CRISPR/Cas9 and TALEN-mediated knock-in approaches in
234 zebrafish. *Methods* 69:142–150
- 235 Auer TO, Durore K, De Cian A, Concordet JP, Del Bene F (2014) Highly efficient CRISPR/Cas9-
236 mediated knock-in in zebrafish by homology-independent DNA repair. *Genome Res*
237 24:142–153
- 238 Auer TO, Xiao T, Bercier V, Gebhardt C, Durore K, Concordet J-P, Wyart C, Suster M,
239 Kawakami K, Wittbrodt J, Baier H, Del Bene F (2015) Deletion of a kinesin I motor unmasks
240 a mechanism of homeostatic branching control by neurotrophin-3. *Elife* 4:418
- 241 Balciuniene J, Nagelberg D, Walsh KT, Camerota D, Georgette D, Biemar F, Bellipanni G,
242 Balciunas D (2013) Efficient disruption of zebrafish genes using a Gal4-containing gene
243 trap. *BMC Genomics* 14:619
- 244 Bedell VM, Wang Y, Campbell JM, Poshusta TL, Starker CG, Krug RG II, Tan W, Penheiter SG,
245 Ma AC, Leung AYH, Fahrenkrug SC, Carlson DF, Voytas DF, Clark KJ, Essner JJ, Ekker SC
246 (2012) In vivo genome editing using a high-efficiency TALEN system. *Nature* 491:114–118
- 247 Branda CS, Dymecki SM (2004) Talking about a revolution: the impact of site-specific
248 recombinases on genetic analyses in mice. *Dev Cell* 6:7–28
- 249 Camp E, Lardelli M (2001) Tyrosinase gene expression in zebrafish embryos. *Dev Genes Evol*
250 211:150–153
- 251 Campbell PD, Marlow FL (2013) Temporal and tissue specific gene expression patterns of the
252 zebrafish kinesin-1 heavy chain family, kif5s, during development. *Gene Expr Patterns*
253 13:271–279
- 254 Carrington B, Varshney GK, Burgess SM, Sood R (2015) CRISPR-STAT: an easy and reliable
255 PCR-based method to evaluate target-specific sgRNA activity. *Nucl Acids Res* 43:e157–e157
- 256 Chang N, Sun C, Gao L, Zhu D, Xu X, Zhu X, Xiong J-W, Xi JJ (2013) Genome editing with
257 RNA-guided Cas9 nuclease in zebrafish embryos. *Cell Res* 23:465–472
- 258 Davison JM, Akitake CM, Goll MG, Rhee JM, Gosse N, Baier H, Halpern ME, Leach SD, Parsons MJ
259 (2007) Transactivation from Gal4-VP16 transgenic insertions for tissue-specific cell labeling and
260 ablation in zebrafish. *Dev Biol* 304:811–824
- 261 Di Donato V, De Santis F, Auer TO, Testa N, Sánchez-Iranzo H, Mercader N, Concordet J-P,
262 Del Bene F (2016) 2C-Cas9: a versatile tool for clonal analysis of gene function. *Genome*
263 *Res* 26:681–692
- 264 He MD, Zhang FH, Wang HL, Wang HP, Zhu ZY, Sun YH (2015) Efficient ligase 3-dependent
265 microhomology-mediated end joining repair of DNA double-strand breaks in zebrafish
266 embryos. *Mutat Res* 780:86–96
- 267 Heermann S, Schütz L, Lemke S, Krieglstein K, Wittbrodt J (2015) Eye morphogenesis driven by
268 epithelial flow into the optic cup facilitated by modulation of bone morphogenetic protein.
269 *Elife* 4:373
- 270 Heidenreich M, Zhang F (2016) Applications of CRISPR-Cas systems in neuroscience. *Nat Rev*
271 *Neurosci* 17:36–44
- 272 Hisano Y, Sakuma T, Nakade S, Ohga R, Ota S, Okamoto H, Yamamoto T, Kawahara A (2015)
273 Precise in-frame integration of exogenous DNA mediated by CRISPR/Cas9 system in
274 zebrafish. *Sci Rep* 5:8841
- 275 Hoshijima K, Jurynek MJ, Grunwald DJ (2016) Precise editing of the zebrafish genome made
276 simple and efficient. *Dev Cell* 36:654–667

Hruscha A, Krawitz P, Rechenberg A, Heinrich V, Hecht J, Haass C, Schmid B (2013) Efficient CRISPR/Cas9 genome editing with low off-target effects in zebrafish. <i>Development</i> 140:4982–4987	277 278 279
Hwang WY, Fu Y, Reyon D, Maeder ML, Kaini P, Sander JD, Joung JK, Peterson RT, Yeh J-RJ (2013a) Heritable and precise zebrafish genome editing using a CRISPR-Cas system. <i>PLoS One</i> 8:e68708	280 281 282
Hwang WY, Fu Y, Reyon D, Maeder ML, Tsai SQ, Sander JD, Peterson RT, Yeh J-RJ, Joung JK (2013b) Efficient genome editing in zebrafish using a CRISPR-Cas system. <i>Nat Biotechnol</i> 31:227–229	283 284 285
Irion U, Krauss J, Nüsslein-Volhard C (2014) Precise and efficient genome editing in zebrafish using the CRISPR/Cas9 system. <i>Development</i> 141:4827–4830	286 287
Kawakami K, Abe G, Asada T, Asakawa K, Fukuda R, Ito A, Lal P, Mouri N, Muto A, Suster ML, Takakubo H, Urasaki A, Wada H, Yoshida M (2010) zTrap: zebrafish gene trap and enhancer trap database. <i>BMC Dev Biol</i> 10:105	288 289 290
Kimura Y, Hisano Y, Kawahara A, Higashijima S-I (2014) Efficient generation of knock-in transgenic zebrafish carrying reporter/driver genes by CRISPR/Cas9-mediated genome engineering. <i>Sci Rep</i> 4:6545	291 292 293
Li J, Zhang BB, Ren YG, SY G, Xiang YH, JL D (2015) Intron targeting-mediated and endogenous gene integrity-maintaining knockin in zebrafish using the CRISPR/Cas9 system. <i>Cell Res</i> 25:634–637	294 295 296
Pan X, Wan H, Chia W, Tong Y, Gong Z (2005) Demonstration of site-directed recombination in transgenic zebrafish using the Cre/loxP system. <i>Transgenic Res</i> 14:217–223	297 298
Platt RJ, Chen S, Zhou Y, Yim MJ, Swiech L, Kempton HR, Dahlman JE, Parnas O, Eisenhaure TM, Jovanovic M, Graham DB, Jhunjhunwala S, Heidenreich M, Xavier RJ, Langer R, Anderson DG, Hacohen N, Regev A, Feng G, Sharp PA, Zhang F (2014) CRISPR-Cas9 knockin mice for genome editing and cancer modeling. <i>Cell</i> 159:440–455	299 300 301 302
Port F, Chen H-M, Lee T, Bullock SL (2014) Optimized CRISPR/Cas tools for efficient germline and somatic genome engineering in <i>Drosophila</i> . <i>Proc Natl Acad Sci U S A</i> 111:E2967–E2976	303 304
Provost E, Rhee J, Leach SD (2007) Viral 2A peptides allow expression of multiple proteins from a single ORF in transgenic zebrafish embryos. <i>Genesis</i> 45:625–629	305 306
Prykhozhij SV, Rajan V, Berman JN (2016) A guide to computational tools and design strategies for genome editing experiments in zebrafish using CRISPR/Cas9. <i>Zebrafish</i> 13:70–73	307 308
Robles E, Filosa A, Baier H (2013) Precise lamination of retinal axons generates multiple parallel input pathways in the tectum. <i>J Neurosci</i> 33:5027–5039	309 310
Scott EK, Baier H (2009) The cellular architecture of the larval zebrafish tectum, as revealed by gal4 enhancer trap lines. <i>Front Neural Circ</i> 3:13	311 312
Scott EK, Mason L, Arrenberg AB, Ziv L, Gosse NJ, Xiao T, Chi NC, Asakawa K, Kawakami K, Baier H (2007) Targeting neural circuitry in zebrafish using GAL4 enhancer trapping. <i>Nat Publ Group</i> 4:323–326	313 314 315
Shen Z, Zhang X, Chai Y, Zhu Z, Yi P, Feng G, Li W, Ou G (2014) Conditional knockouts generated by engineered CRISPR-Cas9 endonuclease reveal the roles of coronin in <i>C. elegans</i> neural development. <i>Dev Cell</i> 30:625–636	316 317 318
Shin J, Chen J, Solnica-Krezel L (2014) Efficient homologous recombination-mediated genome engineering in zebrafish using TALE nucleases. <i>Development</i> 141:3807–3818	319 320
Zu Y, Tong X, Wang Z, Liu D, Pan R, Li Z, Hu Y, Luo Z, Huang P, Wu Q, Zhu Z, Zhang B, Lin S (2013) TALEN-mediated precise genome modification by homologous recombination in zebrafish. <i>Nat Meth</i> 10:329–331	321 322 323

RESEARCH ARTICLE

Neuronal Ndr4 Is Essential for Nodes of Ranvier Organization in Zebrafish

Laura Fontenas^{1#a}, Flavia De Santis^{2a}, Vincenzo Di Donato^{2a}, Cindy Degerny¹, Béatrice Chambraud¹, Filippo Del Bene², Marcel Tawk^{1*}

1 U1195, Inserm, University Paris Sud, University Paris-Saclay, Kremlin-Bicêtre, France, **2** Institut Curie, PSL Research University, Paris, France

☉ These authors contributed equally to this work.

^a Current address: Department of Biology, University of Virginia, Charlottesville, Virginia, United States of America

* marcel.tawk@inserm.fr



 OPEN ACCESS

Citation: Fontenas L, De Santis F, Di Donato V, Degerny C, Chambraud B, Del Bene F, et al. (2016) Neuronal Ndr4 Is Essential for Nodes of Ranvier Organization in Zebrafish. *PLoS Genet* 12(11): e1006459. doi:10.1371/journal.pgen.1006459

Editor: David Lyons, Centre for Neuroregeneration, Edinburgh, UNITED KINGDOM

Received: May 3, 2016

Accepted: November 3, 2016

Published: November 30, 2016

Copyright: © 2016 Fontenas et al. This is an open access article distributed under the terms of the [Creative Commons Attribution License](https://creativecommons.org/licenses/by/4.0/), which permits unrestricted use, distribution, and reproduction in any medium, provided the original author and source are credited.

Data Availability Statement: All relevant data are within the paper and its Supporting Information files.

Funding: The work has been funded by Inserm, Université Paris-Sud and Université Paris-Saclay to MT. The funders had no role in study design, data collection and analysis, decision to publish, or preparation of the manuscript.

Competing Interests: The authors have declared that no competing interests exist.

Abstract

Axon ensheathment by specialized glial cells is an important process for fast propagation of action potentials. The rapid electrical conduction along myelinated axons is mainly due to its saltatory nature characterized by the accumulation of ion channels at the nodes of Ranvier. However, how these ion channels are transported and anchored along axons is not fully understood. We have identified N-myc downstream-regulated gene 4, *ndrg4*, as a novel factor that regulates sodium channel clustering in zebrafish. Analysis of chimeric larvae indicates that *ndrg4* functions autonomously within neurons for sodium channel clustering at the nodes. Molecular analysis of *ndrg4* mutants shows that expression of *snap25* and *nsf* are sharply decreased, revealing a role of *ndrg4* in controlling vesicle exocytosis. This uncovers a previously unknown function of *ndrg4* in regulating vesicle docking and nodes of Ranvier organization, at least through its ability to finely tune the expression of the t-SNARE/NSF machinery.

Author Summary

Myelination is an important process that enables fast propagation of action potential along the axons. Schwann cells (SCs) are the specialized glial cells that ensure the ensheathment of the corresponding axons in the Peripheral Nervous System. In order to do so, SCs and axons need to communicate to organize the myelinating segments and the clustering of sodium channels at the nodes of Ranvier. We have investigated the early events of myelination in the zebrafish embryo. We here identify *ndrg4* as a novel neuronal factor essential for sodium channel clustering at the nodes. Immuno-labeling analysis show defective vesicle patterning along the axons of *ndrg4* mutants, while timelapse experiments monitoring the presence and the transport of these vesicles reveal a normal behavior. Molecular analysis unravels a novel function of *ndrg4* in controlling the expression of the t-SNARE/NSF machinery required for vesicle docking and release. However, inhibiting specifically regulated synaptic vesicle release does not lead to sodium channel clustering defects. We thus propose that *ndrg4* can regulate this process, at least partially,

through its ability to regulate the expression of key components of the t-SNARE/NSF machinery, responsible for clustering of sodium channels along myelinated axons.

Introduction

Myelination is a vertebrate adaptation that ensures the fast propagation of action potentials along the axons. Schwann Cells (SCs) are one of the myelinating glial cells of the Peripheral Nervous System (PNS) while Oligodendrocytes (OLs) are responsible for myelin wrapping in the Central Nervous System (CNS) [1–7]. While myelin sheaths insulate axons and inhibit current leakage, nodes of Ranvier found at regular intervals, gather voltage-gated sodium channels in clusters, and therefore are the only places where action potentials are regenerated, allowing their rapid propagation along axons [8–10]. Defective myelin sheaths or nodes of Ranvier prevent the efficient conduction of action potentials and severely impairs axonal function. Several signaling pathways, mainly intrinsic to SCs, have been identified as being positive or negative regulators of peripheral myelination [11–14]. Analysis of zebrafish mutants lacking SCs (e.g. *erbb2*, *erbb3*, *sox10/cl*) shows defects in sodium channel clustering and positioning [15], suggesting that SCs give essential instructive cues for the proper organization of myelinated axons. However, less is known about neuronal factors that ensure a proper myelin organization so that ion channels are mainly concentrated at the repetitive nodes of Ranvier along myelinated axons.

To better understand the molecular mechanisms governing peripheral myelination, and since the formation of the nodes depends on the interaction between neurons and glia, we undertook a differential screen to look for genes that are dysregulated in the absence of SCs in zebrafish. We compared the transcriptomes of the GFP+ and GFP- cells in the *foxd3::GFP* transgenic line (through FACS sorting), in groups of embryos that contain or not Schwann cells (following a *sox10* knockdown). We have identified a neuronal factor, *ndrg4*, as a major regulator of sodium channel clustering at the nodes of Ranvier.

Ndrq4 belongs to the NDRG (N-myc Downstream-Regulated Gene) family, which includes four related members, known to be important in tumorigenesis and linked to a range of cancers [16,17]. The function of *Ndrq4* itself has been extensively studied in cancer although conflicting results showed that *Ndrq4* has either a tumor-suppressive or an oncogenic function depending on the tissue [17]. NDRG1 is the most widely studied protein, namely for its role in peripheral myelination since a mutation in this gene leads to a severe autosomal recessive demyelinating neuropathy, NDRG1-linked Charcot-Marie-Tooth Disease (CMT4D) [18–20]. While NDRG1 function in myelination is well established, the role of NDRG4 in this process is still unknown. The latter is mainly expressed in the nervous system and the heart of mice and zebrafish [21]. In the mouse embryo, an indirect role of NDRG4 in severe ventricular hypoplasia has been proposed [22] while in zebrafish, *Ndrq4* is required for normal myocyte proliferation during early cardiac development [21]. Given its expression in the brain, it has been suggested that NDRG4 might play an important role within the CNS. Indeed, the expression of brain-derived neurotrophic factor (BDNF) is reduced in the cortex of *Ndrq4* KO mice that leads to spatial learning and memory defects [23]. A possible role of NDRG4 in neuronal differentiation and neurite formation has also been proposed following *Ndrq4* manipulation in PC12 cells [24]. Finally, a significant decrease in NDRG4 expression has been reported in Alzheimer disease brains [25].

Here, we identify a novel function for zebrafish *ndrg4*, in controlling vesicle fusion and release by regulating, among others, the levels of the t-SNARE protein, Snap25 (Synaptosomal

Associated Protein 25KDa), known to be required for the docking and merging of vesicles with the cell membrane during exocytosis [26,27]. Thus, in addition to their pronounced heart defects, the zebrafish *ndrg4* mutants are paralyzed. Our results reveal a previously unknown neuronal role for *ndrg4* in sodium channel clustering that is most likely due to its ability to regulate the expression of key components of the t-SNARE/NSF machinery.

Results

Sodium channel clustering is dependent on *ndrg4* function

Having identified a dysregulation in the expression of *ndrg4* in a differential screen of normal and SCs deficient embryos, we wanted to assess its function during PNS myelination, thus, we generated a *ndrg4* mutant using CRISPR/Cas9 technology [28]. The introduced mutation begets a deletion in the *ndrg4* DNA sequence and introduces a premature stop codon in the *ndrg4* mRNA sequence leading to a nonsense-mediated decay of the corresponding mRNA transcript (Fig 1A, 1B, 1E and 1F). A concomitant knockdown approach using a specific *ndrg4* splice blocking Morpholino (MO; 0.6 pmole/embryo) and a control 5 base pair mismatch *ndrg4* MO (0.6 pmole/embryo) was simultaneously used during this study ([21] and S1 Fig). A pronounced heart edema and a complete paralysis of the embryos were the first obvious defects observed in these mutants and morphants starting from 48 hours post fertilization (hpf) (the earliest time point analyzed here) (Fig 1C and 1D; S1 Fig). *Ndr4* homozygous mutants and morphants failed to respond to touch test at 3 days post fertilization (dpf) (S1, S2 and S3 Movies). The embryos looked thinner and shorter in comparison to controls and had slightly smaller eyes (Fig 1C and 1D; S1 Fig). We first observed, using *in situ* hybridization, that the majority of *ndrg4* mutants (30 out of 38 embryos) showed no obvious change in the expression of *myelin basic protein (mbp)* at 4dpf (Fig 2A–2C), a major protein of the myelin sheath and commonly used marker of myelination, compared to control embryos (75 out of 80 embryos). This result suggests that *ndrg4* function is not required *per se* for *mbp* expression.

We next investigated sodium channel distribution and organization along the PLLn. Using whole mount immunohistochemistry for voltage-gated sodium channels (anti-panNa_vCh) and axons (anti-acetylated tubulin) at 4 dpf, we visualized many sodium channels concentrated in clusters at the nodes of Ranvier within the control PLLn (Fig 2D–2F and 2M). However, in *ndrg4* mutants and morphants, we noticed that sodium channels were not clustered at the nodes of Ranvier (Fig 2G–2I and 2J–2L). We quantified the number of nodes of Ranvier within the PLLn in the last 8 somites starting from the most posterior neuromast of the larvae. We counted an average of 31 ± 2.49 nodes of Ranvier in control axons ($n = 13$ embryos), whereas we found only 0.5 ± 0.8 nodes in the *ndrg4* mutants ($n = 14$ embryos) and 11 ± 5.20 nodes in *ndrg4* morphants ($n = 13$ embryos) (Fig 2N). We have also looked at the clustering of sodium channels in the *sox10:mRFP* transgenic line that labels membrane extensions of SCs [29]. We could see clusters of sodium channels localized in the gaps between adjacent internodal segments in controls at 4dpf (average of 4.42 ± 1.08 clusters per somite; 4 different embryos) (S1G Fig), while fewer clusters were observed in these gaps in *ndrg4* morphants (average of 1.90 ± 0.84 clusters per somite; 5 different embryos; $p < 0.0001$) (S1G Fig). This result suggests that *ndrg4* function is required for sodium channel clustering along the axons.

We next labeled embryos with antibodies against a sequence (FIGQY) conserved in neurofascin family of adhesion molecules, and recognize the neurofascin 186. This latter is also localized at nodes of Ranvier in mammals and zebrafish, and shown to co-localize with NaCh clusters in zebrafish larvae [10,30–33]. Similar results were observed; we noticed that the FIGQY antigen labeling was diffused in *ndrg4* mutants and morphants (Fig 2G'–2L'), in comparison to the clustered labeling observed in controls (Fig 2D'–2F'). We counted an average of

Fig 1. Characterization of the *ndrg4* mutant. (A) Schematic representation of the *ndrg4* genomic locus. The extended region on the *exon 2* represents the sequence targeted by the CRISPR/Cas9 system. Red: sgRNA binding site. Blue: PAM sequence. *ndrg4*⁺ corresponds to the wild-type allele; *ndrg4*^{*31} and *ndrg4*^{*34} are the loss-of-function alleles used in this study. (B) Schematic of *ndrg4* protein product. In *ndrg4*^{*31} and *ndrg4*^{*34} mutant fish, the deletions result in a frameshift generating a premature STOP codon at the level of the amino acids 31 and 34 (of 352) in the ndr family domain. Lateral views of a control (C) and a *ndrg4* mutant (D) embryos at 72 hpf. The arrows point to the heart, note the pronounced heart edema (white asterisk) observed in the *ndrg4* mutant. Lateral view of *ndrg4* mRNA expression in a control (E) and a *ndrg4*^{-/-} embryo (F) at 48hpf. Note the absence of *ndrg4* expression in the mutant. Scale bar = 200 μ m.

doi:10.1371/journal.pgen.1006459.g001

30.86 \pm 0.54 clusters in the last 8 somites within the PLLn in control embryos (n = 14 embryos) whereas we found only 1.29 \pm 0.29 in *ndrg4* mutants (n = 14 embryos) and 6.69 \pm 0.86 in *ndrg4* morphants (n = 13 embryos) (Fig 2O and 2P). This result suggests that initial clustering of neurofascin at the nodes is also dependent on *ndrg4* function.

Ndr4 is not required for PLLn growth or early SCs development

To test whether SC and axonal development occurs normally in *ndrg4* mutants and morphants, we first performed a whole mount acetylated tubulin immunostaining for axonal labeling. We observed no significant difference in PLLn axonal outgrowth (Fig 3A–3C) between mutants (n = 14 embryos), morphants (n = 18 embryos) and controls (n = 20 embryos) at 4 dpf, indicating that axonal growth and maintenance are not defective in *ndrg4* mutants. We then examined *sox10* mRNA expression at 72 hpf. Sox10 is a transcription factor that labels neural crest cells including SC progenitors [34–36]. *Ndr4* mutants (n = 11 embryos) (Fig 3F) and morphants (n = 12 embryos) (Fig 3E) were comparable to controls (n = 32 embryos) (Fig 3D), showing a similar expression of *sox10* along the PLLn, confirming the normal development and distribution of SCs. We also took advantage of the *foxd3::GFP* larvae which express the Green Fluorescent Protein (GFP) in SCs [37] to look for SCs migration in *ndrg4* morphants. We observed no significant difference in SC migration and maintenance between morphants (n = 20 embryos) and controls (n = 16 embryos) at 3 dpf (Fig 3G and 3H). Moreover, since the NDRG proteins are known to play a significant role in cancer, we assessed SC proliferation throughout their development. For this purpose, we performed an anti-phosphorylated histone 3 (PH3) labeling in *foxd3::gfp* larvae at 30, 48 and 72 hpf. Quantification of PH3 positive SCs did not show any significant difference between controls (10 embryos at 30hpf, 23 at 48hpf and 12 at 72hpf) (S2A Fig) and morphants (7 embryos at 30hpf, 11 at 48hpf and 10 at 72hpf) (S2B Fig). The quantification of this phenotype showed that the rate of SC proliferation was not significantly different in *ndrg4* morphant embryos throughout development (S2C Fig). These data suggest that *ndrg4* function is not required for early SC development and axonal growth. To further investigate later aspects of axonal development and SC myelination, we analyzed the ultrastructure of axons in the PLLn using Transmitted Electron Microscopy (TEM). The total number of axons in *ndrg4* mutants and morphants was slightly but not significantly decreased in comparison to controls; we counted an average of 43.6 \pm 2.69 axons in controls (n = 10 nerves from 9 different embryos) at 4dpf, 38.93 \pm 1.66 axons in *ndrg4* mutants (n = 11 nerves from 7 different embryos) and 35.8 \pm 4.4 axons in *ndrg4* morphants (n = 5 nerves from 3 different embryos) (Fig 3I–3K). However, the number of myelinated axons was significantly reduced in *ndrg4* mutants and morphants in comparison to controls, we could count an average of 5.36 \pm 0.49 myelinated axons in *ndrg4* mutants and 4.2 \pm 1.24 in *ndrg4* morphants in comparison to an average of 10.7 \pm 0.68 myelinated axons in controls (Fig 3L). This result suggests that *ndrg4* function may, directly or indirectly, amend SC ability to myelinate but it is not essential for SC myelination as seen for sodium channel clustering.

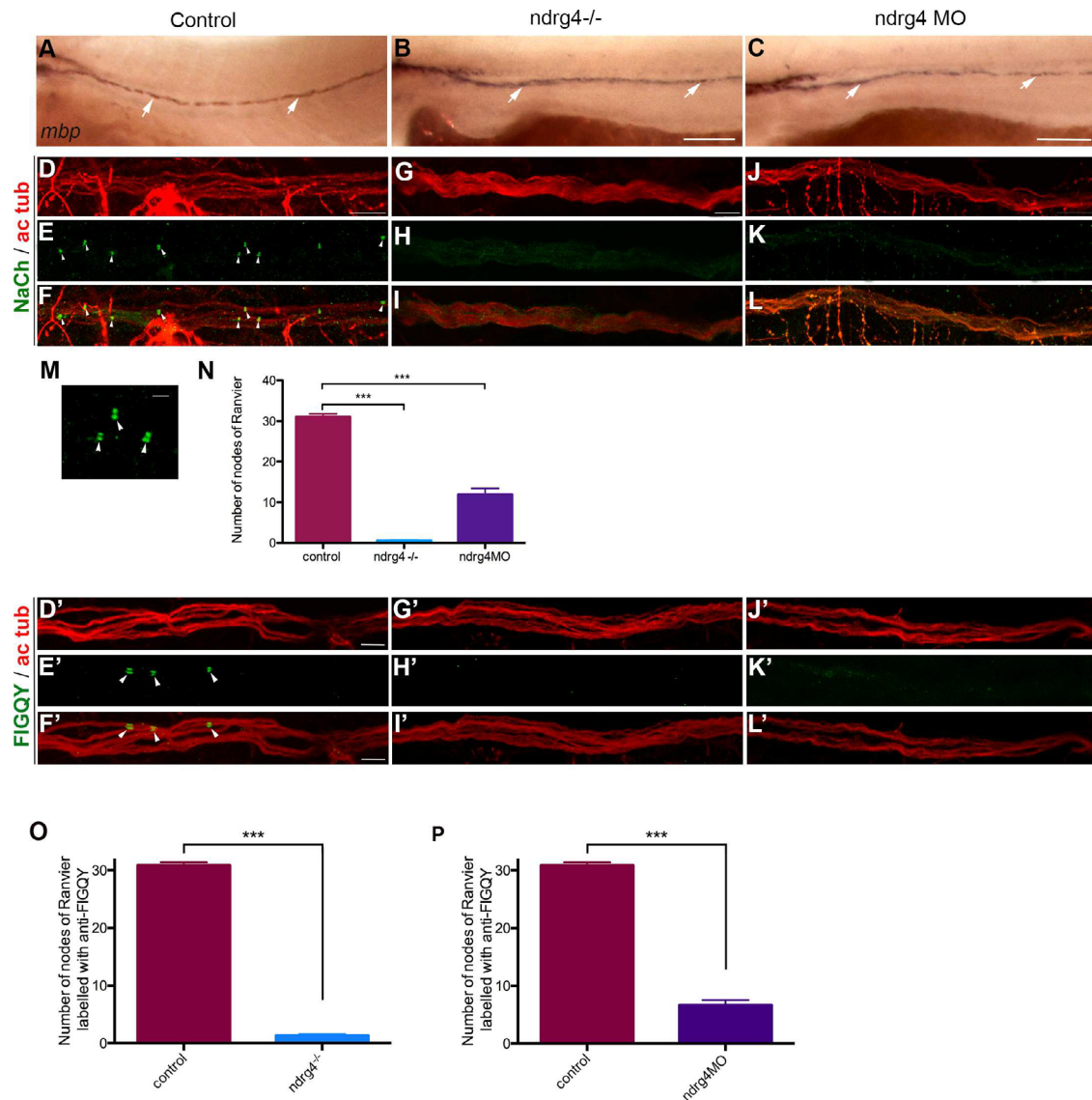


Fig 2. *ndrg4* is required for sodium channel and neurofascin clustering in the peripheral nervous system. (A-C) Lateral view of *mbp* RNA expression in control (A), *ndrg4* mutant (B) and morphant (C) embryos at 4 dpf. Arrows indicate *mbp*-expressing cells along the PLLn. Scale bars = 200µm. (D-L) Acetylated tubulin (ac tub; red) and sodium channels (NaCh; green) immunohistochemistry of a (D-F) control, *ndrg4* mutant (G-I) and *ndrg4* morphant (J-L) PLLn at 4 dpf. Scale bars = 5µm. (M) High magnification of three nodes of Ranvier (arrowheads) from a control nerve. Scale bar = 100nm. (N) A significant decrease in the number of sodium channels clusters is observed in *ndrg4* mutants and morphants in comparison to controls ($p < 0.001$). Acetylated tubulin (ac tub; red) and FIGQY (green) immunohistochemistry of a (D'-F') control, *ndrg4* mutant (G'-I') and *ndrg4* morphant (J'-L') PLLn at 4 dpf. Scale bars = 5 µm. (O,P) A significant decrease in the number of FIGQY labeled clusters is observed in *ndrg4* mutants and morphants in comparison to controls ($p < 0.001$).

doi:10.1371/journal.pgen.1006459.g002

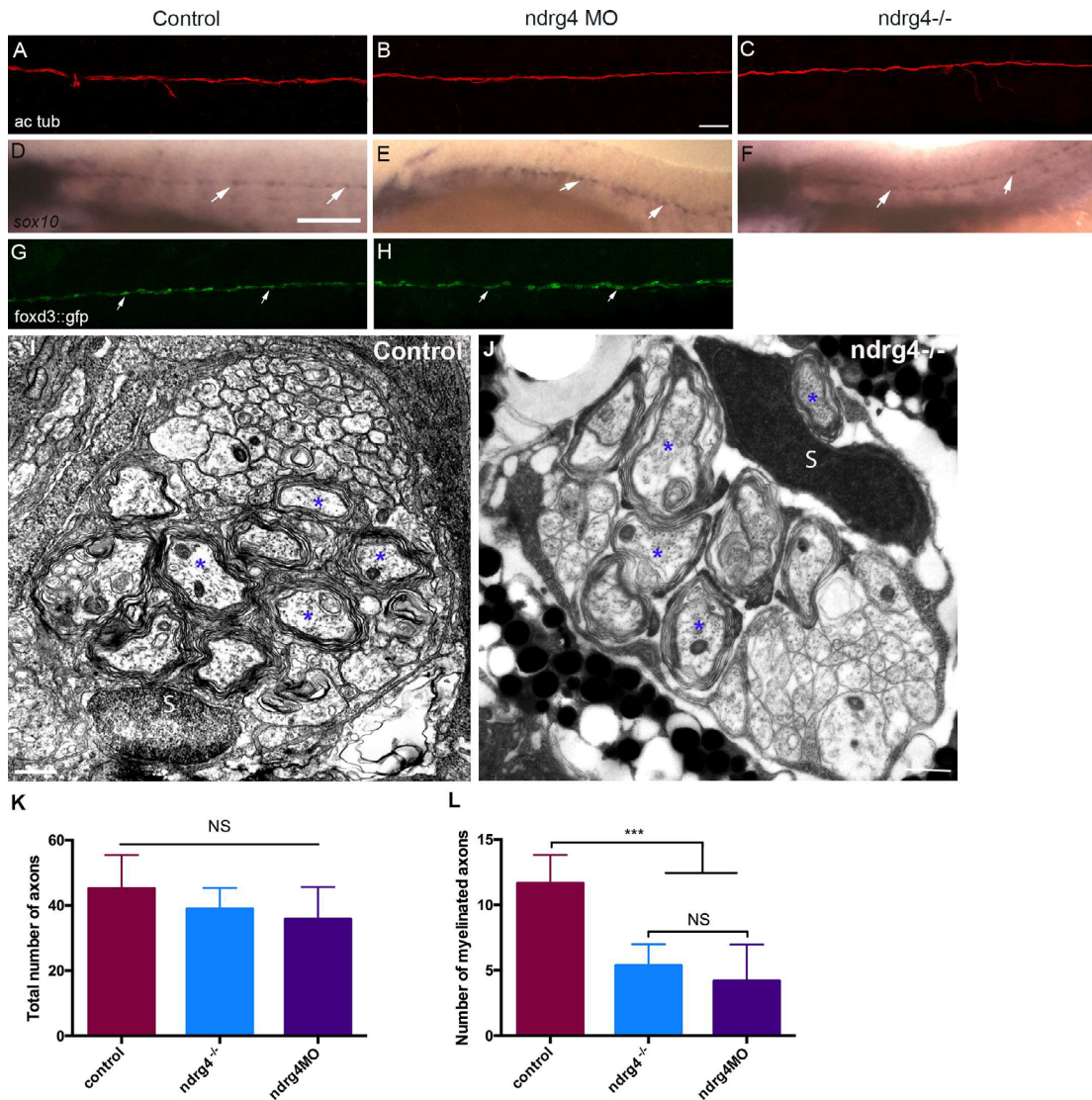


Fig 3. *ndrg4* is not required for axonal outgrowth or early Schwann cell development. Acetylated tubulin expression in control (A), *ndrg4* mutant (C) and morphant (B) embryos at 4 dpf showing the PLLn nerve. Scale bar = 45µm. (d-f) Whole mount *in situ* hybridization of a (d) control embryo, *ndrg4* mutant (F) and *ndrg4* morphant (E) showing *sox10* expression in PLLn SCs (arrows) at 3 dpf. Scale bar = 200µm. Lateral view of a control *foxd3::GFP* embryo (G), a *ndrg4* morphant (H) at 3 dpf showing SCs (arrows) along the PLLn. Transmission electron micrographs showing cross-section through (I) control and *ndrg4* mutant (J). Control PLLn shows an average of 10.7 myelinated axons (blue asterisks). (J) An average of 5.36 myelinated axons (blue asterisks) is observed in the *ndrg4* mutant's PLLn. (S: Schwann cell). Scale bars = 0.5µm. (K,L) Quantification of the total number of axons and the number myelinated axons in controls, *ndrg4* mutants and *ndrg4* morphants. NS: Non Significant.

doi:10.1371/journal.pgen.1006459.g003

NdrG4 is expressed in the Posterior Lateral Line ganglion (PLLg) but not in SCs

Overall, our results strongly suggest that *ndrg4* function is required for nodes of Ranvier organization. To investigate whether its function is neuronal or intrinsic to SCs, we first looked at *ndrg4* expression. Like mammalian *NdrG4* [20,23], zebrafish *ndrg4* is mainly expressed in the developing nervous system and heart [21]. Using *in situ* hybridization, we here confirm *ndrg4* expression within the brain, the eyes and the PLLg at 30 hpf (S3 Fig). The expression of *ndrg4* persists in the nervous system and specifically in the PLLg until at least 72 hpf (S3 Fig). However, *ndrg4* was not observed in SCs at any of these time points. This indicates that, at least in the zebrafish PNS, *ndrg4* is expressed in neuronal cells and not in glia.

NdrG4 function is required in neurons for sodium channel clustering

SC activity and axon-SCs interaction are both required for clustering of sodium channels at the nodes of Ranvier [10,15]. Therefore, we asked whether *ndrg4* function is required in neurons or in SCs despite a clear *ndrg4* mRNA expression in neurons and not in the glia of the zebrafish PNS (present data and [21]). A similar distribution profile was also observed for NDRG4 protein in the mouse CNS [20,23]. We therefore chose to specifically manipulate *ndrg4* function in the PLLg. In order to do so, we first generated mosaic PLLg of WT and *ndrg4* morphant cells by introducing *ndrg4* morphant cells, co-injected with *mCherry* mRNA, into a WT background. In such chimeras, no or very few sodium channel clustering (0.05 ± 0.23 cluster per somite) was observed along the PLLn axons derived from *ndrg4* morphant PLLg neurons (19 somites from 4 different embryos) (Fig 4A–4G) in comparison to control PLLg cells (14 somites from 4 different embryos) where sodium channel clustering was always observed (2.1 ± 1.8 clusters per somite, $p < 0.001$) (Fig 4H–4K). We then introduced WT cells, labeled with *mCherry*, into a *ndrg4* morphant background whereby SCs are defective for *ndrg4* but the introduced PLLg neurons express normal levels of *ndrg4*. In this case, we can observe normal sodium channel clustering along these axons (2.6 ± 1.2 clusters per somite) (Fig 4L–4N; 3 different embryos) while surrounding axons show little or no sign of sodium clustering. The same result was obtained when introducing WT cells into a *ndrg4*^{-/-} background, where normal sodium channel clustering was observed along the WT axons (2.2 ± 1.3 clusters per somite) (Fig 4O–4Q; 2 different chimeras). This result indicates that *ndrg4* function is required cell autonomously in neurons for sodium channel clustering.

NdrG4 function is required for the expression of key genes essential for vesicle docking

To understand the molecular mechanisms governing neuronal *ndrg4* function that leads to such defects, we undertook a differential microarray analysis looking for downstream targets that are dysregulated at 3dpf following *ndrg4* knockdown. Total RNAs were extracted and compared between two groups of either 1. control embryos or 2. *ndrg4* morphants (see [Materials and Methods](#)). In addition to a significant decrease in the expression of a number of genes known to be involved in hematopoiesis, related to *ndrg4* expression and function in the heart, e.g. *alas2* (Fold change (FC) 41, [38]); *klfd* (FC 17, [39]), that we will not discuss here, one particular major group of genes related to *ndrg4* function in the nervous system was discerned. It appeared that *ndrg4* significantly modulates the expression of numerous genes involved in vesicular release (e.g. *caly*, *syt1a*, *snap25*, *nsf*) and synaptic activity (e.g. *syn2*, *rims2*, *sypa*) (S1 Table). These data pointed to a previously unknown role for *ndrg4* in regulating the expression

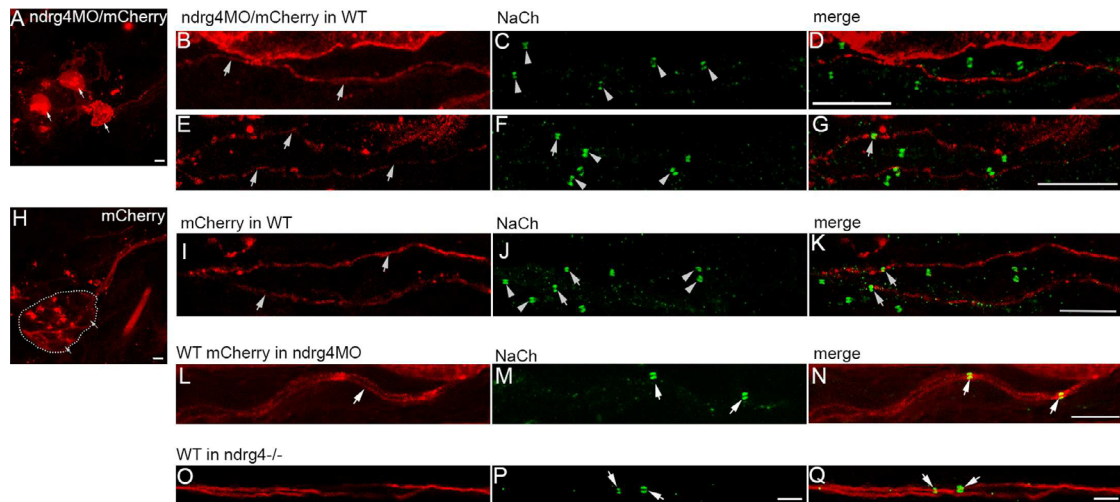


Fig 4. Chimeric embryos show evidence of ndrg4 requirement in neurons for sodium channel clustering. (A) ndrg4MO mCherry labeled PLL neurons shown by arrows. (b,e) ndrg4MO mCherry labeled axons of the PLLn in two different chimeric embryos; (c,f) sodium channels along the PLLn of ndrg4MO mCherry labeled (arrow) and of control (arrowheads) axons; (d,g) merge of the two labelings. Sodium channel clustering is absent in ndrg4MO axons (mCherry labeled) while control ones in the same PLLn show normal clustering. (H) Control mCherry labeled neurons indicated by arrows. The dashed line indicates the margin of the PLLg. (I) Control mCherry labeled axons (arrows). (J) Sodium channel clusters along the PLLn in control labeled (arrows) and other non-labeled (arrowheads) axons. (K) Merge of the two labelings. For (a, H) scale bars = 5µm. For (b-G; I-K) scale bars = 10µm. (L-N) WT mCherry labeled axons in ndrg4 morphant embryos are shown in (L, arrow) and the corresponding sodium channels in (M, arrows). Note the clustering of the nodes in the WT labeled axons while the other ndrg4 deficient axons show no sign of sodium channel clustering. (N) Merge of the two labelings. Scale bar = 7 µm. (O-Q) WT mCherry labeled axons in ndrg4^{-/-} are shown in (O) and the corresponding sodium channels in (P, arrows). (Q) Merge of the two labelings showing clustered sodium channels along the WT axons (arrows). Scale bar = 5 µm.

doi:10.1371/journal.pgen.1006459.g004

of several key genes required for vesicle docking and fusion during exocytosis and synaptic activity.

To further confirm these results in ndrg4 mutants, we performed quantitative PCR (qPCR), western blots and whole mount immunocytochemistry experiments to look for specific changes in the expression of the main corresponding genes and proteins. Indeed, we observed a 65, 48 and 62 per cent decrease in the expression of n-ethylmaleimide sensitive factor a (nsfa), synaptotagmin1a (sytl1a) and syntaxin binding protein1b (stxbp1b) respectively in ndrg4 mutants in comparison to controls (Fig 5A). However, the expression of the v-SNARE vamp2 (synaptobrevin), that is localized to vesicles and not to target membranes, was not altered (Fig 5A). Moreover, we could detect a 72 per cent decrease in the expression of Snap25 protein in ndrg4 mutants in comparison to controls (Fig 5I and 5K) at 3dpf. Similarly, ndrg4 knockdown led to a 90 per cent decrease in Snap25 protein expression (Fig 5H and 5J) (n = 3 independent experiments, p<0.001) in comparison to controls, showing a very sharp decrease in the expression of this key protein involved in vesicle docking and release. We next looked for Snap25 protein expression specifically in the PLLg and PLLn using whole mount immunocytochemistry at 4 dpf. We could observe a significant decrease in the expression of Snap25 along the PLLn and PLLg of ndrg4 mutants and morphants (Fig 5C and 5D, S1I and S1K Fig) compared to controls (Fig 5B, S1H and S1K Fig).

This result validates the overall decrease in the expression of different components essential for vesicle docking and release and for synaptic activity in ndrg4 mutants. Moreover, it shows the decrease in Snap25 expression in the PLLn and PLLg of ndrg4 mutants and morphants.

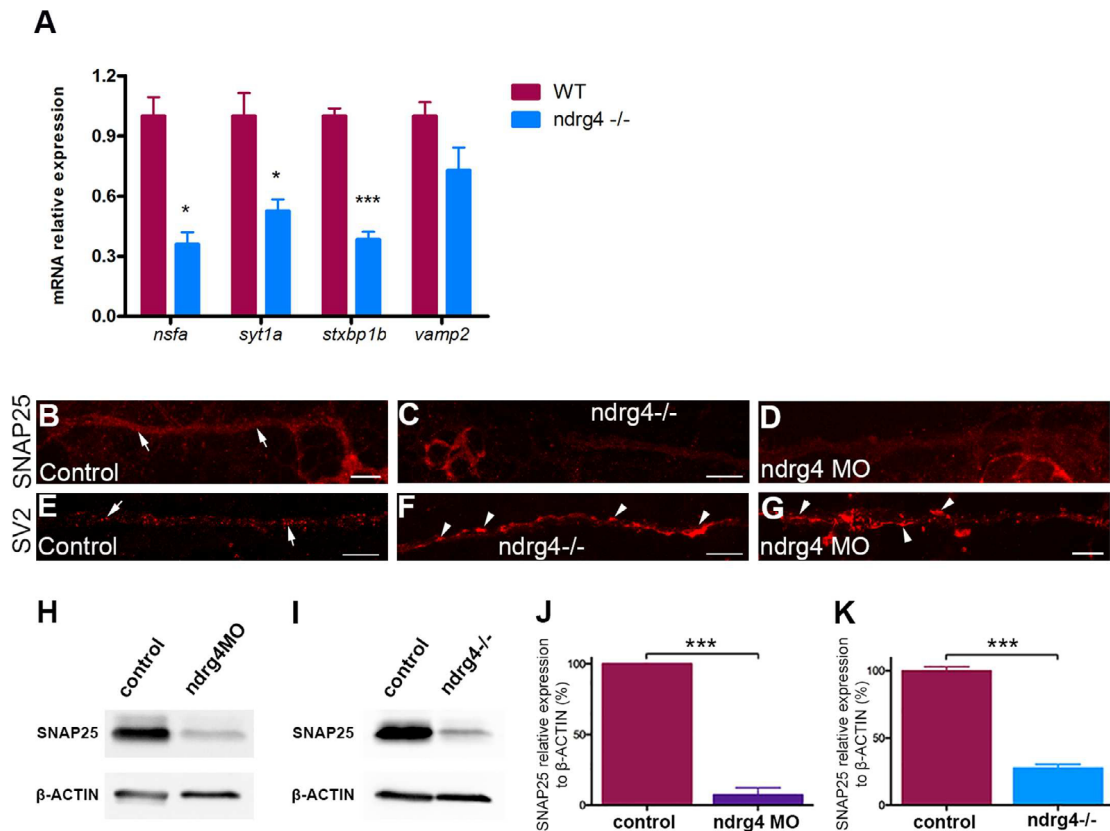


Fig 5. ndrg4 function is required for the expression of several genes that are essential for vesicle docking. (A) qPCR showing a significant decrease in the expression of *nsfa*, *syt1a*, *stxbp1b* but not *vamp2* in *ndrg4* mutants with mRNA relative expression to *ef1a*. Controls from 3 different experiments have deliberately been set to 100 per cent. (n = 3 independent experiments of 30 embryos each). (B-D) Lateral views showing Snap25 expression in the PLLn axons at 4 dpf. Snap25 is visible all along the PLLn (arrows) in controls (B), but detected to a lesser extent in the *ndrg4* mutants (C) and morphants (D) PLLn. (E-G) Lateral views of SV2 immunostaining, labeling synaptic vesicles at 4 dpf. (E) Synaptic vesicles are regularly distributed in the control PLLn (arrows) whereas they form agglomerates (arrowheads) in *ndrg4* mutants (F) and morphants (G). Scale bars = 10µm. (H-K) Western blots showing a sharp decrease in Snap25 protein expression in *ndrg4* mutants and morphants. Snap25 expression is significantly decreased in *ndrg4* morphants (H,J) and mutants (I,K) with protein relative expression to beta-actin. Controls from 3 different experiments have deliberately been set to 100 per cent. (n = 3 independent experiments of 30 embryos each). For the mutants study, the average of three groups of controls has been set to 100 per cent.

doi:10.1371/journal.pgen.1006459.g005

Vesicle patterning is defective in *ndrg4* mutants but the formation of vesicles and their transport are normal

Since the expression of several main components required for vesicular docking and release is significantly affected in *ndrg4* mutants, we took a closer look at the distribution of vesicles along the PLLn at 4dpf using an anti-SV2 antibody. While synaptic vesicles showed a regular dotted pattern along the nerve of control embryos (n = 22 embryos) (Fig 5E), we could observe irregular agglomerates (Fig 5F and 5G) in *ndrg4* mutants (n = 14 embryos) and morphants (n = 10 embryos), suggesting a defect in their release but not their formation.

It has been shown that the clustering of the channels at the nodes relies on vesicular axonal transport [40,41]. Thus, to test a possible role of *ndrg4* in longitudinal vesicular trafficking, that might explain the lack of sodium channel clustering along the axons, we monitored mitochondrial and vesicular movements along the axons using time-lapse imaging. For this purpose, we injected *mito::GFP* and *rab5::YFP* mRNAs at one cell stage and the PLL nerve vesicular trafficking was analyzed at 48 hpf. Mitochondrial average velocity was comparable between controls (S4 Movie; $0.73 \pm 0.09 \mu\text{m}\cdot\text{s}^{-1}$; 56 mitochondria from 5 embryos) and *ndrg4* morphants (S5 Movie; $0.76 \pm 0.2 \mu\text{m}\cdot\text{s}^{-1}$; 79 mitochondria from 5 embryos). Rab5 vesicles average velocity was rather slightly but not significantly increased in *ndrg4* morphants (S6 Movie; $1.82 \pm 0.55 \mu\text{m}\cdot\text{s}^{-1}$; 91 vesicles from 5 embryos) in comparison to controls (S7 Movie; $1.31 \pm 0.44 \mu\text{m}\cdot\text{s}^{-1}$; 100 vesicles from 5 embryos). Altogether, these results suggest that *ndrg4* is not required, *per se*, for vesicular formation or longitudinal transport along the axons.

Snap25 knockdown leads to a decrease in the clustering of sodium channels along the PLLn

Our analysis shows that *ndrg4* can regulate the expression of several key factors involved in vesicular docking and release (S1 Table and Fig 5), including *snap25* and *nsf*. While it has been shown that *nsf* is essential for sodium channel clustering at the nodes [33], we wanted to assess whether *snap25* is also involved in this process, since these two proteins are part of the t-SNARE/NSF machinery required for vesicle docking and release [27]. To test this hypothesis, we injected a specific 5'UTR morpholino against *snap25a* and *b* in zebrafish [42]. Zebrafish embryos injected with 0,6 pmoles of *snap25* MO showed a significant reduction in their ability to move or to respond to a touch stimulus at 3dpf (S8 Movie). This reflects the requirement of Snap25 in synaptic vesicle transmission while no major morphological nor PLLn axonal outgrowth defects were observed (Fig 6A–6C, 6D, 6F and 6H). However, a significant reduction in the number of sodium channel and neurofascin clustering was observed along the PLLn (Fig 6E–6K). We could observe 30.94 ± 2.536 sodium channel clusters in control embryos ($n = 17$ embryos) in comparison to 13.90 ± 5.6 in *snap25* morphants ($n = 20$ embryos). Similar results were obtained for anti-FIGQY labeling, we could observe 30.86 ± 0.54 clusters in control embryos ($n = 14$ embryos) in comparison to 15.78 ± 1.42 clusters in *snap25* morphants ($n = 14$ embryos). Co-injection of *snap25b* mRNA (300 pg) along with *snap25* MO was able to rescue the sodium channel clustering defects (31.75 ± 3.53 clusters; $n = 16$ embryos) and the evoked touch response test (S9 Movie), showing the specificity of this knockdown approach (Fig 6E–6J). This result strongly suggests that Snap25, like Nsf, can also regulate the clustering of sodium channels and neurofascin along the PLLn in zebrafish.

We have also analyzed axonal ensheathment in *snap25* morphants using TEM. Results show no significant difference in the total number of axons (44 ± 2.5 axons in *snap25* morphants; $n = 9$ nerves from 7 different embryos vs 43.6 ± 2.69 axons in controls; $n = 10$ nerves from 9 different embryos) nor in the number of myelinated axons in these morphants in comparison to controls (9.13 ± 0.71 myelinated axons in *snap25* morphants vs 10.7 ± 0.68 myelinated axons in controls) (Fig 6L and 6M). This result indicates that reducing the levels of *snap25* does not lead to obvious myelination defects, while it significantly decreases the clustering of sodium channels and neurofascin along the PLLn, at least at the concentration used in this study.

Snap25 over-expression slightly but significantly enhances clustering of sodium channels in *ndrg4* mutants

To test whether the decrease in the expression of Snap25 is involved in the sodium channel clustering defect observed in *ndrg4* mutants, we injected *snap25b* mRNA (150 pg) in *ndrg4*

Fig 6. snap25 can regulate the clustering of sodium channels and neurofascin along the PLLn and increase the clustering of sodium channels in ndrg4 mutants. (A-C) lateral views of control (A), snap25 morphant (B) and snap25 MO+*snap25b* mRNA (C) embryos at 72hpf. (D,F,H) lateral views of acetylated tubulin staining showing the PLLn in control (D), snap25 morphant (F) and snap25 MO+*snap25b* mRNA (H) embryos at 4dpf. (E-I') lateral views of sodium channels and acetylated tubulin staining along the PLLn of control (E-E'), snap25 morphant (G-G') and snap25MO+ *snap25b* mRNA (I-I') embryos at 4dpf. (J,K) Quantification of the sodium channel and neurofascin clustering, data are represented as mean±sem. Scale bars = 200 μm, 60 μm and 5 μm in (C), (F) and (I,I') respectively. Transmission electron micrographs showing cross-section through (L) control and (M) snap25 morphant's PLLn at 4 dpf. (L) Control PLLn shows an average of 10.7 myelinated axons (blue asterisks). (M) An average of 9.13 myelinated axons (blue asterisks) is also observed in the snap25 morphant embryo's PLLn. (S: Schwann cell). Scale bars = 0.5μm. (N) Quantification of the number of nodes seen in the PLLn in controls, ndrg4 morphants and ndrg4 morphants injected with 150pg of *snap25b* mRNA. (O) Quantification of the number of nodes seen in the PLLn in controls, ndrg4 mutants and ndrg4 mutants injected with 150pg of *snap25b* mRNA.

doi:10.1371/journal.pgen.1006459.g006

mutants and morphants. Indeed, we could observe a slight but significant increase in the number of sodium channel clustering in the injected embryos in comparison to non-injected mutants or morphants (Fig 6N and 6O), while the overexpression of Snap25 did not alter the number of sodium channel clusters in controls. We could count an average of 1.15 ± 0.22 ($n = 14$ embryos) and 6.85 ± 1.15 ($n = 13$ embryos) clusters in ndrg4 mutants and morphants respectively in comparison to an average of 4.35 ± 0.44 ($n = 13$ embryos) and 15.6 ± 1.1 ($n = 13$ embryos) clusters in snap25 mRNA injected ones. This result suggests that the decrease in Snap25 expression is partially responsible for the sodium channel clustering defect observed in these mutants and morphants.

Tetanus toxin injected embryos do not show obvious nodes organization or peripheral myelination defects

Recently, it has been reported that synaptic activity can regulate myelin thickness and biases axon selection in the CNS [43,44] but it is not required *per se* for sodium channel clustering in the PNS [33]. To specifically test the role of synaptic vesicle release in myelin organization of the PLLn, we used this time the Tetanus Toxin light chain (TeNT) to investigate whether the defects observed in ndrg4 mutants are related to its role in synaptic vesicle release. Therefore, we injected *TeNT* mRNA at one cell stage so that all cells in the nervous system are affected and we analyzed the embryos at 3 and 4 dpf. This resulted, first, in a significant decrease in motility when comparing TeNT injected embryos to control ones and only embryos that showed a reduced motility were chosen for further analysis. To examine axonal integrity and SC migration, we injected *TeNT* in the foxd3::GFP line and then performed an acetylated tubulin staining at 3 dpf. We did not observe any obvious difference in axonal integrity or SC development and distribution between *TeNT* injected embryos ($n = 14$ embryos) (Fig 7C–7C") and controls ($n = 24$ embryos) (Fig 7A–7A"). We then looked for sodium channel clustering in *TeNT* injected embryos, and we observed no difference in the number or organization of these channels along the axons in the injected embryos (average of 28.7 nodes from 21 embryos) in comparison to controls (average of 25.5 nodes from 12 embryos) (Fig 7B–7B", 7D–7D" and 7J). We then checked the nerve ultrastructure by TEM at 4 dpf (Fig 7E and 7F) and we counted an average number of 6 myelinated axons per nerve in *TeNT* embryos (4 nerves from 3 different larvae) (Fig 7E) and in control embryos (4 nerves from 4 different larvae) (Fig 7F).

These results show that TeNT injected embryos do not show obvious sodium channel clustering and early myelin compaction defects in the PLLn.

Discussion

The identification of ndrg4 in a differential screen looking for dysregulated genes in the absence of SCs in zebrafish, led us to generate and analyze the ndrg4 mutant. We show that

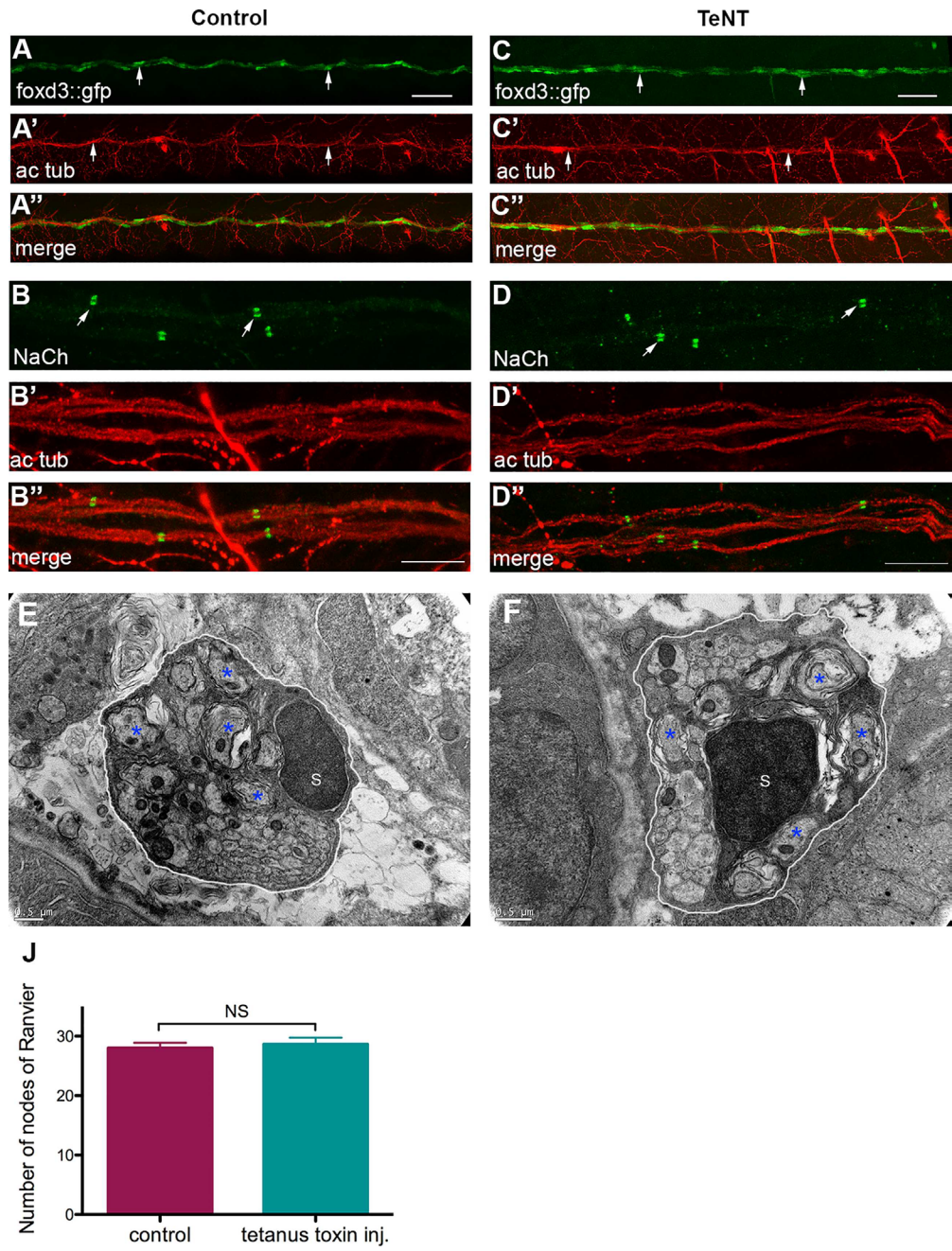


Fig 7. Tetanus toxin injection does not impair sodium channel clustering and myelination in the PNS. (A) Lateral view of a control foxd3::GFP embryo at 3 dpf. Arrows indicate SCs along the PLLn. (A') Acetylated tubulin expression in the same control embryo at 3 dpf. Arrows show the PLLn axons. (A'') Merge of (A) and (A'). (C) Lateral view of a *TeNT* injected foxd3::GFP embryo at 3 dpf. Arrows indicate SCs along the PLLn. (C') Acetylated tubulin expression in the same *TeNT* injected embryo at 3 dpf. Arrows indicate the PLLn axons. (C'') Merge of (C) and (C'). Scale bars = 50µm. Sodium channel labeling in control (B) and *TeNT* injected embryo (D) and their corresponding axons of the PLLn, (B') and (D') respectively. (B'') merge of (B) and (B'), (D'') merge of (D) and (D'). Scale bars = 10µm. (E,F) Transmission electron micrographs showing cross-section through (E) control and (F) *TeNT* injected embryos' PLLn at 4 dpf. (E) Control PLLn shows an average of 6 myelinated axons (blue asterisks). (F) An average of 6 myelinated axons (blue asterisks) is also observed in the *TeNT* injected embryo's PLLn. (S: Schwann cell). Scale bars = 0.5µm. (J) Quantification of the number of nodes seen in the PLLn shows no significant difference between controls and *TeNT* injected embryos.

doi:10.1371/journal.pgen.1006459.g007

ndrg4 is a novel factor required within neurons for the clustering of sodium channels along the peripheral axons. *Ndrq4* mutants have severe heart defects, consistent with the potential role of *NDRG4* in heart development and function previously reported in humans. However, *Ndrq4* mice knockout show no sign of heart dysfunction [21,23,25,45–47], suggesting that the zebrafish *ndrg4* mutant is a more suitable model to study the role of *ndrg4* in this process. The *ndrg4* mutants also show little or no mobility, most likely due to the sharp decrease in the expression of key genes involved in vesicle fusion and release therefore inhibiting synaptic neurotransmission and activity. Labeling of SV2 vesicles in *ndrg4* mutants show clearly that these vesicles are present along the axons but tend to agglomerate, suggesting a defect in their release. Reducing the levels of Snap25 in zebrafish embryos leads to a significant decrease in the clustering of sodium channels and over-expression of Snap25 in *ndrg4* mutants slightly but significantly increases the clustering of sodium channels along the PLLn. Moreover, monitoring vesicle transport along these axons shows no obvious abnormality in comparison to controls. Overall, these results point to a rather global vesicle docking and release defect along the *ndrg4* mutant axons rather than to an abnormal vesicle formation and transport. Moreover, they indicate that these processes can be dissociated. The reduction in the number of myelinated axons observed in *ndrg4* mutants and morphants' PLLn suggests that its function is not required *per se* for SC radial sorting or myelination. The myelin defect might be the result of a delay in the development of these embryos given their severe heart defects or a defective axonal-SCs interaction that alters SC myelination process. However, *ndrg4* mutants do not survive beyond 5–6 dpf to test this hypothesis. Overall, this establishes *ndrg4* as a novel member of the *Ndrq* family, to add to *NDRG1*, that plays a fundamental role in the organization of myelinated axons in the PNS.

A novel neuronal *ndrg4* function that regulates sodium channel clustering

We here identify a novel neuronal function for zebrafish *ndrg4* required for sodium channel and neurofascin clustering along the PLLn. *Ndrq4* regulates, among others, the expression of several key genes involved in vesicle fusion and release [26,27]. It has been shown that ion channels, particularly Nav1.2 channels, require vesicular axonal transport from the neuronal cell body to be later anchored at the sites of the nodes [40,41]. This process is mediated by ankyrin-G and kinesin-1, however less is known about other fundamental players required for ion channel docking. One particular mutant that shows comparable myelinated axons organization defects to *ndrg4* is the *nsf* mutant. Neuronal *nsf* is autonomously required for sodium channel clustering in the PLLn [33,48] and is characterized as an essential component for vesicle fusion and release by interacting with and dissociating the SNARE complex [27,49,50]. Moreover, other data show *nsf* requirement for Ca²⁺ channels localization and function in nerve terminals [51].

Overall, based on previous studies and our data presented here, it is now clear that i) both *nsf* and *ndrg4* mutants cause a very severe defect in sodium channel and neurofascin clustering along the axons, ii) *ndrg4* loss leads to a sharp decrease in Snap25 and *nsf* expression, iii) *snap25* knockdown leads to a significant decrease in sodium channel clustering, iv) *snap25* over-expression slightly but significantly enhances sodium channel clustering in *ndrg4* mutants and v) both NSF and SNAP25 have a fundamental role, *in vivo*, in vesicular docking and release. We thus propose that key components of the NSF/t-SNARE machinery, tightly controlled by *ndrg4*, are most likely playing an essential role in sodium channel and neurofascin clustering in the PNS, independent of their role in synaptic vesicle release. It has been shown that axonal adhesion molecules e.g. neurofascin are diffusible and cluster at the nodes from adjacent axonal domain while sodium channel clustering relies on vesicular axonal transport in the PNS [41]. Our data show that sodium channel and neurofascin clustering are both defective in *ndrg4* mutants and *snap25* morphants, and similar results were obtained with *nsf* mutant [33]. Given that axonal vesicular transport is not dependent on *ndrg4* function but vesicle docking is, one possibility is that the initial anchoring of neurofascin and sodium channels along the axons might rely on vesicle docking. It would be interesting to test whether these fundamental components of the t-SNARE/NSF machinery are also involved in sodium channel and neurofascin clustering at the nodes in mice, and to carefully analyze the clustering of sodium channels and neurofascin in *Ndr4* KO mice. *Ndr4*^{-/-} mice exhibits inferior performance in escape latency and total path lengths in the MWM task in comparison to controls but this is not comparable to the total lack of mobility seen in zebrafish *ndrg4* mutants. Moreover, *Ndr4*^{-/-} mice do not show any heart defects [23] in contrast to zebrafish mutants. Whether *ndrg4* function in the heart and nodes assembly is specific to zebrafish or a possible redundancy would explain the lack of defects in *Ndr4* KO mice is to be tested in the future.

Ndr4 in vesicle fusion and synaptic activity

Several lines of evidence presented here suggest a potential role of *ndrg4* in controlling synaptic vesicle release *in vivo* (S1 Table). Numerous studies indicated a role of synaptic activity in myelination and nodes of Ranvier establishment but conflicting results emerged [52,53]. However, the first *in vivo* evidence, using zebrafish, showed no significant requirement of synaptic activity in PNS sodium channel clustering and *mbp* expression using tetrodotoxin (TTX) and neomycin [33]. We here injected TeNT at one cell stage so that the whole nervous system is affected and whereby the Ca²⁺ triggered exocytosis is specifically down-regulated while the constitutive one is not impaired [54]. We show using TEM that the PNS myelin is comparable to controls and that nodes organization is also similar to controls suggesting that synaptic vesicle release is not required, *per se*, for PNS myelin organization. However, whether these drugs have the same effect on synaptic vesicle release in the PNS, as shown in the CNS [44,55], should be carefully tested in the future. Synaptic vesicle release might be responsible for myelin ensheathment in the CNS as it has been proposed a synaptic-like interaction between OLs and axons [43,44,56], nevertheless its role in nodes organization has not been tested yet. SNAP25 and NSF have been shown to be involved in both types of constitutive and regulated exocytosis as SNARE proteins and NSF are essential for all intracellular membrane fusion events [26,27,57]. We here show that Snap25 expression is decreased within neurons and along the axons of the PLLg in the *ndrg4* mutants and morphants, suggesting a role of *ndrg4* in controlling both regulated and constitutive vesicle release. However, a defect in the latter is more likely to be responsible for nodes disorganization in these mutants. A recent study shows a role of *ndrg4* in exocytosis by regulating Fibronectin recycling and secretion via its interaction with the Blood Vessel Epicardial Substance (Bves) to control epicardial cell movement [58].

Ndr4 is mainly expressed in the nervous system and heart showing a rather specific temporal and local control of snap5 and nsf expression by *ndrg4* during nervous system development. Indeed, the mRNA expression of *ndrg4*, *snap25* and *nsf* are identical at 48 and 72 hpf, (at least in the PLLg; [S4 Fig](#) and [\[33\]](#)).

Overall, these data reveal an unknown neuronal function of *ndrg4* in vesicle release and peripheral myelinated axons organization that is most likely due to its role in controlling the expression of key components of the t-SNARE/NSF machinery.

Materials and Methods

Embryo care

Embryos were staged and cared for according to standard protocols. Foxd3::GFP [\[37\]](#), Sox10::mRFP [\[29\]](#) and HuC::GFP [\[59\]](#) stable transgenic lines, that label SCs and neurons, some of which previously described in [\[60\]](#) were used in this study. All animal experiments were conducted with approved protocols at Inserm.

ndrg4 CRISPR mutagenesis

sgRNA generation. sgRNA guide sequence (GGTGATCCGTGGCGCTCCCA), targeting *ndrg4* exon 2, was cloned into the DR274 (Addgene 42250) vector digested with BsaI. *In vitro* transcription of the sgRNA was performed using the Megascript T7 transcription kit (Ambion AM1334) and sgRNA was purified using RNeasy Mini Kit (Qiagen).

Injections. To induce targeted mutagenesis at the *ndrg4* locus, 200 ng/ul of sgRNA were injected into one-cell stage zebrafish embryos together with Cas9 endonuclease (NEB M0386M; final concentration: 25 μ M). Pools of embryos were digested to extract genomic DNA (to perform PCR and DNA sequencing experiments).

Injected embryos were grown to adulthood and screened for mutation in their offspring. Two different mutants that showed a deletion of 10 and 11 nucleotides respectively were used in this study (See [Fig 1](#)).

Whole embryos DNA extraction and mutation analysis. Embryos were digested for 1 h at 55°C in 0.5mL lysis buffer (10 mM Tris, pH 8.0, 10 mM NaCl, 10 mM EDTA, and 2% SDS) with proteinase K (0.17 mg/mL, Roche Diagnostics) to extract genomic DNA. To verify cleavage at targeted sequence, *ndrg4* exon 2 was PCR amplified and digested with the restriction enzyme HaeII. The restriction site, placed in the sgRNA-binding region, would be removed upon Indel mutations at the *ndrg4* locus. To estimate the rate of mutations *ndrg4* amplicons were cloned into the pCR-bluntII-TOPO vector (life technologies 450245). Single amplicons were sent for sequencing and mutant alleles were identified by comparison to the wild-type unmodified sequence. Primers used for the PCR were: *ndrg4* fw: 5'-CCTGCAAACAAGCAA GCCA-3' and *ndrg4* rev: 5'-ATCATCCTCGTCTCAGCTG-3'.

Microinjections

Splice blocking *ndrg4*-MO (5'-TGCATTCATCTTACCCTTGAGGCAT-3'), 5mis *ndrg4*-MO (5'-TGgATTgATCTTAgCCTTcAGGgAT-3'), described in [\(21\)](#), and 5'UTR *snap25*-MO (5'-AGCTGCTCTCCAAGTGGCTCTTACT-3') described in [\(42\)](#) were purchased from Gene Tools.

We used a corresponding *ndrg4* 5-mis MO as a control in all our experiments. There were no significant difference between control injected embryos and Wild Type (WT) ones. For convenience, we refer to control as WT, non *ndrg4*^{-/-} mutants and 5-mis MO injected embryos in the Figures, unless it is stated otherwise.

For *ndrg4* rescue experiment, *ndrg4* mRNA was synthesized using SP6 mMessage mMachine System after linearization with NotI. For *snap25* rescue and overexpression experiments, *snap25b* mRNA was synthesized using T3 mMessage mMachine System after linearization with ApaI.

For TeNT experiments, tetanus toxin light chain cDNA was purchased from Addgene. Synthetic *TeNT* mRNA was generated using SP6 mMessage mMachine System after linearization with SacII and injected at 150 pg per embryo. Rab5::YFP (a gift from Carl-Philipp Heisenberg) and mito::GFP (a gift from Dominik Paquet) mRNAs were synthesized using SP6 mMessage mMachine System after linearization with NotI and injected at 200 pg per embryo.

In situ hybridization

In situ hybridization was performed following standard protocols previously described in [60] using *mbp* [48] and *sox10* probes [61]. *ndrg4*, and *snap25b* cDNA clones were purchased from Source BioScience UK. *ndrg4*, *snap25b* antisense probes were synthesized using mMessage mMachine System (Ambion) and T7 polymerase after linearization with EcoRI for *ndrg4* and NotI for *snap25b*.

Microarray hybridization

RNA was extracted from two groups of zebrafish embryos (1. control embryos and 2. *ndrg4* morphants) at 3dpf, cDNA generated and applied to Zebrafish_v3 4x44K array (Agilent Technologies). Significantly different genes were first selected using *GeneSpring* 12.0 (Agilent Technologies) and then filtered using t-test and genes with a p value of less than 0.05 were filtered out.

Quantitative real-time RT-PCR

RNA was extracted using Trizol reagent (Life Technologies) and miRNeasy Mini kit (Qiagen) according to manufacturer's instructions. For mRNA quantitation, Reverse Transcription (RT) was performed using High Capacity cDNA Reverse Transcription Kit (Life Technologies). Quantitative real-time PCR (qPCR) was performed using Power SYBR-Green Master Mix (Biorad) on an Applied 7500 Real-Time PCR system. Primers used for qPCR are listed here:

Nsf1a,
forward: CGCGGCTTCTTCGAGTAACA
reverse: GAAGTGTGATCTCCGTCAGGTT
Syt1a,
Forward: AAAGGGAAGAGACGGCTGTG
Reverse: GGAGCCAGGCAGAAGCTTTA
Stxbp1b,
Forward: ACGCTGAAAGAGTACCCAGC
Reverse: CTCCCAAAGTGGGGTCATCC
Vamp2,
Forward: CGCAACATTCCTACCCACT
Reverse: GTGAGAAGTCGTTGCTCCCA

mRNA expression levels in wild type or *ndrg4* mutant zebrafish were determined by RT-qPCR. mRNA amount was normalized to that of EF1-a mRNA then expressed as a relative amount to WT (data represent the mean \pm SD of triplicates).

Immunofluorescence

The following antibodies and dilutions were used: mouse anti-acetylated tubulin (Sigma; 1:500), rabbit anti-PH3 (Millipore; 1:500), mouse anti-SNAP25 (Synaptic Systems; 1:200), mouse anti-sodium channels (pan) clone K58/35 (Sigma; 1:500), mouse anti-SV2 (DSHB; 1:200), rabbit anti FIGQY (a gift from Matthew Rasband; 1:500). Primary antibodies were detected with appropriate secondary antibodies conjugated to either Alexa 488 or Alexa 568 (Molecular probes) at a 1:1000 dilution.

For immunostaining, embryos were fixed in 4% paraformaldehyde 1X PBS overnight at 4°C and stained as whole mounts. Sodium channels, SNAP25 and SV2 immunostainings were performed as described for Na_vCh staining in [33].

Images were taken on a Zeiss LSM510 system and a Leica SP8 confocal microscope.

Live imaging

Embryos were anesthetized with tricaine and embedded in 1.5% low melting point agarose. For mito::GFP and rab5::YFP tracking experiments, PLLn was examined at 48 hpf from a lateral view. A series of 10 minutes time-lapses were recorded. Recordings were performed at 28°C using a Leica SP8 confocal microscope. Larval movements stimulated by touch-response test were performed at room temperature and recorded using a Zeiss Lumar.V12 stereoscope and Zeiss AxioCam MRc camera.

Western blot

Proteins were extracted from pools of embryos as previously described in [62] with 10μl lysis buffer (1M Tris HCl pH 6.8, glycerol 40% and SDS 10%) per embryo. Protein content was determined using the Pierce BCA protein assay. 25 μg proteins were loaded on gel. Western blots were performed according to standard methods using the following antibodies: mouse anti-snap25 (Synaptic Systems; 1:1000), mouse anti-β-actin (Sigma, clone AC-15; 1:10,000) and appropriate HRP-conjugated secondary antibodies (Jackson immuno research).

Transmission electron microscopy

At 4 dpf, embryos were fixed in a solution of 2% glutaraldehyde, 2% paraformaldehyde and 0.1M sodium cacodylate pH 7.3 overnight at 4°C. This was followed by a post-fixation step in cacodylate-buffered 1% osmium tetroxide (OsO₄, Serva) for 1h at 4°C and in 2% uranyl acetate for 1h at room temperature. The tissue was then dehydrated and embedded in epoxy resin. Sections were contrasted with saturated uranyl acetate solution and were examined with a 1011 electron microscope (JEOL) and a digital camera (Gatan).

Chimeric analysis

Donor cells were injected with 0.6pmoles of ndrG4MO and mCherry mRNA (300ng/μl) or with mCherry mRNA (300ng/μl) and introduced into a WT background. mCherry WT cells were also introduced into ndrG4 morphant background. In all cases, only embryos that presented labeling in the nervous system were further analyzed for sodium channel clustering.

Statistical analysis

Means and standard deviations were calculated with Microsoft Excel version 14.4.3 or Graph Pad Prism 5. Means were compared by the two-tailed Student's *t* test or one-way ANOVA according to the experiment. *p*<0.05 was considered statistically significant.

Ethics statement

All experiments were carried out in accordance to the official regulatory standards of the Department of Val de Marne (agreement number D 94-043-013 to the animal facility of Bâtiment Pincus, Institut Biomédical de Bicêtre).

Supporting Information

S1 Fig. *ndrg4* morphant and mutant phenotype. (A-C) Overall morphology of a control embryo (A), *ndrg4* morphant embryo (B), *ndrg4* MO+*ndrg4* mRNA co-injected embryo (C), at 48hpf. (B) *ndrg4* morphant embryo displays smaller head and eyes and is slightly thinner. (C) Co-injection of *ndrg4* MO and mRNA rescue this phenotype. Scale bars = 500 μ m. (D-F) Acetylated tubulin and sodium channels staining of a *ndrg4* MO+mRNA co-injected embryo showing clustered sodium channels along the PLLn (34.2 \pm 3.2; n = 12 embryos) similar to controls. Scale bar = 5 μ m. (G) Sodium channels staining in *sox10::mRFP* transgenic line in controls and *ndrg4* morphants. Arrowheads indicate the clustering of sodium channels while arrows point to nodal gaps. Note the absence of sodium channels clustering at the nodes in *ndrg4* morphants. Scale bar = 5 μ m. (H-J) Snap25 immunostaining in HuC::GFP larvae at 3dpf. (H) Control embryos show Snap25 expression in PLLg neurons (arrows). (I) A reduced Snap25 expression was observed within the PLLg in *ndrg4* morphants. (J) Rescue of Snap25 expression in the PLLg in *ndrg4*MO+mRNA co-injected embryos. Scale bars = 5 μ m. (K) Snap25 expression in the PLLg of control and *ndrg4*^{-/-} embryos. Note the significant decrease in the expression of Snap25 within the PLLg of *ndrg4*^{-/-} in comparison to controls. (TIF)

S2 Fig. *ndrg4* is not required for SC proliferation. PH3 immunohistochemistry in (A) control and (B) *ndrg4* morphant *foxd3::GFP* embryos at 48 hpf. Arrows indicate dividing PLLn SCs. Scale bar = 100 μ m. (C) Quantification of PH3 positive SCs in controls and *ndrg4* morphants shows no significant differences between the two groups at 30 hpf, 48 hpf and 72 hpf. (TIF)

S3 Fig. *ndrg4* mRNA is expressed in the PLL ganglion and not in SCs. (A-C) *In situ* hybridization showing *ndrg4* mRNA expression in the brain, eye and in the PLL ganglion (arrow) at 30 hpf (A), 48 hpf (B) and 72 hpf (C). Scale bar = 200 μ m. (TIF)

S4 Fig. *Snap25* mRNA is expressed in the PLL ganglion. *In situ* hybridization showing *snap25b* mRNA expression in the brain, eye and in the PLL ganglion (arrow) at 48 hpf and 72 hpf. Scale bar = 200 μ m. (TIF)

S1 Movie. Touch response mobility of 3dpf WT larvae.
(MP4)

S2 Movie. The *ndrg4* mutants are paralyzed and do not respond to a touch-evoked motility test at 3dpf.
(MP4)

S3 Movie. The *ndrg4* morphant is paralyzed and shows no response following touch-evoked motility test at 48hpf.
(MP4)

S4 Movie. Real-time imaging of mitochondria in a control PLLn at 48 hpf. Forty-eight hours embryo expressing GFP in mitochondria after *mito::GFP* mRNA injection; the embryo

was imaged every 4 seconds for 6 minutes by confocal microscopy. Lateral view; anterior to the left and dorsal to the top.

(MOV)

S5 Movie. Real-time imaging of mitochondria in a *ndrg4* morphant PLLn at 48 hpf. Forty-eight hours *ndrg4* morphant expressing GFP in mitochondria after *mito::GFP* mRNA injection; the embryo was imaged every 4 seconds for 6 minutes by confocal microscopy. Lateral view; anterior to the left and dorsal to the top.

(MOV)

S6 Movie. Real-time imaging of Rab5 positive vesicles in an *ndrg4* morphant PLLn at 48 hpf. Forty-eight hours *ndrg4* morphant expressing YFP in early endosomes after *Rab5::YFP* mRNA injection; the embryo was imaged every 425 milliseconds for 2 minutes by confocal microscopy. Lateral view; anterior to the left and dorsal to the top.

(MOV)

S7 Movie. Real-time imaging of Rab5 positive vesicles in a control PLLn at 48 hpf. Forty-eight hours embryo expressing YFP in early endosomes after *Rab5::YFP* mRNA injection; the embryo was imaged every 425 milliseconds for 2 minutes by confocal microscopy. Lateral view; anterior to the left and dorsal to the top.

(MOV)

S8 Movie. The *snap25* morphants show little or no movement.

(MP4)

S9 Movie. Co-injection of *snap25* MO and *snap25b* mRNA restores defective evoked touch response observed in *snap25* morphants at 3dpf.

(MP4)

S1 Table. A selection of genes involved in vesicular docking and release or synaptic activity that are down regulated in *ndrg4* morphants in comparison to controls at 3dpf. Genes are sorted in a descending order related to their fold change.

(DOC)

Acknowledgments

We would like to thank Kelly Monk for plasmids, Matthew Rasband for the anti-FIQY antibody, Philippe Leclerc and Olivier Trassard for technical assistance in confocal microscopy and imaging, Alain Schmitt for assistance in Transmission Electron Microscopy, Pierre-Henri Commere for help in FACS sorting at Institut Pasteur, Dan Mejlachowicz and Judith Melki for technical assistance in qPCR, Matthew Voas for helpful discussions, Elisabeth Traiffort and Michael Schumacher for comments on the manuscript.

Author Contributions

Conceptualization: LF MT.

Data curation: LF MT.

Formal analysis: LF CD BC MT.

Funding acquisition: MT.

Investigation: LF FDS VDD CD BC MT.

Methodology: LF FDS VDD FDB MT.

Project administration: MT.

Resources: CD BC FDB MT.

Supervision: MT.

Validation: LF CD BC MT.

Visualization: LF MT CD.

Writing – original draft: LF MT.

Writing – review & editing: LF MT.

References

1. Ahrendsen JT, Macklin W (2013) Signaling mechanisms regulating myelination in the central nervous system. *Neurosci Bull* 29: 199–215. doi: [10.1007/s12264-013-1322-2](https://doi.org/10.1007/s12264-013-1322-2) PMID: [23558589](https://pubmed.ncbi.nlm.nih.gov/23558589/)
2. Jessen KR, Mirsky R (2005) The origin and development of glial cells in peripheral nerves. *Nat Rev Neurosci* 6: 671–682. doi: [10.1038/nrn1746](https://doi.org/10.1038/nrn1746) PMID: [16136171](https://pubmed.ncbi.nlm.nih.gov/16136171/)
3. Jessen KR, Mirsky R (2010) Control of Schwann cell myelination. *F1000 Biol Rep* 2.
4. Kucenas S, Wang WD, Knapik EW, Appel B (2009) A selective glial barrier at motor axon exit points prevents oligodendrocyte migration from the spinal cord. *J Neurosci* 29: 15187–15194. doi: [10.1523/JNEUROSCI.4193-09.2009](https://doi.org/10.1523/JNEUROSCI.4193-09.2009) PMID: [19955371](https://pubmed.ncbi.nlm.nih.gov/19955371/)
5. Lyons DA, Talbot WS (2014) Glial cell development and function in zebrafish. *Cold Spring Harb Perspect Biol* 7: a020586. doi: [10.1101/cshperspect.a020586](https://doi.org/10.1101/cshperspect.a020586) PMID: [25395296](https://pubmed.ncbi.nlm.nih.gov/25395296/)
6. Sherman DL, Brophy PJ (2005) Mechanisms of axon ensheathment and myelin growth. *Nat Rev Neurosci* 6: 683–690. doi: [10.1038/nrn1743](https://doi.org/10.1038/nrn1743) PMID: [16136172](https://pubmed.ncbi.nlm.nih.gov/16136172/)
7. Smith CJ, Morris AD, Welsh TG, Kucenas S (2014) Contact-mediated inhibition between oligodendrocyte progenitor cells and motor exit point glia establishes the spinal cord transition zone. *PLoS Biol* 12: e1001961. doi: [10.1371/journal.pbio.1001961](https://doi.org/10.1371/journal.pbio.1001961) PMID: [25268888](https://pubmed.ncbi.nlm.nih.gov/25268888/)
8. Black JA, Kocsis JD, Waxman SG (1990) Ion channel organization of the myelinated fiber. *Trends Neurosci* 13: 48–54. PMID: [1690930](https://pubmed.ncbi.nlm.nih.gov/1690930/)
9. Poliak S, Peles E (2003) The local differentiation of myelinated axons at nodes of Ranvier. *Nat Rev Neurosci* 4: 968–980. doi: [10.1038/nrn1253](https://doi.org/10.1038/nrn1253) PMID: [14682359](https://pubmed.ncbi.nlm.nih.gov/14682359/)
10. Salzer JL, Brophy PJ, Peles E (2008) Molecular domains of myelinated axons in the peripheral nervous system. *Glia* 56: 1532–1540. doi: [10.1002/glia.20750](https://doi.org/10.1002/glia.20750) PMID: [18803321](https://pubmed.ncbi.nlm.nih.gov/18803321/)
11. Parkinson DB, Bhaskaran A, Arthur-Farraj P, Noon LA, Woodhoo A, et al. (2008) c-Jun is a negative regulator of myelination. *J Cell Biol* 181: 625–637. doi: [10.1083/jcb.200803013](https://doi.org/10.1083/jcb.200803013) PMID: [18490512](https://pubmed.ncbi.nlm.nih.gov/18490512/)
12. Pereira JA, Lebrun-Julien F, Suter U (2012) Molecular mechanisms regulating myelination in the peripheral nervous system. *Trends Neurosci* 35: 123–134. doi: [10.1016/j.tins.2011.11.006](https://doi.org/10.1016/j.tins.2011.11.006) PMID: [22192173](https://pubmed.ncbi.nlm.nih.gov/22192173/)
13. Salzer JL (2012) Axonal regulation of Schwann cell ensheathment and myelination. *J Peripher Nerv Syst* 17 Suppl 3: 14–19.
14. Woodhoo A, Alonso MB, Droggiti A, Turmaine M, D'Antonio M, et al. (2009) Notch controls embryonic Schwann cell differentiation, postnatal myelination and adult plasticity. *Nat Neurosci* 12: 839–847. doi: [10.1038/nn.2323](https://doi.org/10.1038/nn.2323) PMID: [19525946](https://pubmed.ncbi.nlm.nih.gov/19525946/)
15. Voas MG, Glenn TD, Raphael AR, Talbot WS (2009) Schwann cells inhibit ectopic clustering of axonal sodium channels. *J Neurosci* 29: 14408–14414. doi: [10.1523/JNEUROSCI.0841-09.2009](https://doi.org/10.1523/JNEUROSCI.0841-09.2009) PMID: [19923275](https://pubmed.ncbi.nlm.nih.gov/19923275/)
16. Melotte V, Qu X, Ongenaert M, van Crielinge W, de Bruine AP, et al. (2010) The N-myc downstream regulated gene (NDRG) family: diverse functions, multiple applications. *Faseb J* 24: 4153–4166. doi: [10.1096/fj.09-151464](https://doi.org/10.1096/fj.09-151464) PMID: [20667976](https://pubmed.ncbi.nlm.nih.gov/20667976/)
17. Yang X, An L, Li X (2013) NDRG3 and NDRG4, two novel tumor-related genes. *Biomed Pharmacother* 67: 681–684. doi: [10.1016/j.biopha.2013.04.009](https://doi.org/10.1016/j.biopha.2013.04.009) PMID: [23725756](https://pubmed.ncbi.nlm.nih.gov/23725756/)
18. Kalaydjieva L, Nikolova A, Turnev I, Petrova J, Hristova A, et al. (1998) Hereditary motor and sensory neuropathy—Lom, a novel demyelinating neuropathy associated with deafness in gypsies. Clinical, electrophysiological and nerve biopsy findings. *Brain* 121 (Pt 3): 399–408.

19. King RH, Chandler D, Lopaticki S, Huang D, Blake J, et al. (2011) NdrG1 in development and maintenance of the myelin sheath. *Neurobiol Dis* 42: 368–380. doi: [10.1016/j.nbd.2011.01.030](https://doi.org/10.1016/j.nbd.2011.01.030) PMID: [21303696](https://pubmed.ncbi.nlm.nih.gov/21303696/)
20. Okuda T, Higashi Y, Kokame K, Tanaka C, Kondoh H, et al. (2004) NdrG1-deficient mice exhibit a progressive demyelinating disorder of peripheral nerves. *Mol Cell Biol* 24: 3949–3956. doi: [10.1128/MCB.24.9.3949-3956.2004](https://doi.org/10.1128/MCB.24.9.3949-3956.2004) PMID: [15082788](https://pubmed.ncbi.nlm.nih.gov/15082788/)
21. Qu X, Jia H, Garrity DM, Tompkins K, Batts L, et al. (2008) NdrG4 is required for normal myocyte proliferation during early cardiac development in zebrafish. *Dev Biol* 317: 486–496. doi: [10.1016/j.ydbio.2008.02.044](https://doi.org/10.1016/j.ydbio.2008.02.044) PMID: [18407257](https://pubmed.ncbi.nlm.nih.gov/18407257/)
22. Dupays L, Kotecha S, Angst B, Mohun TJ (2009) Tbx2 misexpression impairs deployment of second heart field derived progenitor cells to the arterial pole of the embryonic heart. *Dev Biol* 333: 121–131. doi: [10.1016/j.ydbio.2009.06.025](https://doi.org/10.1016/j.ydbio.2009.06.025) PMID: [19563797](https://pubmed.ncbi.nlm.nih.gov/19563797/)
23. Yamamoto H, Kokame K, Okuda T, Nakajo Y, Yanamoto H, et al. (2011) NDRG4 protein-deficient mice exhibit spatial learning deficits and vulnerabilities to cerebral ischemia. *J Biol Chem* 286: 26158–26165. doi: [10.1074/jbc.M111.256446](https://doi.org/10.1074/jbc.M111.256446) PMID: [21636852](https://pubmed.ncbi.nlm.nih.gov/21636852/)
24. Wang JF, Hill DJ (2009) Identification and action of N-myc downstream regulated gene 4 A2 in rat pancreas. *J Endocrinol* 201: 15–25. doi: [10.1677/JOE-08-0296](https://doi.org/10.1677/JOE-08-0296) PMID: [19193716](https://pubmed.ncbi.nlm.nih.gov/19193716/)
25. Zhou RH, Kokame K, Tsukamoto Y, Yutani C, Kato H, et al. (2001) Characterization of the human NDRG gene family: a newly identified member, NDRG4, is specifically expressed in brain and heart. *Genomics* 73: 86–97. doi: [10.1006/geno.2000.6496](https://doi.org/10.1006/geno.2000.6496) PMID: [11352569](https://pubmed.ncbi.nlm.nih.gov/11352569/)
26. Burgoyne RD, Morgan A (2003) Secretory granule exocytosis. *Physiol Rev* 83: 581–632. doi: [10.1152/physrev.00031.2002](https://doi.org/10.1152/physrev.00031.2002) PMID: [12663867](https://pubmed.ncbi.nlm.nih.gov/12663867/)
27. Tolar LA, Pallanck L (1998) NSF function in neurotransmitter release involves rearrangement of the SNARE complex downstream of synaptic vesicle docking. *J Neurosci* 18: 10250–10256. PMID: [9852562](https://pubmed.ncbi.nlm.nih.gov/9852562/)
28. Hwang WY, Fu Y, Reyon D, Maeder ML, Tsai SQ, et al. (2013) Efficient genome editing in zebrafish using a CRISPR-Cas system. *Nat Biotechnol* 31: 227–229. doi: [10.1038/nbt.2501](https://doi.org/10.1038/nbt.2501) PMID: [23360964](https://pubmed.ncbi.nlm.nih.gov/23360964/)
29. Kucenas S, Takada N, Park HC, Woodruff E, Broadie K, et al. (2008) CNS-derived glia ensheath peripheral nerves and mediate motor root development. *Nat Neurosci* 11: 143–151. doi: [10.1038/nn2025](https://doi.org/10.1038/nn2025) PMID: [18176560](https://pubmed.ncbi.nlm.nih.gov/18176560/)
30. Amor V, Feinberg K, Eshed-Eisenbach Y, Vainshtein A, Frechter S, et al. (2014) Long-term maintenance of Na⁺ channels at nodes of Ranvier depends on glial contact mediated by gliomedin and NrCAM. *J Neurosci* 34: 5089–5098. doi: [10.1523/JNEUROSCI.4752-13.2014](https://doi.org/10.1523/JNEUROSCI.4752-13.2014) PMID: [24719088](https://pubmed.ncbi.nlm.nih.gov/24719088/)
31. Hortsch M (2000) Structural and functional evolution of the L1 family: are four adhesion molecules better than one? *Mol Cell Neurosci* 15: 1–10. doi: [10.1006/mcne.1999.0809](https://doi.org/10.1006/mcne.1999.0809) PMID: [10662501](https://pubmed.ncbi.nlm.nih.gov/10662501/)
32. Salzer JL (2003) Polarized domains of myelinated axons. *Neuron* 40: 297–318. PMID: [14556710](https://pubmed.ncbi.nlm.nih.gov/14556710/)
33. Woods IG, Lyons DA, Voas MG, Pogoda HM, Talbot WS (2006) nsf is essential for organization of myelinated axons in zebrafish. *Curr Biol* 16: 636–648. doi: [10.1016/j.cub.2006.02.067](https://doi.org/10.1016/j.cub.2006.02.067) PMID: [16581508](https://pubmed.ncbi.nlm.nih.gov/16581508/)
34. Dutton KA, Pauliny A, Lopes SS, Elworthy S, Carney TJ, et al. (2001) Zebrafish colourless encodes sox10 and specifies non-ectomesenchymal neural crest fates. *Development* 128: 4113–4125. PMID: [11684650](https://pubmed.ncbi.nlm.nih.gov/11684650/)
35. Finsch M, Schreiner S, Kichko T, Reeh P, Tamm ER, et al. (2010) Sox10 is required for Schwann cell identity and progression beyond the immature Schwann cell stage. *J Cell Biol* 189: 701–712. doi: [10.1083/jcb.200912142](https://doi.org/10.1083/jcb.200912142) PMID: [20457761](https://pubmed.ncbi.nlm.nih.gov/20457761/)
36. Weider M, Kuspert M, Bischof M, Vogl MR, Hornig J, et al. (2012) Chromatin-remodeling factor Brg1 is required for Schwann cell differentiation and myelination. *Dev Cell* 23: 193–201. doi: [10.1016/j.devcel.2012.05.017](https://doi.org/10.1016/j.devcel.2012.05.017) PMID: [22814607](https://pubmed.ncbi.nlm.nih.gov/22814607/)
37. Gilmour DT, Maischein HM, Nusslein-Volhard C (2002) Migration and function of a glial subtype in the vertebrate peripheral nervous system. *Neuron* 34: 577–588. PMID: [12062041](https://pubmed.ncbi.nlm.nih.gov/12062041/)
38. Cazzola M, May A, Bergamaschi G, Cerani P, Rosti V, et al. (2000) Familial-skewed X-chromosome inactivation as a predisposing factor for late-onset X-linked sideroblastic anemia in carrier females. *Blood* 96: 4363–4365. PMID: [11110715](https://pubmed.ncbi.nlm.nih.gov/11110715/)
39. Pang CJ, Lemsaddek W, Alhashem YN, Bondzi C, Redmond LC, et al. (2012) Kruppel-like factor 1 (KLF1), KLF2, and Myc control a regulatory network essential for embryonic erythropoiesis. *Mol Cell Biol* 32: 2628–2644. doi: [10.1128/MCB.00104-12](https://doi.org/10.1128/MCB.00104-12) PMID: [22566683](https://pubmed.ncbi.nlm.nih.gov/22566683/)
40. Barry J, Gu Y, Jukkola P, O'Neill B, Gu H, et al. (2013) Ankyrin-G directly binds to kinesin-1 to transport voltage-gated Na⁺ channels into axons. *Dev Cell* 28: 117–131.

41. Zhang Y, Bekku Y, Dzhashiashvili Y, Armenti S, Meng X, et al. (2012) Assembly and maintenance of nodes of ranvier rely on distinct sources of proteins and targeting mechanisms. *Neuron* 73: 92–107. doi: [10.1016/j.neuron.2011.10.016](https://doi.org/10.1016/j.neuron.2011.10.016) PMID: [22243749](https://pubmed.ncbi.nlm.nih.gov/22243749/)
42. Wei C, Thatcher EJ, Olena AF, Cha DJ, Perdigoto AL, et al. (2013) miR-153 regulates SNAP-25, synaptic transmission, and neuronal development. *PLoS One* 8: e57080. doi: [10.1371/journal.pone.0057080](https://doi.org/10.1371/journal.pone.0057080) PMID: [23451149](https://pubmed.ncbi.nlm.nih.gov/23451149/)
43. Hines JH, Ravanello AM, Schwindt R, Scott EK, Appel B (2015) Neuronal activity biases axon selection for myelination in vivo. *Nat Neurosci* 18: 683–689. doi: [10.1038/nn.3992](https://doi.org/10.1038/nn.3992) PMID: [25849987](https://pubmed.ncbi.nlm.nih.gov/25849987/)
44. Mensch S, Baraban M, Almeida R, Czopka T, Ausborn J, et al. (2015) Synaptic vesicle release regulates myelin sheath number of individual oligodendrocytes in vivo. *Nat Neurosci* 18: 628–630. doi: [10.1038/nn.3991](https://doi.org/10.1038/nn.3991) PMID: [25849985](https://pubmed.ncbi.nlm.nih.gov/25849985/)
45. Milani DJ, Peterson TA, Ruskin JN, Peterson RT, MacRae CA (2003) Drugs that induce repolarization abnormalities cause bradycardia in zebrafish. *Circulation* 107: 1355–1358. PMID: [12642353](https://pubmed.ncbi.nlm.nih.gov/12642353/)
46. Newton-Cheh C, Eijgelsheim M, Rice KM, de Bakker PI, Yin X, et al. (2009) Common variants at ten loci influence QT interval duration in the QTGEN Study. *Nat Genet* 41: 399–406. doi: [10.1038/ng.364](https://doi.org/10.1038/ng.364) PMID: [19305406](https://pubmed.ncbi.nlm.nih.gov/19305406/)
47. Pfeufer A, van Noord C, Marcianti KD, Arking DE, Larson MG, et al. (2010) Genome-wide association study of PR interval. *Nat Genet* 42: 153–159. doi: [10.1038/ng.517](https://doi.org/10.1038/ng.517) PMID: [20062060](https://pubmed.ncbi.nlm.nih.gov/20062060/)
48. Pogoda HM, Sternheim N, Lyons DA, Diamond B, Hawkins TA, et al. (2006) A genetic screen identifies genes essential for development of myelinated axons in zebrafish. *Dev Biol* 298: 118–131. doi: [10.1016/j.ydbio.2006.06.021](https://doi.org/10.1016/j.ydbio.2006.06.021) PMID: [16875686](https://pubmed.ncbi.nlm.nih.gov/16875686/)
49. Edgeworth J, Freemont P, Hogg N (1989) Ionomycin-regulated phosphorylation of the myeloid calcium-binding protein p14. *Nature* 342: 189–192. doi: [10.1038/342189a0](https://doi.org/10.1038/342189a0) PMID: [2478889](https://pubmed.ncbi.nlm.nih.gov/2478889/)
50. Kawasaki F, Mattiuz AM, Ordway RW (1998) Synaptic physiology and ultrastructure in comatose mutants define an in vivo role for NSF in neurotransmitter release. *J Neurosci* 18: 10241–10249. PMID: [9852561](https://pubmed.ncbi.nlm.nih.gov/9852561/)
51. Mochida S, Westenbroek RE, Yokoyama CT, Zhong H, Myers SJ, et al. (2003) Requirement for the synaptic protein interaction site for reconstitution of synaptic transmission by P/Q-type calcium channels. *Proc Natl Acad Sci U S A* 100: 2819–2824. doi: [10.1073/pnas.262787699](https://doi.org/10.1073/pnas.262787699) PMID: [12601156](https://pubmed.ncbi.nlm.nih.gov/12601156/)
52. Stevens B, Tanner S, Fields RD (1998) Control of myelination by specific patterns of neural impulses. *J Neurosci* 18: 9303–9311. PMID: [9801369](https://pubmed.ncbi.nlm.nih.gov/9801369/)
53. Waxman SG (1997) Axon-glia interactions: building a smart nerve fiber. *Curr Biol* 7: R406–410. PMID: [9210363](https://pubmed.ncbi.nlm.nih.gov/9210363/)
54. Khvotchev MV, Ren M, Takamori S, Jahn R, Sudhof TC (2003) Divergent functions of neuronal Rab11b in Ca²⁺-regulated versus constitutive exocytosis. *J Neurosci* 23: 10531–10539. PMID: [14627637](https://pubmed.ncbi.nlm.nih.gov/14627637/)
55. Koudelka S, Voas MG, Almeida RG, Baraban M, Soetaert J, et al. (2016) Individual Neuronal Subtypes Exhibit Diversity in CNS Myelination Mediated by Synaptic Vesicle Release. *Curr Biol* 26: 1447–1455. doi: [10.1016/j.cub.2016.03.070](https://doi.org/10.1016/j.cub.2016.03.070) PMID: [27161502](https://pubmed.ncbi.nlm.nih.gov/27161502/)
56. Almeida RG, Lyons DA (2014) On the resemblance of synapse formation and CNS myelination. *Neuroscience* 276: 98–108. doi: [10.1016/j.neuroscience.2013.08.062](https://doi.org/10.1016/j.neuroscience.2013.08.062) PMID: [24035825](https://pubmed.ncbi.nlm.nih.gov/24035825/)
57. Li WM, Webb SE, Lee KW, Miller AL (2006) Recruitment and SNARE-mediated fusion of vesicles in furrow membrane remodeling during cytokinesis in zebrafish embryos. *Exp Cell Res* 312: 3260–3275. doi: [10.1016/j.yexcr.2006.06.028](https://doi.org/10.1016/j.yexcr.2006.06.028) PMID: [16876784](https://pubmed.ncbi.nlm.nih.gov/16876784/)
58. Benesh EC, Miller PM, Pfaltzgraff ER, Grega-Larson NE, Hager HA, et al. (2013) Bves and NDRG4 regulate directional epicardial cell migration through autocrine extracellular matrix deposition. *Mol Biol Cell* 24: 3496–3510. doi: [10.1091/mbc.E12-07-0539](https://doi.org/10.1091/mbc.E12-07-0539) PMID: [24048452](https://pubmed.ncbi.nlm.nih.gov/24048452/)
59. Park HC, Kim CH, Bae YK, Yeo SY, Kim SH, et al. (2000) Analysis of upstream elements in the HuC promoter leads to the establishment of transgenic zebrafish with fluorescent neurons. *Dev Biol* 227: 279–293. doi: [10.1006/dbio.2000.9898](https://doi.org/10.1006/dbio.2000.9898) PMID: [11071755](https://pubmed.ncbi.nlm.nih.gov/11071755/)
60. Tawk M, Makoukji J, Belle M, Fonte C, Trousson A, et al. (2011) Wnt/beta-catenin signaling is an essential and direct driver of myelin gene expression and myelinogenesis. *J Neurosci* 31: 3729–3742. doi: [10.1523/JNEUROSCI.4270-10.2011](https://doi.org/10.1523/JNEUROSCI.4270-10.2011) PMID: [21389228](https://pubmed.ncbi.nlm.nih.gov/21389228/)
61. Monk KR, Naylor SG, Glenn TD, Mercurio S, Perlin JR, et al. (2009) A G protein-coupled receptor is essential for Schwann cells to initiate myelination. *Science* 325: 1402–1405. doi: [10.1126/science.1173474](https://doi.org/10.1126/science.1173474) PMID: [19745155](https://pubmed.ncbi.nlm.nih.gov/19745155/)
62. Giustiniani J, Chambraud B, Sardin E, Dounane O, Guillemeau K, et al. (2014) Immunophilin FKBP52 induces Tau-P301L filamentous assembly in vitro and modulates its activity in a model of tauopathy. *Proc Natl Acad Sci U S A* 111: 4584–4589. doi: [10.1073/pnas.1402645111](https://doi.org/10.1073/pnas.1402645111) PMID: [24623856](https://pubmed.ncbi.nlm.nih.gov/24623856/)

Clonal analysis of gene loss of function and tissue-specific gene deletion in zebrafish via CRISPR/Cas9 technology

F. De Santis^a, V. Di Donato^a, F. Del Bene¹

PSL Research University, Paris, France

¹Corresponding author: E-mail: filippo.del-bene@curie.fr

CHAPTER OUTLINE

Introduction	172
Tissue-Specific Knockout in Animal Models	172
Clonal Analysis of Gene Loss of Function	173
State of the Art in Zebrafish Tissue-Specific Gene Inactivation	174
Clonal Analysis of Gene Inactivation in Zebrafish	175
1. Methods for Tissue-Specific Gene Inactivation and Clonal Analysis of Mutant Cells 175	
1.1 Rationale for the Design of a Vector System for CRISPR/Cas9-Induced Conditional Gene Disruption via Gal4/UAS	175
1.2 Experimental Workflow	176
1.2.1 Overview of the method	176
1.2.2 Technical procedure.....	176
1.3 Rationale for the Design of a Vector System for Clonal Analysis of Mutant Cells by Combining the Gal4/UAS With the Cre/loxP System	181
1.4 Experimental Workflow	182
1.5 Strategies for the Detection of Gene Loss of Function.....	182
1.5.1 Detection of protein loss in Cas9-expressing cells.....	182
1.5.2 Molecular assessment of the mutagenesis efficiency via fluorescence-activated cell sorting and genome locus sequencing	184
2. Discussion	185
References	186

^aThese two authors contributed equally to this work.

Methods in Cell Biology, Volume 135, ISSN 0091-679X, <http://dx.doi.org/10.1016/bs.mcb.2016.03.006>
© 2016 Elsevier Inc. All rights reserved.

Abstract

In the last few years the development of CRISPR/Cas 9-mediated genome editing techniques has allowed the efficient generation of loss-of-function alleles in several model organisms including zebrafish. However, these methods are mainly devoted to target-specific genomic loci leading to the creation of constitutive knock-out models. On the contrary, the analysis of gene function via tissue- or cell-specific mutagenesis remains challenging in zebrafish. To circumvent this limitation, we present here a simple and versatile protocol to achieve tissue-specific gene disruption based on the Cas9 expression under the control of the Gal4/upstream activating sequence binary system. In our method, we couple Cas9 with green fluorescent protein or Cre reporter gene expression. This strategy allows us to induce somatic mutations in genetically labeled cell clones or single cells, and to follow them *in vivo* via reporter gene expression. Importantly, because none of the tools that we present here are restricted to zebrafish, similar approaches are readily applicable in virtually any organism where transgenesis and DNA injection are feasible.

INTRODUCTION

TISSUE-SPECIFIC KNOCKOUT IN ANIMAL MODELS

The generation of transgenic animals carrying constitutive knockout alleles represents one of the most powerful approaches to investigate gene function. However, stable gene disruption can be linked to embryonic lethality, compensation mechanisms, and pleiotropic phenotypes that might limit the analysis of mutant animals. In these cases, the possibility of inducing targeted mutagenesis in a precisely controlled spatiotemporal manner represents a great advantage in reverse genetic studies. To date, different strategies have been developed to induce tissue-specific loss of function in diverse model organisms. The golden standard techniques for conditional mutagenesis in mouse and fruit fly (*Drosophila melanogaster*) rely on the Cre/loxP and flippase (Flp)/flippase recognition target (FRT) systems (Bouabe & Okkenhaug, 2013; Theodosiou & Xu, 1998). The first approach applies homologous recombination techniques to generate animals carrying a floxed target allele, in which loxP sites are inserted at the 5' and 3' ends of the selected locus. Cre recombinase catalyzes site-specific recombination events in genomic regions containing loxP sites and can be used to excise the floxed target allele, generating gene inactivation. By crossing animals carrying a floxed sequence to driver lines in which Cre expression is controlled by a tissue-specific promoter, it is possible to induce the excision of the target locus in the desired cell population, allowing for the generation of conditional gene disruption (Kuhn, Schwenk, Aguet, & Rajewsky, 1995). A modified version of the Cre enzyme, in which the recombinase is fused to the estrogen receptor (Cre-ER), allows tamoxifen-induced temporal control of Cre activity (Feil et al., 1996). The Flp/FRT technology is an analogous strategy based on the activity of the Flp enzyme, catalyzing site-directed recombination of DNA

sequences flanked by FRT sites (Choi et al., 2009; Golic & Lindquist, 1989). Most recently, CRISPR (clustered regularly interspaced short palindromic repeats)/Cas (CRISPR-associated)—based approaches have been introduced to generate tissue-specific loss of function. The system is based on the combined activity of two components: a single guide RNA (sgRNA) containing 20 nucleotides complementary to the target genomic sequence and the Cas9 endonuclease catalyzing double-strand breaks (DSBs) at the targeted locus. In addition to the efficient generation of constitutive mutant alleles (produced by the imperfect DNA repair mechanisms occurring after Cas9-induced cleavage), the CRISPR/Cas9 technique has been used to insert loxP sites at the desired loci, thus generating floxed alleles for Cre-based conditional mutagenesis (Yang et al., 2013). In addition, it has been shown that it is possible to induce conditional knockout by coupling inducible expression of the *Cas9* enzyme with constitutive expression of sgRNAs (driven by U6 promoters recognized by type III RNA polymerase). In mouse, the generation of a floxed *Cas9* allele (in which a *loxP-STOP-loxP* cassette is placed between a constitutive CAG promoter and the coding sequence (CDS) of the endonuclease) has been used to achieve Cre-dependent spatiotemporal regulation of *Cas9* expression (Platt et al., 2014). Similarly, control of *Cas9* activity was obtained in *Drosophila* by using the Gal4/upstream activating sequence (UAS) binary system (Port, Chen, Lee, & Bullock, 2014). In this strategy, the use of a tissue-specific promoter to drive the transcription of the Gal4 transactivator enables conditional activation of the *Cas9* enzyme, whose expression is controlled by the UAS recognized by Gal4.

CLONAL ANALYSIS OF GENE LOSS OF FUNCTION

To further improve the resolution of loss-of-function studies it is possible to manipulate gene activity in individual cells or single-cell clones and analyze the resulting phenotype within an otherwise wild-type tissue. Different strategies have been developed to generate chimeric animals in which the fate of clones derived from a mutant progenitor can be followed in a wild-type environment. In mouse, homozygous mutant embryonic stem cells, carrying the desired mutation together with an independent genetic marker, can be transplanted into host wild-type blastocysts to give rise to chimeric animals (Rossant & Spence, 1998). Similarly, transplantation strategies can be performed in *Drosophila* by introducing cells derived from a mutant donor embryo into wild-type hosts (Technau & Campos-Ortega, 1986). Nevertheless, transplantation-based approaches are often technically challenging and can only be applied to the analysis of genes acting early in development. Alternative methods are based on the Cre/loxP system and offer the possibility of inducing both targeted gene disruption and activation of a reporter for lineage tracing of mutant cells (Nakazawa, Taniguchi, Okumura, Maeda, & Matsuno, 2012; Zong, Espinosa, Su, Muzumdar, & Luo, 2005). In *Drosophila* multiple strategies have been developed over the years to generate marked clones in genetic mosaics combining

the flexibility of Gal4/UAS and Flp/FRT systems (Griffin, Binari, & Perrimon, 2014). Lately, a novel CRISPR-based strategy has been proposed in mouse. The technique takes advantage of in utero electroporation of a CRISPR-based plasmid to obtain gene inactivation together with a Piggybac transposase vector to express fluorescent reporters for lineage tracing of cells with loss-of-function mutations (Chen, Rosiene, Che, Becker, & LoTurco, 2015).

STATE OF THE ART IN ZEBRAFISH TISSUE-SPECIFIC GENE INACTIVATION

Despite the introduction in the last years of multiple approaches to induce targeted mutagenesis in the zebrafish genome, spatiotemporal control of gene inactivation remains challenging. Strategies based on the already described Cre/loxP and Flp/FRT systems have been also developed in zebrafish to achieve tissue-specific gene disruption (Ni et al., 2012). In this case, the generation of conditional alleles is induced by transgenic insertion of an inverted gene-trap cassette in an intronic region of a gene. Because the mutagenicity of the transgene is orientation dependent, Cre- and Flp-mediated recombination enables a switch from a state of conditional rescue in one orientation to a state of conditional knockout in the other. Nevertheless, the targeting of a precise locus is not possible with this method that relies on random transgene integration. More recently to circumvent this limitation, several techniques based on the TALEN or CRISPR/Cas9 systems have been established to introduce DNA fragments of variable size at predefined genomic locations (Auer & Del Bene, 2014). Among the different applications of these genome editing approaches, the efficient insertion of loxP sites in a targeted fashion has been achieved via TALEN-mediated DSB and subsequent homology-directed repair (Bedell et al., 2012). Although such a tool allows the creation of conditional alleles, the long generation time of zebrafish transgenic lines carrying stable genomic integrations of floxed alleles represents an important constraint. An alternative way to inactivate target genes in a tissue-specific manner has been developed by combining the CRISPR/Cas9 and Tol2 technologies (Ablain, Durand, Yang, Zhou, & Zon, 2015). In this report, a modular construct provides cell-type-specific expression of the Cas9 endonuclease (*Tissue-specific promoter:cas9*) and ubiquitous transcription of the sgRNA by a U6 promoter (*U6:sgRNA*). While mosaic phenotypes can be induced by transient expression of the plasmid, its inclusion into the genome by Tol2 transposition results in higher levels of tissue-restricted gene inactivation. The versatility of the vector system relies on the possibility to readily change the promoter driving *Cas9* transcription and the sgRNA to target a specific open reading frame (ORF) to obtain spatially controlled gene loss of function. A similar approach has been proposed lately to achieve also a tight temporal regulation of Cas9 expression (Yin et al., 2015). This methodology is based on the generation of two transgenic lines: one carries a transgene allowing heat-shock induction of Cas9 expression after Cre mRNA injection (*hp70:loxP-mCherry-STOP-loxP-cas9*); the

other harbors U6 cassettes for the transcription of sgRNAs (*U6:sgRNA*). Therefore, double carriers would show tissue-specific phenotypes subsequent to heat-shock and Cre activation.

CLONAL ANALYSIS OF GENE INACTIVATION IN ZEBRAFISH

CRISPRs-based methods for conditional mutagenesis represent a valid alternative to Cre- and Flp-mediated techniques. However, to date, their application has been limited to the induction and the analysis of tissue-specific gene disruption resulting in visually detectable phenotypes. In fact, genetic labeling of mutant cells, required for the examination of phenotypes that are not readily detectable, is not addressed by these systems.

In this chapter, we present two approaches that combine the Gal4/UAS (Asakawa & Kawakami, 2008) and CRISPR/Cas9 systems in order to induce simultaneously cell-type-specific locus inactivation and fluorescent marking of the targeted cells (Di Donato et al. *Genome Research Accepted*). The first strategy that we describe permits the identification of *Cas9*-expressing cells by concomitant expression of the green fluorescent protein (GFP) and Cas9, both driven by the activation of a UAS sequence (*UAS:Cas9T2AGFP*). Thus, GFP-positive cells can be detected in the spatiotemporal domain of Gal4 expression, which is defined by a chosen tissue-specific promoter. The second strategy provides a tool that enables both the permanent labeling of *Cas9*-expressing cells and the visualization of their clonal progeny, through UAS-dependent coexpression of the Cas9 endonuclease and Cre recombinase (*UAS:Cas9T2ACre*).

For both methods, the vector system used contains two U6 promoters allowing the simultaneous targeting of two sequences at any genomic locus of interest, to increase the percentage of out-of-frame mutations and large deletions.

1. METHODS FOR TISSUE-SPECIFIC GENE INACTIVATION AND CLONAL ANALYSIS OF MUTANT CELLS

1.1 RATIONALE FOR THE DESIGN OF A VECTOR SYSTEM FOR CRISPR/Cas9-Induced Conditional Gene Disruption via Gal4/UAS

CRISPR/Cas9-mediated tissue-specific gene inactivation and concomitant visualization of mutant cells requires: (1) spatiotemporal regulation of the expression of the Cas9 endonuclease; (2) expression of sgRNAs; (3) a fluorescent transgene to label cells where Cas9/sgRNA complex is present. The cell-type-specific expression of the Cas9 enzyme is achieved by using the yeast Gal4/UAS system in which the Gal4 transcriptional activator drives the expression of transgenes linked to the UAS. In our vector design, the CDS of the Cas9, flanked by two SV40 nuclear localization signals, is placed downstream of a 5xUAS cassette. To monitor *Cas9*

expression, we use a viral T2A self-cleaving peptide followed by the GFP CDS enabling the synthesis of the fluorescent reporter from the same transcript (*UAS:Cas9T2AGFP*). Two U6 promoters are subcloned in the same construct to drive ubiquitous transcription of the sgRNAs. BsmBI and BsaI restriction sites allow the cloning of the 20-bp target sequence at the transcription start site (TSS = +1) of the U6 promoters (Figs. 1A and 2). The vector contains Tol2 sites for efficient transposition of the transgenic cassette in the fish genome.

1.2 EXPERIMENTAL WORKFLOW

1.2.1 Overview of the method

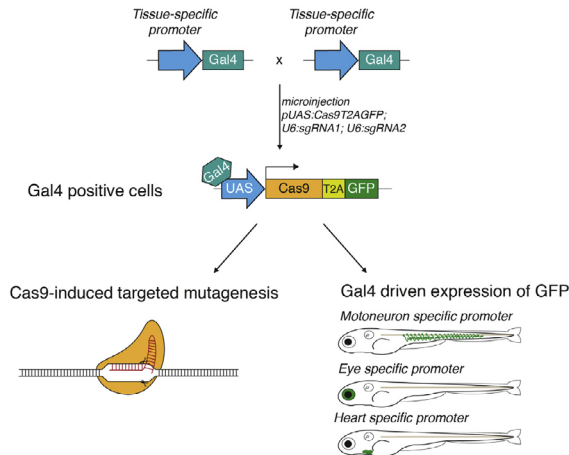
The induction of conditional gene inactivation via the Gal4/UAS system consists of three steps. Step 1: design of sgRNAs targeting the genomic locus of interest and assessment of their mutagenesis efficiency. Step 2: cloning of the target sequences of the sgRNAs displaying the highest mutation rate at the TSS of the U6 promoters in the *pUAS:Cas9T2AGFP* plasmid (Fig. 1C and D). Step 3: microinjection of *pUAS:Cas9T2AGFP;U6:sgRNA1;U6:sgRNA2* plasmid for transient expression or generation of a transgenic line carrying stable genomic integration of the cassette (Fig. 1E).

1.2.2 Technical procedure

Step 1: Design of sgRNAs targeting the genomic locus of interest and assessment of their mutagenesis efficiency

sgRNA design

- Select a target site for sgRNA synthesis by using one of the available online tools (ie, <http://crispor.tefor.net/crispor.cgi>; <http://crispr.mit.edu/>; <http://zifit.partners.org/ZiFiT/>; <http://www.broadinstitute.org/rnai/public/analysis-tools/sgrna-design>; <https://chopchop.rc.fas.harvard.edu/>; <http://www.crisprscan.org/>; <http://crispr.cos.uni-heidelberg.de/help.html>).
- Filter the research for oligonucleotides suitable for cloning at the TSS of the T7 in the pDR274 vector (Addgene ref 42250).
 - Oligonucleotides cloning in the pDR274 vector*
 - Digest 1–5 µg of the pDR274 plasmid with BsaI overnight at 37°C.
 - Run the digestion product on a 0.8% agarose gel and extract the linear plasmid with a gel and polymerase chain reaction (PCR) extraction kit.
 - Mix 3 µL of 100 µM forward and reverse oligonucleotides containing the target sequence and add 14 µL of TE buffer (10 mM Tris-Cl, pH 7.5. 1 mM EDTA).
 - Heat the mixture 10 min at 95°C and cool down for 30 min at room temperature to allow the annealing of the oligonucleotides.
 - Ligate 2 µL of annealed oligonucleotides and 100 ng of the digested pDR274 plasmid.
 - Transform the reaction in DH5α competent cells.

**FIGURE 2**

Schematic of conditional gene inactivation and genetic labeling of *Cas9*-expressing cells after injection of the *pUAS:Cas9T2AGFP;U6sgRNA1;U6sgRNA2* plasmid in specific Gal4 driver lines.

- Plate on LB (Lysogeny broth)-kanamycin plates.
- The next day, pick two colonies from the transformation plate. Inoculate each colony into 2 mL of LB-kanamycin medium and incubate at 37°C overnight with agitation.
- Isolate DNA using a Miniprep kit.
- Sequence the plasmid with M13 forward primer to verify the presence of the target sequence.
 - sgRNA in vitro synthesis*
- Use the pDR274 plasmid containing the target sequence as template for a PCR reaction with the primers:
 - Fw oligo: 5'-GCTCGTCCTGAATGATATGCGACC-3'
 - Rev oligo: 5'-CCAGTAGTGATCGACACTGCTCG-3'
- Set up the PCR reaction as follows:
 - pDR274 template: 10 ng
 - 5X buffer HF: 10 µL
 - dNTP (10 mM): 1 µL
 - Primers (10 µM): 2.5 µL each
 - DMSO: 1.5 µL
 - Phusion polymerase: 0.5 µL
 - H₂O up to 50 µL

Use the program:

98° 30 s
 –
 98° 30 s
 58° 20 s } ×35
 72° 20 s
 –
 72° 5 min

The expected size of the band is 253 bp.

The PCR product will contain a T7 promoter sequence and the sgRNA sequence.

- Gel purify the amplicon and elute in 20 µL. The PCR product will be used as template for the sgRNA synthesis.
 - Proceed with sgRNA synthesis using the MegaScript T7 kit (AMBION—AM1334) assembling the reaction in a final volume of 20 µL as described below:
 - 8 µL of PCR product
 - +2 µL 10X transcription buffer
 - +2 µL of each NTP
 - +2 µL of T7 RNA polymerase
 - Transcribe for 4 h at 37°C.
 - Add 1 µL of TurboDNase: 15 min 37°C.
 - Recover RNA with RNA purification with RNeasy Mini Kit (QIAGEN—74104) according to the manufacturer's instructions and perform a double elution with 30 µL of water (Rnase/Dnase free).
 - Check the quality of the sgRNA on a 2% agarose gel and with a spectrophotometer.
 - Microinjection of sgRNA in fish embryos*
 - Prepare injection solution as follows:
 - 300 ng/µL sgRNA
 - 25 µM Cas9 protein (NEB-M0386M or an equivalent homemade protein)
 - 1X Cas9 10X buffer
 - H₂O
 - Inject 1 nL of solution into one-cell—stage wild-type embryos.
 - Estimation of the mutagenesis rate*
 - Perform genomic extraction on a pool of 25 injected embryos.
 - Amplify by PCR the genomic locus containing the sequence targeted by sgRNAs used.
 - Clone PCR amplicons into the pCRII-TOPO (Zero Blunt TOPO PCR Cloning Kit, ThermoFisher Scientific—K2800-02) vector and sequence DNA recovered from 20 colonies.
 - The frequency of insertion and deletion (indel) mutations at the targeted locus is estimated by comparison with the wild-type allele.
- Step 2: Generation of pUAS:CAS9T2AGFP;U6:sgRNA1;U6:sgRNA2 construct

Design of the oligonucleotides for cloning at the TSS of U6 promoters

Two U6 promoters flank the *UAS:CAS9T2AGFP* cassette. They contain at the +1 position restriction sites for BsaI and BsmBI suitable for the cloning of desired target sequences. U6 promoters require transcription to start with a guanine nucleotide (G). Design the oligonucleotides as follows:

BsaI site (Fig. 1C):

For a target sequence starting with a G add the overhang CTC- to the 5' of the 20-nt target and the AAAC- overhang to the 5' of the reverse complement of the last 19 nt of the target (removing the final C).

Example:

Target: 5'-GCAGATACACATACAGATAC-3'

Fw oligo: 5'-CTCGCAGATACACATACAGATAC -3'

Rev oligo: 5'-AAACGTATCAGTATGTGTATCTG- 3'

For a target sequence not starting with a G substitute the first nucleotide with a G and proceed as previously described.

Example:

Target: 5'-CAGATACACATACAGATACA-3'

Fw oligo: 5'-CTCGAGATACACATACAGATACA -3'

Rev oligo: 5'-AAACTGTATCAGTATGTGTATCT- 3'

BsmBI site (Fig. 1D):

For a target sequence starting with a G add the overhang AGCTC- to the 5' of the 20-nt target and the TAAAC- overhang to the 5' of the reverse complement of the 20-nt target.

Example:

Target: 5'-GCAGATACACATACAGATAC-3'

Fw oligo: 5'-AGCTCGCAGATACACATACAGATAC -3'

Rev oligo: 5'-TAAACGTATCAGTATGTGTATCTGC- 3'

For a target sequence not starting with a G substitute the first nucleotide with a G and proceed as previously described.

Example:

Target: 5'-CAGATACACATACAGATACA-3'

Fw oligo: 5'-AGCTCGAGATACACATACAGATACA -3'

Rev oligo: 5'-TAAACTGTATCAGTATGTGTATCTC- 3'

Oligonucleotides cloning in the pUAS:CAS9T2AGFP;U6:sgRNA1;U6:sgRNA2 vector (Fig. 1C and D)

- Digest 1–2 µg of the pUAS:CAS9T2AGFP;U6:sgRNA1;U6:sgRNA2 vector with BsaI overnight at 37°C.
- Run the digestion product on a 0.8% agarose gel and extract the linear plasmid with a gel extraction kit.
- Mix 3 µL of 100 µM forward and reverse oligonucleotides containing the target sequence and overhangs for BsaI cloning and add 14 µL of TE buffer.
- Heat the mixture 10 min at 95°C and cool down for 30 min at room temperature to allow the annealing of the oligonucleotides.
- Ligate 2 µL of annealed oligonucleotides and 100 ng of the digested pUAS:CAS9T2AGFP;U6:sgRNA1;U6:sgRNA2 plasmid (Fig. 1C).

- Transform the reaction in TOP10 competent cells (ThermoFisher Scientific—K2800-02).
- Plate on LB-ampicillin plates
- The next day, pick two colonies from the transformation plate. Inoculate each colony into 2 ml of LB-ampicillin medium and incubate at 37°C overnight with agitation.
- Purify DNA using a miniprep kit
- Sequence the plasmid with T7 specific primer to verify the presence of the target sequence
- Repeat the entire process with BsmBI enzyme using oligonucleotides containing overhangs for BsmBI cloning (Fig. 1D), digesting the plasmid where the first target sequence at the BsaI site has already been inserted.
- Sequence the plasmid for correct insertion of the Sp6 specific primer.

Step 3: Establishing tissue-specific gene inactivation (Fig. 1E and 2)

Microinjection of pUAS:CAS9T2AGFP;U6:sgRNA1;U6:sgRNA2 plasmid

- Choose a specific Gal4 driver line based on the population of cells where gene function needs to be analyzed.
- Set up mating couples of the chosen Gal4 transgenic line.
- Prepare the injection mix as described:
 - 30 ng/μL of pUAS:CAS9T2AGFP;U6:sgRNA1;U6:sgRNA2 construct
 - +50 ng/μL of Tol2 mRNA
 - +RNase, DNase-free water up to 5 μL
- Inject with pUAS:CAS9T2AGFP;U6:sgRNA1;U6:sgRNA2 into one-cell-stage embryos from an incross of a *Tg(Tissue-specific:Gal4)* line.
- Screen embryos with GFP-positive cells in the expected Gal4 expression pattern.
- If a stable *UAS:CAS9T2AGFP;U6:sgRNA1;U6:sgRNA2* is needed, raise the embryos to adulthood after injection in wild-type embryos.
- Screen for F0 adults carrying the transgene in the germline and cross them with the chosen Gal4 transgenic line.

1.3 RATIONALE FOR THE DESIGN OF A VECTOR SYSTEM FOR CLONAL ANALYSIS OF MUTANT CELLS BY COMBINING THE Gal4/UAS WITH THE CRE/LOXP SYSTEM

The use of a GFP reporter to mark *Cas9*-expressing cells allows for the phenotypic analysis of potentially mutant cells during the time span of activity of the promoter driving Gal4 transcription. Long-term tracking of these cells needs a strategy to permanently mark the cells displaying a loss-of-function phenotype. To stably label the population of *Cas9*-expressing cells, we replaced the GFP CDS in the pUAS:CAS9T2AGFP;U6:sgRNA1;U6:sgRNA2 with the ORF of the Cre recombinase (Fig. 1B). Thus, potentially mutant cells can be visualized by using fish lines carrying a transgene where a ubiquitous promoter drives the expression of a fluorescent reporter upon Cre-mediated excision of a floxed STOP sequence. The tissue-specific

promoter regulating Gal4 transcription guarantees synchronized translation of Cas9 and Cre enzymes from the same mRNA, ensuring targeted mutagenesis at the chosen genomic locus and expression of the floxed reporter within the same cell. The fluorescence of the reporter will be stable throughout the entire life of the fish and, most importantly, will be inherited in all the cells deriving from the same *Cas9*-expressing progenitor (Fig. 3). Our strategy, named 2C-Cas9 (Cre-mediated recombination for Clonal analysis of **Cas9** mutant cells) offers the possibility to induce site-specific mutagenesis in a selected cell population and, at the same time, enables genetic labeling of the clones derived from the targeted cells (Di Donato et al. *Genome Research accepted*).

1.4 EXPERIMENTAL WORKFLOW

The procedures for the cloning of the target sequences in the plasmid and for the microinjection of the resulting transgenesis vector have been previously described and are summarized in Fig. 1C,D and F. The injection of the pUAS:*CAS9T2ACre*; *U6:sgRNA1*; *U6:sgRNA2* plasmid is done in a cross between the selected Gal4 driver line and a transgenic line carrying a floxed allele. Different floxed lines can be used (Di Donato et al. *Genome Research accepted*; Bertrand et al., 2010; Hans et al., 2011; Mosimann et al., 2011).

1.5 STRATEGIES FOR THE DETECTION OF GENE LOSS OF FUNCTION

By using the 2C-Cas9 approach, all the *Cas9*-expressing cells can be identified by the expression of a fluorescent reporter. Nevertheless, the marked cells will represent a heterogeneous population in which each cell (or clone) will have independently induced mutations (some of them might not be out-of-frame mutations). To simplify the statistical analysis of the phenotypes arising from 2C-Cas9-mediated targeted gene disruption it is necessary to evaluate the proportion of mutant cells within the labeled population.

1.5.1 Detection of protein loss in *Cas9*-expressing cells

The most direct approach to identify the cells carrying *null* mutations is to perform immunohistochemistry (IHC) experiments by using an antibody recognizing the protein encoded by the targeted gene. This strategy requires a double staining to detect simultaneously the fluorescent reporter linked to *Cas9* expression and the protein coded by the targeted locus. The absence of colocalization will reveal efficient gene disruption.

1.5.1.1 Protocol for IHC on whole mount embryos

- Fix embryos in 4% paraformaldehyde in 1X PBS (pH 7.4) for 2 h at room temperature or overnight at 4°C.
- Wash three times in 1X PBS/0.1% Tween-20 (PBS-Tw), for 5 min each time.
- Incubate for 20 min in ice-cold acetone.

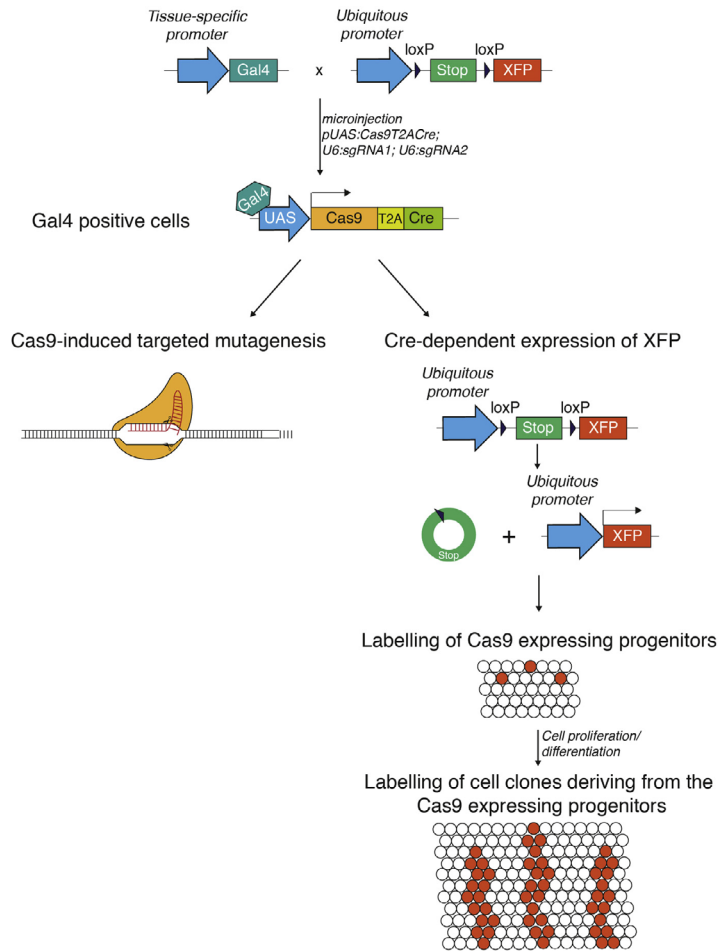


FIGURE 3
Schematic of tissue-specific gene disruption and permanent clonal labeling of Cas9-expressing cells after injection of the *pUAS:Cas9T2ACre;U6sgRNA1;U6sgRNA2* plasmid in a cross of a specific Gal4 driver to a floxed reporter line (2C-Cas9). (See color plate)

- Rehydrate in three steps (75%; 50%; 25% acetone in PBS).
- Wash twice in PBS-Tw, 5 min each.
- Incubate with 1 mg/mL collagenase diluted in PBS according to the stage (1 dpf, day post fertilization: 10 min; 2 dpf: 20 min; 3 dpf: 75 min; 4 and 5 dpf: 120 min).
- Wash three times in PBS-Tw, 5 min each.
- Incubate for 1 h at room temperature in blocking solution (2% BSA; 0.5% Triton-X100 in PBS).
- Wash three times in PBS-Tw, 5 min each.
- Incubate overnight at 4°C with primary antibodies diluted in blocking solution at the appropriate concentrations.
- Wash three times in PBS-Tw, 5 min each.
- Incubate overnight at 4°C with secondary antibodies diluted in blocking solution at the appropriate concentrations.
- Wash three times in PBS-Tw, 5 min each.
- Mount for imaging in 1% low-melting agarose.

1.5.1.2 Protocol for IHC on cryosections

- Fix embryos in 4% paraformaldehyde in 1X PBS (pH 7.4) for 2 h at room temperature or overnight at 4°C.
- Incubate overnight in 30% sucrose; 0.02% sodium azide; PBS solution.
- Embed the embryos in Tissue-Tek O.C.T. compound after removal of the sucrose and place the resulting blocks on dry ice before sectioning.
- Section the blocks with a thickness of 14 µm and mount the sections on Fisherbrand Superfrost plus slides (No 12-550-15).
- Wash twice in PBS-Tw, 5 min each time.
- Incubate for 1 h at room temperature in blocking solution (10% normal goat serum in PBS-Tw).
- Incubate overnight at 4°C with primary antibodies diluted in blocking solution.
- Wash three times in PBS-Tw, 5 min each.
- Incubate for 2 h with secondary antibodies diluted in blocking solution.
- Wash five times in PBS-Tw, 5 min each.
- Add Vectashield drops on the sections and place coverslips on the slides.

1.5.2 Molecular assessment of the mutagenesis efficiency via fluorescence-activated cell sorting and genome locus sequencing

The molecular assessment of the mutagenesis efficiency of the 2C-Cas9 system in the selected Gal4 line requires the isolation of the fluorescent *Cas9*-expressing cells. Fluorescence-activated cell sorting (FACS) might be used to isolate the marked *Cas9*-expressing cells from the wild-type nonfluorescent cell population. After separation, total DNA can be extracted from the two pools of cells and the targeted locus can be analyzed to screen for the presence and the frequency of out-of-frame mutations.

1.5.2.1 Protocol for FACS

- Dissociate the embryos ($n > 200$) as previously described by [Manoli & Driever \(2012\)](#).
- Perform cell sorting and collect cells in lysis buffer (E.G. NucleoSpin Tissue kit; Macherey–Nagel—740952.10).
- Extract genomic DNA following kit instructions.
- PCR amplify the targeted genomic loci.
- Clone PCR amplicons into the pCR-bluntII-TOPO vector.
- Isolate plasmid DNA from single colonies.
- Sequence the plasmids and identify mutant alleles by comparison with the wild-type sequence.

2. DISCUSSION

In this chapter we describe a new tool allowing, with a single plasmid injection, both conditional mutagenesis and lineage tracing of potentially mutant cells. The flexibility of the approach is based on the use of the Gal4/UAS system to drive *Cas9* expression. Many Gal4 driver transgenic lines showing diverse cell-type-specific expression patterns are available to the zebrafish community. The transient or stable UAS-dependent expression of *Cas9*, coupled with constitutive transcription of gene-specific sgRNAs, allows the inactivation of any gene of interest in any Gal4 line. Therefore, gene disruption can be achieved in multiple tissues by generating a unique transgenesis vector, containing gene-specific sgRNA, to be injected into different Gal4 driver lines. Unambiguous identification of cells displaying loss-of-function phenotypes is provided by the expression of a reporter gene (GFP or Cre) together with Cas9 endonuclease. While GFP fluorescence enables visualization of *Cas9*-expressing cells during the activity time window of the chosen Gal4 line, the use of Cre allows permanent labeling and clonal analysis of potentially mutated cells even after *Gal4* expression has terminated. Both methods represent a valuable alternative to laborious transplantation experiments that represent, to date, the only method to analyze cell-autonomous behavior of mutant cells in a wild-type genetic background. Furthermore, the analysis of genetic chimeras resulting from transplantations is restricted to early phenotypes and does not allow the investigation of the role of genes and pathways that are used repeatedly during development. If well established, Cre/loxP-based approaches for conditional gene inactivation in zebrafish would overcome these issues. Nevertheless they would need long generation time and are currently limited by the low efficiency of homologous recombination-based genomic manipulations.

Although the system described here is useful to score conditional loss-of-function phenotypes by using genetic fluorescent labeling, it does not mark exclusively populations of cells carrying *null* alleles but all *Cas9*-expressing cells. Because this is a mixed population of cells, only a percentage will harbor out-of-frame mutations.

We propose to discriminate mutant from wild-type cells by performing immunofluorescence experiments to detect loss of protein by the targeted gene at a single-cell level. Alternatively, molecular analysis of gene disruption can be performed, after DNA extraction from FACS-sorted fluorescent cells, to estimate the proportion of truly mutant cells within the labeled population.

Several parameters need to be considered to obtain highly penetrant tissue-specific phenotypes by using the 2C-Cas9 system. The selection of sgRNA displaying efficient mutagenesis rates is crucial to successfully induce DSBs at the target genomic locus. In addition, to achieve loss of function in the cases where indel mutations do not disrupt the ORF of the targeted gene, designing of sgRNAs targeting essential functional domains of a protein can be advantageous. The injection of our vector system into a heterozygous mutant background, where one allele carries a *null* mutation, represents another way to enhance the efficiency of gene disruption. Furthermore, the use of a strong Gal4 driver line, leading to a high intracellular expression of Cas9 endonuclease levels, is recommended. In the future, additional improvements in the *Cas9* expression cassette may be needed. A possibility could be the incorporation into our vector system of noncoding elements of the zebrafish genome that have been shown to boost expression of transgenes in UAS-based plasmids (Horstick et al., 2015).

The strategy presented in this chapter can be widely applied for the analysis of gene function in single cells or in clonal populations, from larval stage to adulthood. The genetic labeling of potentially mutant cells generated by the 2C-Cas9 method provides a versatile technique to correlate phenotype and genotype, a challenge that cannot be addressed with other currently available genetic tools in zebrafish.

REFERENCES

- Ablain, J., Durand, E. M., Yang, S., Zhou, Y., & Zon, L. I. (2015). A CRISPR/Cas9 vector system for tissue-specific gene disruption in zebrafish. *Developmental Cell*, 32(6), 756–764. <http://dx.doi.org/10.1016/j.devcel.2015.01.032>.
- Asakawa, K., & Kawakami, K. (2008). Targeted gene expression by the Gal4-UAS system in zebrafish. *Development, Growth & Differentiation*, 50(6), 391–399. <http://dx.doi.org/10.1111/j.1440-169X.2008.01044.x>. pii:DGD1044.
- Auer, T. O., & Del Bene, F. (2014). CRISPR/Cas9 and TALEN-mediated knock-in approaches in zebrafish. *Methods*. <http://dx.doi.org/10.1016/j.ymeth.2014.03.027>.
- Bedell, V. M., Wang, Y., Campbell, J. M., Poshusta, T. L., Starker, C. G., Krug, R. G., 2nd, ... Ekker, S. C. (2012). In vivo genome editing using a high-efficiency TALEN system. *Nature*, 491(7422), 114–118. <http://dx.doi.org/10.1038/nature11537>.
- Bertrand, J. Y., Chi, N. C., Santoso, B., Teng, S., Stainier, D. Y., & Traver, D. (2010). Haematopoietic stem cells derive directly from aortic endothelium during development. *Nature*, 464(7285), 108–111. <http://dx.doi.org/10.1038/nature08738>.
- Bouabe, H., & Okkenhaug, K. (2013). Gene targeting in mice: a review. *Methods in Molecular Biology*, 1064, 315–336. http://dx.doi.org/10.1007/978-1-62703-601-6_23.

- Chen, F., Rosiene, J., Che, A., Becker, A., & LoTurco, J. (2015). Tracking and transforming neocortical progenitors by CRISPR/Cas9 gene targeting and piggyBac transposase lineage labeling. *Development*, *142*(20), 3601–3611. <http://dx.doi.org/10.1242/dev.118836>.
- Choi, C. M., Vilain, S., Langen, M., Van Kelst, S., De Geest, N., Yan, J., ... Hassan, B. A. (2009). Conditional mutagenesis in *Drosophila*. *Science*, *324*(5923), 54. <http://dx.doi.org/10.1126/science.1168275>.
- Feil, R., Brocard, J., Mascrez, B., LeMeur, M., Metzger, D., & Chambon, P. (1996). Ligand-activated site-specific recombination in mice. *Proceedings of the National Academy of Sciences of the United States of America*, *93*(20), 10887–10890. Retrieved from <http://www.ncbi.nlm.nih.gov/pubmed/8855277>.
- Golic, K. G., & Lindquist, S. (1989). The FLP recombinase of yeast catalyzes site-specific recombination in the *Drosophila* genome. *Cell*, *59*(3), 499–509. Retrieved from <http://www.ncbi.nlm.nih.gov/pubmed/2509077>.
- Griffin, R., Binari, R., & Perrimon, N. (2014). Genetic odyssey to generate marked clones in *Drosophila* mosaics. *Proceedings of the National Academy of Sciences of the United States of America*, *111*(13), 4756–4763. <http://dx.doi.org/10.1073/pnas.1403218111>.
- Hans, S., Freudenreich, D., Geffarth, M., Kaslin, J., Machate, A., & Brand, M. (2011). Generation of a non-leaky heat shock-inducible Cre line for conditional Cre/lox strategies in zebrafish. *Developmental Dynamics*, *240*(1), 108–115. <http://dx.doi.org/10.1002/dvdy.22497>.
- Horstick, E. J., Jordan, D. C., Bergeron, S. A., Tabor, K. M., Serpe, M., Feldman, B., & Burgess, H. A. (2015). Increased functional protein expression using nucleotide sequence features enriched in highly expressed genes in zebrafish. *Nucleic Acids Research*, *43*(7), e48. <http://dx.doi.org/10.1093/nar/gkv035>.
- Kuhn, R., Schwenk, F., Aguet, M., & Rajewsky, K. (1995). Inducible gene targeting in mice. *Science*, *269*(5229), 1427–1429. Retrieved from <http://www.ncbi.nlm.nih.gov/pubmed/7660125>.
- Manoli, M., & Driever, W. (2012). Fluorescence-activated cell sorting (FACS) of fluorescently tagged cells from zebrafish larvae for RNA isolation. *Cold Spring Harbor Protocols*, *2012*(8). <http://dx.doi.org/10.1101/pdb.prot069633>.
- Mosimann, C., Kaufman, C. K., Li, P., Pugach, E. K., Tamplin, O. J., & Zon, L. I. (2011). Ubiquitous transgene expression and Cre-based recombination driven by the ubiquitin promoter in zebrafish. *Development*, *138*(1), 169–177. <http://dx.doi.org/10.1242/dev.059345>.
- Nakazawa, N., Taniguchi, K., Okumura, T., Maeda, R., & Matsuno, K. (2012). A novel Cre/loxP system for mosaic gene expression in the *Drosophila* embryo. *Developmental Dynamics*, *241*(5), 965–974. <http://dx.doi.org/10.1002/dvdy.23784>.
- Ni, T. T., Lu, J., Zhu, M., Maddison, L. A., Boyd, K. L., Huskey, L., ... Chen, W. (2012). Conditional control of gene function by an invertible gene trap in zebrafish. *Proceedings of the National Academy of Sciences of the United States of America*, *109*(38), 15389–15394. <http://dx.doi.org/10.1073/pnas.1206131109>.
- Platt, R. J., Chen, S., Zhou, Y., Yim, M. J., Swiech, L., Kempton, H. R., ... Zhang, F. (2014). CRISPR-Cas9 knockin mice for genome editing and cancer modeling. *Cell*, *159*(2), 440–455. <http://dx.doi.org/10.1016/j.cell.2014.09.014>.
- Port, F., Chen, H. M., Lee, T., & Bullock, S. L. (2014). Optimized CRISPR/Cas tools for efficient germline and somatic genome engineering in *Drosophila*. *Proceedings of the National Academy of Sciences of the United States of America*, *111*(29), E2967–E2976. <http://dx.doi.org/10.1073/pnas.1405500111>.

- Rossant, J., & Spence, A. (1998). Chimeras and mosaics in mouse mutant analysis. *Trends in Genetics*, *14*(9), 358–363. Retrieved from <http://www.ncbi.nlm.nih.gov/pubmed/9769731>.
- Techau, G., & Campos-Ortega, J. (1986). Lineage analysis of transplanted individual cells in embryos of *Drosophila melanogaster*. *Roux's Archives of Developmental Biology*, *195*(8), 489–498. <http://dx.doi.org/10.1007/BF00375889>.
- Theodosiou, N. A., & Xu, T. (1998). Use of FLP/FRT system to study *Drosophila* development. *Methods*, *14*(4), 355–365. <http://dx.doi.org/10.1006/meth.1998.0591>.
- Yang, H., Wang, H., Shivalila, C. S., Cheng, A. W., Shi, L., & Jaenisch, R. (2013). One-step generation of mice carrying reporter and conditional alleles by CRISPR/Cas-mediated genome engineering. *Cell*, *154*(6), 1370–1379. <http://dx.doi.org/10.1016/j.cell.2013.08.022>.
- Yin, L., Maddison, L. A., Li, M., Kara, N., LaFave, M. C., Varshney, G. K., ... Chen, W. (2015). Multiplex conditional mutagenesis using transgenic expression of Cas9 and sgRNAs. *Genetics*, *200*(2), 431–441. <http://dx.doi.org/10.1534/genetics.115.176917>.
- Zong, H., Espinosa, J. S., Su, H. H., Muzumdar, M. D., & Luo, L. (2005). Mosaic analysis with double markers in mice. *Cell*, *121*(3), 479–492. <http://dx.doi.org/10.1016/j.cell.2005.02.012>.